The Role of Cdx in Mesoderm Cell Fate Specification

Tanya Foley

Thesis submitted in partial fulfillment of the requirements
for the PhD degree in Cellular and Molecular Medicine

October 20, 2021

Department of Cellular and Molecular Medicine
Faculty of Medicine University of Ottawa

© Tanya Foley, Ottawa, Canada, 2022

AUTHORIZATIONS

Figure 1 (Bassalert et al., 2018). Reproduced with permission from Springer Nature publishing group.

This Agreement between Tanya Foley ("You") and Elsevier ("Elsevier") consists of yourlicense details and the terms and conditions provided by Elsevier and Copyright ClearanceCenter.

License Number	5125461142459
License date	Aug 10, 2021
Licensed Content Publisher	Elsevier
Licensed Content Publication	Elsevier Books
Licensed Content Title	Current Topics in Developmental Biology
Licensed Content Author	Cécilia Bassalert,Lorena Valverde-Estrella,ClaireChazaud
Licensed Content Date	Jan 1, 2018
Licensed Content Pages	24
Start Page	81
End Page	104
Type of Use	reuse in a thesis/dissertation
Portion	figures/tables/illustrations
Number of figures/tables/illustrations	1
Format	both print and electronic
Are you the author of this Elsevierchapter?	No
Will you be translating?	No
Title	Roles of Cdx Transcription Factors During MesodermSpecification
Institution name	University of Ottawa
Expected presentation date	Oct 2021
Portions	Figure 1

Figure 3 (Lu et al., 2001). Reproduced with permission from Elsevier publishing group.

This Agreement between Tanya Foley ("You") and Elsevier ("Elsevier") consists of yourlicense details and the terms and conditions provided by Elsevier and Copyright ClearanceCenter.

License Number	5125470468997
License date	Aug 10, 2021
Licensed Content Publisher	Elsevier
Licensed Content Publication	Current Opinion in Genetics & Development
Licensed Content Title	From fertilization to gastrulation: axis formation in themouse embryo
Licensed Content Author	Cindy C Lu,Jane Brennan,Elizabeth J Robertson
Licensed Content Date	Aug 1, 2001
Licensed Content Volume	11
Licensed Content Issue	4
Licensed Content Pages	9
Start Page	384
End Page	392
Type of Use	reuse in a thesis/dissertation
Portion	figures/tables/illustrations
Number offigures/tables/illustrations	1
Format	both print and electronic
Are you the author of this Elsevierarticle?	No
Will you be translating?	No
Title	Roles of Cdx Transcription Factors During MesodermSpecification
Institution name	University of Ottawa
Expected presentation date	Oct 2021
Portions	1

Figure 4 (Liu et al., 2018). Reproduced with permission from Oxford University Press publishing group.

This Agreement between Tanya Foley ("You") and Oxford University Press ("Oxford University Press") consists of your license details and the terms and conditions provided by Oxford University Press and Copyright Clearance Center.

License Number	5162091035467
License date	Oct 04, 2021
Licensed content publisher	Oxford University Press
Licensed content publication	Acta Biochimica et Biophysica Sinica
Licensed content title	TGF-β signaling pathway in early mouse development and embryonic stem cells
Licensed content author	Liu, Chang; Peng, Guangdun
Licensed content date	Nov 28, 2017
Type of Use	Thesis/Dissertation
Title of your work	Roles of Cdx Transcription Factors During Mesoderm Specification
Publisher of your work	University of Ottawa
Expected publication date	Oct 2021
Title	Roles of Cdx Transcription Factors During Mesoderm Specification
Institution name	University of Ottawa
Expected presentation date	Oct 2021
Portions Figure	3

Figure 5 (Bardot et al., 2020). Reproduced with permission from Elsevier publishing group.

This Agreement between Tanya Foley ("You") and Elsevier ("Elsevier") consists of yourlicense details and the terms and conditions provided by Elsevier and Copyright ClearanceCenter.

License Number	5125481244778
License date	Aug 10, 2021
Licensed Content Publisher	Elsevier
Licensed ContentPublication	Mechanisms of Development
Licensed Content Title	Mouse gastrulation: Coordination of tissue patterning,specification and diversification of cell fate
Licensed Content Author	Evan S. Bardot,Anna-Katerina Hadjantonakis
Licensed Content Date	Sep 1, 2020
Licensed Content Volume	163
Licensed Content Issue	n/a
Licensed Content Pages	1
Start Page	103617
End Page	0

Type of Use	reuse in a thesis/dissertation
Portion	figures/tables/illustrations
Number offigures/tables/illustrations	1
Format	both print and electronic
Are you the author of thisElsevier article?	No
Will you be translating?	No
Title	Roles of Cdx Transcription Factors During MesodermSpecification
Institution name	University of Ottawa
Expected presentation date	Oct 2021
Portions	Figure 1

Figure 6 (Cui et al., 2018). Reproduced with permission from John Wiley and Sons publishing group.

This Agreement between Tanya Foley ("You") and John Wiley and Sons ("John Wiley andSons") consists of your license details and the terms and conditions provided by John Wileyand Sons and Copyright Clearance Center.

License Number	5125490085689
License date	Aug 10, 2021
Licensed ContentPublisher	John Wiley and Sons
Licensed ContentPublication	Development, Growth & Differentiation
Licensed ContentTitle	Mouse gastrulation: Attributes of transcription factor regulatorynetwork for epiblast patterning
Licensed ContentAuthor	Naihe Jing, Patrick P. L. Tam, Guangdun Peng, et al
Licensed ContentDate	Oct 18, 2018
Licensed ContentVolume	60
Licensed ContentIssue	8
Licensed ContentPages	10
Type of use	Dissertation/Thesis
Requestor type	University/Academic
Format	Print and electronic
Portion	Figure/table
Number offigures/tables	1
Will you betranslating?	No
Title	Roles of Cdx Transcription Factors During Mesoderm Specification
Institution name	University of Ottawa
Expectedpresentation date	Oct 2021
Portions	Figure 4

Figure 7 (Tam and Behringer, 1997). Reproduced with permission from Elsevier publishing group.

This Agreement between Tanya Foley ("You") and Elsevier ("Elsevier") consists of yourlicense details and the terms and conditions provided by Elsevier and Copyright ClearanceCenter.

License Number	5162091335167
License date	Oct 04, 2021
Licensed Content Publisher	Elsevier
Licensed Content Publication	Mechanisms of Development
Licensed Content Title	Mouse gastrulation: the formation of a mammalian bodyplan
Licensed Content Author	Patrick P.L Tam,Richard R Behringer
Licensed Content Date	Nov 1, 1997
Licensed Content Volume	68
Licensed Content Issue	1-2
Licensed Content Pages	23
Start Page	3
End Page	25
Type of Use	reuse in a thesis/dissertation
Portion	figures/tables/illustrations
Number offigures/tables/illustrations	1
Format	both print and electronic
Are you the author of this Elsevierarticle?	No
Will you be translating?	No
Title	Roles of Cdx Transcription Factors During Mesoderm Specification
Institution name	University of Ottawa
Expected presentation date	Oct 2021
Portions	Figure 1

Figure 8 (Berenguer et al., 2020). Reproduced under the terms of the Creative Commons Attribution License, which permits unrestricted use, distribution, and reproduction in any medium, provided the original author and source are credited.

Copyright: © 2020 Berenguer et al. This is an open access article distributed under the terms of the Creative Commons Attribution License, which permits unrestricted use, distribution, and reproduction in any medium, provided the original author and source are credited.

Figure 9 (Beddington and Robertson, 1998). Reproduced with permission from Elsevier publishing group.

This Agreement between Tanya Foley ("You") and Elsevier ("Elsevier") consists of your license details and the terms and conditions provided by Elsevier and Copyright Clearance Center.

License Number	5162100020895
License date	Oct 04, 2021
Licensed Content Publisher	Elsevier
Licensed Content Publication	Trends in Genetics
Licensed Content Title	Anterior patterning in mouse
Licensed Content Author	Rosa S.P Beddington, Elizabeth J Robertson
Licensed Content Date	Jul 1, 1998
Licensed Content Volume	14
Licensed Content Issue	7
Licensed Content Pages	8
Start Page	277
End Page	284
Type of Use	reuse in a thesis/dissertation
Portion	figures/tables/illustrations
Number offigures/tables/illustrations	1
Format	both print and electronic
Are you the author of this Elsevierarticle?	No
Will you be translating?	No
Title	Roles of Cdx Transcription Factors During Mesoderm Specification
Institution name	University of Ottawa
Expected presentation date	Oct 2021
Portions	Figure 1

Figure 10 (Yamane, 2018). Reproduced under the terms of the Creative Commons Attribution License, which permits unrestricted use, distribution, and reproduction in any medium, provided the original author and source are credited.

Copyright © 2018 Yamane. This is an open-access article distributed under the terms of the Creative Commons Attribution License (CC BY). The use, distribution or reproduction in other forums is permitted, provided the original author(s) and the copyright owner(s) are credited and that the original publication in this journal is cited, in accordance with accepted academic practice. No use, distribution or reproduction is permitted which does not comply with these terms.

Figure 11 (Gavrilov and Lacy, 2013). Reproduced with permission from Elsevier publishing group.

This Agreement between Tanya Foley ("You") and Elsevier ("Elsevier") consists of yourlicense details and the terms and conditions provided by Elsevier and Copyright ClearanceCenter.

License Number	5125930097770
License date	Aug 11, 2021
Licensed ContentPublisher	Elsevier
Licensed ContentPublication	Current Opinion in Genetics & Development
Licensed Content Title	Genetic dissection of ventral folding morphogenesis in mouse:embryonic visceral endoderm-supplied BMP2 positions head andheart
Licensed Content Author	Svetlana Gavrilov,Elizabeth Lacy
Licensed Content Date	Aug 1, 2013
Licensed Content Volume	23
Licensed Content Issue	4
Licensed Content Pages	9
Start Page	461
End Page	469
Type of Use	reuse in a thesis/dissertation
Portion	figures/tables/illustrations
Number offigures/tables/illustrations	1
Format	both print and electronic
Are you the author of thisElsevier article?	No
Will you be translating?	No
Title	Roles of Cdx Transcription Factors During MesodermSpecification
Institution name	University of Ottawa
Expected presentationdate	Oct 2021
Portions	Figure 2

Figure 12 (Arora et al., 2012). Reproduced with permission from Elsevier publishing group.

This Agreement between Tanya Foley ("You") and Elsevier ("Elsevier") consists of yourlicense details and the terms and conditions provided by Elsevier and Copyright ClearanceCenter.

License Number	5125501502535
License date	Aug 10, 2021
Licensed Content Publisher	Elsevier
Licensed Content Publication	Blood
Licensed Content Title	The murine allantois: a model system for the study ofblood vessel formation
Licensed Content Author	Ripla Arora,Virginia E. Papaioannou
Licensed Content Date	Sep 27, 2012
Licensed Content Volume	120
Licensed Content Issue	13
Licensed Content Pages	11
Start Page	2562
End Page	2572
Type of Use	reuse in a thesis/dissertation
Portion	figures/tables/illustrations
Number offigures/tables/illustrations	1
Format	both print and electronic
Are you the author of thisElsevier article?	No
Will you be translating?	No
Title	Roles of Cdx Transcription Factors During MesodermSpecification
Institution name	University of Ottawa
Expected presentation date	Oct 2021

Figure 13 (Jones et al., 2006). Reproduced with permission from The American Physiology Society
publishing group.

This Agreement between Tanya Foley ("You") and The American Physiological Society("The American Physiological Society") consists of your license details and the terms andconditions provided by The American Physiological Society and Copyright ClearanceCenter.

The publisher has provided special terms related to this request that can be found at the endof the Publisher's Terms and Conditions.

License Number	5125920009702
License date	Aug 11, 2021
Licensed Content Publisher	The American Physiological Society
Licensed Content Publication	Physiology
Licensed Content Title	What Determines Blood Vessel Structure? GeneticPrespecification vs. Hemodynamics
Licensed Content Author	Elizabeth A. V. Jones, Ferdinand le Noble, Anne Eichmann
Licensed Content Date	Dec 1, 2006
Licensed Content Volume	21
Licensed Content Issue	6
Type of Use	Thesis/Dissertation
Requestor type	non-profit academic/educational
Readers being charged a feefor this work	No
Format	print and electronic
Portion	figures/tables/images
Number offigures/tables/images	1
Will you be translating?	no
World Rights	no
Title	Roles of Cdx Transcription Factors During MesodermSpecification
Institution name	University of Ottawa
Expected presentation date	Oct 2021
Portions	Figure 1

Figure 14 (Van Handel et al., 2012). Adapted with permission from Elsevier publishing group.

This Agreement between Tanya Foley ("You") and Elsevier ("Elsevier") consists of yourlicense details and the terms and conditions provided by Elsevier and Copyright ClearanceCenter.

License Number	5125510794080
License date	Aug 10, 2021
Licensed ContentPublisher	Elsevier
Licensed ContentPublication	Cell
Licensed Content Title	Scl Represses Cardiomyogenesis in Prospective HemogenicEndothelium and Endocardium
Licensed Content Author	Ben Van Handel,Amélie Montel-Hagen,RajkumarSasidharan,Haruko Nakano,Roberto Ferrari,Cornelis J.Boogerd,Johann Schredelseker,Yanling Wang,Sean Hunter,TõnisOrg,Jian Zhou,Xinmin Li,Matteo Pellegrini,Jau-NianChen,Stuart H. Orkin et al.
Licensed Content Date	Aug 3, 2012
Licensed Content Volume	150
Licensed Content Issue	3
Licensed Content Pages	16
Start Page 590	
End Page	605
Type of Use	reuse in a thesis/dissertation
Portion	figures/tables/illustrations
Number offigures/tables/illustrations	1
Format	both print and electronic
Are you the author of thisElsevier article?	No
Will you be translating?	No
Title	Roles of Cdx Transcription Factors During MesodermSpecification
Institution name	University of Ottawa
Expected presentationdate	Oct 2021
Portions	Graphical abstract

Figure 15 (Jagannathan-Bogdan and Zon, 2013). Reproduced with permission from The Company of Biologists Ltd publishing group.

Development

Article:Hematopoiesis.	
Order License ID	Pending
ISSN	1477-9129
Type of Use	Republish in a thesis/dissertation
Publisher	COMPANY OFBIOLOGISTS,
Portion	Image/photo/illustration
LICENSED CONTENT	
Publication Title	Development
Article Title	Hematopoiesis.
Author/Editor	Company of Biologists.
Date	01/01/1987
Language	English
Country	United Kingdom of Great Britain and Northern Ireland
Rightsholder	The Company ofBiologists Ltd.
Publication Type	e-Journal
Start Page	2463
End Page	2467
Issue	12
Volume	140
URL	http://dev.biologists.org/
REQUEST DETAILS	
Portion Type	Image/photo/illustration
Number of images /photos / illustrations	1
Format (select all thatapply)	Print, Electronic
Who will republish thecontent?	Academic institution
Duration of Use	Life of current and all future editions
Lifetime Unit Quantity	Up to 499
Rights Requested	Main product
Distribution	Canada
Translation	Original language of publication
Copies for the disabled?	No
Minor editingprivileges?	Yes
Incidental promotionaluse?	No
Currency	CAD
NEW WORK DETAILS	
Title	The Role of Cdx inMesoderm Developmentand Cell Fate Specification
Instructor name	Tanya Foley
Institution name	University of Ottawa
Expected presentationdate	2021-10-20

Figure 17 (Meilhac and Buckingham, 2018). Reproduced with permission from Springer Nature publishing group.

This Agreement between Tanya Foley ("You") and Springer Nature ("Springer Nature")consists of your license details and the terms and conditions provided by Springer Natureand Copyright Clearance Center.

License Number	5125511071729
License date	Aug 10, 2021
Licensed Content Publisher	Springer Nature
Licensed Content Publication	Nature Reviews Cardiology
Licensed Content Title	The deployment of cell lineages that form the mammalianheart
Licensed Content Author	Sigolène M. Meilhac et al
Licensed Content Date	Sep 28, 2018
Type of Use	Thesis/Dissertation
Requestor type	academic/university or research institute
Format	print and electronic
Portion	figures/tables/illustrations
Number offigures/tables/illustrations	1
High-res required	no
Will you be translating?	no
Circulation/distribution	1 - 29
Author of this Springer Naturecontent	no
Title	Roles of Cdx Transcription Factors During MesodermSpecification
Institution name	University of Ottawa
Expected presentation date	Oct 2021
Portions	Figure 3

Figure 18 (Xi et al., 2013). Reproduced with permission from Springer Nature publishing group.

This Agreement between Tanya Foley ("You") and Springer Nature ("Springer Nature")consists of your license details and the terms and conditions provided by Springer Natureand Copyright Clearance Center.

License Number	5125511289142
License date	Aug 10, 2021
Licensed ContentPublisher	Springer Nature
Licensed ContentPublication	Nature Reviews Molecular Cell Biology
Licensed Content Title	Mending broken hearts: cardiac development as a basis for adultheart regeneration and repair
Licensed Content Author	Mei Xin et al
Licensed Content Date	Jul 10, 2013
Type of Use	Thesis/Dissertation
Requestor type	academic/university or research institute
Format	print and electronic
Portion	figures/tables/illustrations
Number of figures/tables/illustrations	1
High-res required	no
Will you be translating?	no
Circulation/distribution	1 - 29
Author of this SpringerNature content	no
Title	Roles of Cdx Transcription Factors During MesodermSpecification
Institution name	University of Ottawa
Expected presentationdate	Oct 2021
Portions	Figure in Box 2

Figure 19 (Keyte and Hutson, 2012). Reproduced with permission from Elsevier publishing group.

This Agreement between Tanya Foley ("You") and Elsevier ("Elsevier") consists of yourlicense details and the terms and conditions provided by Elsevier and Copyright ClearanceCenter.

License Number	5125511429912
License date	Aug 10, 2021
Licensed Content Publisher	Elsevier
Licensed Content Publication	Differentiation
Licensed Content Title	The neural crest in cardiac congenital anomalies
Licensed Content Author	Anna Keyte,Mary Redmond Hutson
Licensed Content Date	Jul 1, 2012
Licensed Content Volume	84
Licensed Content Issue	1
Licensed Content Pages	16
Start Page	25
End Page	40
Type of Use	reuse in a thesis/dissertation
Portion	figures/tables/illustrations
Number offigures/tables/illustrations	1
Format	both print and electronic
Are you the author of this Elsevierarticle?	No
Will you be translating?	No
Title	Roles of Cdx Transcription Factors During MesodermSpecification
Institution name	University of Ottawa
Expected presentation date	Oct 2021
Portions	Figure 1

Figure 20 (Lohnes, 2003). Reproduced with permission from John Wiley and Sons publishing group.

This Agreement between Tanya Foley ("You") and John Wiley and Sons ("John Wiley andSons") consists of your license details and the terms and conditions provided by John Wileyand Sons and Copyright Clearance Center.

License Number	5125520188510
License date	Aug 10, 2021
Licensed ContentPublisher	John Wiley and Sons
Licensed ContentPublication	BioEssays
Licensed Content Title	The Cdx1 homeodomain protein: an integrator of posteriorsignaling in the mouse
Licensed ContentAuthor	David Lohnes
Licensed Content Date	Sep 17, 2003
Licensed ContentVolume	25
Licensed Content Issue	10
Licensed Content Pages	10
Type of use	Dissertation/Thesis
Requestor type	University/Academic
Format	Print and electronic
Portion	Figure/table
Number offigures/tables	1
Will you be translating?	No
Title	Roles of Cdx Transcription Factors During Mesoderm Specification
Institution name	University of Ottawa
Expected presentationdate	Oct 2021
Portions	Figure 1

Figure 21 (Pilon et al., 2007). Reproduced with permission from The Company of Biologists Ltd publishing group.

Publication Title	Development
Article Title	Wnt signaling is a keymediator of Cdx1expression in vivo.
Author/Editor	Company of Biologists.
Date	01/01/1987
Language	English
Country	United Kingdom of GreatBritain and NorthernIreland
Rightsholder	The Company ofBiologists Ltd.
Publication Type	e-Journal
Start Page	2315
End Page	2323
Issue	12
Volume	134
URL	http://dev.biologists.org/

REQUEST DETAILS

Portion Type	Image/photo/illustration
Number of images /photos / illustrations	1
Format (select all thatapply)	Print, Electronic
Who will republish thecontent?	Academic institution
Duration of Use	Life of current edition
Lifetime Unit Quantity	Up to 499
Rights Requested	Main product
Distribution	Worldwide
Translation	Original language ofpublication
Copies for the disabled?	No
Minor editingprivileges?	Yes
Incidental promotionaluse?	No
Currency	CAD

NEW WORK DETAILS

Title	Role of Cdx FactorsDuring MesodermSpecification
Instructor name	Tanya Foley
Institution name	University of Ottawa
Expected presentation date	2021-10-01

ADDITIONAL DETAILS

Order referencenumber	N/A
The requesting person /organization to appearon the license	Tanya Foley

Figure 22 (Blaussen.com staff, 2014). Reproduced with permission from the Wikimedia Foundation.

This work is free and may be used by anyone for any purpose. If you wish to use this content, you do not need to request permission as long as you follow any licensing requirements mentioned on this page.

The Wikimedia Foundation has received an e-mail confirming that the copyright holder has approved publication under the terms mentioned on this page. This correspondence has been reviewed by a Volunteer Response Team (VRT) member and stored in our permission archive. The correspondence is available to trusted volunteers as ticket #2013061010006654.

Figure 24, 25, 27 (Guo et al., 2004). Reproduced with permission from the Taylor and Francis publishing group.

The role of Cdx proteins in intestinal development and cancer
Author: Rong-Jun Guo, , Eun Ran Suh, et al
Publication: Cancer Biology & Therapy
Publisher: Taylor & Francis
Date: Jul 1, 2004
Rights managed by Taylor & Francis
Thesis/Dissertation Reuse Request
Taylor & Francis is pleased to offer reuses of its content for a thesis or dissertation free of charge contingent on resubmission of permission request if work is published.

Figure 28 (Savory et al., 2011a). Reproduced with permission from The Company of Biologists Ltd publishing group.

Article:	Cdx mediates neural tube closure through transcriptional regulation of the planar cell polarity gene Ptk7.
Order License ID	Pending
ISSN	1477-9129
Type of Use	Republish in athesis/dissertation
Publisher	COMPANY OF BIOLOGISTS,
Portion	Image/photo/illustration
Publication Title	Development
Article Title	Cdx mediates neuraltube closure through transcriptional regulation of the planar cell polarity gene Ptk7.
Author/Editor	Company of Biologists.
Date	01/01/1987
Language	English
Country	United Kingdom of Great Britain and Northern Ireland
Rightsholder	The Company of Biologists Ltd.
Publication Type	e-Journal
Start Page	1361
End Page	1370
Issue	7
Volume	138
URL	http://dev.biologists.org/
REQUEST DETAILS	
Portion Type	Image/photo/illustration
Number of images /photos / illustrations	1
Format (select all thatapply)	Print, Electronic
Who will republish thecontent?	Academic institution
Duration of Use	Life of current edition
Lifetime Unit Quantity	Up to 499
Rights Requested	Main product
Distribution	Worldwide
Translation	Original language ofpublication
Copies for the disabled?	No
Minor editingprivileges?	Yes
Incidental promotionaluse?	No
Currency	CAD
NEW WORK DETAILS	
Title	Role of Cdx FactorsDuring Mesoderm Specification
Instructor name	Tanya Foley
Institution name	University of Ottawa
Expected presentationdate	2021-10-01

Figure 29 (Nguyen et al., 2017). Reproduced under the terms of the Creative Commons Attribution
License, which permits unrestricted use, distribution, and reproduction in any medium, provided the original author and source are credited.

Creative Commons
This is an open access article distributed under the terms of the Creative Commons CC-BY license, which permits unrestricted use, distribution, and reproduction in any medium, provided the original work is properly cited.
You are not required to obtain permission to reuse this article.

Figures 30, 31 (Ho and Crabtree, 2010). Reproduced with permission from Springer Nature publishing group.

This Agreement between Tanya Foley ("You") and Springer Nature ("Springer Nature") consists of your license details and the terms and conditions provided by Springer Natureand Copyright Clearance Center.

License Number	5125531030848
License date	Aug 10, 2021
Licensed Content Publisher	Springer Nature
Licensed Content Publication	Nature
Licensed Content Title	Chromatin remodelling during development
Licensed Content Author	Lena Ho et al
Licensed Content Date	Jan 27, 2010
Type of Use	Thesis/Dissertation
Requestor type	academic/university or research institute
Format	print and electronic
Portion	figures/tables/illustrations
Number offigures/tables/illustrations	2
High-res required	no
Will you be translating?	no
Circulation/distribution	1 - 29
Author of this Springer Naturecontent	no
Title	Roles of Cdx Transcription Factors During MesodermSpecification
Institution name	University of Ottawa
Expected presentation date	Oct 2021
Portions	Box 1 and Figure 1

Figures 33- 46 (Foley et al., 2019). Reprroduced with Permission from the Company of Biologists Publishing group.

Order Date	18-Oct-2021
Order License ID	1155081-1
ISSN	1477-9129
Type of Use	Republish in a thesis/dissertation
Publisher	COMPANY OF BIOLOGISTS,
Portion	Chapter/article
LICENSED CONTENT	
Publication Title	Development
Article Title	Role of Cdx factors in early mesodermal fate decisions.
Author/Editor	Company of Biologists.
Date	01/01/1987
Language	English
Country	United Kingdom of Great Britain and Northern Ireland
Rightsholder	The Company of Biologists Ltd.
Publication Type	e-Journal
Issue	7
Volume	146
URL	http://dev.biologists.org/
REQUEST DETAILS	
Portion Type	Chapter/article
Page range(s)	1-11
Total number of pages	11
Format (select all that apply)	Print, Electronic
Who will republish the content?	Academic institution
Duration of Use	Life of current and all future editions
Lifetime Unit Quantity	Up to 499
Rights Requested	Main product
Distribution	Canada
Translation	Original language of publication
Copies for the disabled?	No
Minor editing privileges?	Yes
Incidental promotional use?	No
Currency	CAD
NEW WORK DETAILS	
Title	The Role of Cdx in Mesoderm Development and Cell Fate Specification
Instructor name	Tanya Foley
Institution name	University of Ottawa
Expected presentation date	2021-10-20

ABSTRACT

Roles for the Cdx transcription factors during anteroposterior patterning and development of the posterior embryo have been well described, yet little is known about Cdx functions during mesoderm specification. In the studies presented here, novel roles for Cdx during gastrulation are presented. In the first of two studies, the role of Cdx factors during cardiac mesoderm specification is investigated. We demonstrate that Cdx factors epigenetically restrict cardiac progenitor specification, preventing the ectopic expression of cardiogenic genes within progenitor mesodermal populations. We provide evidence to suggest that this occurs through interaction with Brg1, a subunit of the SWI/SNF chromatin remodeling complex, and propose a molecular mechanism by which Cdx-mediated recruitment of the SWI/SNF complex is required to maintain repression of cardiac targets at developmental stages where Cdx transcription factors are no longer expressed.

Following this, Cdx-dependent gene expression programs were identified in the extra-embryonic yolk sac. RNA-sequencing of Cdx-mutant yolk sacs revealed novel Cdx-dependent gene targets involved in ion and nutrient transport, functions analogous to those previously described for Cdx in the adult intestinal epithelium. Subsequent experimentation revealed that, for a subset of these targets, regulation correlates with the maintenance of H3K27me3 marks. Finally, we provide evidence to suggest Cdx-dependent H3K27me3 marks are established at early developmental stages, when yolk sac progenitors are specified from the streak.

Together, these studies describe novel roles for Cdx factors in mesoderm specification during gastrulation, and evoke molecular mechanisms by which Cdx might program early mesodermal populations for gene expression at later developmental stages through interactions with epigenetic regulatory complexes.

TABLE OF CONTENTS

AUTHORIZATIONS ii

ABSTRACT xxiii

TABLE OF CONTENTS xxiv

LIST OF TABLES xxvii

LIST OF FIGURES xxviii

LIST OF ABBREVIATIONS xxxi

ACKNOWLEDGEMENTS xxxiv

CHAPTER 1 – GENERAL INTRODUCTION 1

The pre-implantation embryo 2

Anteroposterior axis formation 4

Gastrulation and formation of the germ layers 7

Extra-embryonic membranes 14

Primitive hematopoiesis 18

Transcriptional regulation of primitive hematopoiesis 21

Cardiogenesis 24

Cdx transcription factors in the early embryo 31

Cdx factors in the intestine 35

Conditional Cdx2-deletion 39

Functional overlap among Cdx factors 41

Cdx interacting partners and transcription 43

SWI/SNF and BAF chromatin remodeling complexes 43

Polycomb Repressive Complex 2 46

RATIONALE 51

HYPOTHESIS 51

OBJECTIVES 51

CHAPTER 2 – ROLE OF CDX FACTORS IN EARLY MESODERMAL FATE DECISIONS 52

Author Contributions 54

Abstract 55

Introduction 56

Results 59

Cdx2 occupancy is enriched at transcription factor loci 59
Cdx function is required for normal cardiac gene expression and heart tube morphogenesis 64
Cdx represses cardiac gene expression in the yolk sac 66
Mesodermal Cdx function is essential for heart tube morphogenesis 67
Cardiogenesis required Cdx function in the yolk sac 69
Cdx2 expression is coincident with cardiac progenitor specification 71
Cdx2 co-occupies cardiogenic loci with Brg1 73
Discussion 82
Cdx2 as a master developmental regulator 82
Cdx and mesodermal specification 84
Cdx factors as integrators of extracellular signaling 87
Cdx and chromatin remodeling 88
Materials and Methods 90
Mice 90
Antibodies 90
Chromatin immunoprecipitation (ChIP) and ChIP-seq 90
GO term analysis 92
In situ hybridization 92
Reverse-transcription quantitative PCR (RT-qPCR) 92
RNA-seq 93
FAIRE-PCR 93
Acknowledgements 95
CHAPTER 3 – CDX REGULATES GENE EXPRESSION THROUGH PRC2-MEDIATED EPIGENETIC MECHANISMS 96
Author Contributions 98
Abstract 99
Introduction 100
Results 104
Differential gene expression in Cdx mutant yolk sacs 104
Cdx impacts expression of genes associated with nutrient and ion transport 109

Identification of novel Cdx target genes in the yolk sac 111
Cdx impacts PRC2-dependent gene regulation 113
Discussion 118
Cdx and the yolk sac 118
Cdx primes gene expression programs 120
Cdx2 and PRC2 122
Conclusions 123
Materials and Methods 125
Mice 125
Histology 125
Antibodies 125
Chromatin immunoprecipitation (ChIP) 126
Reverse-transcription quantitative PCR (RT-qPCR) 127
Bulk RNA-sequencing 128
Acknowledgements 129
CHAPTER 4 – GENERAL DISCUSSION 130
Overview 131
Cardiac defects in Cdx mutant embryos 132
Ectopic cardiac gene expression in DKO embryos 133
Cdx2 occupancy across the genome 134
Cdx and the SWI/SNF complex 137
Temporal overlap between Cdx occupancy and regulatory partners at genomic targets 139
Functional significance of H3K27me3 at Cdx target genes 142
Conserved Cdx functions in the mouse extra-embryonic yolk sac and adult intestine 144
Conclusions 146
REFERENCES 148
APPENDIX 180

LIST OF TABLES

Table 1. Select transcription and signaling factors with peak scores below 800

Table 2. Oligonucleotide sequences for ChIP-PCR

Table 3. Oligonucleotide sequences for qRT-PCR

Table 4. Oligonucleotide sequences for semi-quantitative RT-PCR

Table 5. Oligonucleotide sequences for FAIRE-PCR

Table 6. List of ChIP-PCR primer sequences

Table 7. List of qRT-PCR primer sequences

Table 8. List of RT-PCR primer sequences

LIST OF FIGURES

Figure 1. Pre-implantation embryonic development (E2.75-E5.5)
Figure 2. The mouse egg cylinder
Figure 3. The pre-gastrulation embryo (E6.0-E6.5)
Figure 4. Gastrulation and the embryonic germ layers
Figure 5. Signaling pathways involved in anteroposterior patterning
Figure 6. Lineage specification in the primitive streak
Figure 7. The mesodermal wings
Figure 8. Somitogenesis in the mouse embryo
Figure 9. The murine node
Figure 10. Extra-embryonic membranes associated with murine development
Figure 11. Embryonic turning and positioning of the yolk sac
Figure 12. Chorioallantoic fusion and formation of the placenta
Figure 13. Mouse primitive hematopoiesis
Figure 14. Hemogenic endothelium lines the yolk sac vasculature
Figure 15. Transition from primitive to definitive hematopoiesis.
Figure 16. Flk1 expression in mesodermal lineages.
Figure 17. Cardiac progenitors migrate anterolaterally from the primitive streak
Figure 18. Transcriptional regulation of cardiac morphogenesis
Figure 19. Cardiac neural crest cells
Figure 20. Nested Cdx expression in the early embryo
Figure 21. Anterior homeotic transformations in *Cdx1*$^{-/-}$ mutants
Figure 22. The segments of the adult intestine.
Figure 23. The crypt-villus axis of the small intestine
Figure 24. Cdx expression along the anteroposterior axis of the intestine
Figure 25. Cdx expression along the crypt-villus axis
Figure 26. Conditional Cdx2 gene deletion
Figure 27. Sequence similarity among Cdx family members
Figure 28. Cdx1-Cdx2 compound mutants
Figure 29. SWI/SNF complex subunits interact with Cdx2
Figure 30. Mouse SWI/SNF chromatin remodeling complex
Figure 31. Cell- and tissue-type-specific SWI/SNF complexes

Figure 32. Polycomb Repressive Complex 2
Figure 33. Cdx2 binding distribution
Figure 34. Enriched Cdx2 binding at hematopoietic and cardiac gene loci
Figure 35. Cardiac defects and altered expression of heart field markers in Cdx mutants
Figure 36. Tamoxifen-mediated Cdx deletion induces a cardiac phenotype
Figure 37. Cardiac genes are ectopically expressed in Cdx-deficient yolk sacs
Figure 38. Aberrant cardiac morphogenesis in *Cdx1*$^{-/-}$*Cdx2*$^{F/F}$*Mesp1*$^{+/Cre}$ mutants
Figure 39. Disrupted yolk sac vascularization in *Cdx1*$^{-/-}$*Cdx2*$^{-/-}$*Mesp1*$^{+/Cre}$ mutants.
Figure 40. Cdx2 is expressed in mesodermal progenitors
Figure 41. Cdx1 expression in E6.5-E7.75 embryos by single-cell RNA-seq
Figure 42. Cdx4 expression in E6.5-E7.75 embryos by single-cell RNA-seq
Figure 43. Cdx1, Cdx2, and Cdx4 are expressed in E6.5 whole embryos
Figure 44. Cdx2 expression relative to cardiac and hematopoietic marker genes in E6.25-7.5 embryos
Figure 45. Cdx2 and Brg1 co-occupy cardiac transcription factor loci
Figure 46. Proposed model for Cdx function in early mesoderm
Figure 47. Cdx mutants display the expected phenotypes despite incomplete Cdx2 depletion
Figure 48. 2D PCA comparison of RNA-seq datasets
Figure 49. *Scl/Tal-1* expression in *Cdx1*$^{+}$ and *Cdx4*$^{+}$ cells
Figure 50. Log_2 transformed gene counts for six RNA-seq datasets
Figure 51. RNA-seq analysis of Cdx-dependent gene expression yolk sacs
Figure 52. Genes involved in ion transport, blood vessel development, epithelial cell function, and metabolism are differentially expressed in DKO yolk sacs
Figure 53. Differential gene expression in Cdx mutant yolk sacs
Figure 54. Cdx2 directly regulates *Tbx4* and *Sox9*
Figure 55. Cdx regulates *Ezh2* expression in the yolk sac
Figure 56. Cdx impacts H3K27me3 density at Cdx target genes
Figure 57. Model for Cdx function
Appendix Figure 58. DKO embryoid bodies produce spontaneously beating colonies
Appendix Figure 59. cTnT is ectopically expressed in DKO embryos and yolk sacs
Appendix Figure 60. Cdx2 and Brg1 share genomic binding sites
Appendix Figure 61. Cdx2 and Brg1 overlap at targets associated with vascular morphogenesis

Appendix Figure 62. Cdx2 and Suz12 share genomic binding sites
Appendix Figure 63. Cdx2 and Suz12 overlap at targets associated with transcriptional regulation
Appendix Figure 64. Cdx2 and H3K27me3 share genomic binding sites
Appendix Figure 65. Cdx2 and H3K27me3 overlap at targets associated with cardiac development
Appendix Figure 66. Cdx2 and Baf250a are co-expressed in single cells at E6.5-E7.75
Appendix Figure 67. Cdx2 interacts with Suz12
Appendix Figure 68. Cdx2 occupied sits overlap with binding by Suz12 and H3K27me3 in mesodermal precursors
Appendix Figure 69. H3K27me3 levels are increased at a subset of cardiogenic and hematopoietic Cdx-targets in Cdx-mutant yolk sacs
Appendix Figure 70. Cdx-mutant embryos have highly variable levels of total H3K27me3
Appendix Figure 71. Cdx2 and markers of visceral endoderm are co-expressed in single cells at E6.5-E7.75.

LIST OF ABBREVIATIONS

Abbreviation	Meaning
A	anterior
AAA	anterior arch of the atlas
AGM	aorta-gonad-mesonephros
AP	anteroposterior
APC	adenomatous polyposis coli
ATP	adenosine triphosphate
AVE	anterior visceral endoderm
BAF	Brahma/Brg1 associated factor
Bmp	bone morphogenetic protein
Brg1	Brahma-related protein 1
Brm	Brahma
C (C1-C7)	cervical vertebrae (1-7)
CDRE	Cdx response element
ChIP	chromatin immunoprecipitation
cNCCs	cardiac neural crest cells
Co-IP	co-immunoprecipitation
Cre-ER^{T}	tamoxifen-inducible Cre-recombinase fused to an estrogen receptor ligand-binding domain
DKO	double knock-out
DNA	deoxyribonucleic acid
DV	dorsoventral
DVE	distal visceral endoderm
E	embryonic day
EBs	embryoid bodies
EDTA	ethylenediaminetetraacetic acid
EMT	epithelial-to-mesenchymal transition
En	definitive endoderm
Epi	epiblast
esBAF	embryonic stem cell-specific BAF complex
ESC	embryonic stem cell

Exm	extra-embryonic mesoderm
Ezh	Enhancer of zeste
Fb	forebrain
Fgf	fibroblast growth factor
Fgfr	fibroblast growth factor receptor
FHF	first heart field
Flk1	vascular endothelial growth factor receptor 2
H2AK119ub	histone H2 lysine 119 mono-ubiquitination
H3K27me3	histone H3 lysine 27 trimethylation
HCl	hydrochloric acid
HEK	human embryonic kidney
hESC	human embryonic stem cell
Hsp90	heat shock protein 90
ICM	inner cell mass
IgG	Immunoglobulin Type G
Ihh	Indian hedgehog
iPSC	induced pluripotent stem cell
Kb	kilobase
L	left
Lpm	lateral plate mesoderm
mESC	mouse embryonic stem cell
MgCl2	magnesium chloride
mRNA	messenger RNA
MS	mass spectrometry
NaCl	sodium chloride
nBAF	neuronal-specific BAF complex
npBAF	neural progenitor-specific BAF complex
P	posterior
PAGE	polyacrylamide gel electrophoresis
PAS	para-aortic splanchnopleura
PCR	polymerase chain reaction
PcG	Polycomb group

PrE	primitive endoderm
PRE	Polycomb response element
PS	primitive streak
PVDF	polyvinylidene fluoride
Pxm	paraxial mesoderm
qPCR	quantitative PCR
PRC	Polycomb Repressive Complex
Ptc	Patched
R	right
RNA	ribonucleic acid
RT-PCR	reverse transcription PCR
Seq	sequencing
Ser	serine
SDS	sodium dodecyl sulphate
SHF	second heart field
Shh	Sonic hedgehog
SILAC	stable isotope labelling of amino acids in cell culture
SWI/SNF	Switch/Sucrose Non-Fermentable
T	Brachyury
T1	first thoracic vertebra
TA	transit amplifying
TE	trophectoderm
TGFβ	transforming growth factor beta
Tris	tris(hydroxymethyl)aminomethane
TrxG	Trithorax group
TSS	transcriptional start site
VE	visceral endoderm
VER	ventral ectodermal ridge
VEGF	vascular endothelial growth factor
VEGFR	vascular endothelial growth factor receptor
Wnt	wingless

ACKNOWLEDGEMENTS

My deepest gratitude to Dr. David Lohnes, my supervisor and mentor. It has been a privilege to spend these formative years in your lab. You have taught me that good science requires patience, and that the value of an experiment lies within its controls. Your encouragement and confidence in my abilities has profoundly influenced the way I approach new challenges, and your mentorship has provided me with a strong foundation for the exciting future that lies ahead. I am deeply appreciative of your commitment to my learning and your kindness, which has made all the difference.

My sincere thanks to the members of my Thesis Advisory Committee: Dr. Marc Ekker, Dr. Marjorie Brand, and Dr. Nadine Wiper-Bergeron. The contributions made by each of you have greatly enhanced my learning, and I appreciate the time and effort you have invested in my education.

A heartfelt thank you to Dr. Joanne Savory. I have learned so much from you during our time in the lab together. The care and attention with which you approach your work has set an example I have tried my best to follow, and I have benefitted greatly from your willingness to discuss ideas, provide feedback, and offer guidance. Your influence on me has been greater than you know.

Much appreciation for the contributions of my lab-mates. Bradley Hess, Adriana Gambarotta, Dr. Simon Chewchuk, Dr. Sanzida Jahan, Dr. Wei Lin, Dr. Kirk Mulatz, Dr. Randy Ringuette, Yalun Zhu, Thinh Nguyen, and the ever-enthusiastic Faiyaz Zaman, thank you. I am a better scientist and teammate for having studied alongside each of you.

To my family – my Mom and Dad, who instilled in me the values and determination that make me who I am, and whose love and support has been unwavering. I could not have accomplished this without you. Thank you to my brother, Tyler, whose support is constant. I continue to learn from you each day, and am grateful to have you as my sibling and friend. Grandma Shirley, the other pea in my pod, thank you for your love, encouragement, and concern about my state of employment. Sincere thanks and appreciation to Anil and Judy, whose love and reassurance has been like a warm cup of tea,

a very welcome comfort during these final years of study. To Asif, Asma, Ashar, and Abhar, a constant source of strength and love, and a reminder that hope is a beautiful thing, thank you.

This experience would have been far less magical had I not shared it with the friends I met along the way. Olanta, my work-wife and forever coffee date. Thank you for being there morning, noon, and night, and for sharing this experience with me. Maneka, who truly believes that anything is possible, your influence has had a profound impact on me. Thank you for everything. Andréanne and Fatima, you have both inspired me to work hard since the very beginning. Thank you for keeping me going and believing in me. Candice, a light in the lab, thank you for the lessons in trickle-down therapy and for your company during long days that became late evenings. Nima, who radiates positivity, thank you for sharing both your canoe and your love for Canadian Maple donuts.

I am grateful for the Lovely Ladies, Samantha, Nicky, Roxanne, and Chloé, who have shared this journey in its entirety with me. I cannot wait to see what the future holds for each of us, I have no doubt it is very bright. I owe many thanks to the members of the Ottawa Cricket Club, not only for their friendship, but also for making sure I stay well fed and for giving me a place to be each weekend.

Finally, to my partner and best friend, Themiya, thank you for your unconditional love and support. You have changed me as a person, and I will forever be grateful for the impact you have had on my life. Thank you for selflessly offering me understanding and encouragement each day. I am so lucky to be sharing this journey with you.

CHAPTER 1 – GENERAL INTRODUCTION

The pre-implantation embryo

Mouse development begins with fertilization of the oocyte and formation of the zygote at embryonic day 0.5 (E0.5). The zygote rapidly undergoes several rounds of cellular cleavage followed by compaction. This is a process by which cells within the embryo transform from a loose cluster of cells into a tightly packed mass known as the morula, named in Latin for its mulberry-like appearance (Figure 1A; White et al., 2016). At approximately E3.5, and through complex mechanisms that are not fully understood, the morula segregates into two lineages, forming the inner cell mass (ICM) and the surrounding trophectoderm (TE; Maître, 2017). Initially, the transcription factor *Cdx2* is expressed at low levels throughout the morula, but becomes restricted to cells of the TE. As such, Cdx2 expression distinguishes the TE from *Oct4*$^{+}$ cells of the ICM (Niwa et al., 2005; Yamanaka et al., 2006; Beck et al., 1995; Strumpf et al., 2005; van den Akker et al., 2002). The TE will differentiate further to form the extra-embryonic ectoderm, and later contributes to the placenta, while cells of the ICM will give rise to all other extra-embryonic membranes, as well as all tissue types within the embryo proper (Gardner et al., 1973; Papaioannou, 1982).

Once the TE and ICM are established, a fluid-filled cavity known as the blastocoel develops within the ICM through cavitation, displacing the ICM to one side of the embryo (Figure 1B, C). As a result, the embryo adopts an elongated cup-like morphology as the pro-amniotic cavity is formed, transitioning from a blastocyst to an egg cylinder (Christodoulou et al., 2018). With this, cells within the ICM differentiate to form two lineages, the epiblast and primitive endoderm (Figure 1C; Gardner, 1982; 1983; 1989). Soon after they are specified, cells committed to the primitive endoderm lineage physically segregate from those committed to the epiblast, sorting to the surface to form an epithelial layer enveloping the epiblast (Figure 1D; Morris et al., 2010; Frenkenberg et al., 2011; Rossant et al., 2003; Plusa et al., 2008). The primitive endoderm then gives rise to the visceral endoderm and parietal

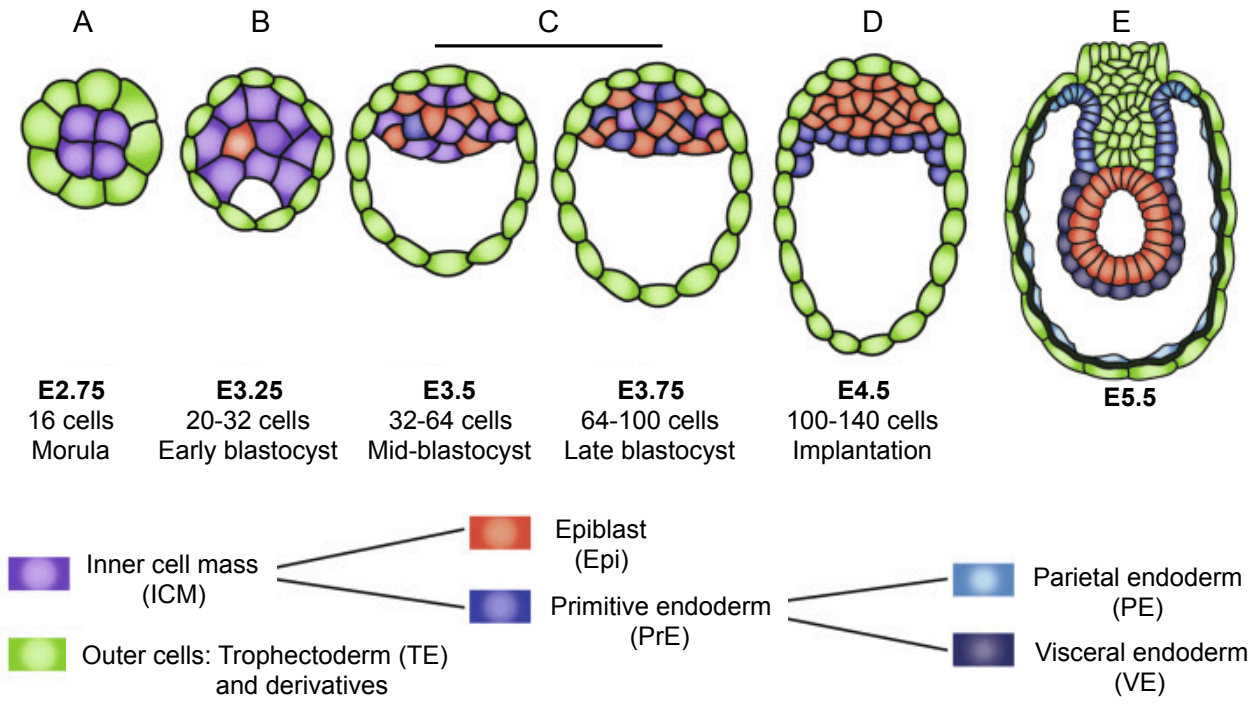


Figure 1. Pre-implantation embryonic development (E2.75-E5.5). After fertilization, the embryo undergoes cellular cleavage combined with compaction to form the morula (A), which then transitions to the blastocyst stage (B) with the formation if the inner cell mass (ICM; purple), the trophectoderm (TE; green), and a fluid-filled cavity known as the blastocoel. Cells within the ICM diverge to form the epiblast (Epi; red), which eventually forms the embryo proper, and the primitive endoderm (PrE; royal blue), which contributes to extra-embryonic membranes (C). Cells of the PrE physically segregate from cells of the ICM (D) before diverging to form two lineages, the parietal endoderm (PE; light blue) and visceral endoderm (VE; dark blue). The PE lines the TE within the blastocoel, while the VE remains associated with the epiblast (E). At E5.5, implantation occurs as the embryo assumes a cup-like morphology and the amniotic cavity forms. Figure reproduced with permission (Bassalert et al., 2018).

endoderm (Figure 1E). The visceral endoderm remains associated with the surface of the epiblast to form the visceral yolk sac, while the parietal endoderm extends away from the epiblast and into the blastocoel to form the parietal yolk sac, a monolayer that lines the wall of the TE (Duval, 1981; Sobotta, 1911; Stern and Downs, 2012; Gardner and Beddington, 1988). Together, these membranes regulate nutrient and waste exchange in the early embryo.

Anteroposterior axis formation

At approximately E5.5, implantation occurs as the egg cylinder burrows into the endometrium of the maternal uterine horn. At this stage, the embryo is composed of the inner epiblast, extra-embryonic ectoderm (derived from the trophectoderm), and the visceral endoderm (Figure 2). During implantation, the embryo is radially symmetrical, with only a discernable proximal-distal axis. Nodal signaling from the proximal epiblast, which is inhibited more proximally by BMP signaling in the extra-embryonic ectoderm (Ben-Haim et al., 2006; Arnold and Robertson, 2009; Lu and Robertson, 2004; Takaoka et al., 2017; Yamamoto et al., 2009), induces the differentiation of the distal visceral endoderm (DVE). The DVE migrates to the prospective anterior embryo, inducing the formation of the anterior visceral endoderm (AVE). The AVE is a signaling centre in the anterior embryo composed of *Hhex*$^{+}$ cells whose formation is the first symmetry-breaking event in embryonic development (Figure 3; Takaoka et al., 2001; Abe et al., 2018; Antonica et al., 2019; Shioi et al., 2017). The AVE has a critical function during early development, as it establishes the anterior-posterior embryonic axis. Once specified, the AVE induces the differentiation of anterior head structures within the epiblast while also inhibiting posteriorizing Wnt and Nodal signaling from the extra-embryonic ectoderm (Yamamoto et al., 2009; Migeotte et al., 2010; Omelchenko et al., 2014; Seinivas et al., 2004). As a result, Nodal activity is further restricted to the distal embryo, and graded Wnt signaling becomes highest proximally (Belo et al., 1997; Kemp et al., 2005; Perea-Gomez et al., 2002).

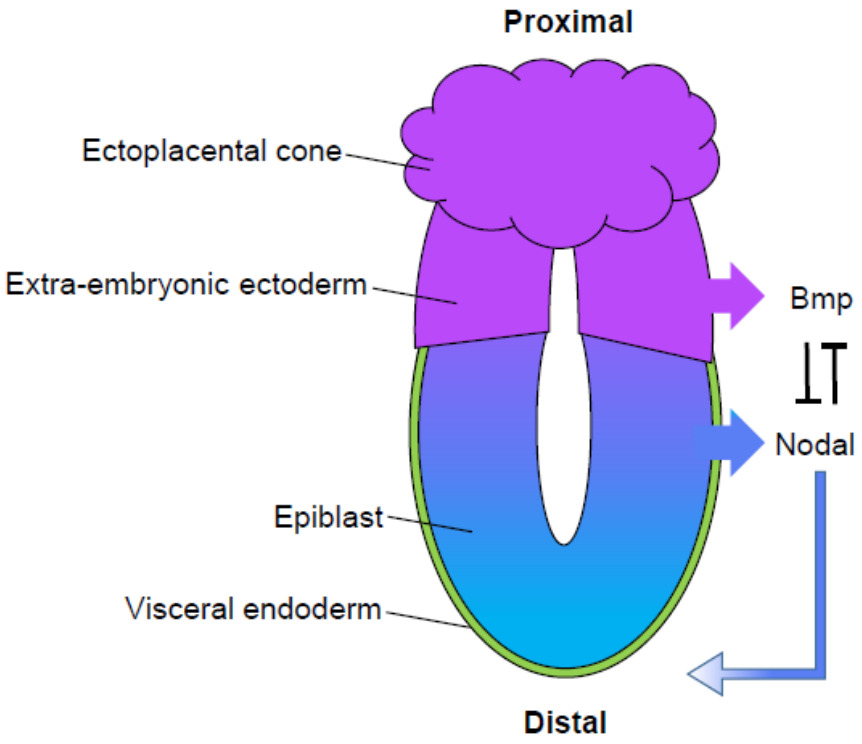


Figure 2. The mouse egg cylinder. At 5.5, the egg cylinder consists of the epiblast (blue), the trophectoderm-derived extra-embryonic ectoderm (purple), and the visceral endoderm (green). Nodal produced by the proximal epiblast induces differentiation of the distal visceral endoderm, while mutually inhibited proximally by Bmp from the extra-embryonic ectoderm.

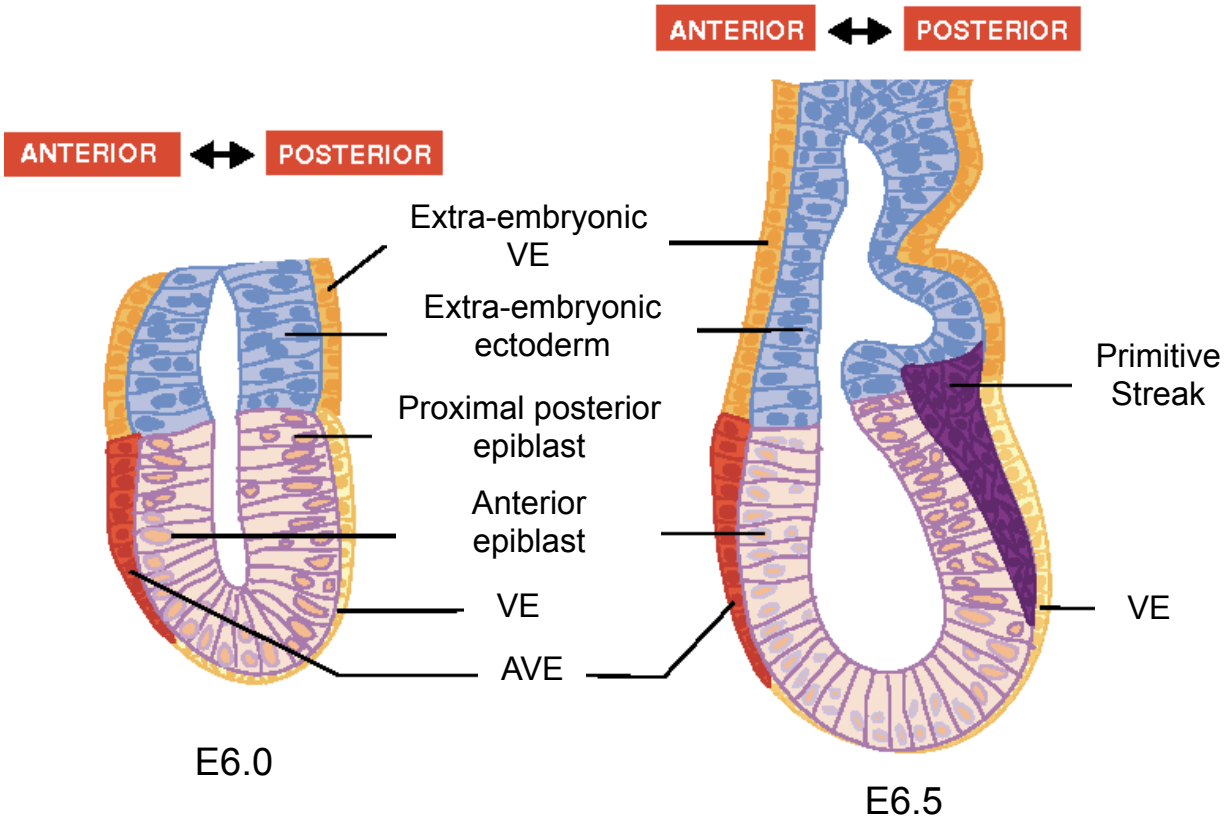


Figure 3. The pre-gastrulation embryo (E6.0-E6.5). Anterior visceral endoderm (AVE, red); Extra-embryonic visceral endoderm (Extra-embryonic VE, orange); Extra-embryonic ectoderm (blue); Epiblast (pink); Visceral endoderm (VE, yellow); Anterior visceral endoderm (AVE, red); Primitive streak (purple). Figure reproduced with permission (Lu et al., 2001).

Gastrulation and formation of the germ layers

Following anteroposterior axis formation, the embryonic body plan is established through gastrulation. Gastrulation begins with the formation of the primitive streak, a groove-like structure in the posterior embryo that forms at E6.5. Epiblast cells, stimulated by Bmp, Wnt, Nodal, and Fgf activity, undergo an epithelial-to-mesenchymal transition (EMT) and invaginate through the midline of the posterior embryo, giving rise to the streak. As cells egress, the same extracellular signaling pathways that simulate cell migration also program cells to mesodermal and endodermal fates (Ciruna and Rossant, 2001; Ciruna et al., 1997; Huelsken et al., 2000; Mohamed et al., 2004; Sun et al., 1999; Winnier et al., 1995). Gastrulation results in the formation of the three embryonic germ layers, the endoderm, mesoderm, and ectoderm (Figure 4; Tam and Gad, 2004). The endoderm eventually gives rise to the digestive system and associated organs, while the mesoderm contains progenitors for skeletal and smooth muscle, the cardiovascular system, blood, and bone, and the ectoderm, derived from the epiblast cells that do not ingress through the streak, gives rise to the nervous system and the epidermis.

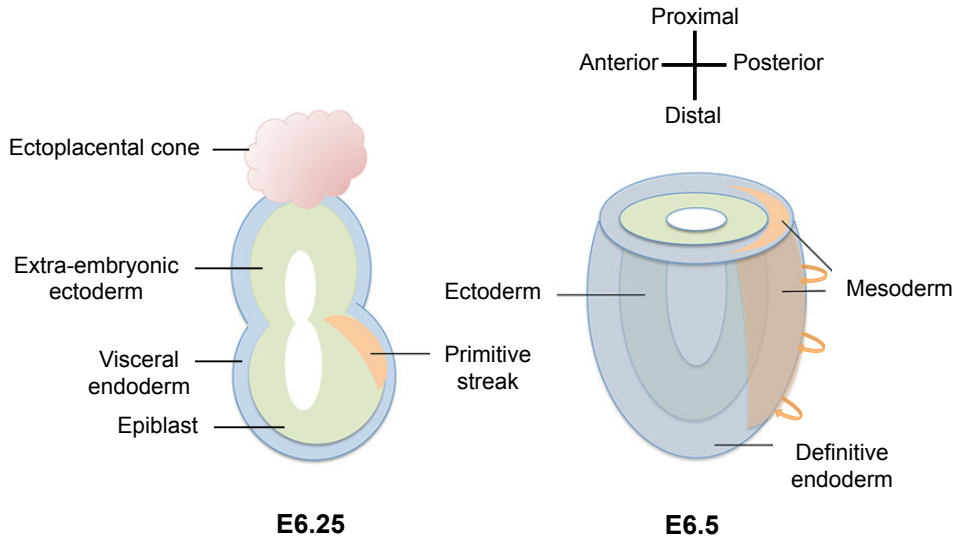


Figure 4. Gastrulation and the embryonic germ layers. At E6.25, gastrulation begins with the formation of the primitive streak in the posterior region of the embryo. Epiblast cells migrate through the streak to form the mesodermal layer as they egress between the definitive endoderm and the ectoderm. Figure reproduced with permission (Liu et al., 2018).

Epiblast cells are highly plastic before gastrulation, but become restricted to specific fates once migrating through the primitive streak (Lawson et al., 1991; Lawson and Hage, 1994; Parameswaram and Tam, 1995; Tam and Zhou, 1996). As epiblast cells migrate through the streak, they are exposed to graded extracellular signals along the anteroposterior axis (Figure 5A, B). After inducing epiblast cell migration, Wnt, Bmp, Fgf, and Nodal act in a combinatorial manner to specify progenitors to their fates (Bellairs, 1986; Hashimoto and Nakatsuji, 1989; Tam et al., 1993). As a result, mesodermal lineages exit the streak in a specific pattern that is evolutionarily conserved (Figure 6; Lawson et al., 1991; Parameswaran and Tam, 1995; Tam et al., 1997; Kinder et al., 1999). Extra-embryonic mesoderm is the first population to egress from the streak, specified in response to input from graded Bmp, Wnt, and Fgf signals with low input from the Nodal pathway. Upon exiting the streak, this progenitor population migrates extra-embryonically where it contributes to membranes, including the amnion, chorion, allantois, and visceral yolk sac (Watson and Cross, 2005). These extra-embryonic structures are required to support the growth of the conceptus through various developmental stages by providing nutrients and removing waste until the placenta forms at a later stage.

In contrast to extra-embryonic mesoderm, subsequent mesodermal populations migrate anterolaterally as they egress from the streak, giving rise to mesodermal cell types within the embryo proper. These include the lateral plate mesoderm (LPM) and paraxial mesoderm (PM), which are next to be specified. Together, the LPM and PM form the mesodermal wings and they generate a layer between the endoderm and ectoderm (Figure 7; Davidson and Zon, 2004; Lawson et al., 1991; Rosenquist, 1970; Tam and Beddington, 1987). The LPM emerges from the posterior region of the mid-streak in response to high levels of BMP signaling combined with input from the Nodal, Wnt, and Fgf pathways (Ferretti and Hadjantonakis, 2019; Nishimatsu and Thomsen, 1998; Furthauer et al., 2004; Rossant and Tam, 2009; Schier and Talbot, 2005). LPM contains progenitors for the heart, blood, vasculature, kidneys,

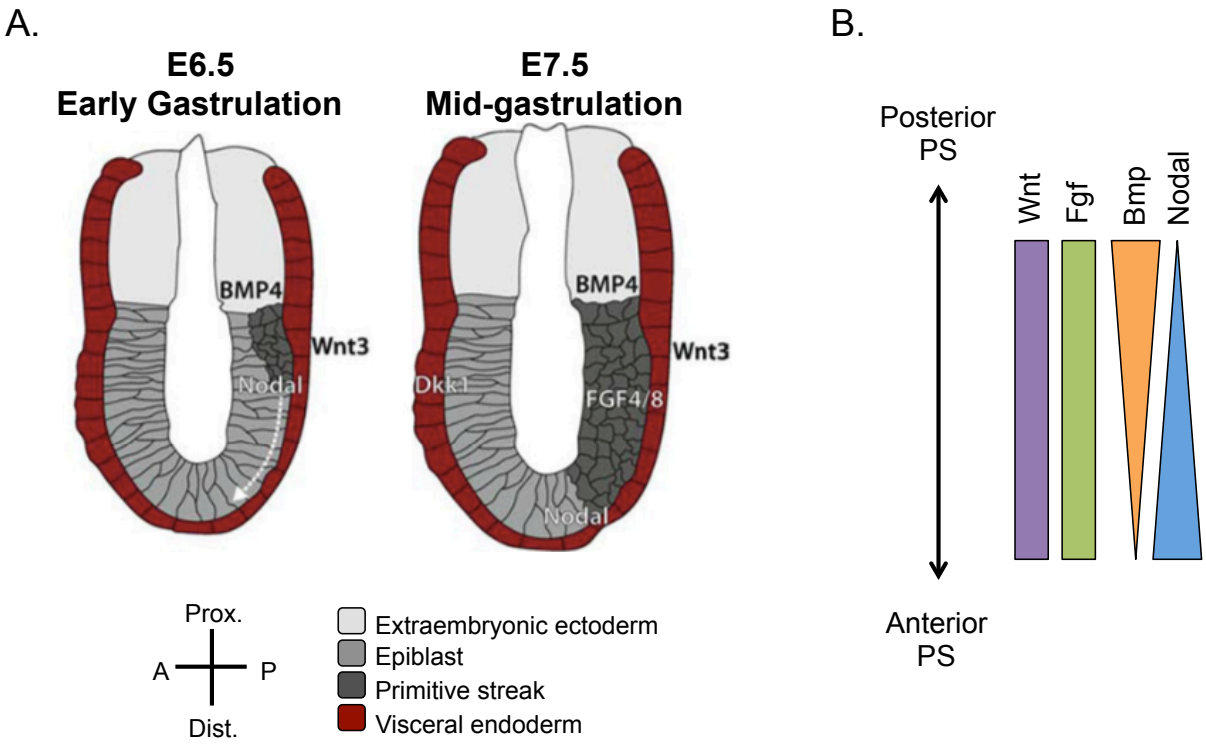


Figure 5. Signaling pathways involved in anteroposterior patterning. A. Bmp, Wnt, Fgf and Nodal signaling pathways act in combination in the posterior embryo to pattern epiblast cells to mesoderm and definitive endoderm as they egress through the primitive streak. Bmp, Wnt, and Nodal signaling are initially high in the posterior embryo during the induction of the primitive streak (E6.5). At E7.5, Wnt and Fgf signaling are uniformly active along the length of the streak, while Bmp ligands are localized to the posterior region and Nodal signaling is highest in the anterior streak, near the node. Figure reproduced with permission (Bardot et al., 2020). **B.** Schematic representation of signaling activities along the anteroposterior axis of the streak, with uniform Wnt (purple) and Fgf (green) signaling along the length of the streak, Bmp (orange) signaling highest in the posterior region, and Nodal (blue) signaling highest in the anterior portion of the primitive streak.

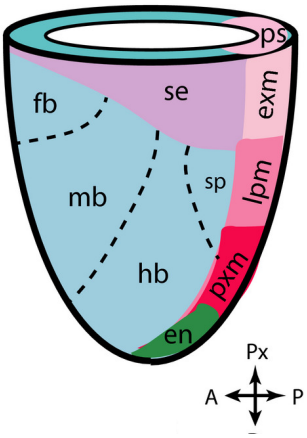


Figure 6. Lineage specification in the primitive streak. Extra-embryonic mesoderm (exm, light pink) is first to egress from the primitive streak, exiting from the posterior-most region, followed by lateral plate mesoderm (lpm, dark pink), paraxial mesoderm (pxm, red), and definitive endoderm (en, green) most anteriorly. Ectodermal lineages derived from the epiblast include surface ectoderm (se, purple) and progenitors for the forebrain (fb, blue), midbrain (mb, blue), hindbrain (hb, blue), and spinal cord (sp blue). Proximal (Px), distal (D), anterior (A), and posterior (P) axes are depicted with arrows below. Figure reproduced with permission (Cui et al., 2018).

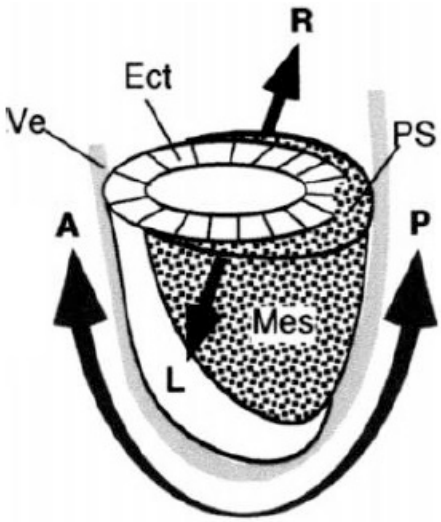


Figure 7. The mesodermal wings. During gastrulation, mesoderm egresses from the streak to form bilateral sheets of tissue that eventually join in the anterior region, referred to as the mesodermal wings. Mes, mesoderm: Ve, visceral endoderm; Ect, ectoderm; PS, primitive streak. The anterior-posterior (A-P) and right-left (R-L) axes are indicated by arrows. Figure reproduced with permission (Tam and Behringer, 1997).

smooth muscle, and limbs (Lane and Smith, 1999; Selleck and Stern, 1991; Warga and Nusslein-Volhard, 1999), and migrates to the lateral region of the embryo upon exiting the streak.

PM, also known as presomitic mesoderm (PSM), egresses anterior to the LPM, and contains highly proliferative progenitors for the vertebrae and associated skeletal muscle, as well as the dermis (Cooke and Zeeman, 1976). Once specified, PSM occupies the caudal region of the embryo and undergoes periodic segmentation commencing at E8.0. This segmentation forms the somites, bilateral blocks of epithelial tissue adjacent to the neural tube that form in an anterior-to-posterior direction (Figure 8). In mice, this process is regulated by oscillations in Wnt, Notch, and Fgf signaling, producing ~65 pairs of somites (Cooke and Zeeman, 1976; Dequeant and Pourquie, 2008).

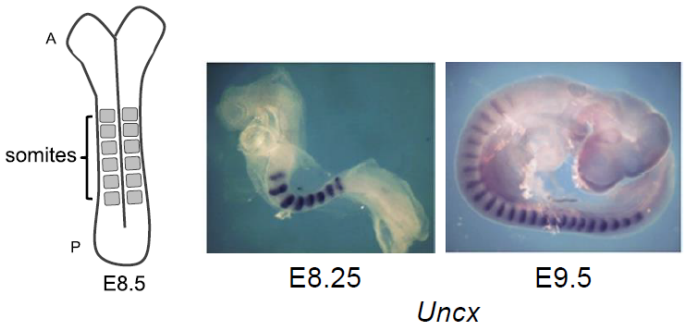


Figure 8. Somitogenesis in the mouse embryo. In situ hybridization staining for *Uncx* trancripts reveals somites, bilateral blocks of trunk tissue along the neural tube, in E8.5 and E9.5 embryos. A, anterior; P, posterior. Figure adapted with permission (Berenguer et al., 2020).

The final population specified from the epiblast during gastrulation is the definitive endoderm, which is unique from the primitive endoderm and visceral endoderm derived from the ICM earlier in development. At approximately E7.5, a small cup-like structure known as the node emerges within the distal tip of the embryo, bordering the anterior-most region of the primitive streak (Figure 9). The node,

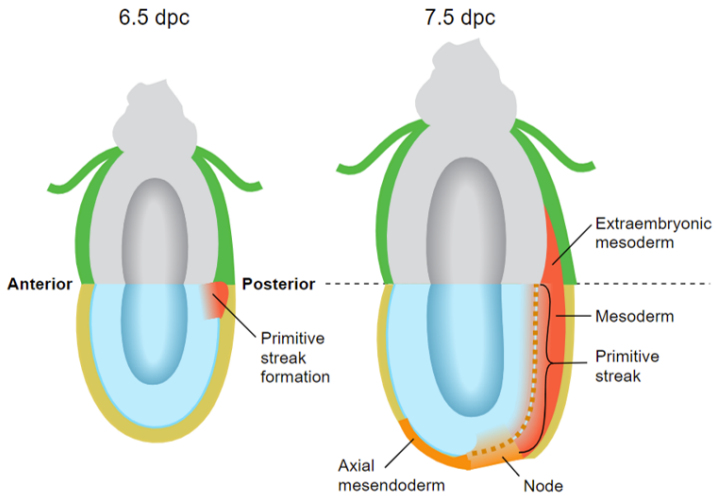


Figure 9. The murine node. The primitive streak elongates anteriorly toward the distal tip of the egg cylinder, eventually reaching the node, a cup-like structure that emerges in this region at E7.5. Grey, extra-embryonic ectoderm; green, extra-embryonic visceral endoderm; blue, epiblast; yellow, embryonic visceralendoderm; red, primitive streak; orange, mesendoderm specified during gastrulation. Figure reproduced with permission (Beddington and Robertson, 1998).

known as Spemann's organizer in amphibians and Hensen's node in birds, functions as another signaling centre to provide cues for tissue patterning, orientation, and position during gastrulation (Spemann, 1938; Hamburger, 1988). At this stage, increased BMP signaling in the posterior embryo further inhibits Nodal, restricting its activity to the node where it specifies migratory epiblast cells to definitive endoderm as they egress from the streak (Schier 2003; Schier and Talbot, 2005; Shen, 2007; Mendjan et al., 2014). Through further differentiation and patterning events, progeny of the definitive endoderm will form the lining of the respiratory system and digestive tract, as well as the liver and pancreas, among other tissues (Wells and Melton, 1999).

In addition to its role in specifying definitive endoderm, the node also functions to establish left-right asymmetry (Brennan et al., 2001, 2002). Cells within the node each contain a single cilium. Clockwise rotation by these cilia produces a leftward flow of extra-embryonic fluid, which carries Nodal and other signalling molecules to the left side of the embryo (Sulik et al., 1994; Nonaka et al.,

1998; Afzelius et al., 1976; Pedersen et al., 1976; Takeda et al., 1999; Okada et al., 1999; Supp et al., 1999; Nonaka et al., 2002; Wright, 2001; Shiratori et al., 2001; Sajoh et al., 2000). In addition, transplantation studies using murine embryos have shown that grafts from the node of one embryo can induce the formation of a secondary axis in another, demonstrating that the Node harbors organizer function intrinsic to the cells within this structure (Beddington, 1994).

Initially, the Fgf and Wnt signaling pathways are uniformly active along the length of the streak, but become restricted to the posterior-most region of the embryo at later developmental stages, from E8.5 onwards (Mendjan et al., 2014). Bmp activity is highest in the posterior region of the streak, initially produced by the distal extra-embryonic ectoderm at the egg cylinder stage. In contrast, the concentration of Nodal ligand is highest in the anterior-most region of the primitive streak, near the node (Aulehla and Pourquié, 2010; Conlon et al., 1994; Norris and Robertson, 1999). Mutual inhibition between Nodal and Bmp maintains their opposing gradients along this axis (Lawson et al., 1999). Combinatorial signaling by each of these pathways specifies progenitors to their respective fates, with cell fate determined by the time and place at which cells egress from the primitive streak (Wolpert, 1996; Lawson et al., 1991; Tam et al., 1997). As gastrulation progresses, the primitive streak continues to extend toward the distal tip of the embryo until E9.5, at which point epiblast cells are no longer migratory and gastrulation ceases. At this stage, the primitive streak is resolved into the tailbud through a structure known as the ventral ectodermal ridge (VER; Wilson and Beddington, 1996).

Our understanding of the signaling pathways active in the early embryo and their impact on cell fate determination has allowed for both mouse and human models of in vitro differentiation to be developed. This approach uses culture conditions that mimic extracellular signaling cues to guide the differentiation of embryonic stem cells (ESCs), or induced pluripotent stem cells (iPSC), to desired cell fates (Keller, 1995; Smith, 2001). Such studies have shown that mesodermal progenitors can be specified from human iPSCs in response to a range of signaling environments that mimic the

conditions within the primitive streak (Mendjan et al., 2014; Kattman et al., 2011; Mae et al., 2013). Cardiac and hematopoietic cell types are among the cell types that have been most well-studied using this approach (Kattman et al., 2010). More recently, three-dimensional models of embryonic development have been generated, termed gastruloids, formed by the aggregation of ESCs. These cultures exhibit spatiotemporal patterns of gene expression similar to those observed in embryos in vivo (Beccari et al., 2018; van den Brink et al., 2014). The advent of gastruloid cultures will allow for key aspects of mammalian development that are not recapitulated in 2-dimensional culture models to be better studied, including formation of the germ layers, axial organization, and somite segmentation (van den Brink, et al., 2014; Turner et al., 2017; Beccari et al., 2018).

Extra-embryonic membranes

The development of the mouse embryo is supported by a number of extra-embryonic membranes (Figure 10), each of which is composed of mesoderm specified in the posterior-most region of the primitive streak. These tissues provide a means of delivering nutrients and removing waste during the early stages of embryonic development, and consist of the amnion, the allantois, the chorion, and the visceral yolk sac. The innermost of these membranes is the amnion, a fluid-filled sac in which the embryo develops.

The amnion is surrounded by the extra-embryonic yolk sac. After the germ layers are specified, at E7.5, the embryo is U-shaped with the ectoderm positioned on the inside and the endoderm facing outward. The definitive endoderm, specified during gastrulation, displaces the visceral endoderm as it migrates anteriorly to form the primitive gut tube. As a result, most cells of the visceral endoderm are displaced to the extra-embryonic yolk sac (Tam and Behringer, 1997; Thomas et al., 1998; Bielinska et al., 1999; Kwon et al., 2008). As development progresses to E8.5, the mouse embryo turns, thereby reversing this orientation with the endodermal layer facing inward and the ectoderm is positioned

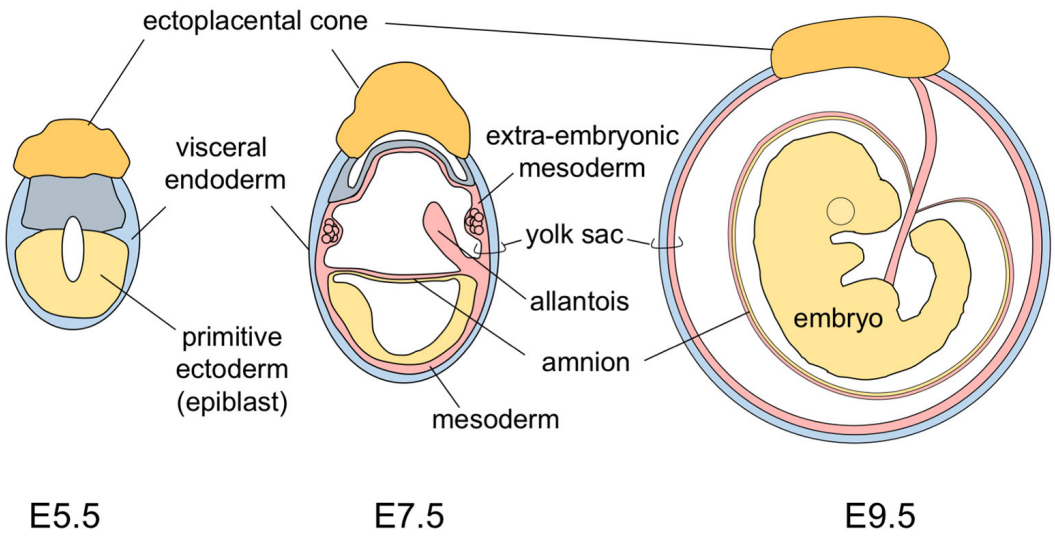


Figure 10. Extra-embryonic membranes associated with murine development. Extra-embryonic membranes at E5.5, E7.5, and E9.5. Figure reproduced with permission (Yamane, 2018).

outward by E9.5 (Figure 11). Embryonic turning distinguishes the mouse embryo from those of other vertebrate species, wherein gastrulation results in the germ layers being oriented such that the ectoderm faces outward and the endoderm inward as these layers are specified and turning is not required. Due to embryonic turning, the murine yolk sac envelops the embryo. This also differs from other vertebrates in which the yolk sac is attached to, but does not surround, the developing embryo. The yolk sac is composed of both mesodermal derivative and visceral endoderm derived from the epiblast prior to gastrulation. Within the mesodermal layer, extra-embryonic vasculature develops, allowing the yolk sac to serve as a means of nutrient and waste exchange while also providing an additional layer of protection to the developing conceptus.

The chorioallantoic placenta is required to maintain the exchange of nutrients and gases during fetal development, and forms at E10.5 through the fusion the allantois and the chorion. The allantois is first visible in the proximal region of the posterior embryo at E7.5, budding from the posterior embryo and extending through the exocoelomic cavity toward the chorion. The chorion is composed of a

trophectoderm-derived outer layer and an inner layer of extra-embryonic mesoderm (Downs and Bertler, 2000; Tam and Beddington, 1987; Gardner, 1983; Kinder et al., 1999; Lawson et al., 1991). Through cell proliferation and the addition of progenitors from the primitive streak, the allantois makes contact with the mesodermal layer of the chorion at E8.5, at which point these two structures fuse to form the chorioallantoic placenta (Figure 12). Once fusion occurs, epithelial cells within the allantois form a vascular plexus that joins with the developing yolk sac vasculature, creating the umbilical vessels (Inman and Downs, 2006; 2007; Downs et al., 1998).

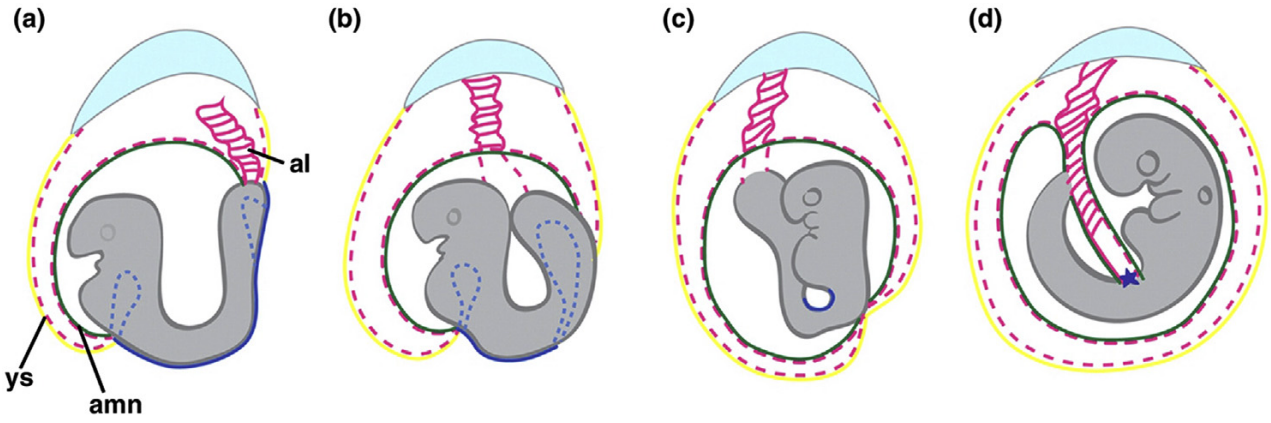


Figure 11. Embryonic turning and positioning of the yolk sac. At E8.5, the mouse embryo undergoes axial turning, which is complete by E9.5. This results in the embryo being encased by the amnion and yolk sac, unlike other vertebrate species in which the yolk sac is attached to, but does not envelop, the embryo. Abbreviations: amn, amnion; ys, yolk sac. Figure reproduced with permission (Gavrilov and Lacy, 2013).

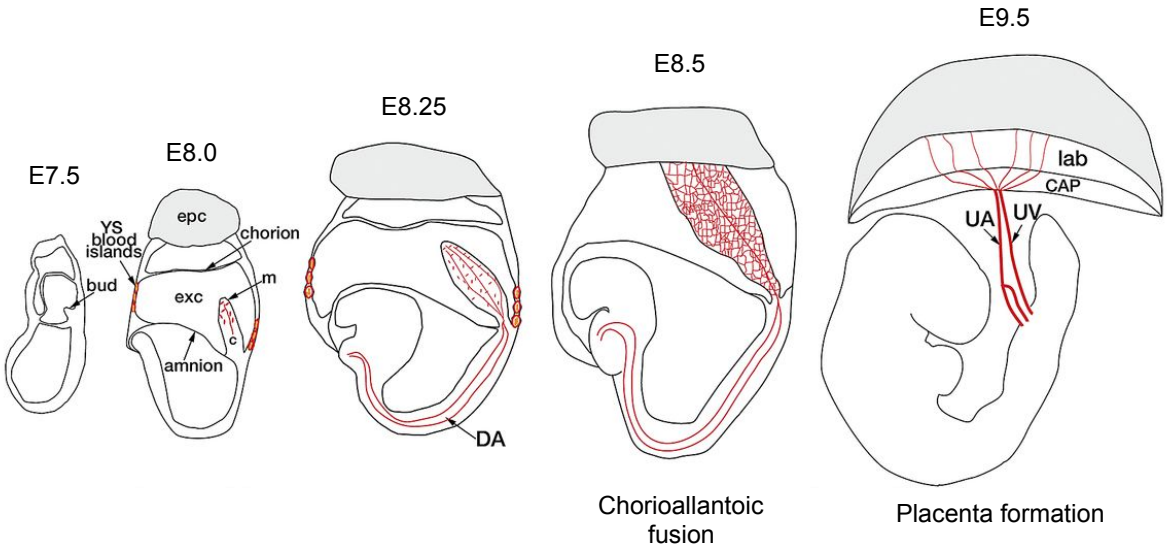


Figure 12. Chorioallantoic fusion and formation of the placenta. At E7.5, the allantois begins to bud from the extra-embryonic mesoderm. The allantois extends into the exocoelomic cavity through a combination of cell proliferation and the addition of progenitors form the primitive streak. At E8.5, and allantois fuses with the chorion while the vascular plexus within joins with the developing yolk sac vasculature to form the umbilical vessels. Figure reproduced with permission (Arora et al., 2012).

In rodents, the yolk sac is composed of two membranes, the inner visceral yolk sac and the outer parietal yolk derived from the primitive endoderm. The visceral yolk sac develops at E7.5, and consists of a layer of extra-embryonic mesoderm, specified in the posterior region of the primitive streak, which lies adjacent to a layer of visceral endoderm, derived from the primitive endoderm and specified prior to gastrulation. Each layer has unique functions, with the mesodermal layer of the visceral yolk sac being the first site of embryonic hematopoiesis, known as primitive hematopoiesis. Hematopoietic progenitors are derived from a population of *Mesp1*$^{+}$ mesoderm specified in the posterior primitive streak at the onset of gastrulation. In the yolk sac, these progenitors form a population of bi-potential precursors, known as hemangioblasts that migrate from the streak to colonise the yolk sac, forming aggregates known as blood islands before differentiating to both primitive erythrocytes and vascular endothelium.

Adjacent to the mesodermal layer of the visceral yolk sac lies a layer of visceral endoderm, which maintains the exchange of nutrients and wastes, facilitated by its proximity to the underlying mesodermal vasculature. Through this function, the visceral endoderm sustains the conceptus until the formation of the chorioallantoic placenta at E10.5 (Casanova and Grabel, 1988; Hogan and Tilly, 1981; Hogan et al., 1994; Boucher and Pedersen, 1996; Cross et al., 1994).

The epithelial cells that compose the visceral endoderm are functionally and morphologically similar to the epithelial lining of the intestine, as both contain microvilli and vesicles required for nutrient uptake (Bielinska et al., 1999). Further, the visceral endoderm also produces a number of plasma proteins, and is transcriptionally similar to the adult liver (Bielinska et al., 1999; Cindrova-Davies et al., 2017). The delivery of nutrients and removal of waste by the visceral endoderm is essential for embryonic development, as disruption of this tissue by chemical injection, or through use of visceral endoderm-targeted antibodies, has teratogenic effects in rodents (Brent et al., 1990; Jollie et al., 1990; Lloyd et al., 1990). In addition, the deletion of genes involved in nutrient transport in the visceral endoderm leads to embryonic lethality by E10.5 (Farese et al., 1995; Copp, 1995).

In addition to maintaining the transport of nutrients and waste, the visceral endoderm also produces inductive signals required for lineage specification, differentiation, and patterning in both the yolk sac mesoderm and the embryo proper (Belaoussoff et al., 1998; Thomas and Beddington, 1996). For example, signaling by Indian hedgehog (Ihh) and vascular endothelial growth factor (Vegf) originating in the visceral endoderm is required for vascularization within the underlying yolk sac mesoderm (Damert et al., 2002).

Primitive hematopoiesis

Hematopoietic progenitors are specified in the posterior primitive streak before they migrate extra-embryonically to populate the yolk sac (Ferkowicz et al., 2003; Huber et al., 2004; Li et al.,

2005). The first wave of embryonic hematopoiesis, primitive hematopoiesis, begins in the extra-embryonic yolk sac at E7.5, with the appearance of blood islands by E8.5 (Figure 13; Haar and Ackerman, 1971; Silver and Palis, 1997; Palis et al., 1995). Blood islands are composed of progenitor cells that form both the first vascular endothelium within the yolk sac and primitive blood. Those cells that will contribute to the vasculature are located more peripherally within progenitor cell clusters, while those fated to primitive blood are positioned more centrally, located within the lumen of developing endothelial tubes (Ferkowicz and Yoder, 2005). A number of studies suggest that both cell types are derived from a common precursor, the hemangioblast (Sabin, 1920; Choi et al., 1998; Nishikawa et al., 1998; Lu et al., 2006; Kennedy et al., 2007). The existence of the hemangioblast, however, has been the subject of considerable debate, with work by others suggesting instead that hematopoietic and endothelial lineages are distinct, derived from separate mesodermal populations specified in the primitive streak (Kinder et al., 1999; Lawson et al., 1991; Furuta et al., 2006; Vogeli et al., 2006; Ferkowicz and Yoder, 2005; Jones et al., 2006).

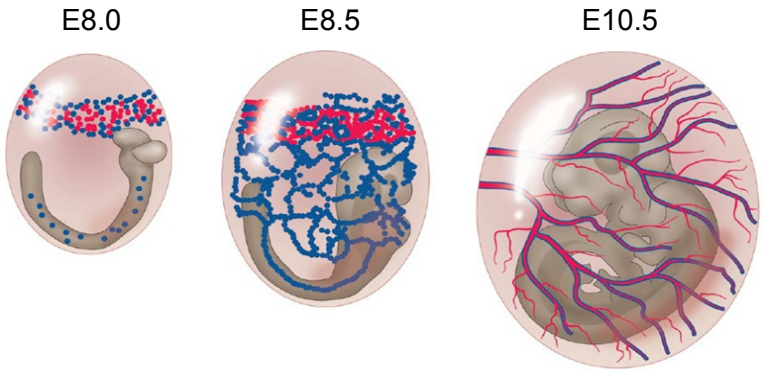


Figure 13. Mouse primitive hematopoiesis. Primitive hematopoiesis begins in the extra-embryonic yolk sac at approximately E7.5 with the formation of blood islands, which become visible by E8.5 and form a band-like structure across the yolk sac. Blood islands contain bi-potential progenitors, known as hemangioblasts, which give rise to both primitive erythrocytes and the yolk sac vasculature. These progenitors give rise to both the vascular plexus and primitive blood by E8.5, and sustain the embryo

until the second wave of hematopoiesis, definitive hematopoiesis, is induced in the embryo proper at E10.5. Figure reproduced with permission (Jones et al., 2006).

Whether distinct progenitors for each lineage exist, or whether they are derived from a common bi-potential precursor, both the vascular endothelium and primitive erythrocytes emerge from blood islands in parallel, becoming visible within the yolk sac by E8.5 (Padron-Barthe et al., 2014; Murray, 1932; Choi et al., 1998). Endothelial cells within the yolk sac form the vascular plexus, which then expands into a larger a capillary network with a honeycomb-like appearance (Jones et al., 2006). The resulting vasculature is thought to be lined with hemogenic endothelium, which buds from the vessel walls and into the lumen and differentiates to form primitive blood (Figure 14; Bertrand et al., 2010; Boisset et al., 2010; Chen et al., 2009; Eilken et al., 2009; Kissa and Herbomel, 2010; Zovein et al., 2008; Lancrin et al., 2009; Dieterlen-Lievre, 1998; Org et al., 2015). Primitive hematopoiesis progresses within the yolk sac until approximately E10.5, at which point a second wave of hematopoiesis, known as definitive hematopoiesis, is initiated across multiple sites within the embryo proper. Such sites include

the fetal liver, spleen, bone marrow, and aorta-gonad-mesonephros (AGM; Figure 15; Moore and Metcalf, 1970; Johnson and Moore, 1975; Medvinsky and Dzierzak, 1996).

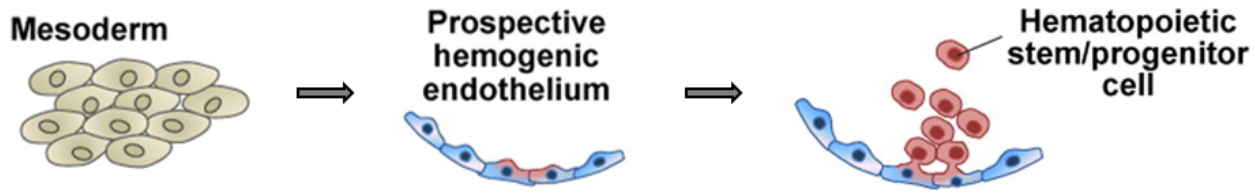


Figure 14. Hemogenic endothelium lines the yolk sac vasculature. Some studies suggest that the yolk sac vasculature is lined by hemogenic endothelium. These endothelial cells are thought to be capable of budding into the lumen from the vessel while differentiating to hematopoietic lineages. Figure adapted with permission (Van Handel et al., 2012).

Transcriptional regulation of primitive hematopoiesis

Hematopoietic progenitors reside within *Mesp1*$^{+}$ mesoderm, specified around E6.5-E7.5 in the posterior primitive streak, and egress soon after extra-embryonic mesoderm is specified (Saga et al., 1996; Saga et al., 1999; Bondue et al., 2008). In addition to hematopoietic mesoderm, progenitors for cardiac mesoderm, vascular endothelium, and precursors to skeletal muscle are also contained within the *Mesp1*$^{+}$ population (Chan et al., 2013). At E7.5, both hematopoietic and cardiac progenitors express the cell surface receptor *Flk1*, otherwise referred to as *Kdr* or *Vegfr2* (Ishitobi et al., 2011; Fehling et al., 2003; Huber et al., 2004; Iida et al., 2005; Kattman et al., 2006). *Flk1* expression is maintained in endothelial progenitors at later stages of differentiation, but is extinguished in hematopoietic and cardiac lineages (Figure 16; Yamaguchi et al., 1993; Kattman et al., 2006; Moretti et al., 2006; Ishitobi et al., 2011).

Hematopoietic progenitors express the helix-loop-helix transcription factor *Scl/Tal-1*, which is first detected in the yolk sac at approximately E8.5 (Shivdasani et al., 1995; Visvader et al., 1998). *Scl/Tal-1* is a master regulator of primitive hematopoiesis, inducing the expression of many downstream transcription factors, including *Runx1*, *Gata1*, *Gata2*, *Hhex* and *Hey2*, among others (Robb et al., 1995; Van Handel et al., 2012; Org et al., 2015). *Scl/Tal-1* expression is required within *Flk1*$^{+}$ precursors for primitive hematopoiesis, as *Scl/Tal-1*$^{-/-}$ mutants lack primitive blood and are lethal between E8.5 and E10.5 (Van Handel et al., 2012; Shivdasani et al., 1995).

In addition to positively regulating the expression of hematopoietic targets, *Scl/Tal-1* is also required to repress cardiogenic gene expression in *Mesp1*$^{+}$ mesoderm destined to become blood (Van Handel et al., 2012; Org et al., 2015). *Scl/Tal-1* does so by binding to epigenetically primed enhancers associated with cardiac gene expression thereby depleting cardiac enhancers of epigenetic marks associated with gene activation (Org et al., 2015). Cardiac genes repressed by *Scl/Tal-1* include the cardiac transcription factors *Gata4, Gata6*, *Hand1*, *Mixl1*, and *Tbx5* (Org et al., 2015). Consistent with

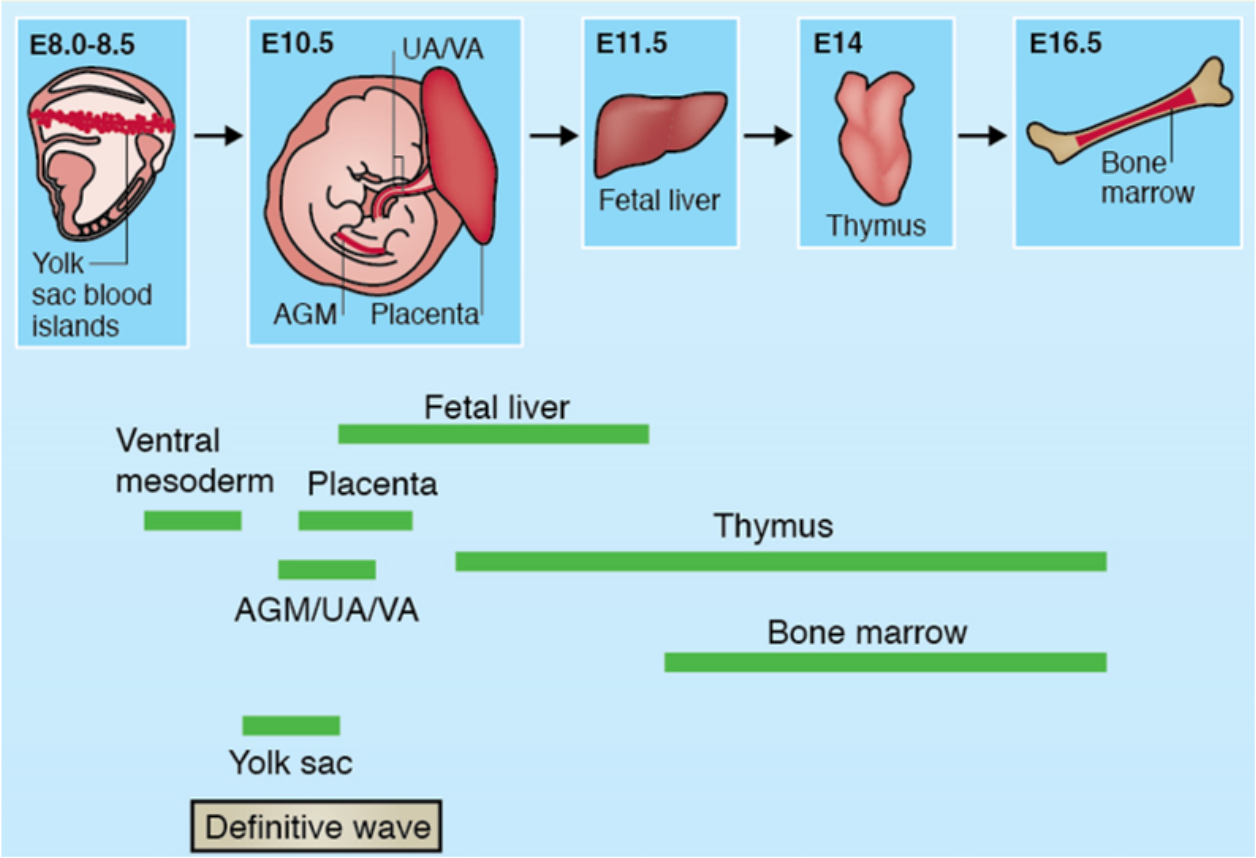


Figure 15. Transition from primitive to definitive hematopoiesis. The first wave of embryonic hematopoiesis takes place in the extra-embryonic yolk sac with the formation of blood islands. Once the vasculature has formed, these primitive erythrocytes colonize other developing organs in which hematopoiesis continues. At E10.5, the aorta-gonad-mesonephros (AGM), the placenta, the umbilical artery, and the vitelline artery induce hematopoietic precursors that, along with yolk sac-derived hematopoietic progenitors, colonize the fetal liver at E11.5. Here, these progenitors cells mature and/or expand, before colonizing the thymus at E14.0 and the bone marrow at E16.5, the latter serving the main hematopoietic niche in adults. Figure adapted with permission (Jagannathan-Bogdan and Zon, 2013).

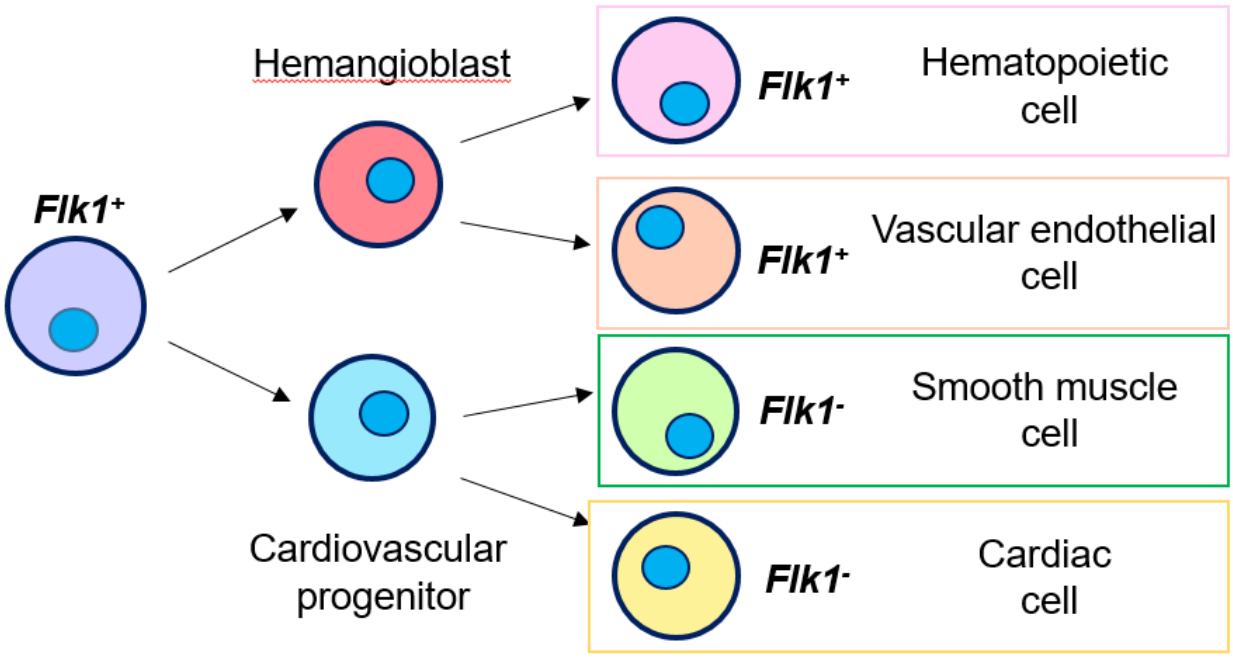


Figure 16. Flk1 expression in mesodermal lineages. Hemangioblasts and cardiovascular progenitors are derived from mesodermal precursors that express Flk1. Flk1 expression is maintained in hematopoietic and vascular endothelial lineages derived from hemangioblasts, while downregulated in smooth muscle and cardiac cells during their differentiation from cardiovascular progenitor cells. Figure adapted with permission (Ishitobi et al., 2011).

this, yolk sac explant cultures deficient for *Scl/Tal-1* not only fail to generate vasculature and primitive blood, but also ectopically express cardiogenic transcripts, including *cTnT*, a marker of cardiomyocytes involved in cell contraction, and are capable of spontaneously generating synchronously beating cell colonies (Org et al., 2015).

Cardiogenesis

In addition to their close functional relationship, cardiac and hematopoietic progenitors are derived from a common *Mesp1*$^{+}$ mesodermal precursor specified in the posterior region of the streak as noted above. Those cells fated to give rise to cardiac mesoderm are specified in response to high levels of Wnt and Bmp signaling at E6.5 followed by Wnt inhibition as cardiac mesoderm egresses from the streak and migrates anterolaterally to the anterior region of the embryo (Saga et al., 1996; Saga et al., 1999; Bondue et al., 2008; Chan 2013). Once specified, cardiac progenitors express the cell surface marker *Flk1* in addition to platelet derived growth factor receptor α (*Pdgfr-α*), allowing this lineage to be distinguished from the hemato-endodethelial lineage, which expresses *Flk1* but not *Pdgfr-α* (Kattman et al., 2011).

Once cardiac progenitors reach the anterior embryo, they form two progenitor populations known as the first and second heart fields (FHF and SHF, respectively; Tam and Schoenwolf, 1999; Xin et al., 2013). At approximately E7.5, the FHF and SHF form the cardiac crescent in the anterior embryo, which lies beneath the head folds (Figure 17). Cells of the first heart field express the cardiac marker *Tbx5* (Bruneau et al., 1999; Devine et al., 2014), absent from the SHF, while the SHF is marked by the expression of *Mef2c* (Verzi et al., 2005; Devine et al., 2014). While some consider these two populations to be distinct, it is possible that the FHF and SHF exist within one continuous population, exhibiting differential expression of cardiac markers in response to the changing environment within the streak as they are specified.

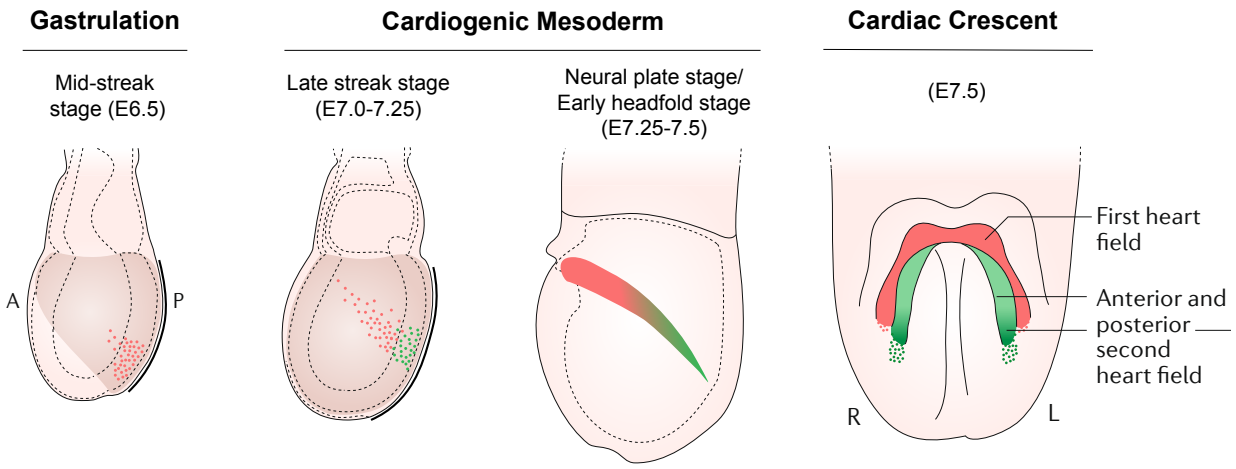


Figure 17. Cardiac progenitors migrate anterolaterally from the primitive streak. Cardiac progenitors migrate anterolaterally from the primitive streak to form the cardiac crescent in the anterior region of the embryo, beneath the head folds, by E7.5. A, anterior; P, posterior; R, right; L, left. Figure reproduced with permission (Meilhac and Buckingham, 2018).

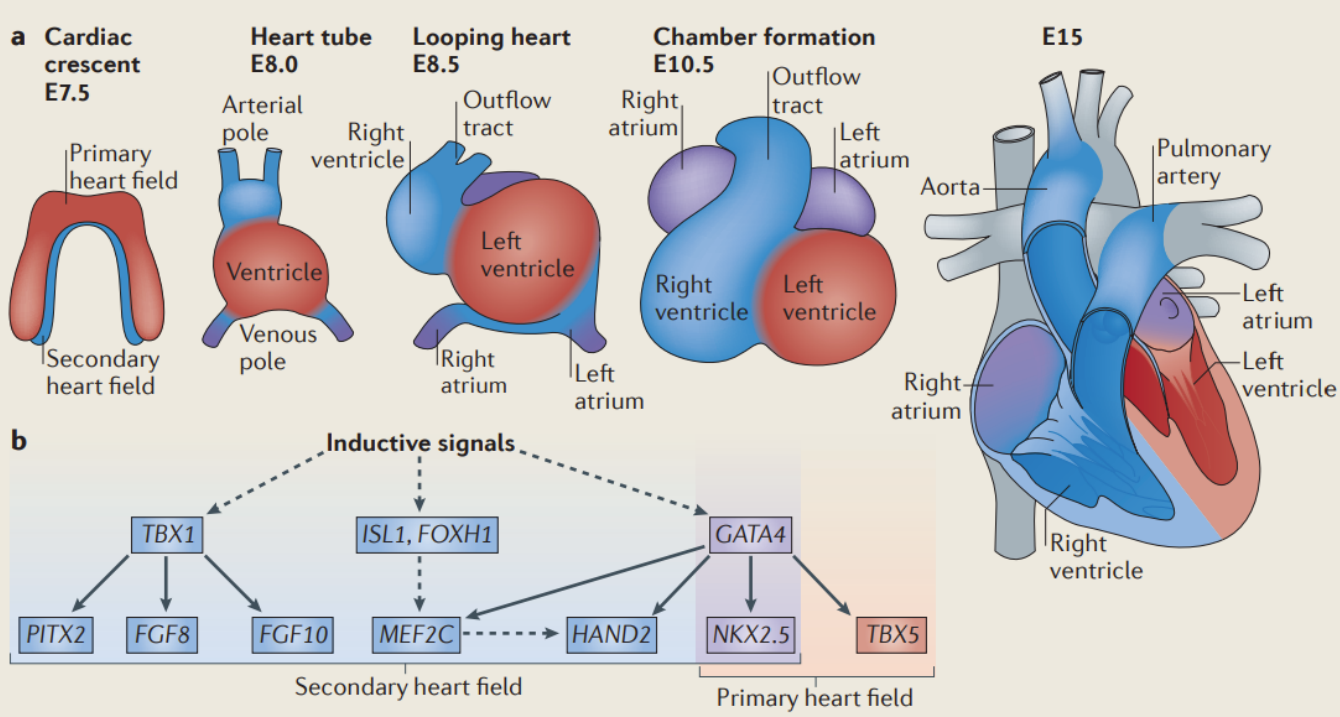


Figure 18. Transcriptional regulation of cardiac morphogenesis. A. Schematic of murine cardiac morphogenesis from E7.5 through to E15.0. The cardiac crescent contains the first (primary) and second (secondary) heart fields. At E8.5, the cardiac crescent fuses at the midline to form the primitive heart tube, which undergoes a series of looping events forming the cardiac chambers. The first heart field contributes to the left ventricle and the atria. The second heart field forms the right ventricle and the outflow tract. **B.** Cardiac morphogenesis is coordinated by a number of transcription factors. Those specific to cells of the first heart field are depicted in red, those of the second heart field are shown in blue, and factors expressed in both heart fields are shown in purple. Figure reproduced with permission (Xi et al., 2013).

At E8.5, cells of the FHF fuse at the midline to form the primitive heart tube which begins to contract while undergoing a series of looping events required to give rise to the cardiac chambers (Figure 18). Through this process, cells of the FHF will form the left ventricle and the atria, while cells of the SHF will give rise to the right ventricle and the outflow tract (Bruneau, 2013). Cardiac morphogenesis and heart looping are finely regulated processes, controlled by a network of transcription factors. Among these, *Tbx5* is first expressed in the FHF at E7.5, and persists in the right and left atria, left ventricle, and left ventricular septum (Bruneau et al., 1999). In humans, aberrant *Tbx5* expression and/or function is associated with Holt-Oram syndrome, characterized by deformities in the upper limbs and cardiac dysfunction. Similar developmental defects have been observed in murine models of *Tbx5* dysfunction, offering evidence for evolutionary conservation of Tbx5 function between these two species (Bruneau et al., 1999).

Within the cardiac mesoderm, the transcription factors *Mef2c* and *Isl1* are exclusively expressed in progenitors of the SHF (Lin et al., 1997; Cai et al., 2003). *Mef2c* expression in the SHF is necessary for cardiac morphogenesis, as mutants deficient for this factor develop only a single ventricle and display defects in both inflow and outflow tract morphogenesis (Buckingham et al., 2005; Lin et al., 1997; Dodou et al., 2004). While *Isl1* is expressed in the allantois, neural tube, and cardiac crescent of the developing embryo, its expression in the heart is also restricted to the SHF where it regulates the development of the right ventricle and outflow tract (Cai et al., 2003).

Nkx2-5 is one of the earliest cardiac markers, expressed in cardiac crescent, initiating at the same stage as *Tbx5* but detected in progenitors of both the FHF and SHF (Harvey, 1996; Lints et al., 1993; Redkar et al., 2001). Mutants lacking *Nkx2-5* expression display a broad range of cardiac defects, including defects in atrial septum formation, impaired outflow tract morphogenesis, poor ventricular trabeculation, and hypoplasia of the left heart. Together, these defects contribute to embryonic lethality at E9.5 (Lyons et al., 1995; Benson et al., 1999; Elliott et al., 2003; Schott et al., 1998; Gutierrez-

Roelens et al., 2002). In humans, *Nkx2-5* mutation leads to tetralogy of Fallot, a cardiac abnormality in which blood circulation to the lungs is deficient and suggesting some degree of evolutionary conservation for *Nkx2-5* function (Goldmuntz et al., 2001).

Also among cardiac transcription factors critical for heart morphogenesis are *Gata4*, *Hand1*, and *Hand2*. *Gata4* expression is induced in cardiac mesoderm as early at E7.5, at the cardiac crescent stage, and is subsequently maintained in both FHF and SHF populations where it, along with *Gata5* and *Gata6*, is required for cardiac development (Grepin et al., 1995; 1997; Narita et al., 1997; Gove et al., 1997; Charron et al., 1999; Gajewski et al., 1999; Reiter et al., 1999). *Gata4* is dispensable for cardiac lineage specification, however *Gata4* deficient mice are embryonic lethal at approximately E9.5 due to aberrant ventral morphogenesis leading to disruptions in heart tube formation (Kuo et al., 1997; Molentin et al., 1997). This is thought to result from *Gata4* function in the endoderm which lies adjacent to the LPM and regulates cardiac morphogenesis through the production of diffusible signals as well as through mechanical mechanisms (Narita et al., 1997; Varner and Taber, 2012).

Hand1 and *Hand2* are induced at the cardiac crescent and heart tube stages. *Hand1* expression is first detected in the developing heart at E8.5, while *Hand2* is strongly expressed within the SHF from E7.75 (Barnes et al., 2011). These transcripts are predominantly distributed in cardiac neural crest cells (cNCC), which migrate from the hindbrain region of the neural tube through the pharyngeal arches and into the developing heart tube where they populate the outflow tract, forming both the valves and arteries of the heart (Figure 19; Kirby and Waldo, 1990; 1995; Farell et al., 1999; Bronner, 2012; Etchevers et al., 2019; Yamagishi, 2020). *Hand1* and *Hand2* expression within cNCCs is induced once these cells reach the heart tube, suggesting a role in tissue patterning and differentiation rather than specification (Vincentz et al., 2008; Yutzey and Kirby, 2002; George and Firulli, 2019). Asymmetric expression of *Hand1* and *Hand2* is also essential for heart looping during cardiac morphogenesis (Xin et al., 2013; Srivastava et al., 2006). While *Hand1* is first expressed in the developing heart tube at

E8.5, it becomes more robust from E9.5-13.5 when it is restricted to the outer curvature of the left ventricle and the outflow tract (Barbosa et al., 2007; Barnes et al., 2010), while *Hand2* is observed in the right ventricle and the outflow tract. Like *Nkx2-5*, misexpression of *Hand1* has also been associated with tetralogy of Fallot, likely due to an interaction between *Hand1* and *Nkx2-5*/*Gata4* that is required for normal cardiac morphogenesis (Lu et al., 2016).

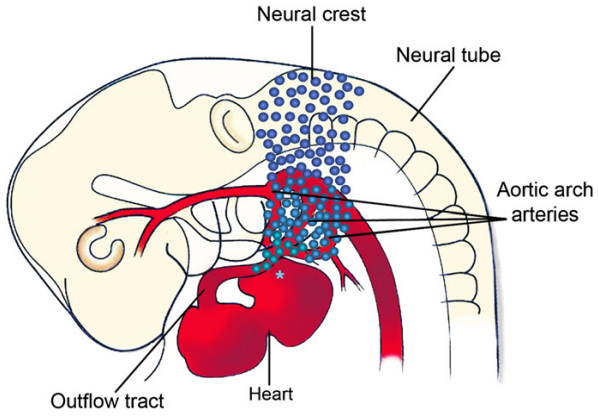


Figure 19. Cardiac neural crest cells. Cardiac neural crest cells (cNCCs) migrate from the neural tube through the pharyngeal arches and into the outflow tract, eventually contributing to cardiac valves and arteries. Figure reproduced with permission (Keyte and Hutson, 2012).

Cardiac morphogenesis is also dependent on inputs from non-mesodermal germ layers. As cardiac progenitors migrate to the anterior embryo, they remain in close contact with the endoderm, which produces signaling molecules that promote cardiac differentiation from within the mesoderm (Narita et al., 1997). The coordinated expression of cardiac transcription factors within the cardiac crescent is regulated, in part, by signaling from the AVE, which promotes cardiac differentiation via inhibition of Wnt signaling. Consistent with this, disruption of the AVE leads to cardiac defects in both frogs and newts (Jacobson, 1961; Nascone and Mercola, 1995; Gannon and Bader, 1995; Alexander et al., 1995). These observations are further supported by co-culture experiments that similarly

demonstrate a requirement for Nodal/Activin signaling from anterior endoderm cells during cardiac morphogenesis (Schultheiss et al., 1995; Yatskievych et al., 1997).

Sonic hedgehog (Shh), secreted by the endoderm rostral to the heart fields within the developing pharynx, is similarly required for cardiac morphogenesis. Shh signals through Patched (Ptc) receptors on the surface of cardiac progenitors within the second heart field. In the presence of Shh ligand, proliferation within this population is inhibited and the appropriate number of cells within the second heart field is maintained. In the absence of Shh signaling, over-proliferation by cells of the second heart field leads to cardiac defects that include abnormalities associated with the arterial pole and aortic arch arteries (Dyer et al., 2009). RA similarly restricts the cardiac progenitor pool (Keegan et al., 2005; Waxman et al., 2008), and is required for heart looping (Heine et al., 1985; Dersch and Zile, 1993; Dickman and Smith, 1996; Wasiak and Lohnes, 1999). Together, these observations demonstrate the importance of signaling molecules from non-mesodermal germ layers during the formation of the heart and their impact on the expression of cardiogenic transcription factors.

In addition to the vast network of transcription factors, the embryonic heart also requires input from hemodynamic forces produced by blood flow for its development. The heart tube begins to contract as soon as it is formed, initiating blood flow through the developing vasculature. Dynamic blood flow produces shear stress within the lumen of the heart tube, which varies in response to changes in the heart tube shape and size, as well as increasing amounts of blood volume and pressure during development (Andres-Delgado and Mercader, 2016; Haack and Abdelilah-Seyfried, 2016). These changes in blood flow are detected by mechanosensors within cardiac cells in the heart tube, and result in the initiation of regulatory responses by downstream signaling cascades that impact cardiac development (Andres-Delgado and Mercader, 2016; Haack and Abdelilah-Seyfried, 2016). Thus, in mutant embryos lacking blood, decreased hemodynamic forces result in cardiac abnormalities, as these signaling cascades are not induced. Such defects include abnormalities in endocardial cell migration

and proliferation, as well as aberrant cardiac valve formation, and appear well before the embryo is dependent on the circulatory system for oxygen and nutrient delivery (Haack and Abdelilah-Seyfried, 2016; Heckel et al., 2015; Koefoed et al., 2014; Midgett and Rugonyi, 2014; Midgett et al., 2017; Hove et al., 2003; Kowalski et al., 2014; Hogers et al., 1999; Hahn and Schwartz, 2009). For instance, mice deficient in *Scl/Tal-1*, which lack primitive blood, display distended pericardial sacs at E9.5 coupled with endocardial defects resulting from impaired migration of these cells (Shivdasani et al., 1995; Bussman et al., 2007; Schumacher et al., 2013).

Cdx transcription factors in the early embryo

Cdx homeobox genes encode transcription factors that are involved in development of the posterior embryo, with the first member of this gene family, *caudal*, having been identified in Drosophila (Mlodzik et al., 1985; Mlodzik and Gehring, 1987; Macdonald and Struhl, 1986; Mlodzik et al., 1990). *Drosophila* c*audal* expression is first induced after fertilization in the *Drosophila* embryo, forming an AP gradient that increases in concentration toward the posterior region of the embryo (Macdonald and Struhl, 1986). As development progresses, *caudal* expression is gradually lost from the anterior embryo, becoming restricted to the posterior pole (Macdonald and Struhl, 1986). *Drosophila* embryos void of *caudal* expression display impairments in gastrulation, AP segment patterning defects, and lack the hindgut, demonstrating its critical role in these processes (Macdonald and Struhl, 1986; Wu and Lengyel, 1998).

Caudal factors are evolutionarily conserved, with three orthologs, *Cdx1*, *Cdx2*, and *Cdx4,* identified in mice (Duprey et al., 1988; James and Kazenwadel, 1991; Gamer and Wright, 1993), *Xcad1*, *Xcad2* and *Xcad3* in *Xenopus* (Blumberg et al., 1991; Northrop and Kimelman, 1994), *cdx1a*, *cdx1b,* and *cdx4* in zebrafish (Davidson et al., 2003; Mulley et al., 2006; Shimizu et al., 2005; 2006; Davidson and Zon, 2006), and *CHox-cad* in chicken (Frumkin et al., 1991). In each of these vertebrate

species, caudal-like members are involved in anteroposterior patterning and are required for the development of the posterior embryo (Van den Akker et al., 2002; Davidson et al., 2003; Lohnes, 2003; Chawengasksophak et al., 2004; Van Nes et al., 2005; Shimizu et al., 2005; 2006; Davidson and Zon, 2006). Cdx functions were initially thought to be mediated primarily by regulation of downstream Hox activity, however more recent work has challenged this paradigm, demonstrating that Cdx also regulates a number of developmental processes through non-Hox targets (Savory et al., 2009a; Savory et al., 2011; Nguyen et al., 2017; Brooke-Bisschop et al., 2017; Foley et al., 2019; Davidson et al., 2003; Davidson and Zon, 2006; Amin et al., 2016).

In the embryo proper, Cdx genes are sequentially activated in the caudal embryo, beginning at the primitive streak stage where they form a nested pattern of expression in all three germ layers (Figure 20; Lohnes, 2003). *Cdx1* is first expressed at E7.5 in the primitive streak. As development progresses, *Cdx1* expression extends along the length of the posterior embryo, with the anterior boundary at the posterior hindbrain (Meyer and Gruss, 1993). *Cdx1* transcripts are expressed in the neural tube, somites, and forelimb buds until E12.5, at which point expression is extinguished with the exception of the endoderm, where *Cdx1* persists in the resulting gut tube and subsequently in the intestinal epithelium throughout adulthood (Duprey et al., 1998).

Cdx1 acts as a posteriorizing factor during vertebral patterning, with *Cdx1*$^{-/-}$ mutants displaying anterior transformations of the cervical and thoracic vertebrae resulting from a posterior shift in *Hox* gene expression (Figure 21; Subramanian et al., 1995). In these mutants, the first cervical vertebra (C1) is fused to the occipital bone, while the second cervical vertebra (C2) displays morphological features of C1, and the third cervical vertebra (C3) takes on the appearance of C2 (Isaacs et al., 1998; van den Akker, 2002; Deschamps et al., 1999; Lohnes, 2003; Subramanian et al., 1995). These patterning defects extend to the thoracic vertebrae, however the lumbar and caudal vertebrae remain unaffected.

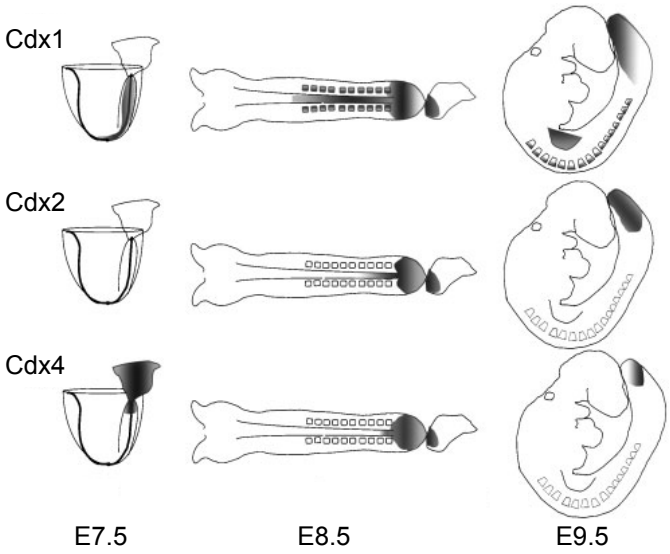


Figure 20. Nested Cdx expression in the early embryo. Cdx1 expression is induced in all three germ layers of the primitive streak beginning at E7.5, and persists in the somites, tail bud, and forelimb bud at later developmental stages. Cdx2 is also expressed in the tail bud, with early studies indicating an onset of expression at E8.5. Cdx4 is expressed at E7.5 in the allantois, and is maintained in the tail bud where its expression is much more spatially restricted at E9.5 compared to the other Cdx family members. Figure reproduced with permission (Lohnes, 2003).

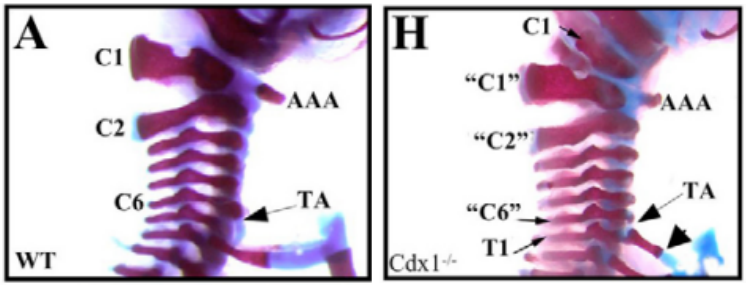


Figure 21. Anterior homeotic transformations in *Cdx1*$^{-/-}$ mutants. Staining of whole mount skeletal preparations from wild type and *Cdx1*$^{-/-}$ mutants were stained for bone (Alizarin red) and cartilage (Alcian blue), revealing anterior transformations in the cervical vertebrae. Anterior transformation of C1, C3, and C7 are indicated by "C1", "C2", and "C6", respectively, with C1 fused to the basoccipital bone in *Cdx1* mutants. C1-C7, cervical vertebrae; T1, first thoracic vertebra; AAA, anterior arch of the atlas (atlas also known as C1); TA, tuberculum anterior; C, cervical vertebrae; TA, tuberculum anterior. Figure reproduced with permission (Pilon et al., 2007).

Apart from these transformations, *Cdx1*-null mutants are phenotypically normal and produce viable offspring (Subramanian et al., 1995).

Cdx2 expression is first detected in the extra-embryonic TE at E3.5 where it is required for trophoblast development (Beck et al., 1995; Chawengsaksophak et al., 2004). Initially, *Cdx2* is uniformly expressed at low levels throughout the early embryo, but becomes restricted to the trophoblast lineage at the 8-cell stage where it represses the expression of ICM-associated transcripts such as *Nanog* and *Oct4* (Ralston and Rossant, 2008; Johnson et al., 1981; Strumpf et al., 2005; Niwa et al., 2005; Tolkunova et al., 2006; Ralston and Rossant, 2008; Yamanaka et al., 2006; Beck et al., 1995; van den Akker et al., 2002). *Cdx2* expression in the TE is required for implantation, with germ-line *Cdx2* deletion resulting in peri-implantation lethality (Beck et al., 1995; Strumpf et al., 2005; Chawengsaksophak et al., 2004).

In the embryo proper, *Cdx2* expression was previously thought to initiate at E8.5 (Beck et al., 1995; Lohnes, 2003; Rayon et al., 2016). Recent studies, however, have detected Cdx2 protein and mRNA within the primitive streak at earlier developmental stages (Foley et al., 2019; Amin et al., 2016). After gastrulation, *Cdx2* expression persists in the tail bud, posterior gut tube, and neural tube until E12.5 (Lohnes, 2003). Like *Cdx1*, *Cdx2* expression is extinguished at E12.5 in all tissues but the posterior endoderm, persisting in the adult intestinal epithelium where it is essential for homeostasis throughout life. $Cdx2^{+/-}$ mutants are viable and produce fertile offspring, yet display anterior homeotic transformations to the posterior cervical and anterior thoracic vertebrae (Chawengsaksophak et al., 1997). While these defects are reminiscent of those described $Cdx1^{-/-}$ embryos, they extend more posteriorly, reflective of the differential patterns of expression for *Cdx1* and *Cdx2* (Lohnes, 2003).

Cdx4 expression is initiated in the posterior embryo at E7.5, with a much more spatially restricted pattern of expression compared to the other two family members (Gamer and Wright, 1993; Lohnes, 2003). At later developmental stages, *Cdx4* is expressed within the neural ectoderm and in the

unsegmented paraxial mesoderm, with its rostral expression boundary marked by the most recently formed somite (Gamer and Wright, 1993). *Cdx4*$^{-/-}$ mutants exhibit no overt phenotypes, however loss of Cdx4 in combination with mutated alleles of Cdx1 or Cdx2 exacerbates phenotypes associated with single mutants for either gene (Faas and Isaacs, 2009; Savory et al., 2011; Van den Akker et al., 2002; van Nes et al., 2006; Young et al., 2009). These phenotypes include impaired axial elongation coupled with stunted allantoic outgrowth in *Cdx2*$^{+/-}$*Cdx4*$^{-/-}$ mutants, resulting in failed chorioallantoic fusion and subsequent embryonic lethality by E10.5 (Chawengsaksophak et al., 2004; van de Ven et al., 2011; van Nes et al., 2006; Savory et al., 2009a; van den Akker et al., 2002) providing further support for functional overlap among family members.

Cdx factors in the intestine

Expression of *Cdx1* and *Cdx2* are maintained in the adult intestinal epithelium, which is derived from the endoderm. The small intestine consists of three segments, the duodenum, jejunum, and ileum (Figure 22). The ileum attaches to the cecum, a small pouch that demarcates the transition from the small intestine to the large intestine, also known as the colon. Columnar epithelial cells line the lumen of the small intestine, forming structures known as crypts and villi, while the epithelial lining of the colon forms only crypts.

Crypts are invaginations that form at the base of the intestinal epithelium, while villi are finger-like protrusions that extend from the crypts into the lumen of the intestine, and facilitate nutrient absorption (Figure 23). Epithelial cells in the small intestine are continuously sloughed from the tip of the villi into the lumen, resulting in a high rate of cellular turnover. To maintain homeostasis, the intestinal epithelium self-renews, with intestinal stem cells in the base of the crypts proliferating and differentiating to replace cells that are continuously lost from the villi. As they differentiate, the stem transit amplifying (TA) cells. TA cells give rise to goblet cells, which secrete mucous into the intestinal

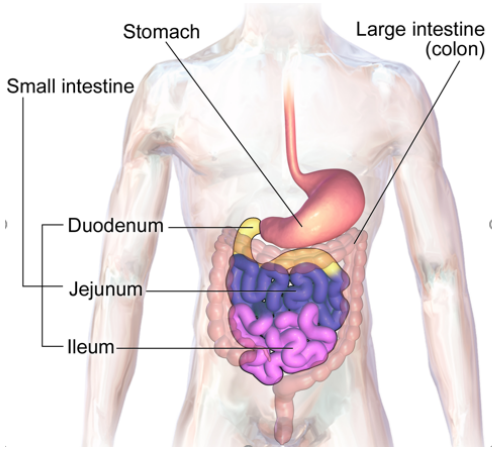


Figure 22. The segments of the adult intestine. The intestinal tract is composed of the small intestine and the large intestine, or colon. The small intestine is composed of three segments, the duodenum, jejunum, and ileum. The ileum attaches to the cecum, a small pouch that transitions the small intestine to the colon. Figure reproduced with permission (Blaussen.com staff, 2014).

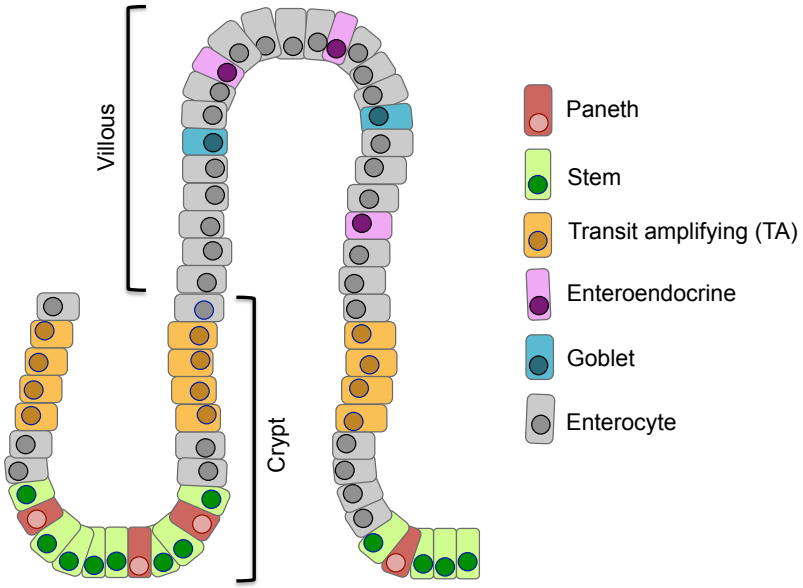


Figure 23. Crypt-villus axis of the small intestine. Intestinal stem cells (green) reside in the base of the crypts. In response to high cell turnover, stem cells differentiate to Transit Amplifying (TA; yellow) cells, which then differentiate further to generate enterocytes (grey), goblet cells (blue), enteroendocrine cells (purple) and Paneth cells (red). Enterocytes, goblet cells, and enteroendocrine cells types continue to migrate apically, populating the villi, while Paneth cells return to the base of the crypts where they maintain the stem cell niche.

lumen, absorptive enterocytes, required for nutrient uptake, enteroendocrine cells, required for hormone production, and Paneth cells, which serve to protect against microbes and to support the stem cell niche. Once specified, goblet cells, enterocytes, and enteroendocrine cells migrate apically to the tips of the villi, while Paneth cells return to the base of the crypts where they reside (Clevers and Bevins, 2013). This process is continuous and results in cellular turnover every 5-6 days within the villi, and every 30 days within the crypts (Lipkin, 1985).

In the intestine, *Cdx1* and *Cdx2* have distinct, yet overlapping, patterns of expression (Figure 24). *Cdx1* expression is graded along the length of the intestine, becoming highest in the distal colon, while *Cdx2* expression is highest in the cecum and proximal colon, decreasing both anteriorly and posteriorly. Cdx1 is also differentially expressed along the crypt-villus axis of the intestinal epithelium, being most abundant in the crypts of both the small intestine and the colon and decreasing along the apicobasal axis (Figure 25). Cdx2 is uniformly expressed but differentially phosphorylated along this axis, with phospho-Cdx2 levels highest in the base of the crypts (Guo et al., 2004). This phosphorylation occurs in the N-terminal transactivation domain and is thought to impact transcriptional activation (Trinh et al., 1999; Rings et al., 2001).

Cdx2 is required to maintain homeostasis and patterning in both the small intestine and the colon. *Cdx2*$^{+/-}$ mice develop lesions in the colon that are void of *Cdx2* expression and contain markers of esophageal and gastric cell types, indicating that Cdx2 imposes posterior identity in the intestine (Chawengsaksophak et al., 1997; Beck et al., 1999; 2003). Similar observations have been made in zebrafish, indicating evolutionarily conserved roles for Cdx in the intestine (Chen et al., 1009; Flores et al., 2008; Faas and Isaacs, 2009).

Conditional homozygous *Cdx2* deletion (see also below) produces an anterior transformation of the epithelial lining within the small intestine. When induced in the early definitive endoderm, the intestinal epithelium adopts an esophageal fate (Gao et al., 2009), while deletion at later developmental

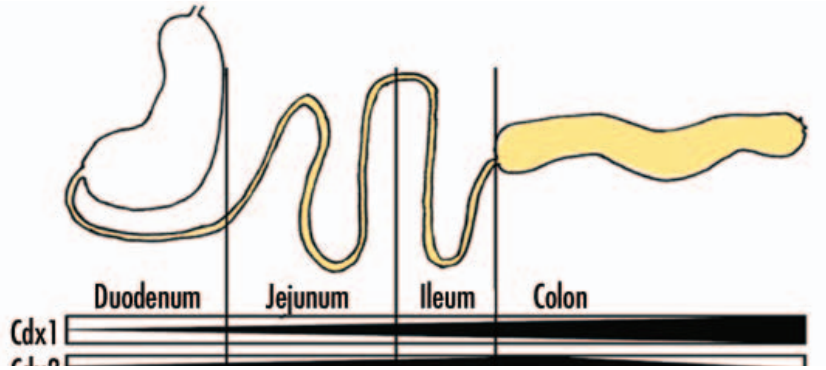


Figure 24. Cdx expression along the anteroposterior axis of the intestine. The small intestine is composed of the duodenum, jejunum, ileum, and is separated from the colon by the cecum. Cdx1 expression increases posteriorly along the AP axis of the intestine, reaching maximal expression in the distal colon. Cdx2 expression increases along the AP axis of the small intestine, reaching its highest expression in the cecum before decreasing in the distal colon. Black shading within rectangles indicates the level of expression. Figure reproduced with permission (Guo et al., 2004).

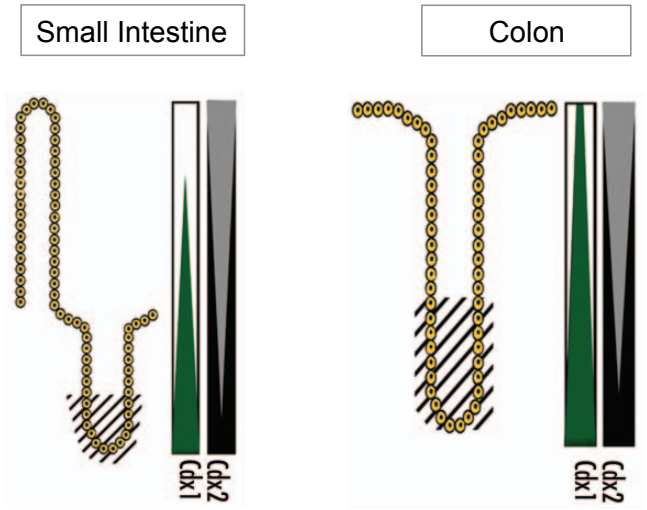


Figure 25. Cdx expression along the crypt-villus axis. In both the small intestine and colon, Cdx1 expression is highest in the base of the crypts, and decreases toward to the tip of the villi in the small intestine as indicated by the green triangles. Cdx2 is uniformly expressed along the crypt-villous axis, but is differentially phosphorylated on Ser-60 with phospho-Cdx2 highest away from the base of the crypts in both the small intestine and the colon, as indicated by the grey triangles. Figure reproduced with permission (Guo et al., 2004).

stages in the intestinal epithelium, both alone and in a *Cdx1*$^{-/-}$ background, results in the ectopic expression of gastric markers in the small intestine accompanied by aberrant villous morphology, with lethality at P0 (Grainger et al., 2010). *Cdx2* depletion in adults results in similar phenotypic changes, including ectopic expression of gastric markers, loss of enterocyte apicobasal polarity, aberrant villus morphology, and disruption of both the TA and stem cell compartments (Hryniuk et al. 2012; Gao et al. 2010; Simmini et al., 2014). Together, these morphological changes lead to poor nutrient absorption and the subsequent demise of the animal within 6-7 days (Verzi et al., 2010; Hryniuk et al., 2012; Gao et al., 2010). Defects in the small intestine of *Cdx2*$^{-/-}$ mice are largely indistinguishable from those observed in *Cdx1*$^{-/-}$*Cdx2*$^{-/-}$ compound mutants, consistent with *Cdx1* being dispensable for intestinal homeostasis (Subramanian et al., 1995; Bonhomme et al., 2008; Grainger et al., 2010; Hryniuk et al., 2012). *Cdx1*$^{-/-}$*Cdx2*$^{-/-}$ mutants, however, exhibit more severe defects in the colon than mice deficient in *Cdx2* alone, including ectopic expression of anterior intestinal markers (Hryniuk et al., 2012).

Conditional Cdx2-deletion

To overcome the embryonic lethality that results from *Cdx2* deletion, our lab derived a conditional knockout model using a tamoxifen-inducible Cre-*loxP* system (Figure 26; Hayashi et al., 2002; Gorman and Bullock, 2000; Nagy, 2000; Rossant and McMahon, 1999). In this model, *Cdx2* deletion is induced by a Cre-recombinase fused to an estrogen receptor ligand-binding domain that responds only to tamoxifen (*Cre-ER*^{T}). In the absence tamoxifen, the Cre-recombinase is sequestered in the cytosol through an interaction with heat shock protein 90 (Hsp90). Upon tamoxifen treatment, Cre-ER^{T} undergoes a conformational change, is released from Hsp90, and translocates to the nucleus where it targets *loxP* sites flanking Exon 2 of *Cdx2* (*Cdx2*$^{fl/fl}$), which contains the DNA-binding homeodomain. Expression of the Cre recombinase is driven by a *β-Actin* promoter (*β–Actin::Cre-ER*^{T}), allowing for ubiquitous ligand-regulated deletion. Thus, with tamoxifen treatment, *Cdx2*$^{-/-}$ mutants can

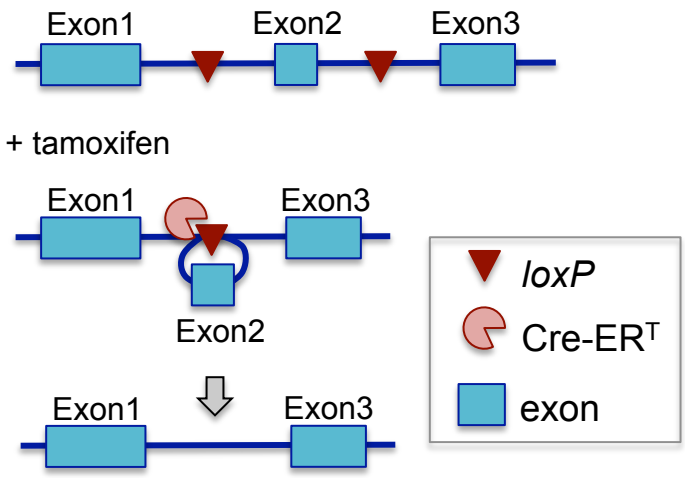


Figure 26. Conditional *Cdx2* gene deletion. Exon 2 of Cdx2 is flanked by *loxP* sites. In the presence of tamoxifen, a tamoxifen-inducible Cre-recombinase, that is otherwise sequestered in the cytoplasm by Hsp90, translocates to the nucleus where it excises Exon 2 of *Cdx2*, which is flanked by *loxP* sites. Exon 2 contains the DNA-binding homeodomain for Cdx2. The excision of this exon results in recombination and the production of a functionally null protein.

be generated for the study of post-implantation Cdx2 function.

Cdx2$^{-/-}$ conditional mutants survive until E12.5, and present a number of defects (Savory et al., 2009a). *Cdx2*$^{-/-}$ embryos are deficient in presomitic mesoderm, resulting in truncation of the posterior embryo caudal to the forelimb bud and defects in somite segmentation (Savory et al., 2009a). Further, the absence of posterior axial tissue leads to failure of chorioallantoic fusion (Savory et al., 2009a). *Cdx4* expression is also attenuated and may also contribute to the *Cdx2*$^{-/-}$ phenotype (Savory et al., 2009a; Chawengsaksophak et al., 2004).

Functional overlap among Cdx factors

Cdx members contain a highly conserved DNA-binding homeodomain which binds to the consensus sequence TTTAT(G), termed a Cdx response elements (CDREs; Dearolf, Topol, and Parker,

1989). Three regions N-terminal to the homeodomain have been identified (A, B, and C in Figure 27) which include a putative nuclear export sequence (Figure 27A), a region within the Cdx transactivation domain of unknown function (Figure 27B), and a region C-terminal to homeodomain whose function is also unknown (Figure 27C; Trinh et al., 1999; Taylor et al., 1997a; Taylor et al., 1997b; Rings et al., 2001; Lynch et al., 2003). The transactivation domain of Cdx2 also harbors a phosphorylation site at serine-60 (Rings et al., 2001) which can impact transcriptional activity (Rings et al., 2001). This residue is, however, not conserved and little else is known about the regulation of Cdx factors by post-translational modification.

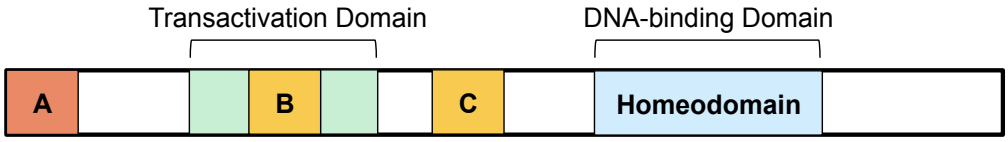


Figure 27. Sequence similarity among Cdx family members. The DNA-binding homeodomain is conserved among Cdx homologs, as well as region A, thought to act as a nuclear export signal, B, located within a transactivation domain, and C, which displays a high degree of sequence similarity between Cdx1 and Cdx2 but whose function remains unknown. Figure reproduced with permission (Guo et al., 2004).

Despite little sequence similarity, there appears to be a high degree of functional overlap among Cdx family members in both the embryo and the adult intestine. In the embryo, both *Cdx1*$^{-/-}$ and *Cdx2*$^{+/-}$ mutants exhibit homeotic transformations of the cervical and thoracic vertebrae associated with shifts in the expression of Hox genes (Subramanian et al., 1995; Chawengsaksophak et al., 1997). *Cdx1* deletion, however, produces transformations that are more anterior than those observed with heterozygous loss of *Cdx2*. These differences are thought to be due to differential patterns of *Cdx1* and *Cdx2* expression, with the *Cdx1* expression boundary being anterior to that of *Cdx2* in wild type animals (Chawensaksophak et al., 2004; Subramanian et al., 1995).

Studies in which mutants containing *Cdx2* "knocked-in" to the *Cdx1* locus ($Cdx1^{Cdx2\text{-}ki/Cdx2\text{-}ki}$) were developed to further explore functional overlap among Cdx members. In this model, *Cdx2* is expressed under *Cdx1* regulatory elements by virtue of homologous recombination mediated knock-in (Savory et al., 2009b). These mutants display no anterior vertebral transformations demonstrating that Cdx2 can substitute for Cdx1, at least for vertebral patterning (Savory et al., 2009b). Similar observations have been made in the distal gut, with no observable phenotypic changes within the colon of $Cdx1^{Cdx2\text{-}ki/Cdx2\text{-}ki}$ adults (Grainger et al., 2013).

To overcome functional overlap among Cdx family members, $Cdx2^{f/f}Actin::CreER^{T}$ mutants were crossed into a $Cdx1^{-/-}$ background and treated as above, producing $Cdx1^{-/-}Cdx2^{-/-}$ compound mutants (Savory et al., 2011a). These compound mutants lack *Cdx4* expression (Savory et al., 2011a), thereby reflecting total Cdx loss of function. These compound mutants exhibited defects not observed in *Cdx2* single mutants, including a more anterior axial truncation and craniorachischisis, a severe defect in neural tube closure resulting in the neural tube remaining open along its length (Figure 28; Savory et al., 2011b). Further, these compound Cdx mutants exhibit defects in somite segmentation, resulting in poorly formed somite boundaries and misexpression of anteroposterior somitic markers (Savory et al., 2011b). These defects are consistent with previous work suggesting functional overlap among Cdx family members (Savory et al., 2011; Hryniuk et al., 2012; van den Akker et al., 2002; van Rooijen et al., 2012).

Cdx interacting partners and transcription

SWI/SNF and BAF chromatin remodeling complexes

Little is known about interacting partners involved in Cdx-dependent transcription. Using stable isotope labelling of amino acids in culture coupled with mass-spectrometry (SILAC-MS), our lab

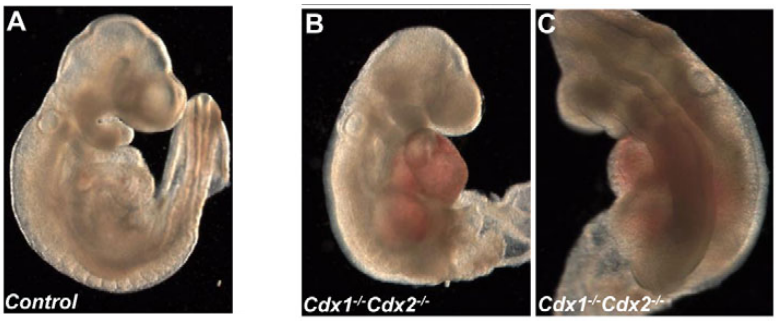


Figure 28. Cdx1-Cdx2 compound mutants. Defects in cardiac development, somite segmentation, axial elongation (B) and neural tube closure (C) are observed in Cdx1-Cdx2 compound mutants compared to wild type controls (A). Figure reproduced with permission (Savory et al., 2011).

identified a number of subunits of the mammalian SWI/SNF chromatin remodelling complex, also known as the Brahma-associated factor (BAF) complex, as potential human CDX2 interacting partners (Figure 29; Nguyen et al., 2017), consistent with prior findings (Yamamichi et al., 2009). The SWI/SNF complex is composed of Trithorax group (TrxG) proteins which are highly conserved from yeast to humans (Cairns et al., 1994; Peterson et al., 1994; Dingwall et al., 1995; Khavari et al., 1993; Kwon et al., 1994; Laurent et al., 1993; Muchardt and Yaniv, 1993; Randazzo et al., 1994; Tamkun et al., 1992; Wang et al., 1996). These complexes reposition nucleosomes in an ATP-dependent manner, regulating chromatin accessibility and thereby impacting gene expression (Cairns et al., 1994; Peterson et al., 1994).

Among SWI/SNF subunits found to interact with Cdx2 was Brahma-related gene 1 (Brg1), one of two catalytic subunits of this complex and critical for development (Khavari et al., 1993; Muchardt and Yaniv, 1993; Chiba et al., 1994; Randazzp et al., 1994; Wang et al., 1996; Bultman et al., 2000). We found a direct protein-protein interaction between Cdx and Brg1, along with their co-occupation of common genomic targets that is conserved among both murine and human tissues (Nguyen et al., 2017;

Gene Name	Unique Peptides	Sequence Coverage [%]	Ratio H/L Normalized	Log Ratio
CDX2	6	17.6	14.40	3.85
BAF250	16	9.9	7.51	2.91
BAF190 (BRG1)	21	16.5	5.27	2.40
BAF53	2	4.7	4.19	2.07
BAF57	2	6.1	2.78	1.48
BAF155	4	6.2	2.70	1.43
BAF170	2	3.5	2.47	1.30

Figure 29. SWI/SNF complex subunits interact with CDX2. SILAC-MS performed in HEK293T cells identified a number of proteins belonging to the SWI/SNF chromatin remodelling complex as CDX2 interacting partners. These included BAF250, BAF53, BAF57, BAF155, and BAF170. The ratio of heavy to light isotope peptides (ratio H/L normalized) is an indicator of relative enrichment. Figure reproduced with permission (Nguyen et al., 2017).

Yamamichi et al., 2009; Foley et al., 2019). In addition to Brg1, a number of core SWI/SNF subunits were recovered from the SILAC analysis. This suggests that Cdx interacts with the entire complex, and that this interaction may be a major means by which Cdx factors regulate gene expression.

SWI/SNF complexes are composed of 10-12 subunits (Figure 30; Ho and Crabtree, 2010). Each complex contains one of two catalytic subunits, either Brahma (Brm) or Brg1 (Chiba et al., 1994; Clapier et al., 2017; Khavari et al., 1993; Kwon et al., 1994; Wang et al., 1996). While Brg1 is essential for development with its deletion resulting in embryonic lethality, initial studies on Brm-knockout mice suggested that Brm is dispensable during development (Reyes et al., 1998). however, residual Brm expression is detected in the Brm mutant, and it remains unclear if this catalytic subunit plays a role during development (Thompson et al., 2015).

Brg1 and Brm subunits exhibit a high degree of sequence homology, with both containing C-terminal bromodomains (Khavari et al., 1993; Muchardt and Yaniv, 1993; Chiba et al., 1994). These domains facilitate binding to acetylated histone tails, suggesting that SWI/SNF complexes read the

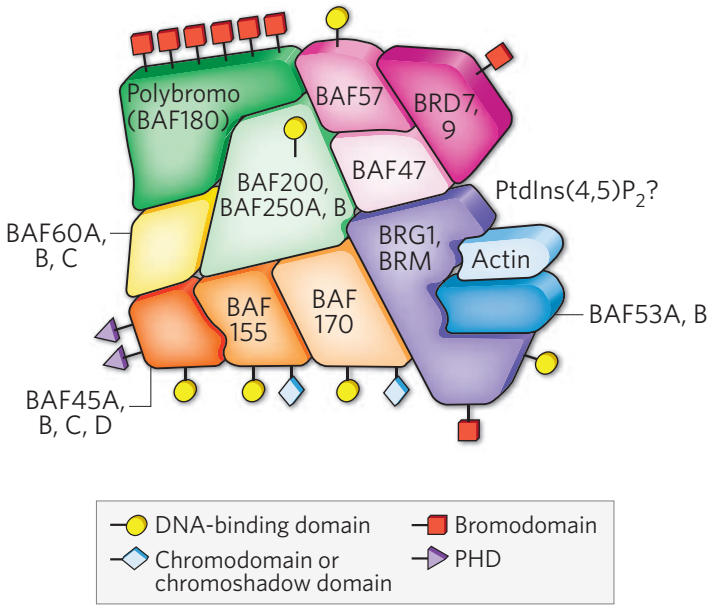


Figure 30. Mouse SWI/SNF chromatin remodelling complex. The SWI/SNF chromatin remodelling complex consists of 10-12 subunits, including cell-type specific components and one of two catalytic subunits, either Brg1 or Brm (purple). Figure reproduced with permission (Ho and Crabtree, 2010).

histone code and translate post-translational modifications of histone tails into changes in chromatin accessibility, thereby impacting gene expression (Meslamani et al., 2016; Moustakim et al., 2016). Despite their sequence similarity, Brg1 and Brm are unable to substitute for one another due to their unique N-terminal domains that facilitate interactions with distinct sets of transcription factors (Kadam and Emerson, 2003; Flowers et al., 2009).

The precise mechanisms that regulate SWI/SNF recruitment to target genes remains unclear. Studies suggest that SWI/SNF complexes are recruited to genomic targets by transcription factors (Yoshinaga et al., 1992; Ostlund Farrants et al., 1997; Neely et al., 1999; Cosma et al., 1999; Krebs et al., 1999; Dimova et al., 1999; Fryer et al., 1998; Kowenz-Leutz and Leutz, 1999; Kadam and Emerson, 2003; Xu et al., 2006; Nguyen et al., 2017; Foley et al., 2019). Transcription factor mediated recruitment, in combination with cell type- and developmental stage-specific expression of diverse

SWI/SNF complexes, are thought to direct SWI/SNF chromatin remodelling activity to specific regions of the genome (Figure 31). Tissue-specific SWI/SNF members assemble with core complex proteins consisting of Baf57, Baf53, Baf155, Baf170, Baf47, and either Brg1 or Brm (Hadidy and Uversky, 2019). Tissue-specific SWI/SNF subunits include Baf60C, required for heart development (Lickert et al., 2004), Baf60A, involved in skeletal muscle differentiation (Puri et al., 2012), and Baf250A/B, required ESC pluripotency (Yan et al., 2008; Celen et al., 2017). A second ESC-specific SWI/SNF complex, known as esBAF, has also been identified, and is characterized by the presence of Brg1 and Baf155 and the absence of Baf170 (Yan et al., 2008; Ho et al., 2009).

The SWI/SNF chromatin remodelling complex, in conjunction with TrxG proteins, are known to oppose gene repression by Polycomb group (PcG) proteins (Ringrose and Paro, 2007; Schuettengruber et al., 2007). While these two classes of protein complexes have antagonistic functions, they maintain the balance between gene activation and repression critical to development and differentiation. Mammalian SWI/SNF is thought to antagonize PcG-mediated repression by evicting Polycomb complexes from their binding sites (Kia et al., 2008; Stanton et al., 2017). Despite this relationship, SWI/SNF-mediated chromatin remodelling does not necessarily result in positive regulation of transcription, as it has the potential to also repress genomic targets. In this regard, Brg1 binding is required to maintain histone H3 lysine 27 trimethyl (H3K27me3)-mediated gene repression at a subset of target genes (Alexander et al., 2015).

Polycomb Repressive Complex 2 (PRC2)

PcG proteins epigenetically regulate gene expression through the addition of histone modifications that establish lineage-specific gene expression programs during development (Bracken et al., 2006). PcG proteins, discovered in *Drosophila,* were named as such for the morphological transformations within the body segments of PcG mutants, as flies in which PcG proteins are disrupted

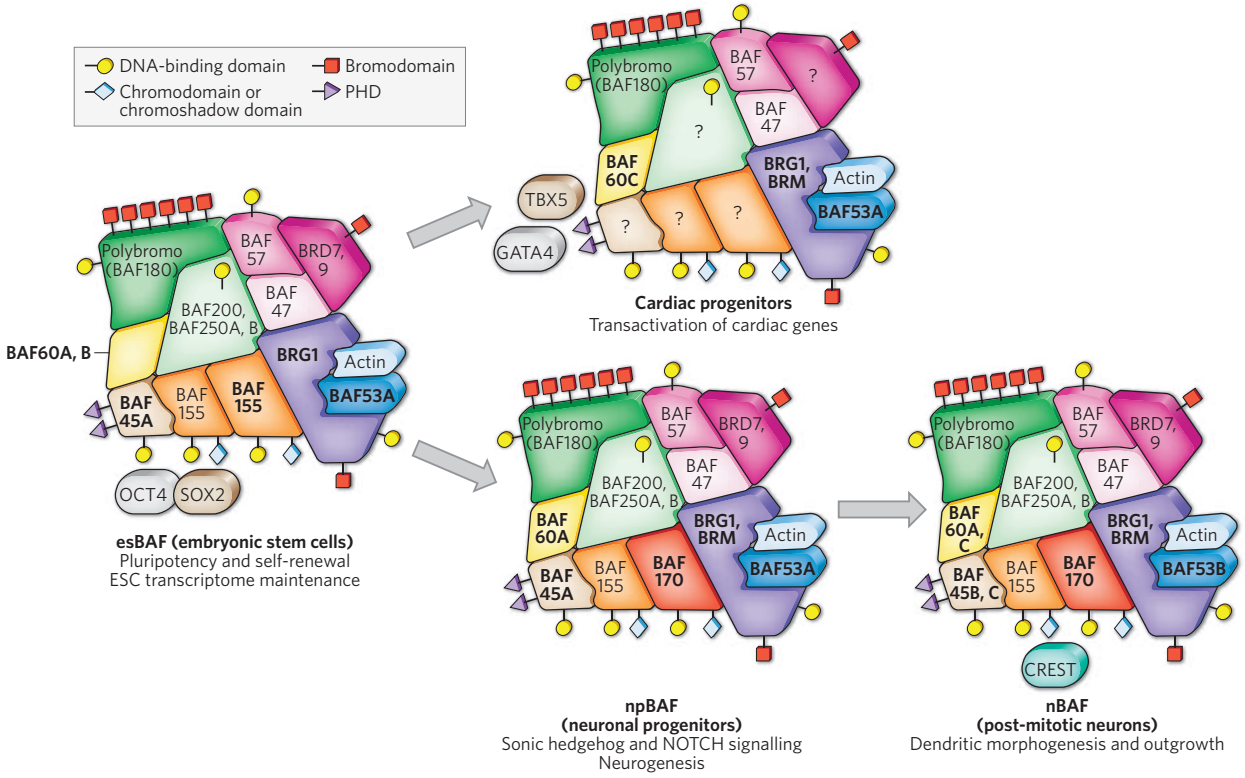


Figure 31. Cell- and tissue-type-specific SWI/SNF complexes. Tissue- and cell-type specific BAF complexes allows for biological specificity, as each complex has distinct functions. The diagram illustrates examples of known tissue- and cell-type-specific BAF complexes, with possible subunits at each position listed. These complexes include the embryonic stem cell-specific BAF complex (esBAF), the neuronal progenitor specific BAF complex (npBAF), the neuronal specific BAF complex (nBAF), and the cardiac progenitor specific BAF complex. Question marks (?) indicate subunits that have not yet been identified with certainty. Subunits that distinguish each of these complexes are indicated in bold type. Figure reproduced with permission (Ho and Crabtree, 2010).

possess additional sex combs, rows of bristles on the front legs of adult males involved in courtship behaviour (Lewis, 1949; Lewis, 1978; Kopp, 2011; Atallah et al., 2009; True et al., 2008). Two mammalian PcG protein complexes have been extensively studied, Polycomb Repressive Complex 1 (PRC1) and 2 (PRC2). PRC1 activity results in the mono-ubiquitination of histone H2A at lysine 119 (H2AK119ub), while PRC2 catalyzes deposition of H3K27me3 (Schuettengruber and Cavalli, 2009; Simon and Kingston, 2009). PRC2 is composed of PcG proteins, and contains four core subunits; Suz12, Eed, RbAp46/47, and one of two mutually exclusive catalytic subunits, either Ezh1 or Ezh2 (Figure 32), along with a number of accessory subunits (Margueron and Reinberg, 2011). Ezh1 and Ezh2 have different patterns of expression, with Ezh1 being ubiquitously expressed, albeit often at low levels, and Ezh2 expressed in proliferating tissues (Margueron et al., 2008). While Ezh1 and Ezh2 are both histone methyltransferases, these subunits differ in their relative catalytic activity, with Ezh2 being more active (Margueron et al., 2008). Despite its reduced methyltransferase activity, Ezh1 appears to be more efficient at compacting chromatin than Ezh2, resulting in more robust gene repression (Margueron et al., 2008).

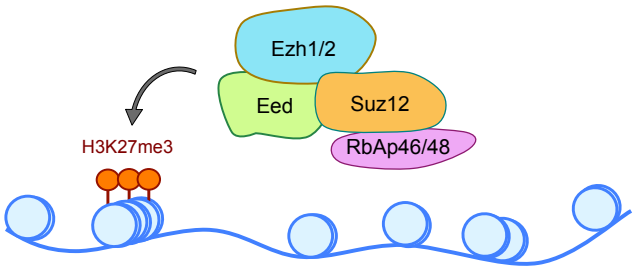


Figure 32. Polycomb Repressive Complex 2. PRC2 contains four core catalytic subunits, Eed, Suz12, RbAp46/48, and one of two catalytic subunits, either Ezh1 or Ezh2. This complex contains histone methyltransferase activity, resulting in H3K27me3 typically associated with gene repression.

Narrow peaks of H3K27me3 on either side of transcriptional start sites are thought to indicate bivalent promoters, as they often overlap with peaks of H3K4me3, an activating mark catalyzed by TrxG proteins (Zhao et al., 2007; Pan et al., 2007; Schuettengruber et al., 2007; Ringrose and Paro, 2007). In addition to TSS-associated peaks, broad regions of H3K27me3 spanning hundreds of kilobases, often covering entire gene bodies, are also observed in the mammalian genome (Zhao et al., 2007; Hawkins et al., 2010). These larger domains are established during lineage commitment and are associated with long-term gene repression by PRC2 (Boyer et al., 2006; Squazzo et al., 2006; Hawkins et al., 2010; Cui et al., 2009).

PRC1 binding overlaps with that of PRC2 at a number of genomic loci (Boyer et al., 2006; Bracken et al., 2006; Lee et al., 2006; Schwartz et al., 2006; Schwartz and Pirotta, 2014). Genomic consensus sequences for PRC binding sites, known as Polycomb response elements (PREs), have been identified in *Drosophila*, however mammalian orthologs for these response elements remain elusive, despite PRC complexes and their genomic targets being highly evolutionarily conserved (Bauer et al., 2015). Studies have shown that H3K27me3 deposited by PRC2 recruits PRC1 to shared targets, leading to the accumulation of H2AK119ub, chromatin compaction and gene silencing (Di Croce and Helin, 2013; Francis et al., 2004). Similarly, PRC2 also appears to be recruited to sites enriched for H2AK199ub (Kalb et al., 2014) and H3K27me3 (Hojfeldt et al., 2018). While a model in which co-recruitment occurs between PRC1 by PRC2 would allow for cooperative binding and efficient repression of gene expression, as previously proposed (Schwartz and Pirrotta, 2014), both PRC1 and PRC2 are capable of binding to target sites in the absence of these marks. Moreover, while PRC1 and PRC2 share common targets (Boyer et al., 2006; Bracken et al., 2006; Lee et al., 2006; Schwartz et al., 2006; Schwartz and Pirotta, 2014), PRC2 is capable of maintaining gene repression at a subset of targets in the absence of PRC1 (Ku et al., 2008; Iovino et al., 2013; Endoh et al., 2012; Cohen et al.,

2018), and vice-versa (Leeb et al, 2010; Tavares et al., 2012) indicating that locus-specific mechanisms of regulation by PRC complexes exist (Brand et al., 2019).

Despite the absence of obvious PRE consensus sequences in the mammalian genome, PRC complexes appear to preferentially bind CpG islands (Boyer et al., 2006; Mendenhall et al., 2010), as well as regions enriched for H3K27me3 (Hansen et al., 2008; Margueron et al., 2009). Given that only a small number of all CpG islands/H3K27me3 sites are occupied by PRC complexes, a second layer of regulation must exist (Brand et al., 2019). While the mechanisms remain unknown, it has been proposed that PRC recruitment may occur through interactions with lineage- and cell-type specific transcription factors (Woo et al., 2010; Yu et al., 2012; Pinello et al., 2014; Arnold et al., 2013).

Studies in differentiating motor neurons and the intestinal epithelium have described a relationship between Cdx transcription factors and the repressive histone modification H3K27me2. During motor neuron differentiation, Cdx2 binding to *Hox* loci results in the clearance of H3K27me3, rendering these loci permissive to expression. In the absence of Cdx2, persistent H3K27me3 represses gene expression, interfering with the induction of normal gene regulatory networks required for neuronal differentiation (Mazzoni et al., 2013). Similarly, Cdx2 binding inhibits the spread of H3K27me3 across genomic targets in the intestinal epithelium, thereby maintaining gene expression by establishing boundaries for this inhibitory histone modification (Saxena et al., 2017). While a physical interaction has not yet been described between Cdx and members of PRC2, these factors appear to share an appositional functional relationship.

Rationale

Cardiac and primitive hematopoietic lineages are specified from a common *Mesp1*$^{+}$ mesodermal progenitor (Kattman et al., 2006; Simoes et al., 2011). Using a Cdx-knockout mouse model, our group has shown that aberrant heart morphogenesis accompanies defects in the first wave of yolk sac hematopoiesis, suggesting that Cdx coordinates the decision between cardiac and hematopoietic lineages. The mechanism by which Cdx regulates this specification event is unknown, but may involve the Cdx-dependent chromatin remodelling complex via SWI/SNF, and/or functional interaction with PRC2-dependent gene silencing.

Hypothesis

I hypothesize that Cdx transcription factors are required to maintain the balance in specification between cardiac and hematopoietic cell fates through epigenetic mechanisms involving interactions with SWI/SNF chromatin remodelling complex and H3K27me3/PRC2.

Objectives

1. Determine the impact of Cdx deletion on the balance between commitment to cardiac and hematopoietic lineages.
2. Describe the molecular mechanisms by which Cdx factors regulate the expression of its target genes within mesodermal lineages, focusing on cardiogenic and yolk sac targets.

CHAPTER 2 - Role of Cdx Factors in Early Mesodermal Fate Decisions

Role of Cdx factors in early mesodermal fate decisions

Tanya E. Foley, Bradley Hess, Joanne G. Savory, Randy Ringuette, David Lohnes

Keywords: Cdx, mouse, Mesoderm, Cell fate, Transcription, Chromatin

Article published March 1 2019 in *Development*, Volume 146, Issue 7, dev170498.

AUTHOR CONTRIBUTIONS

Tanya Foley designed and conducted experiments, performed data analysis, and prepared the manuscript.

Bradley Hess conducted the ChIP-seq experiment.

Joanne Savory generated the *Cdx1*$^{-/-}$*Cdx2*$^{fl/fl}$ mice, helped to design the ChIP-seq experiment, and assisted in ChIP-seq data analysis.

Randy Ringuette conducted one whole mount immunohistochemistry experiment.

David Lohnes helped to design experiments and to write the manuscript.

ABSTRACT

Murine cardiac and hematopoietic progenitors are derived from *Mesp1*$^{+}$ mesoderm. Cdx function impacts both yolk sac hematopoiesis and cardiogenesis in zebrafish, suggesting that Cdx family members regulate early mesoderm cell fate decisions. We found that Cdx2 occupies a number of transcription factor loci during embryogenesis, including key regulators of both cardiac and blood development, and that Cdx function is required for normal expression of the cardiogenic transcription factors *Nkx2-5* and *Tbx5*. Furthermore, Cdx and Brg1, an ATPase subunit of the SWI/SNF chromatin remodeling complex, co-occupy a number of loci, suggesting that Cdx family members regulate target gene expression through alterations in chromatin architecture. Consistent with this, we demonstrate loss of Brg1 occupancy and altered chromatin structure at several cardiogenic genes in Cdx-null mutants. Finally, we provide evidence for an onset of Cdx2 expression at E6.5 coinciding with egression of cardiac progenitors from the primitive streak. Together, these findings suggest that Cdx functions in multi-potential mesoderm to direct early cell fate decisions through transcriptional regulation of several novel target genes, and provide further insight into a potential epigenetic mechanism by which Cdx influences target gene expression.

INTRODUCTION

The murine Cdx genes, *Cdx1*, *Cdx2* and *Cdx4*, encode homeodomain transcription factors related to caudal in Drosophila. With the exception of early expression of *Cdx2* in the trophectoderm of the pre-implantation embryo, Cdx family members are sequentially activated during gastrulation commencing at embryonic day (E) 7.5, forming a nested expression domain in the primitive streak and subsequently in all three germ layers of the tail bud until approximately E13.5 (Beck, et al., 1995; Gamer and Wright, 1993; Meyer and Gruss, 1993; Strumpf et al., 2005). Cdx gene expression is then extinguished in all tissues except the hindgut endoderm and derivative intestinal epithelium, where Cdx1 and Cdx2 are maintained throughout adulthood (Silberg et al., 2000). Whereas $Cdx2^{-/-}$ mutants are peri-implantation lethal, owing to a requirement for this transcription factor in the trophectoderm, $Cdx1^{-/-}$ and $Cdx2^{+/-}$ mice are viable and exhibit homeotic transformations of the cervical and thoracic vertebrae with concomitant shifts in Hox gene expression (Subramanian et al., 1995; Chawengsaksophak et al., 1997). Cdx4-null mutants are phenotypically normal; however, the loss of Cdx4 exacerbates $Cdx1^{-/-}$ or $Cdx2^{+/-}$ phenotypes, indicative of functional overlap between Cdx family members (Faas and Isaacs, 2009; Savory et al., 2011a; van den Akker et al., 2002; van Nes et al., 2006; Young et al., 2009). The derivation and analysis of Cdx2 conditional mutants (Savory et al., 2009a; Stringer et al., 2012) and compound mutant derivatives (van den Akker et al., 2002; Savory et al., 2011a; Verzi et al., 2011; van Rooijen et al., 2012; Stringer et al., 2012; Grainger et al., 2010; Hryniuk et al., 2012) further substantiated the functional overlap between family members. Analysis of these mutants also revealed a requirement for Cdx genes in diverse processes in development and in the adult intestinal track. These include, for example, roles for Cdx proteins in specification and development of the intestine and its homeostasis in the adult (Beck et al., 1999, 2003; Chawengsaksophak et al., 1997; Gao et al., 2009; Grainger et al., 2010; Stringer et al., 2012; Hryniuk et al., 2012), yolk sac hematopoiesis (Lengerke et al., 2007; Wang et al., 2008; Brooke-Bisschop et al., 2017; Davidson and

Zon, 2006; Davidson et al., 2003), neural tube closure, and elaboration of the post-otic embryo (Savory et al., 2009a, 2011; van Rooijen et al., 2012).

Although Cdx function has been shown to be crucial for numerous developmental programs, our understanding of the target genes governing these programs is incomplete. Cdx family members regulate target gene transcription through binding to a cognate response element (CDRE), of the consensus TTTATG, either in the proximity of their target genes (Suh et al., 1994; Subramanian et al., 1995) or at distal enhancer elements (Maier et al., 2005; Taylor et al., 1997; Gaunt, 2017). Although Cdx family members typically positively regulate transcription, there is a growing body of evidence that suggests they can also act as transcriptional repressors. The means by which Cdx factors regulate transcription is also poorly understood, although Cdx function has been shown to impact chromatin architecture (Verzi et al., 2013, 2010; Saxena et al., 2017; Neijts et al., 2017), consistent with their association with Brg1 (Smarca4) and other members of the SWI/SNF chromatin remodeling complex (Yamamichi et al., 2009; Nguyen et al., 2017).

In agreement with their functional overlap (van den Akker et al., 2002; Davidson and Zon, 2006; van Nes et al., 2006; Faas and Isaacs, 2009), Cdx family members appear comparable in their ability to occupy, and regulate, target genes (Charité et al., 1998; Savory et al., 2009a). Targets identified to date include a number of Hox genes, implicated in Cdx-dependent vertebral patterning (Shashikant et al., 1995; Charité et al., 1998; Subramanian et al., 1995; Pownall et al., 1996; Isaacs et al., 1998; van den Akker et al., 2002; Gaunt et al., 2003, 2008), Cyp26A1, which is essential for catabolism of retinoic acid (RA) and crucial for the maintenance of a caudal progenitor population driving axial elongation (Wingert et al., 2007; Savory et al., 2009a; Young et al., 2009; Martin and Kimelman, 2010), genes encoding products involved in intestinal differentiation and homeostasis (Beck et al., 1999, 2003; Chawengsaksophak et al., 1997; Gao et al., 2009; Grainger et al., 2010;

Hryniuk et al., 2012), and targets necessary for yolk sac hematopoiesis (Davidson et al., 2003; Davidson and Zon, 2006; Lengerke et al., 2007; Wang et al., 2008; Brooke-Bisschop et al., 2017).

To establish a more comprehensive understanding of Cdx function during mouse development, we conducted chromatin immunoprecipitation coupled with deep sequencing (ChIP-seq) using material from E8.5 embryos. This analysis revealed Cdx2 to be highly enriched at the loci of genes encoding numerous transcription factors, among which were a number of transcription factors involved in hematopoiesis and cardiogenesis. Consistent with this, we found that loss of Cdx function leads to heart anomalies and misexpression of several cardiogenic genes, including gain of expression of cardiac markers in Cdx mutant yolk sacs concomitant with loss of expression of genes involved in yolk sac hematopoiesis. Finally, Brg1, a catalytic subunit of the SWI/SNF chromatin remodeling complex required for mesodermal differentiation (Alexander et al., 2015) and which interacts functionally with Cdx2 (Yamamichi et al., 2009; Nguyen et al., 2017), co-localized with Cdx2 at a number of cardiogenic loci. Moreover, Brg1 binding and chromatin structure was altered at these genes in Cdx mutants. As Cdx is essential for yolk sac hematopoiesis (Davidson and Zon, 2006; Davidson et al., 2003; Lengerke et al., 2007; Wang et al., 2008; Brooke-Bisschop et al., 2017), these findings suggest that Cdx function regulates chromatin remodeling events necessary for the coordinated expression of transcription factors that direct hematopoietic versus cardiac fates from a common progenitor population.

RESULTS

Cdx2 occupancy is enriched at transcription factor loci

To understand the means by which Cdx family members regulate developmental programs, Cdx2 occupancy in the E8.5 embryo was assessed by chromatin immunoprecipitation followed by deep sequencing (ChIP-seq). Of the 13,991 total peaks returned from this analysis, Cdx2 binding was found to be distributed primarily in introns (32% of peaks) and proximal to transcriptional start sites (20% of peaks; Figure 33A, B). Genomic regions associated with Cdx2 occupancy were also highly enriched for canonical CDREs (Figure 33C; Dearolf et al., 1989; Suh et al., 1994; Subramanian et al., 1995).

Putative Cdx target genes were selected for further analyses using a minimum peak score of 800 as a cut-off, based on our recovery of previously characterized Cdx2 targets with peak scores ranging from 800 (e.g. *Dll1*; Grainger et al., 2012) to 3100 (e.g. *Scl*; Savory et al., 2011a; Brooke-Bisschop et al., 2017). Gene ontology (GO) term enrichment analysis was conducted using the 441 peaks annotated to a reference gene that met this threshold. This analysis revealed that Cdx2-occupied loci were significantly enriched for genes involved in transcription, positive and negative regulation of gene expression, and cell fate commitment (Figure 33D), suggesting that Cdx2 coordinates the expression of gene regulatory networks essential to embryonic development. Consistent with this, 226 of the 441 peaks were associated with genes encoding factors related to regulation of transcription, and six corresponded to genes involved in signaling pathways (*Wnt3*, *Wnt7b*, *Wnt11*, *Cyp26A1*, *Bmp2* and *Dll1*). This analysis likely excluded potential candidate targets, owing to the relatively high stringency used for cutoff, as well as additional targets that may not be accessible at the developmental stage employed for this analysis. It is, however, interesting to note that a number of annotated peaks that fall below the cutoff are also enriched for genes encoding transcription factors and signaling molecules (Table 1).

Among transcription-related targets, Cdx2 was enriched at a number of Hox genes (e.g. *Hoxa1*, *Hoxa2*, *Hoxb1*, *Hoxb2*, *Hoxb13*, *Hoxc4* and *Hoxd1*), consistent with the known roles for Cdx family

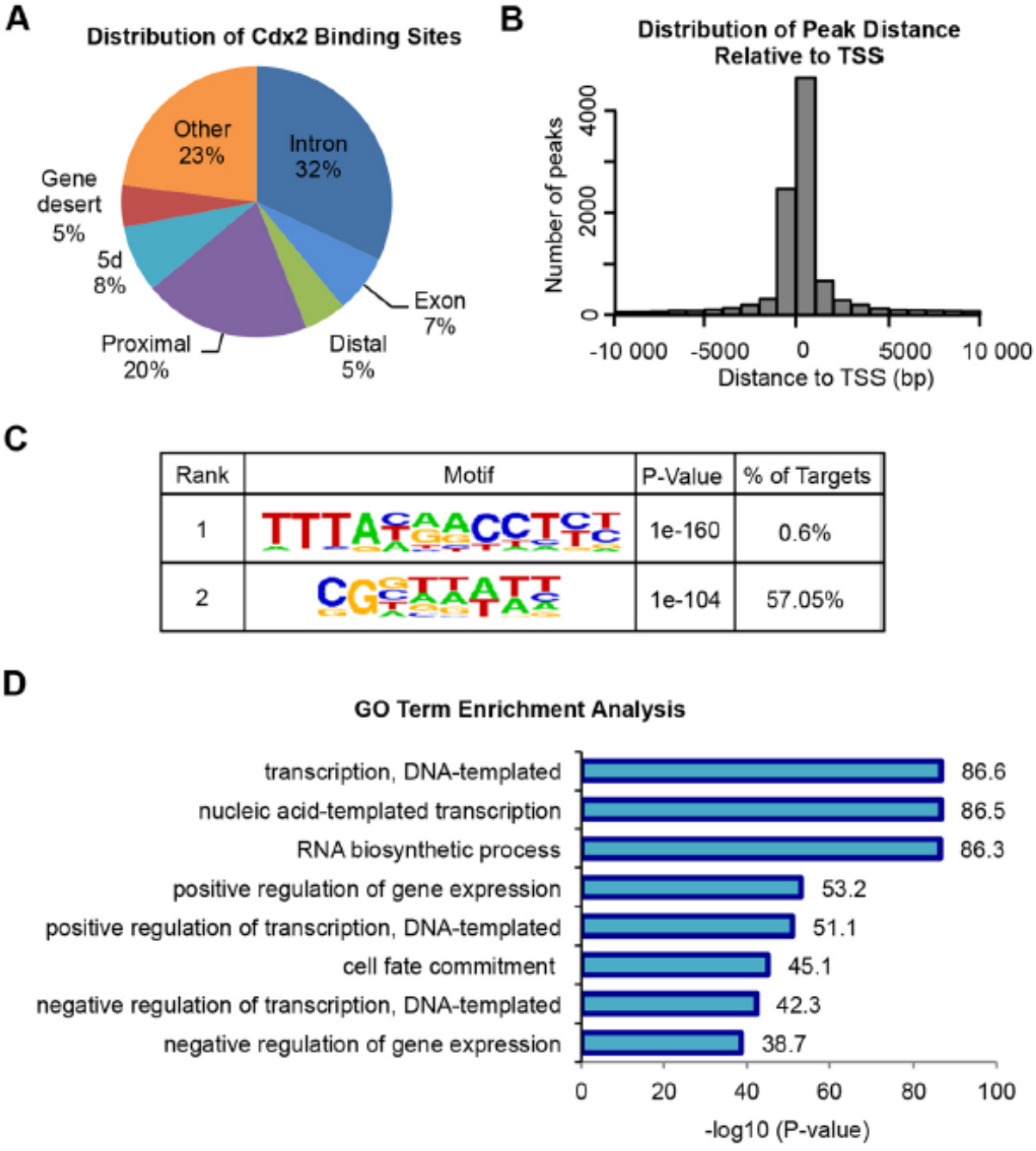


Figure 33. Cdx2 binding distribution. A. Relative distribution of Cdx2 genomic occupancy designated as proximal (within 2 kb of a TSS), distal (2-10 kb upstream of a TSS), 5d (10-100 kb upstream of a TSS), within gene deserts (≥100 kb upstream/downstream of a TSS), or other (all remaining peaks). **B.** Distribution of peak distances relative to the nearest TSS. **C.** Binding motifs with

the greatest enrichment under Cdx2 peaks and their associated P-values. **D.** GO term enrichment analysis of Cdx2-bound loci with peak scores of 800 or greater. A subset of GO terms with a fold enrichment of 5 or greater were considered and sorted by $\log_{10}$(P-value).

Gene Name	Peak Score	Binding Region
Bmpr1a	346.6	Promoter_TSS (NM_009758)
Wnt7b	351.89	Promoter_TSS (NM_009528)
Sox6	351.38	Promoter_TSS (NM_001025560)
Smad5	509.91	Intergenic
Lmo4	488.81	Promoter_TSS (NM_001161770)
Ptch1	178.92	Intergenic
Sox3	468.75	Intergenic
Isl1	423.56	Intergenic
Id2	422.99	Intergenic
Es1	411.90	Intergenic
Notch2	400.99	Promoter_TSS (NM_010928)
Pax2	396.03	Intergenic
Neurog2	390.89	Intergenic
Foxa1	388.42	Intergenic
Dll1	386.31	Intergenic
Gsx2	377.44	Intergenic
Wnt2b	373.98	Promoter_TSS (NM_009520)
Neurod2	339.47	Intergenic
Neurog1	336.61	Intergenic
Sox3	317.70	Intergenic
Lbx2	314.86	Promoter_TSS (NM_010692)
Hoxb1	312.16	Intergenic
Fgf8	308.96	Intergenic
Foxa2	308.16	Intergenic
Esx1	306.91	Intergenic
Nkx3_2	305.43	Intergenic
Bmpr1b	301.93	Intergenic
Smad3	297.39	Promoter_TSS (NM_016769)
Tbx3	293.08	Intergenic
Tbx20	292.35	Intergenic

Table 1. Select transcription and signaling factors with peak scores below 800. Select genes occupied by Cdx2 with a peak score of 800 or greater and the associated genomic peak location.

members in vertebral patterning through regulation of Hox gene expression (Subramanian et al., 1995; Charité et al., 1998; van den Akker et al., 2002; Shashikant et al., 1995; Pownall et al., 1996; Isaacs et al., 1998; Gaunt et al., 2003, 2008). Certain transcriptional regulators of tissue patterning and specification were also enriched for Cdx2 occupancy (e.g. *Twist1*, *Irx2*, *Gsc*, *Pitx1*, *Pax1*, *Pax3*, *Pax9*, *Alx3*, *Sox1*, *Sox2*, *Foxa2* and *Foxd3*).

As previously described (Wang et al., 2008; Brooke-Bisschop et al., 2017), ChIP-seq identified *Scl* (*Tal1*), which encodes a master regulator of hematopoiesis, as a Cdx2 target (Figure 34A; Shivdasani et al., 1995; van Handel et al., 2012; Org et al., 2015). In addition, other regulators of yolk-sac hematopoiesis, including Lyl1, Lmo2 and Meis1, showed significant Cdx2 binding (Figure 34A). Of particular note was the finding of a number of genes encoding cardiogenic transcription factors that were highly enriched for Cdx2 occupancy. Such genes encompassed some of the earliest known markers of cardiac progenitors, including *Gata4*, *Nkx2-5*, *Tbx5* and *Isl1*, as well as genes required for cardiac looping, such as *Hand1* and *Hand2* (Figure 34B; reviewed by Srivastava, 2006).

We validated Cdx2 binding by ChIP-PCR within the genomic loci of select cardiac transcription factors, using primers flanking canonical CDREs within Cdx2 ChIP-seq peaks and chromatin isolated from E8.5 embryos (Figure 34C). This analysis confirmed Cdx2 occupancy at a number of cardiac gene loci, including *Tbx5*, *Gata4*, *Hand1* and *Hand2* (Figure 34D). Cdx2 binding to the promoter region of *Cyp26A1*, a previously characterized Cdx2 target (Savory et al., 2009a), was included as a positive control. Exon 4 of *Wnt3a* is not occupied by Cdx2 (Nguyen et al., 2017) and no increase in Cdx2 binding relative to IgG was seen at this region. Additionally, *Mef2c*, a cardiac marker specific to the second heart field (Verzi et al., 2005), was found to have a peak score of only 56.26 in

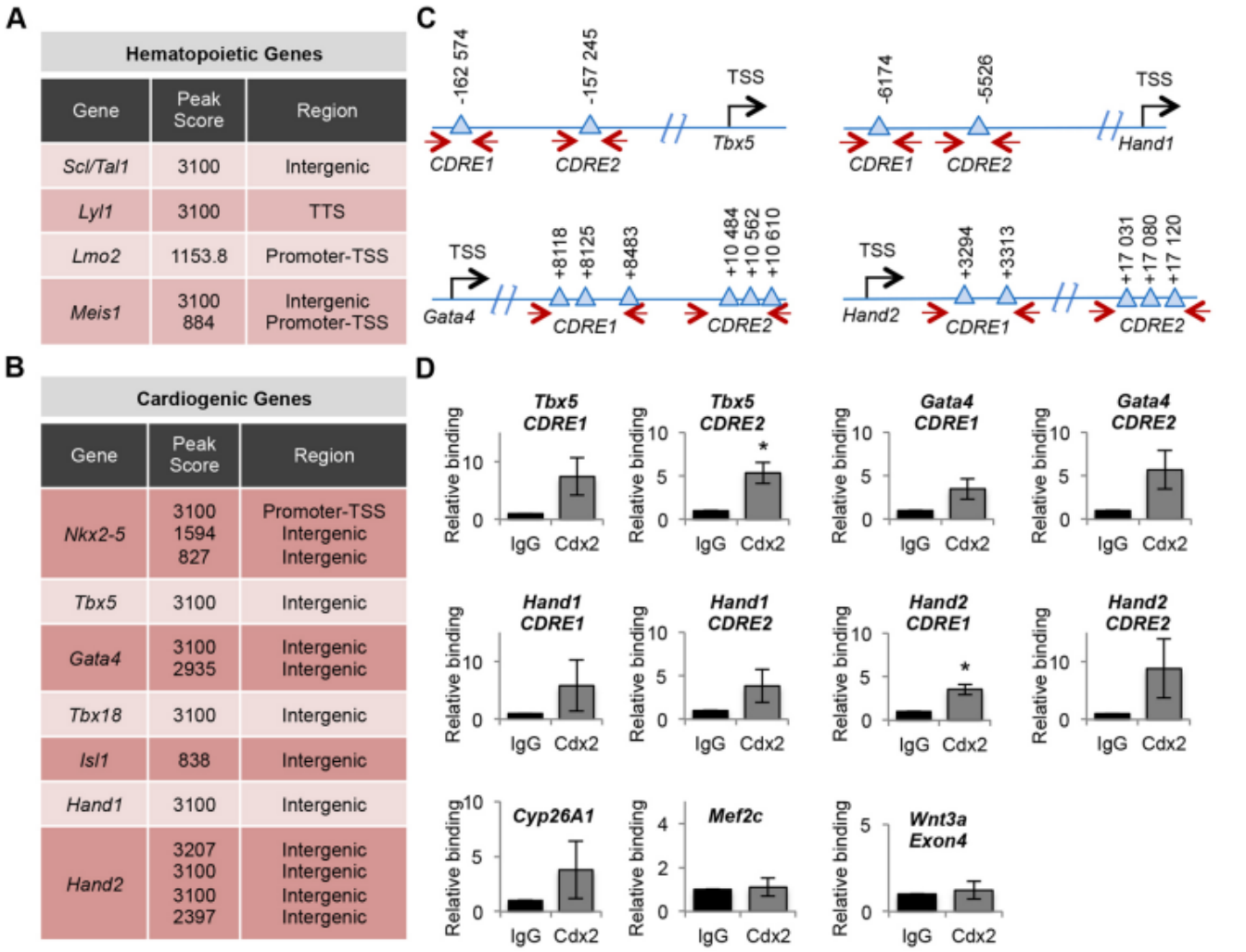


Figure 34. Enriched Cdx2 binding at hematopoietic and cardiac gene loci. A, B. Genes enriched for Cdx2 binding with known roles in hematopoiesis (A) or cardiogenesis (B) identified by ChIP-seq. Peak scores, indicative of the level of Cdx2 binding above background, are noted. **C.** Schematics of CDREs, identified using TRANSFAC analysis of sequences under ChIP-seq peaks. Regions of complementarity for ChIP-PCR primers flanking CDREs (blue triangles) are indicated by red arrows. **D.** Validation of Cdx2 binding at cardiac loci by ChIP-PCR using primers described in C. Error bars represent s.e.m. from three biological replicates. *Cyp26A1* was used as a positive control and *Wnt3a Exon4* and *Mef2c* as negative controls. *P≤0.05 (determined by two-tailed t-test).

the ChIP-seq dataset, and was not detected by ChIP-PCR. Thus, this locus served as a cardiac-specific negative control for Cdx2 binding in these experiments.

Cdx function is required for normal cardiac gene expression and heart tube morphogenesis

Cdx2$^{F/F}$*Actin::Cre-ER*^{T} mutants (Savory et al., 2009a) were crossed with germline *Cdx1*-nulls (Subramanian et al., 1995), generating *Cdx1*$^{-/-}$*Cdx2*$^{F/F}$*Actin::Cre-ER*^{T} compound mutants as previously described (Savory et al., 2011a). Post-implantation *Cdx1-Cdx2* compound conditional null mutants (hereafter referred to as DKO) lose expression of *Cdx4*, becoming functionally Cdx-null and thus circumventing both the peri-implantation lethality of Cdx2-null mutation and functional overlap between family members (Savory et al., 2011a, 2009a; van den Akker et al., 2002; van Nes et al., 2006; Young et al., 2009). DKO mutants in which Cdx2 deletion was induced at E5.5 (i.e. prior to the normal onset of embryonic Cdx expression) developed beating heart tubes at E9.5 but exhibited a distended pericardial sac and aberrant heart tube morphology, and typically died at E10.5 (Savory et al., 2011a; Figure 35A). Additionally, in situ hybridization (ISH) revealed that the ventricular marker *Mlc2v* (*Myl2*) (Franco et al., 1999) was reduced in intensity and spatially restricted in the mutant heart tubes relative to controls (Figure 35B).

The heart defects observed in DKO mutants were variable, potentially as a result of differences in the embryonic stage at which Cdx2 deletion was induced. To investigate this, tamoxifen was administered at E4.5 to assess whether loss of Cdx function at an earlier stage might exacerbate the cardiac phenotype. This earlier deletion, however, resulted in fully penetrant embryonic lethality, likely because of the requirement for Cdx2 during implantation (Chawengsaksophak et al., 1997). Although tamoxifen treatment at E6.5 also resulted in cardiac defects (Figure 36), these were less severe than those elicited by Cdx2 deletion at E5.5, suggesting a narrow developmental window during which loss of Cdx function impacts heart development.

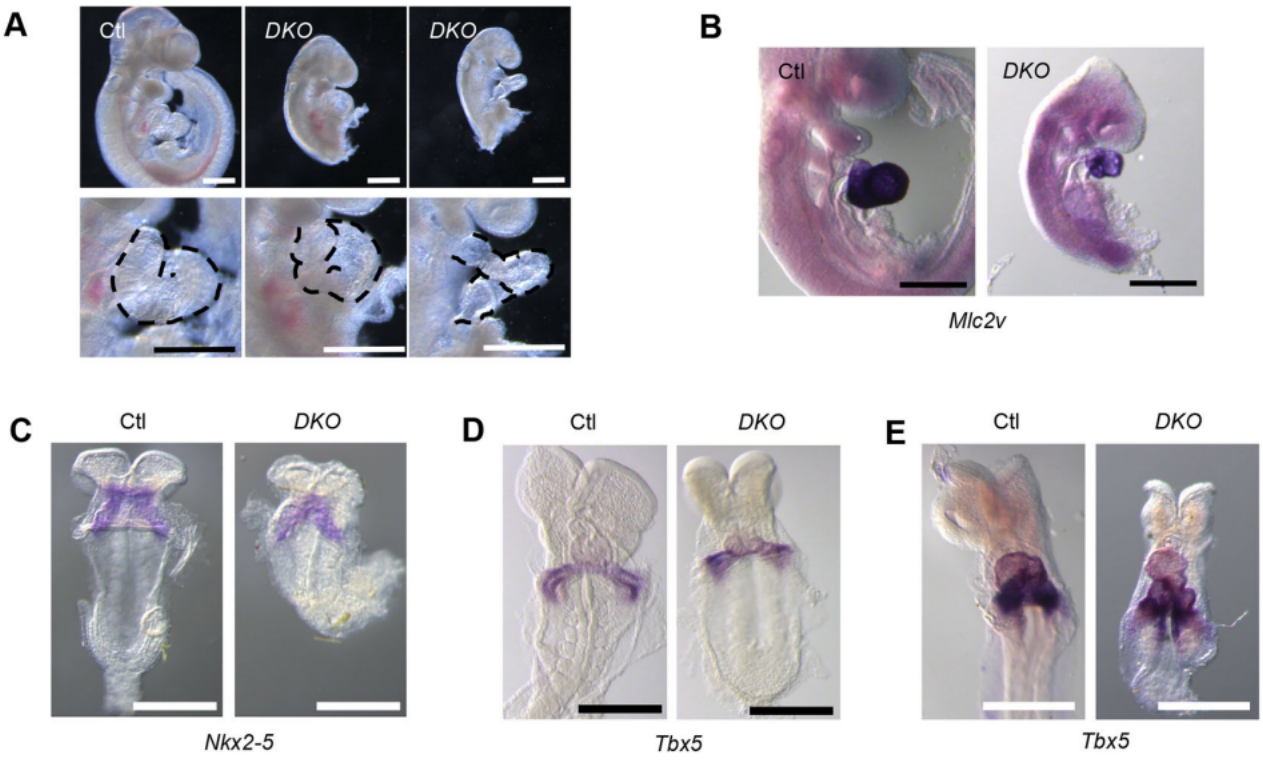


Figure 35. Cardiac defects and altered expression of heart field markers in Cdx mutants. A. Morphological changes to the heart tube in E9.5 Cdx mutants (DKO) relative to a stage-matched control (Ctl). Bottom panels show enlarged images with the heart tubes indicated by dashes. **B.** In situ hybridization for *Mlc2v* in E9.5 DKO embryos and a stage-matched control (Ctl). Images are representative of 3/3 controls and 2/2 mutants. **C.** In situ hybridization analysis of *Nkx2-5* expression in E8.5 wild-type (Ctl) and DKO embryos. *Nkx2-5* expression was affected in 4/4 DKO embryos, and only 1/6 controls. **D.** In situ hybridization analysis of *Tbx5* in E8.5 Ctl and DKO embryos. *Tbx5* expression was affected in 3/3 DKO embryos, compared with 5 controls with normal expression. **E.** In situ hybridization analysis of *Tbx5* in E9.5 Ctl and DKO embryos. *Tbx5* expression was affected in 1/2 DKO embryos compared with 7 normal controls. For each experiment, embryos were stage-matched and processed in parallel. Scale bars: 0.5 mm.

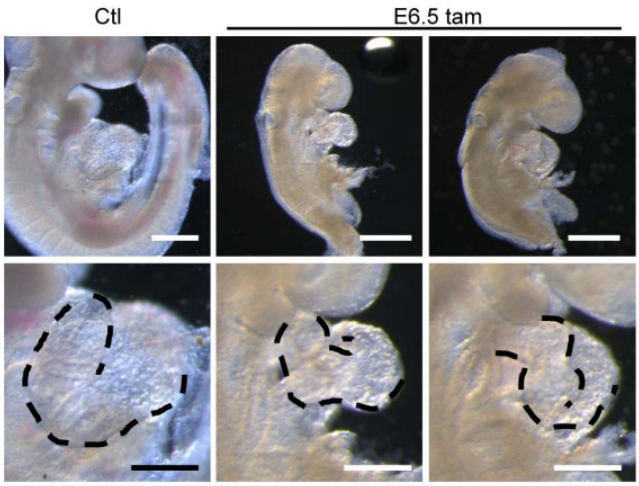


Figure 36. Tamoxifen-mediated Cdx deletion induces a cardiac phenotype. Cardiac defects in E9.5 mutants treated with tamoxifen at E6.5 compared to stage-matched control. Scale bars, 0.5mm (top) and 0.25mm (bottom). Images are representative of 8-9 mutants and 4/7 wild type controls.

To characterize further the effect of Cdx loss of function on cardiogenesis, the expression of *Nkx2-5* and *Tbx5*, early markers of cardiac progenitors (Bruneau et al., 1999; Komuro and Izumo, 1993; Lints et al., 1993) and highly enriched for Cdx2 occupancy (Figure 34B), were assessed by ISH. At E8.5, *Nkx2-5* transcripts were distributed in a triangle-like expression domain in DKO embryos rather than the cardiac crescent labeling typically observed in controls (Figure 35). At this stage, *Tbx5* transcripts were also localized to the cardiac crescent in control embryos, whereas DKO mutants exhibited broader lateral distribution of *Tbx5*-positive cells that tapered toward the midline (Figure 35D). At E9.5, *Tbx5* expression in DKO embryos was even less spatially restricted relative to controls (Figure 35E), consistent with prior observations in *cdx1a/4*-deficient zebrafish embryos (Lengerke et al., 2011).

Cdx represses cardiac gene expression in the yolk sac

Prior work has shown that Cdx function is required for proper yolk sac vascularization and hematopoiesis, and this may occur, in part, through Cdx-dependent regulation of *Scl* expression

(BrookeBisschop et al., 2017; Wang et al., 2008). In this regard, both cardiac and yolk sac hematopoietic progenitors are derived from a common pool of multi-potential *Mesp1*$^{+}$ mesodermal precursors (Chan et al., 2013). *Mesp1*$^{+}$ mesoderm fated to give rise to early blood lineages must therefore initiate the expression of a hematopoietic gene expression program while simultaneously repressing the expression of genes involved in cardiogenesis (Chan et al., 2013). To determine whether the loss of hematopoietic potential in DKO mutant yolk sacs is accompanied by ectopic cardiac differentiation, indicative of a fate switch in the absence of Cdx, cardiac gene expression was assessed by qRT-PCR in E8.5 and E9.5 DKO yolk sacs and compared with littermate controls. Ectopic expression of *Tbx5* was observed in mutant yolk sacs at both stages (Figure 37A), consistent with a role for Cdx in repressing cardiac differentiation in this lineage. In contrast, variable changes in expression were observed for yolk sac *Nkx2-5* and *cTnT* (*Tnnt2*) (Figure 37B, C), suggesting that such Cdx-dependent repression may be specific to *Tbx5*.

Mesodermal Cdx function is essential for heart tube morphogenesis

In addition to mesoderm-intrinsic processes, signals from both the endoderm and the ectoderm impact heart development (Zaffran and Frasch, 2002). As the conditional mouse model employed here uses a *CMV-Actin::Cre-ER*^{T} transgene to induce global *Cdx2* gene deletion, the loss of Cdx function on cardiogenesis may occur through non-mesodermal pathways. To investigate this, we utilized a *Mesp1-Cre* knock-in allele (*Mesp1*$^{+/Cre}$; Saga et al., 1999) to effect Cdx2 deletion. *Mesp1* expression initiates at E6.5, and descendant cells contribute to cardiac progenitors of both the first and second heart fields, hematopoietic and endothelial progenitors in the yolk sac, and myogenic mesoderm (Devine et al., 2014; Chan et al., 2013; Saga et al., 1999).

At E11.5, *Cdx1*$^{-/-}$*Cdx2*$^{F/F}$*Mesp1*$^{+/Cre}$ mutants appeared smaller than littermate controls, lacked red blood cells, exhibited a malformed heart with pericardial edema (Figure 38A), and were never

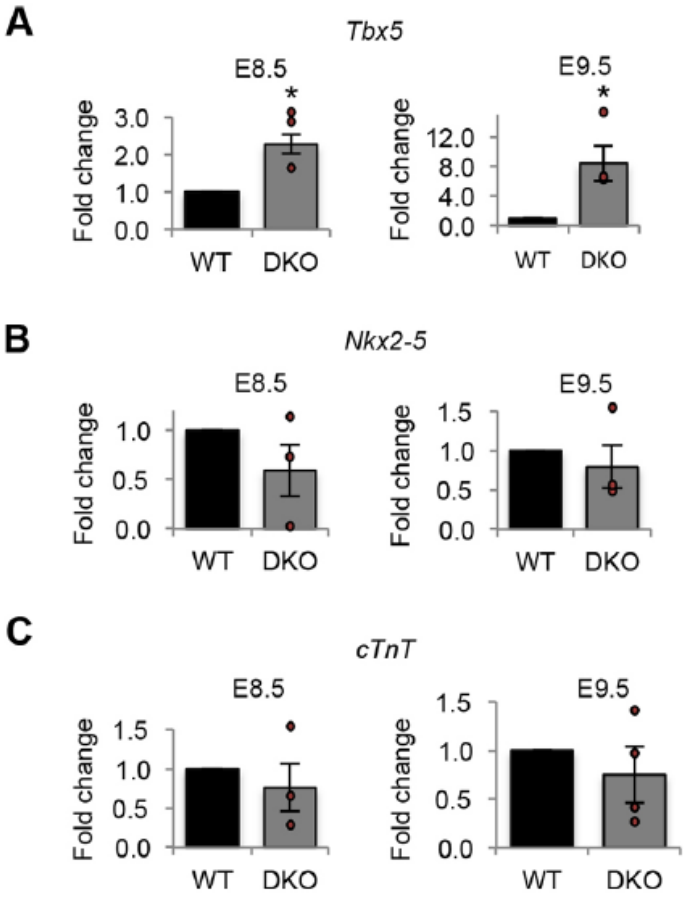


Figure 37. Cardiac genes are ectopically expressed in Cdx-deficient yolk sacs. A-C. *Tbx5* (A), *Nkx2-5* (B) and *cTnT* (C) expression levels were assessed in E8.5 and E9.5 yolk sacs collected from DKO or littermate control (WT) embryos by qRT-PCR or RT-PCR. Error bars represent s.e.m. from a minimum of three independent experiments. *P≤0.05 (determined by two-tailed t-test).

recovered beyond E12.5. E8.0 *Cdx1*$^{-/-}$*Cdx2*$^{F/F}$*Mesp1*$^{+/Cre}$ mutants and littermate controls were assessed for *Nkx2-5* expression, which marks cardiac progenitors of both the first and second heart fields (Stanley et al., 2002). In contrast to Cdx DKO mutants, *Nkx2-5* expression in these embryos was indistinguishable from controls (Figure 38B), suggesting that the cardiac defects observed in *Cdx1*$^{-/-}$*Cdx2*$^{F/F}$*Mesp1*$^{+/Cre}$ mutants either manifest after E8.0, or occur through mechanisms that do not impact *Nkx2-5*.

In E9.5 embryos, expression of Mlc2v was comparable in the prospective ventricles in *Cdx1*$^{-/-}$*Cdx2*$^{F/F}$*Mesp1*$^{+/Cre}$ mutants and littermate controls (Figure 38C, D). However, the positioning of the heart was affected in the mutants, which also exhibited a narrowed outflow track (Figure 38D, arrowhead) and underdevelopment of the right ventricle. These observations suggest that *Mesp1*$^{+/Cre}$-mediated deletion of Cdx2 results in a milder cardiac phenotype than that elicited by *CMV-Actin::CreER*^{T}. Consistent with this, although the tail buds of E9.5 *Cdx1*$^{-/-}$*Cdx2*$^{F/F}$*Mesp1*$^{+/Cre}$ embryos were foreshortened relative to controls, they did not exhibit the severe axial truncation consistently observed in DKO mutants (Figure 38C; Savory et al., 2011a). These differences may be due to Cdx deletion in axial progenitors in the tail bud of *Cdx1*$^{-/-}$*Cdx2*$^{F/F}$ *CMV-Actin::CreER*^{T} mutants, whereas *Mesp1*$^{+/Cre}$ is not anticipated to impact this niche (Saga et al., 1999; Chan et al., 2013).

Cre-negative *Cdx1*$^{-/-}$*Cdx2*$^{F/F}$ embryos did not display obvious cardiac defects, nor did *Cre*$^{+}$ littermates heterozygous for *Cdx2* (*Cdx1*$^{-/-}$*Cdx2*$^{+/F}$*Mesp1*$^{+/Cre}$; data not shown), consistent with prior findings (Subramanian et al., 1995; van den Akker et al., 2002). These defects were also not induced by expression of Cre alone in either model (*Mesp1-Cre* or *CMV-Actin::CreER*^{T}), with or without tamoxifen treatment (data not shown).

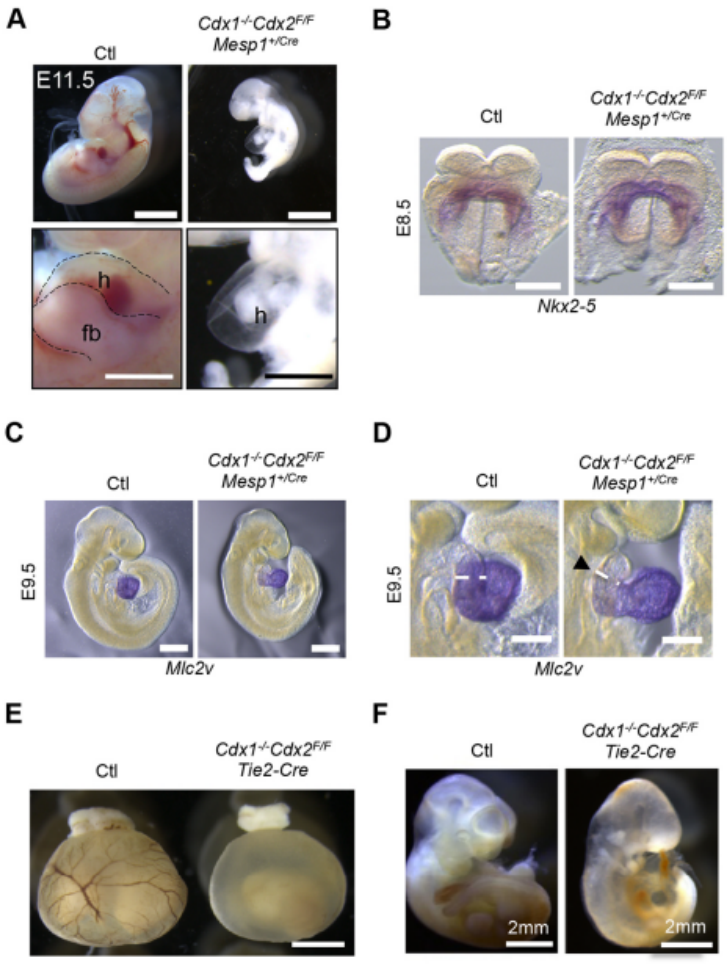


Figure 38. Aberrant cardiac morphogenesis in *Cdx1*$^{-/-}$*Cdx2*$^{F/F}$*Mesp1*$^{+/Cre}$ mutants. **A.** Representative images of a *Cdx1*$^{-/-}$*Cdx2*$^{F/F}$*Mesp1*$^{+/Cre}$ mutant and littermate control (Ctl) at E11.5. An enlarged view of the mutant heart shown in the panel below illustrates a distended pericardial sac, malpositioning of the heart, and the absence of blood typical of these mutants. Images are representative of 7/9 mutants and 14 littermate controls. fb, forelimb bud; h, heart. **B-D.** In situ hybridization analysis of *Nkx2-5* and *Mlc2v* in *Cdx1*$^{-/-}$*Cdx2*$^{F/F}$*Mesp1*$^{+/Cre}$ mutants and littermate controls. Images are representative of 1 mutant and 8 littermate controls for *Nkx2-5* staining, and 2/3 mutants and 5 littermate controls for *Mlc2v* staining. Axial truncation in E9.5 *Cdx1*$^{-/-}$*Cdx2*$^{F/F}$*Mesp1*$^{+/Cre}$ mutants is shown in D. Arrowhead indicates the outflow tract, which is narrowed in the *Cdx1*$^{-/-}$*Cdx2*$^{F/F}$*Mesp1*$^{+/Cre}$ mutant, as demonstrated by the dashed line. **E.** Representative images of *Cdx1*$^{-/-}$*Cdx2*$^{F/F}$*Tie2-Cre* (n=3) and littermate control (n=3) yolk sacs at E10.5. **F.** Representative images of 4/4 *Cdx1*$^{-/-}$*Cdx2*$^{F/F}$*Tie2-Cre* mutant embryos and 1/1 littermate control at E10.5. Scale bars: 0.25 mm (B, C); 0.5 mm (D); 1 mm (A, bottom); 2 mm (A, top; E, F).

Cardiogenesis requires Cdx function in the yolk sac

In addition to aberrant cardiac morphogenesis, *Cdx1*$^{-/-}$*Cdx2*$^{F/F}$*Mesp1*$^{+/Cre}$ mutants exhibited defective yolk sac vascularization similar to that observed in DKO mutants (Figure 39; Brooke-Bisschop et al., 2017). Deficiency in yolk sac hematopoiesis can lead to pericardial edema (Shivdasani et al., 1995; Moser et al., 2004). It is therefore possible that the cardiac defects in Cdx mutants are secondary to the failure of yolk sac hematopoiesis. To assess this, a *Tie2*$^{+/Cre}$ transgenic line, in which expression of the Cre recombinase is largely restricted to endothelial and hematopoietic lineages (Tang et al., 2010), was used to delete *Cdx2* in a *Cdx1*-null background as previously described (Brooke-Bisschop et al., 2017). In addition to being smaller than littermate controls and deficient in yolk sac hematopoiesis (Figure 38E, F; Brooke-Bisschop et al., 2017), *Cdx1*$^{-/-}$*Cdx2*$^{F/F}$*Tie2*$^{+/Cre}$ embryos displayed aberrant cardiac morphology at E10.5, with distended pericardial sacs and a narrow, misshapen heart tube (Figure 38F). It may be that the loss of Cdx function impacts cardiac development secondary to yolk sac hematopoiesis; however, misexpression of *Tbx5* and *Nkx2-5* in DKO mutant embryos was observed at E8.5, before circulatory defects are anticipated to influence cardiac morphogenesis. Furthermore, Cdx2 binding occurs at the genomic loci of a number of cardiac targets, also at E8.5 (Figure 33B-D). Although it is impossible to distinguish between the two, these data suggest that the aberrant cardiac morphogenesis observed in Cdx mutants likely results from a combination of defects that are both primary and secondary to Cdx deletion.

Cdx2 expression is coincident with cardiac progenitor specification

Cdx2 expression has been reported in the chorion, ectoplacental cone, primitive streak and allantois as early as E7.5 (Beck et al., 1995); however, the contribution made by *Cdx2*$^{+}$ cells and their descendants to the cardiac lineage is unknown. Moreover, this pattern of *Cdx2* expression is inconsistent with a role in cardiac mesoderm specification from *Mesp1*$^{+}$ progenitors, which commences

at E6.5 (Saga et al., 1996; 2000; Bondue et al., 2008). To address these discrepancies, we analyzed single cell RNA-seq data generated by Scialdone and colleagues (Scialdone et al., 2016), which revealed that Cdx2 transcripts are indeed present in the murine embryo as early as E6.5 (Figure 40A-D). Cdx1 transcripts were also identified at this stage, whereas Cdx4 transcripts were rare (Figures 41, 42). *Cdx2*$^{+}$ cells were found within the epiblast at E6.5 in nascent mesoderm, posterior mesoderm, allantois and blood progenitors, among others (Figure 40C). Whole-mount immunohistochemistry also

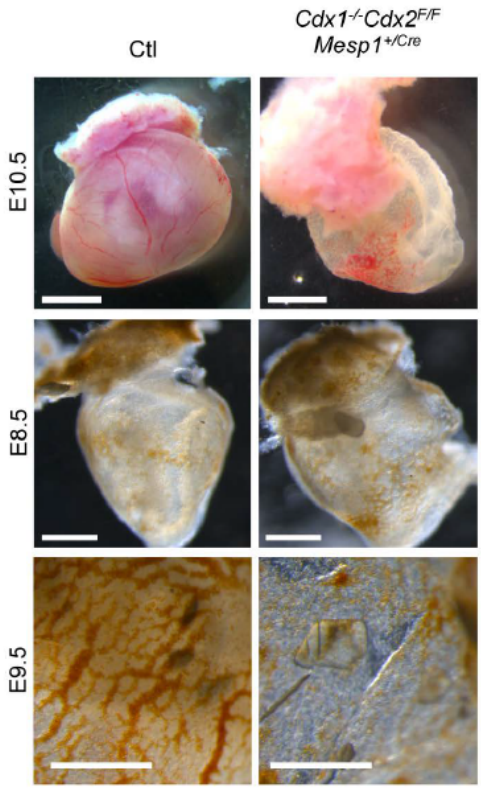


Figure 39. Disrupted yolk sac vascularization in *Cdx1*$^{-/-}$*Cdx2*$^{-/-}$*Mesp1*$^{+/Cre}$ mutants. *Cdx1*$^{-/-}$*Cdx2*$^{F/F}$*Mesp1*$^{+/Cre}$ and littermate control embryos with affixed yolk sacs collected at E10.5, E8.5, and E9.5 and DAB stained. Scale bars, 2mm (top panel) and 0.5mm (middle and bottom panel). Images at E10.5 are representative of 3/4 mutants and 7/7 controls; E9.5, 2/3 murtants and 3/3 controls; E8.5, 1/1 mutant and 4/4 controls.

revealed Cdx2 in the E6.5 embryo, including the anterior region of the primitive streak (Figure 40E), corresponding with the region associated with cardiac mesoderm specification and egression. In addition, *Cdx2* transcripts were detected in E6.5 embryos by RT-PCR in both embryonic and extraembryonic material (Figure 40F), and *Cdx1*, and to a lesser extent *Cdx4*, were also expressed (Figure 43). Consistent with previous reports (Beck et al., 1995; Mcdole and Zheng, 2012), Cdx2 levels were more robust at E7.5 (Figure 40E). Taken together, these data demonstrate that Cdx2 is present in the appropriate region and at the appropriate developmental stage to be able to impact cardiac progenitors directly.

Cdx2-positive cells frequently co-expressed *Mesp1* (Figure 40G), but rarely expressed *Tbx5* or *Mef2c*, markers of the first and second heart fields, respectively (Figure 40I,J; Bruneau et al., 1999; Verzi et al., 2005). Although there was a weak correlation between Cdx2 expression and that of additional heart markers (Figure 44), these genes, as well as Cdx, are also expressed in other mesodermal lineages. Correlations between *Cdx1* or *Cdx4* expression and the expression of *Mesp1*, *Tbx5* and *Mef2c* were similar to those observed between Cdx2 and these transcripts (Scialdone et al., 2016; data not shown), in agreement with functional overlap among Cdx family members. Conversely, a subset of $Cdx2^{+}$ cells co-expressed *Scl* (Figure 40H) and other hematopoietic markers (Figure 44). Taken together, these data are consistent with a role for Cdx2 in repressing cardiogenic, and promoting hematopoietic, differentiation in $Mesp1^{+}$ progenitors.

Cdx2 co-occupies cardiogenic loci with Brg1

Brg1, the catalytic subunit of the SWI/SNF chromatin remodeling complex, is required for mesoderm induction and cardiac progenitor specification in differentiating embryonic stem cells (ESCs; Alexander et al., 2015), as well as heart development (Stankunas et al., 2008; Hang et al., 2010). Cdx2physically associates with Brg1, and other members of the SWI/SNF complex, and Cdx2-

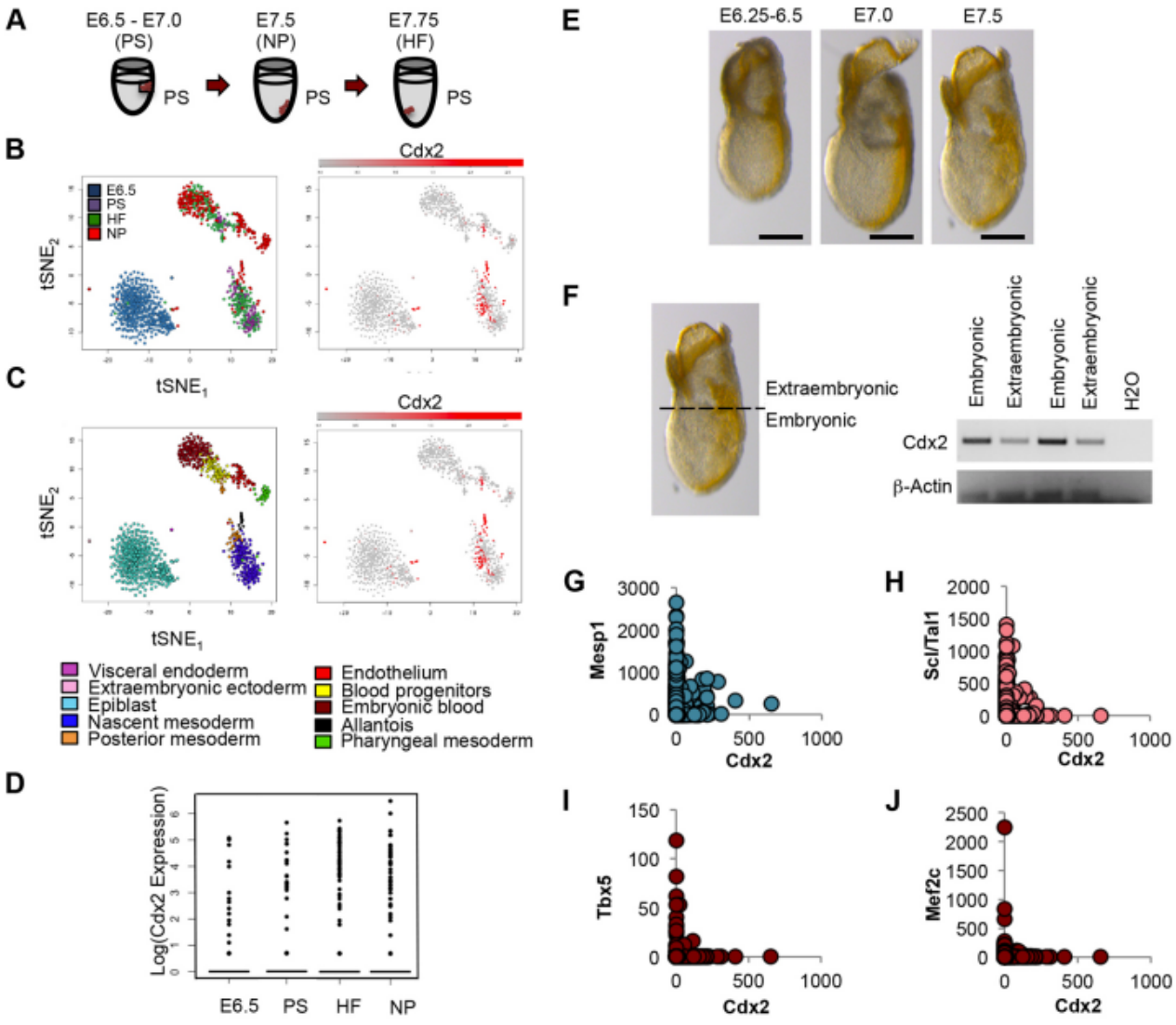

A
E6.5 - E7.0
(PS)
E7.5
(NP)
E7.75
(HF)
PS
PS
PS
B
Cdx2
E6.5
PS
HF
NP
tSNE2
tSNE1
C
Cdx2
tSNE2
tSNE1
Visceral endoderm
Extraembryonic ectoderm
Epiblast
Nascent mesoderm
Posterior mesoderm
Endothelium
Blood progenitors
Embryonic blood
Allantois
Pharyngeal mesoderm
D
Log(Cdx2 Expression)
E6.5
PS
HF
NP
E
E6.25-6.5
E7.0
E7.5
F
Extraembryonic
Embryonic
Embryonic
Extraembryonic
Embryonic
Extraembryonic
H2O
Cdx2
β-Actin
G
Mesp1
Cdx2
H
Scl/Tal1
Cdx2
I
Tbx5
Cdx2
J
Mef2c
Cdx2

Figure 40. Cdx2 is expressed in mesodermal progenitors. A. Schematic of embryonic development between E6.5 and E7.75 corresponding to the time points at which single cell RNA-seq (Scialdone et al., 2016) was performed as shown in B, C. Red circles represent cardiac progenitors as they are specified and migrate anterolaterally to form the heart fields. HF, head fold; NP, neural plate; PS, primitive streak. **B.** Cdx2 transcripts in cells isolated from embryos at E6.5 (epiblast, blue), primitive streak (E7.0, purple), head fold (E7.5, green) and neural plate (E7.75, red) stages. **C.** Cells in B were color-coded according to cell lineage as indicated in the key. tSNE, t-distributed stochastic neighbor embedding. **D.** Cdx2 transcript abundance was plotted as log expression according to embryonic stage using the single cell RNA-seq dataset generated by Scialdone and colleagues (Scialdone et al., 2016). **E.** Immunohistochemistry illustrating the presence of Cdx2 protein in the primitive streak region of wild-type embryos at E6.5-E7.5. Scale bars: 0.25 mm. **F.** Left: Image of an E7.5 embryo with the boundary between the embryo proper and the extra-embryonic region indicated by a dashed line. Right: Cdx2 transcripts were detected in both embryonic and extra-embryonic material from independent E6.5 embryos by RT-PCR. β-Actin was used as a loading control. **G-J.** Single cell RNA-seq data (Scialdone et al., 2016) was used to assess correlations between cells expressing *Cdx2* and *Mesp1* (mesoderm; **G**), *Tbx5* (first heart field; *I*), *Mef2c* (second heart field; **J**), or *Scl* (hematopoietic progenitors; **H**) between E6.5 and E7.75.

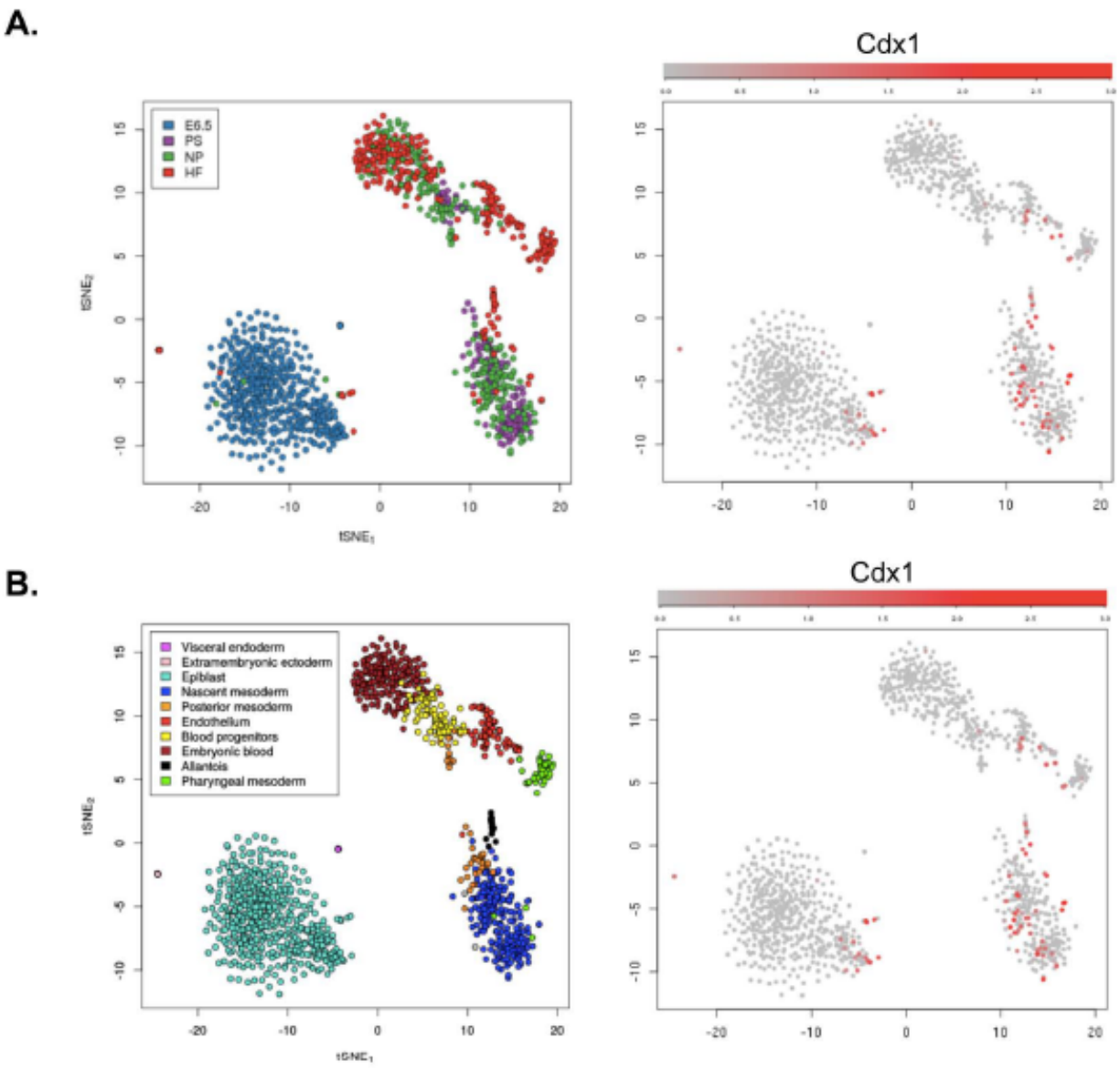


Figure 41. Cdx1 expression in E6.5-E7.75 embryos by single-cell RNA-seq. A. *Cdx1* transcripts were detected in cells isolated from embryos at E6.5 (epiblast, blue), primitive streak stage (E7.0, purple), neural plate stage (E7.5, green), and head fold stage (E7.75, red) embryos (Scialdone et al., 2016). **B.** Cdx1 transcripts were detected in cells associated with a number of progenitor lineages, including epiblast cells (turquoise), nascent mesoderm (blue), posterior mesoderm (orange), pharyngeal mesoderm (green), endothelium (red), blood progenitors (yellow), and extraembryonic ectoderm (pink).

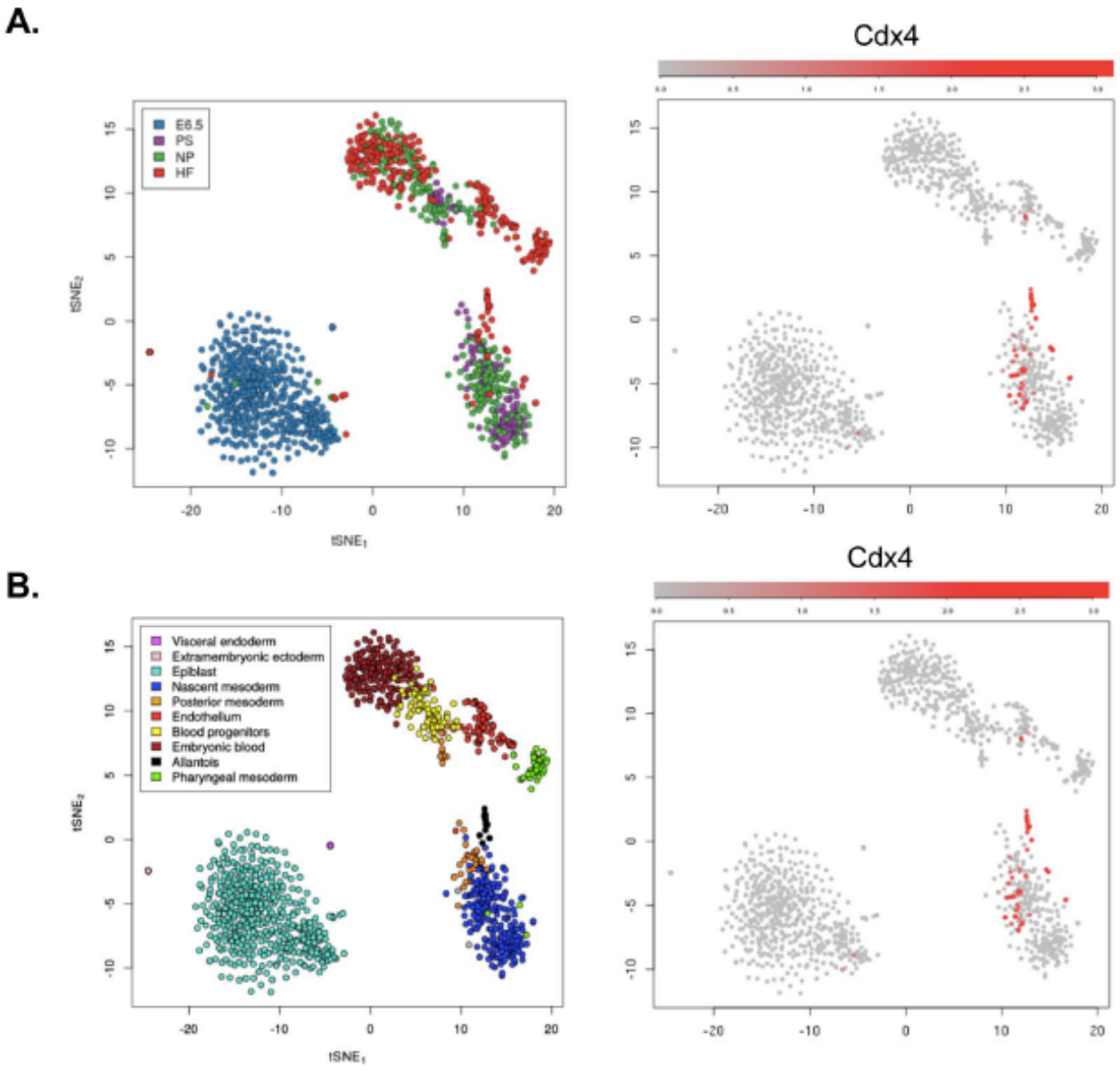


Figure 42. Cdx4 expression in E6.5-E7.75 embryos by single-cell RNA-seq. A. *Cdx4* transcripts were detected in cells isolated from embryos at E6.5 (epiblast, blue), primitive streak stage (E7.0, purple), neural plate stage (E7.5, green), and head fold stage (E7.75, red) embryos (Scialdone et al., 2016). **B.** *Cdx4* transcripts were detected in cells associated with a number of progenitor lineages, including epiblast cells (turquoise), endothelium (red), allantois (black), nascent mesoderm (Blue), and posterior mesoderm (orange).

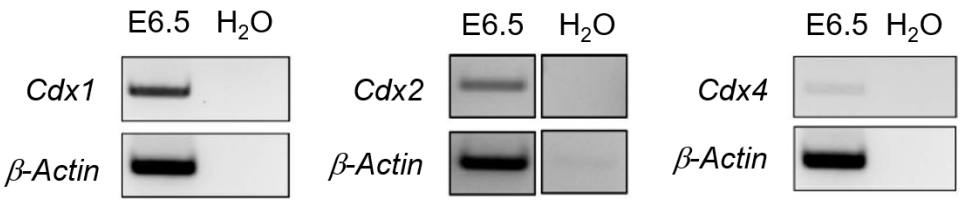


Figure 43. Cdx1, Cdx2, and Cdx4 are expressed in E6.5 whole embryos. *Cdx1*, *Cdx2*, and *Cdx4* transcripts were detected in pooled litters of E6.5 embryos by RT-PCR. *β-Actin* was used as a loading control. RT-PCR images are representative of four independent experiments in which similar results were obtained.

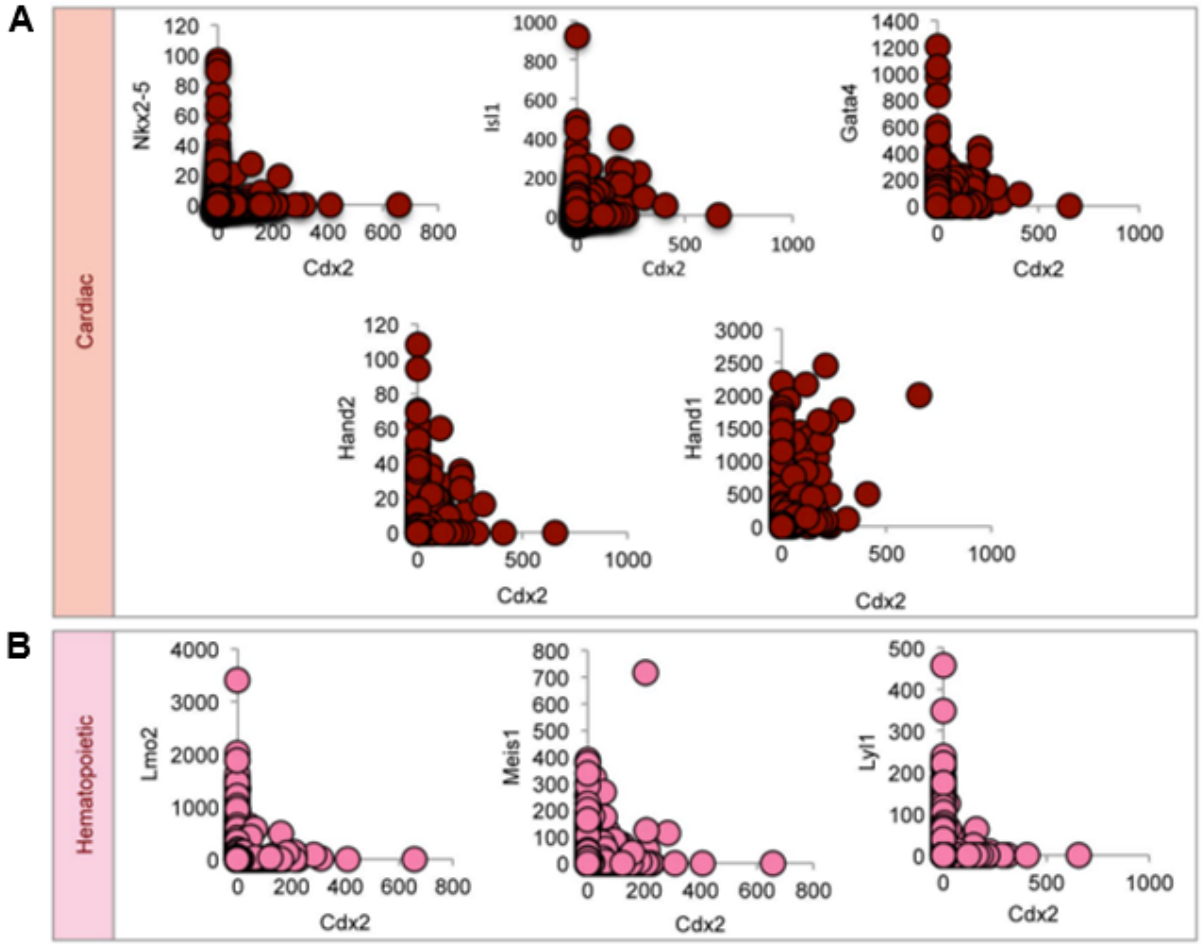


Figure 44. Cdx2 expression relative to cardiac and hematopoietic marker genes in E6.25-7.5 embryos. Correlation plots were generated using a single-cell RNA-seq dataset generated by Scialdone and colleagues (Scialdone et al., 2016) using E6.25-7.5 whole embryos to demonstrate co-expression of *Cdx2* and select cardiac (A) and hematopoietic (B) transcripts.

dependent expression of at least some targets is associated with chromatin remodeling events (Nguyen et al., 2017; Verzi et al., 2010, 2013). To determine whether a similar association between Cdx2 and Brg1 was observed at cardiogenic loci, the Cdx2 ChIP-seq data were intersected for Brg1 chromatin occupation derived from ChIP-seq analysis of ESCs at the mesoderm stage of directed differentiation to cardiomyocytes (Alexander et al., 2015). This exercise revealed a number of cardiac loci occupied by both Cdx2 and Brg1, including *Tbx5*, *Nkx2-5*, *Gata4*, *Hand1* and *Hand2*, whereas the *Isl1* locus was occupied by Cdx2 only (Figure 45A).

To determine whether Brg1 occupies Cdx2-bound cardiac genes in a Cdx-dependent manner, ChIP-PCR was performed for Brg1, comparing wild-type with DKO embryos at E9.5 (Figure 45B). Brg1 binding was impaired within Cdx2-occupied regions of *Tbx5*, *Gata4* and *Nkx2*-5 genes as well as the previously characterized Cdx targets *Cyp26A1* and *Dll1* (Savory et al., 2009a; Grainger et al., 2012). These findings are consistent with a model whereby Cdx2 recruits Brg1 to select cardiac targets to regulate gene expression via SWI/SNF chromatin remodeling.

To determine whether impaired Brg1 binding to cardiac targets results in altered chromatin organization, formaldehyde-assisted isolation of regulatory elements (FAIRE)-PCR was used to compare chromatin accessibility between wild type and DKO mutants. Given the ectopic cardiac gene expression observed in yolk sacs, and that hematopoietic yolk sac mesoderm shares a common *Mesp1*$^{+}$ progenitor with the cardiac lineage, yolk sacs from wild-type and DKO embryos at E9.5 were used for these experiments. Changes in chromatin accessibility at Cdx2-occupied CDREs were observed at *Tbx5*, *Gata4* and *Nkx2-5* loci, whereas accessibility at the *β-actin* locus remained unaffected in DKO yolk sacs, and thus served as a negative control (Figure 45C). Although these changes were variable and did not reach statistical significance, likely owing to the cellular heterogeneity of the yolk sac, they are consistent with Cdx-dependent chromatin organization and in agreement with prior observations in other systems (Verzi et al., 2010, 2013; Nguyen et al., 2017; Saxena et al., 2017).

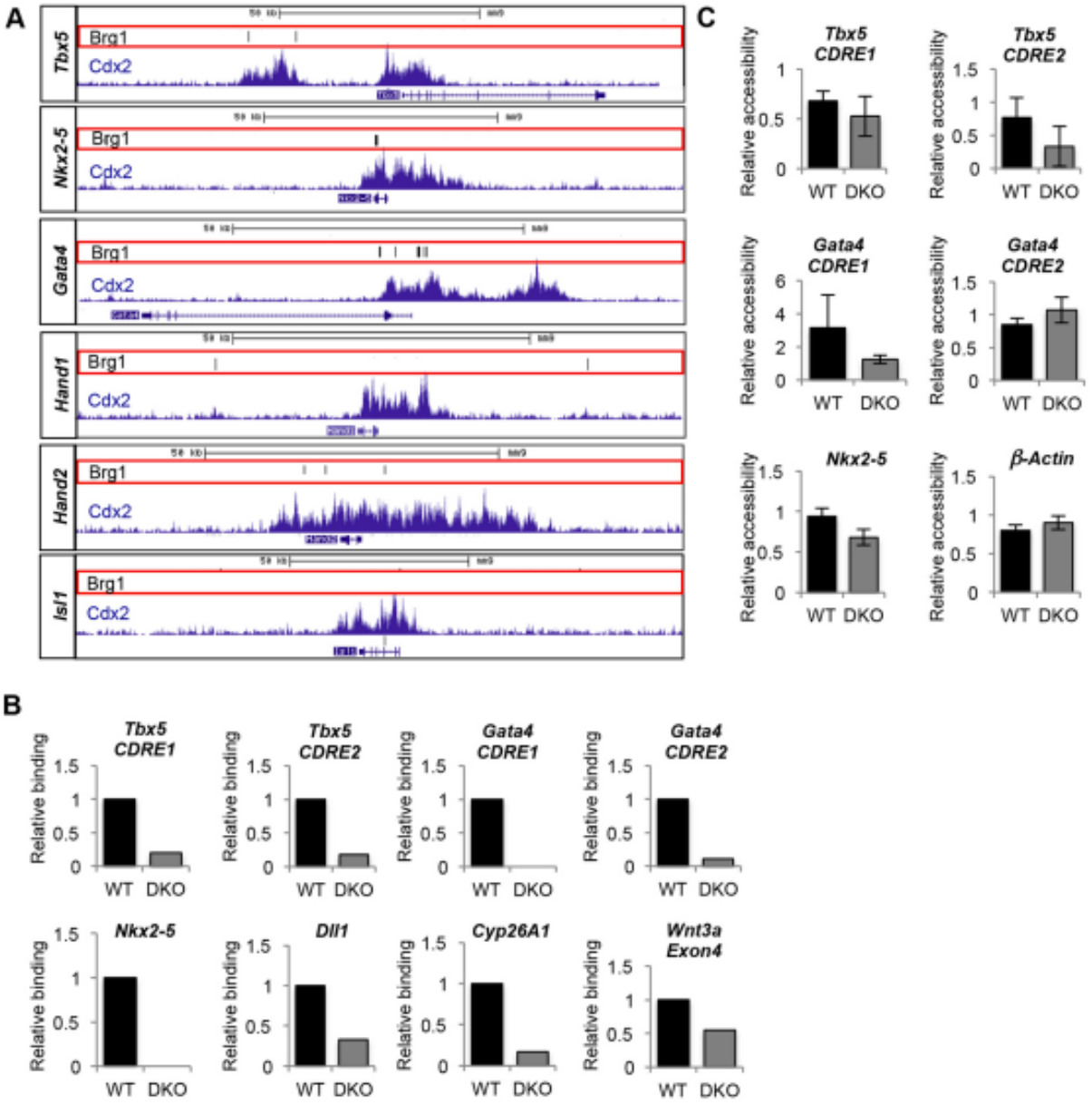


Figure 45. Cdx2 and Brg1 co-occupy cardiac transcription factor loci. A. Brg1 ChIP-seq tracks from ESCs at the mesoderm stage of directed differentiation to cardiomyocytes (Alexander et al., 2015) were intersected with Cdx2 ChIP-seq data from E8.5 embryos at *Tbx5*, *Nkx2-5*, *Gata4*, *Hand1*, *Hand2* and *Isl1* genes. Brg1 tracks are outlined in red with regions of enriched binding indicated by black vertical bars; Cdx2 tracks are indicated below in blue. **B.** ChIP-PCR experiments assessing Brg1 binding at Cdx2-occupied cardiac loci in wild-type (WT) and DKO embryos at E9.5. Graphs are representative of two independent experiments in which similar results were obtained. **C.** FAIRE-PCR-mediated assessment of chromatin accessibility in wild-type and DKO yolk sacs at E9.5. Values were normalized to input. Error bars represent s.e.m. from a minimum of three independent experiments. *β-Actin* was used as a negative control.

DISCUSSION

ChIP-seq analysis of Cdx2 occupancy in E8.5 embryos revealed a marked enrichment at loci encoding transcription factors, suggesting that Cdx coordinates gene regulatory networks essential to numerous developmental processes, a finding consistent with the complex phenotype of Cdx-null mutants (Beck, et al., 1995; Gamer and Wright, 1993; Meyer and Gruss, 1993; van den Akker et al., 2002; Strumpf et al., 2005; Savory et al., 2009a, 2011; van Rooijen et al., 2012). A subset of these transcription factors are involved in cardiogenesis and hematopoiesis, both of which are known roles for Cdx (Lengerke et al., 2007; Wang et al., 2008; Brooke-Bisschop et al., 2017). Cardiac defects observed in Cdx DKO embryos, together with altered gene expression patterns, suggest that Cdx function is required for normal heart development, potentially governing fate decisions between hematopoietic and cardiac lineages from a common progenitor pool. Finally, Brg1 was recruited to a subset of cardiogenic loci in a Cdx-dependent manner. Together with the finding of altered chromatin architecture at some of these genes, these observations lead us to propose a model in which Cdx factors, transiently expressed in mesodermal progenitors within the primitive streak, occupy the loci of fate-determining transcription factors with Brg1 and the SWI/SNF complex, leading to establishment of the chromatin architecture required for the fidelity of subsequent gene expression programs at later developmental stages (Figure 46).

Cdx2 as a master developmental regulator

ChIP-seq analysis revealed that many of the robust Cdx2 peaks localized to transcription factor loci. Consistent with this, GO terms highly over-represented in this dataset included ‘transcription’, ‘positive and negative regulation of gene expression’ and ‘cell fate determination’, suggesting that Cdx2 impacts the expression of a number of transcriptional networks implicated in development. Indeed, transcription factors represented 226 of the 441 annotated peaks exhibiting binding above the

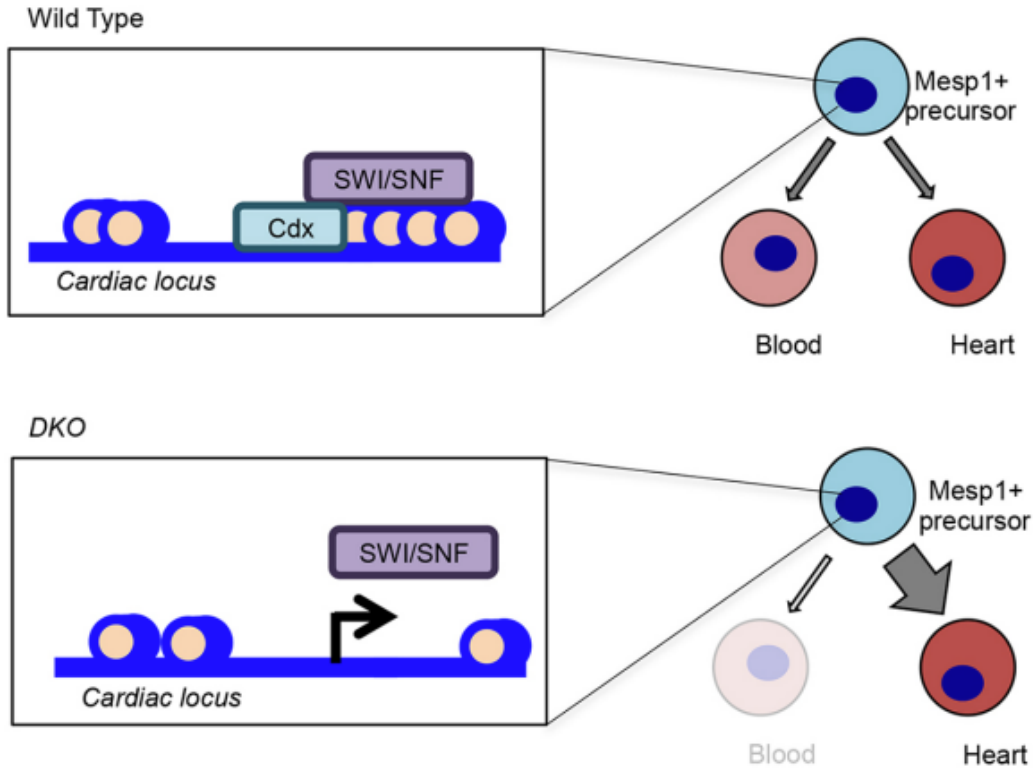


Figure 46. Proposed model for Cdx function in early mesoderm. Cdx recruits Brg1 and the SWI/SNF complex to cardiac loci in wild-type *Mesp1*$^{+}$ mesoderm, resulting in chromatin remodeling and subsequent gene silencing. This, in turn, maintains the balance between differentiation to cardiac and hematopoietic lineages from *Mesp1*$^{+}$ precursors. In Cdx DKO mutants, Brg1 is no longer recruited to cardiac targets, which results in increased chromatin accessibility and ectopic cardiac gene expression, perturbing the balance between commitment to hematopoietic and cardiac cell fates.

threshold of 800. This association is further reflected in some of the phenotypes exhibited by Cdx mutants. For example, *Cdx1*$^{-/-}$ and *Cdx2*$^{+/-}$ mice and compound mutant derivatives thereof typically display vertebral homeotic transformations associated with altered expression of Hox target genes (Subramanian et al., 1995; Chawengsaksophak et al., 1997). Cdx DKO and triple-knockout mutants exhibit precocious axial truncation, which may be ascribed, at least in part, to illicit RA signaling in the tailbud caused by loss of Cyp26A1 expression (Savory et al., 2009a; Young et al., 2009; Martin and Kimelman, 2010).

Cdx and mesodermal specification

Cdx2 was found to be resident at a number of genes encoding regulators of yolk sac hematopoiesis, consistent with previous work underscoring a requirement for Cdx in hematopoiesis in diverse vertebrate species (Brooke-Bisschop et al., 2017; Lengerke et al., 2007; Davidson and Zon, 2006; Davidson et al., 2003; Wang et al., 2008). In the present study, Cdx2 binding was also enriched at the loci of numerous cardiogenic transcription factors (e.g. *Nkx2-5*, *Tbx5*, *Gata4*, *Isl1*, *Hand1* and *Hand2*).

Prior work has suggested a role for Cdx in early mesoderm fate decisions (Mendjan et al., 2014), including suppression of cardiogenesis (Lengerke et al., 2011; Rao et al., 2016). Although the basis underlying these observations is poorly understood, occupancy of cardiogenic and hematopoietic transcription factors by Cdx2, coupled with ectopic cardiogenic gene expression in DKO mutants, is consistent with a role for Cdx2 in suppressing cardiogenesis and promoting hematopoietic gene expression programs within a common *Mesp1*$^{+}$ mesodermal precursor, an event believed to occur during early gastrulation at E6.5 (Saga et al., 1999; Chan et al., 2013). However, the onset of Cdx gene expression in the embryo proper is reported to occur at around E7.5 (Beck et al., 1995; Gamer and Wright, 1993; Meyer and Gruss, 1993; Strumpf et al., 2005), and is therefore inconsistent with a role in

this specification event. Recent single cell RNA-seq performed and published by Scialdone et al. (2016) suggests that these early *Mesp1*+ progenitors do, in fact, express Cdx family members as early as E6.5. This was further supported by whole-mount immunohistochemistry, which revealed Cdx2 protein in the primitive streak at E6.5, thus placing Cdx in the appropriate developmental context to influence early *Mesp1*+ mesoderm specification events. Furthermore, an onset for Cdx function at the early primitive streak stage supports previously described roles for Cdx family members in early post-otic embryonic development (van Rooijen et al., 2012; Chawengsaksophak et al., 2004, 1997; Savory et al., 2009a; Amin et al., 2016; Subramanian et al., 1995) and craniorachichisis (Savory et al., 2011a).

In contrast to its role at hematopoietic loci, Cdx2 occupancy at cardiac loci is likely inhibitory, as previous studies using directed differentiation of mouse and human ESCs in vitro demonstrated increased differentiation to cardiac fates in the absence of Cdx function (Lengerke et al., 2011; Rao et al., 2016) and decreased cardiac gene expression in models of Cdx gain of function (Lengerke et al., 2011). Consistent with this, single cell RNA-seq revealed that all three Cdx family members are expressed in *Mesp1*+ progenitor cells in the mouse, but are not co-expressed with *Tbx5* or *Mef2c*, suggesting that Cdx expression is incompatible with the acquisition of a cardiac fate. A role for Cdx in suppressing cardiogenesis is further evidenced by ectopic *Nkx2-5* and *Tbx5* expression in the cardiac crescent of DKO mutants, and ectopic *Tbx5* expression in DKO yolk sacs.

Our observation that *Tbx5* expression is misregulated in DKO mutants is consistent with previous work in zebrafish that revealed expanded *tbx5a* expression in *cdx1a/4* compound mutants (Lengerke et al., 2011). Moreover, ectopic *Tbx5* expression in DKO mutant yolk sacs indicates that Cdx-deficient yolk sacs maintain sufficient plasticity to be redirected to a cardiac fate. Notably, a similar role has been described for *Scl* (Van Handel et al., 2012; Org et al., 2015), which functions downstream of Cdx (BrookeBisschop et al., 2017; Wang et al., 2008; Davidson and Zon, 2006; Davidson et al., 2003). Although Cdx may impact mesodermal cell fate decisions in part via *Scl*, our

finding of direct binding of Cdx2 to numerous cardiogenic loci, together with the mis-expression of some of these genes in DKO mutants, suggests that Cdx also plays a direct role in repressing cardiogenic gene expression.

Although *Tbx5* expression was consistently upregulated in DKO mutant yolk sacs, random alterations in *Nkx2-5* expression suggests that Cdx factors may not repress all cardiac targets similarly within a given context. In this regard, in the zebrafish, embryonic *nkx2-5* expression remains unaffected in Cdx mutants until they are treated with RA antagonists, suggesting that retinoid-mediated compensatory mechanisms are necessary to effect *nkx2-5* expression in the absence of Cdx (Lengerke et al., 2011). RA signaling not only regulates *Cdx1* expression (Houle et al., 2000, 2003; Prinos et al., 2001) but is also involved in heart development, and altered retinoid signaling can lead to aberrant cardiac mesoderm specification and subsequent defects in cardiac morphogenesis (Zile, 1998; Dickman and Smith, 1996). This suggests that murine Cdx factors are necessary, but not sufficient, for the regulation of certain Cdx targets, such as *Nkx2-5*, and that RA, or other signaling pathways, impact expression of such genes in Cdx mutants.

Defects in yolk sac hematopoiesis, such as those observed in Cdx mutants (Brooke-Bisschop et al., 2017; Lengerke et al., 2008; Wang et al., 2008; Davidson and Zon, 2006; Davidson et al., 2003), can also affect cardiac development (Shivdasani et al., 1995; Moser et al., 2004). Consistent with this, *Cdx1*$^{-/-}$*Cdx2*$^{F/F}$*Tie2-Cre* mutants exhibited aberrant cardiogenesis, suggesting that the absence of blood contributes to cardiac defects in these mutants. Nevertheless, cardiac defects in DKO mutants are preceded by altered expression of *Nkx2-5* and *Tbx5* as early as E8.5, likely before yolk sac hematopoiesis is sufficiently compromised to impact heart tube morphogenesis. Furthermore, Cdx2 binding to a number of cardiac loci supports a direct role for Cdx during heart field specification and argues against aberrant cardiogenesis in DKO mutants being entirely secondary to circulatory deficiencies.

Cdx factors as integrators of extracellular signaling

Although similar morphological defects were observed in Cdx mutant heart tubes produced by *CMV-Actin::CreER*^{T} and *Mesp1-Cre* mediated recombination, perturbations in the expression of cardiac transcription factors were only observed in *CMV-Actin::CreER*^{T} mutants, arguing against Cdx function in *Mesp1*$^{+}$ progenitors as causal to these heart defects. It may be that cell Cdx-dependent non-autonomous cues instructive to cardiac morphogenesis originating from the endoderm and/or ectoderm are disrupted only in the *CMV-Actin::CreER*^{T} mutant model. For instance, *BMP2* expressed in the endoderm (Schultheiss et al., 1997; Somi et al., 2004) is required for the formation of a heart in zebrafish (Frasch, 1995) and *Xenopus* (Shi et al., 2000), as is its homolog *dpp* in Drosophila (Kishimoto et al., 1997). Although cardiac mesoderm is induced in BMP2-deficient mice, subsequent heart morphogenesis is perturbed (Zhang and Bradley, 1996). In this regard, we identified *Bmp2* as a potential Cdx2 target gene by ChIP-seq in E8.5 embryos, the stage at which the heart tube emerges and commences looping. Thus, Cdx regulation of BMP signaling from non-mesodermal germ layers may be preserved in *Mesp1-Cre* driven Cdx mutants, yet lost in *CMV-Actin::CreER*^{T} mutants, possibly contributing to the stronger phenotype in the latter. Further work will be required to examine this potential relationship.

Cdx proteins act as intermediaries that relay caudalizing signals to regulate expression of transcription factors, such as the *Hox* genes (Shashikant et al., 1995; Charité et al., 1998; Subramanian et al., 1995; Pownall et al., 1996; Isaacs et al., 1998; van den Akker et al., 2002; Gaunt et al., 2003, 2008). Consistent with this, previous work has demonstrated Wnt- and RA-dependent regulation of Cdx family members (Houle et al., 2000, 2003; Prinos et al., 2001; Ikeya and Takada, 2001; Pilon et al., 2006). Directed differentiation of ESCs to cardiomyocytes in vitro mimics signaling gradients in the primitive streak, and requires an initial phase of Wnt signaling for mesoderm induction (Lindsley et al., 2006; Gadue et al., 2006; Haegel et al., 1995), followed by Wnt inhibition to permit differentiation

to cardiac cell fates (Lickert et al., 2002; Ueno et al., 2007; Burridge et al., 2012; Yang et al., 2008; Murry and Keller, 2008; Marvin et al., 2001; Schneider and Mercola, 2001; Tzahor and Lassar, 2001); continued Wnt signaling promotes mesodermal progenitor commitment to alternative lineages, including blood (Woll et al., 2008; Wang et al., 2008; Rao et al., 2016). Such models have placed Cdx function downstream of Wnt to repress cardiogenesis, thereby promoting differentiation to such alternative mesodermal lineages (Lengerke et al., 2011; Mendjan et al., 2014; Rao et al., 2016). Thus, cardiac inhibition by Cdx factors as shown here, coupled with activation of hematopoietic regulators, is consistent with their role downstream of Wnt during mesodermal cell fate decisions.

Cdx and chromatin remodeling

Cdx2 has been shown to influence chromatin accessibility in the intestinal epithelium (Verzi et al., 2010, 2013), and interacts with Brg1 at some target loci in other models (Nguyen et al., 2017; Yamamichi et al., 2009). Furthermore, Cdx2 appears to be required for Brg1 recruitment to cardiac genes. Chromatin organization within these regions was also disrupted in DKO yolk sacs, suggesting that the interaction between Cdx2 and Brg1 at cardiac genes impacts chromatin accessibility. It is possible that Cdx2 recruits Brg1 and SWI/SNF chromatin remodeling activity to cardiogenic loci to establish non-permissive chromatin, thereby epigenetically silencing gene expression in non-cardiac lineages at later developmental stages. However, not all Cdx2-bound loci were co-occupied by Brg1. For example, at the Tbx5 gene locus, Brg1 binding was robust at the Cdx2 ChIP-seq peak most distal to the transcriptional start site (TSS), whereas the more proximal peak was occupied by Cdx2 alone (Figure 45A). Cdx2 and Brg1 were also present at the *Hand1* locus, although Brg1-bound regions flanked Cdx2 peaks, suggesting that these factors may both impact *Hand1* expression, but do not co-occupy genomic intervals at this particular gene. Conversely, *Isl1* was occupied by Cdx2 alone, suggesting that regulation by Cdx at some cardiac targets might occur independent of SWI/SNF

complex recruitment. Although we cannot exclude Brg1 occupation of such genes in lineages not surveyed here, and/or at other times, these observations suggest that Cdx2-dependent transcription occurs through Brg1-dependent and -independent mechanisms.

In summary, the findings presented here suggest a model in which Cdx factors regulate gene expression through epigenetic mechanisms following recruitment of the SWI/SNF complex. This putative mechanism allows for *Cdx*$^{+}$ cells and their progeny to initiate the appropriate gene regulatory networks at developmental stages when cell fate decisions are made, after *Cdx* expression is extinguished.

MATERIALS AND METHODS

Mice

Cdx1$^{-/-}$*Cdx2*$^{F/F}$, *CMV-Actin::CreER*^{T}, *Tie2*$^{+/Cre}$, and *Mesp1*$^{+/Cre}$ mouse lines have been previously described (Savory et al., 2009a; Santagati et al., 2005; Saga et al., 1999, 2000; Kisanuki et al., 2001; Tang et al., 2010). *Cdx1*$^{-/-}$*Cdx2*$^{F/F}$ females were paired with *Cdx1*$^{-/-}$*Cdx2*$^{F/F}$ *CMV-Actin::CreER*^{T} males for timed matings, with noon of the day of vaginal plug discovery considered E0.5, and Cdx2 deletion induced with 2 mg tamoxifen in corn oil by oral gavage at E5.5. *Mesp1*$^{+/Cre}$ or *Tie2*$^{+/Cre}$ animals were crossed into the *Cdx1*$^{-/-}$*Cdx2*$^{F/F}$ line, and *Cdx1*$^{-/-}$*Cdx2*$^{+/F}$*Mesp1*$^{+/Cre}$ or *Cdx1*$^{-/-}$*Cdx2*$^{+/F}$*Tie2*$^{+/Cre}$ males were paired with *Cdx1*$^{-/-}$*Cdx2*$^{F/F}$ females for timed matings, as above. Animals were maintained according to the guidelines established by the Canadian Council on Animal Care and Animal Care and Veterinary Services at the University of Ottawa.

Antibodies

Rabbit polyclonal anti-Cdx2 antibodies have been previously described (Savory et al., 2009b). Brg1 antibodies were purchased from Abcam (ab110641). Control rabbit IgG antibodies were purchased from Sigma (i8140).

Chromatin immunoprecipitation (ChIP) and ChIP-seq

Embryos from timed matings were dissected, crosslinked with 1% formaldehyde, and ChIP performed as previously described (Pilon et al., 2006) with the following modifications: chromatin was sonicated for 1-min intervals six times using a Branson Sonifier 450 at output 3 with 30% duty cycle, and 10 µg of polyclonal rabbit-anti-Cdx2 (Savory et al., 2009b) and pre-immune rabbit-anti-IgG (Sigma) was coupled to 200 µl of magnetic protein G Dynabeads (Invitrogen). Samples were purified using the QIAquick PCR Purification Kit (Qiagen) and library preparation and sequencing performed by the Genome Quebec and McGill Innovation Centre using the mm9 reference genome. ChIP experiments

were performed as above using 5 µg of antibody against Cdx2 (Savory et al., 2009b), or IgG control (Sigma), coupled to 50 µl of protein A/G Sepharose beads (Santa Cruz Biotechnology). DNA purification was followed by PCR using primers directed against sequences flanking putative Cdx response elements (CDREs), identified by TRANSFAC, within genomic intervals associated with enriched Cdx2 occupancy as determined by ChIP-seq. Primer sequences are listed in Table 2. ChIP-seq tracks for Brg1 binding in ESCs at the mesoderm stage of differentiation to cardiomycotes in culture (Alexander et al., 2015) were intersected with Cdx2-ChIP seq data using the UCSC genome browser (https://genome.ucsc.edu/).

Table 2. Oligonucleotide sequences for ChIP-PCR.

Gene Name	Primer Sequences	
Gata4 CDREs1	Forward	CACGTGCGCTCCAAAAGTC
	Reverse	GCCCAGAGGGGTTAACGTG
Gata4 CDREs2	Forward	GAAGTATCCCCGCAGCTGTT
	Reverse	AGATAGCAAAGTCTCAAAGTAGCC
Hand1 CDREs1	Forward	GTTGTCTGAGCTTCGTCCCA
	Reverse	CCCGAGAGCAACTACCAGAA
Hand1 CDREs2	Forward	AACTTGCCCAGTCTTGACGA
	Reverse	GAGGTCCTTGGCTCCTATGG
Hand2 CDREs1	Forward	TTAGTGTGGCCCTCTCTCCA
	Reverse	AAGTGTTGTGTGTATGGGGCT
Hand2 CDREs2	Forward	CCCCCGTCATTCTCTGTGTG
	Reverse	GGATGAGAACCACTGACTCTTT
Mef2c	Forward	TCCCCAAAACCCCCTATACCCT
	Reverse	GTAAGTATGAAAATTTGCCCT
Tbx5 CDRE1	Forward	ACCTCTCTGTTCCTATCCAGTG
	Reverse	CGCTTAGTCGACCTCAAGTCTAA
Tbx5 CDRE2	Forward	GCTCGCAGCTCTCACCAAAT
	Reverse	AAACTAGAGGGGATGGGTGC
Wnt3a Exon4	Forward	GCCATCGCCAGTCACATGCACCTCAAGTGC
	Reverse	CTACTTCGAGGTGTGCACGTCATAGACACG
Tbx5 Control Region	Forward	ACACCAAAGCTATGACTTGTCTGGC
	Reverse	ATCCTTAGGTTCCTGAGCTTGACAT
Gata4 Control Region	Forward	AAGTCACTCCGCTCTTCTAGACAA
	Reverse	ATTTAGGTCAGTGTAGTAGCTT
Nkx2-5 Control Region	Forward	AAGCTGCTTCATTTTTCACCCTCCTA
	Reverse	ACTTAAGAGTGACTTGTTTAGCTAA

GO term analysis Cdx2

ChIP-seq peaks with peak scores greater than 800 was assembled and used for GO term enrichment analysis. Gene IDs were uploaded to the Gene Ontology Consortium enrichment analysis tool (www.geneontology.org/page/go-enrichment-analysis), and only those GO terms with a fold enrichment of 5 or greater were considered. GO terms were sorted by P-value and plotted as $-\log_{10}$(P-value).

In situ hybridization

Embryos were dissected at E8.5 or E9.5 in chilled PBS, pooled according to genotype, stage-matched based on somite number (or head morphology in cases of axial truncation) and processed in parallel as described (Houle et al., 2000; Wilkinson et al., 1990). Probes were generated from previously described plasmids encoding *Nkx2-5* (Komuro and Izumo, 1993), *Tbx5* (Bruneau et al., 1999) or *Mlc2v* (Molkentin et al., 1997). Whole-mount immunohistochemistry was performed using antibodies against Cdx family members on E6.0-E7.5 embryos as previously described (Qiu et al., 1997; Savory et al., 2009b).

Reverse-transcription quantitative PCR (RT-qPCR)

Embryos or yolk sacs were collected at E8.5-9.5 and RNA extracted using Trizol (Gibco BRL) according to the manufacturer's instructions. cDNA was synthesized by standard methods and amplified by semi-quantitative RT-PCR with GoTaq (Promega) using a DNA Engine Tetrad 2 (Bio-Rad), or by RT-qPCR using SYBR green (Promega) and the CFX 96 (Bio-Rad) thermocycler. Either *β-actin* or *Gapdh* was used as an input control, and RT-qPCR results were analyzed using the ΔΔCt method. Oligonucleotides (listed in Tables 3 and 4) were validated before use and dissociation curves were considered for each amplicon to ensure specificity.

Table 3. Oligonucleotide sequences for qRT-PCR

Gene Name	Primer Sequences	
Tbx5	Forward	ATGGTCCGTAACTGGCAAAG
	Reverse	ACAAGTTGTCGCATCCAGTG
Gapdh	Forward	GGCCGGTGCTGAGTATGTCG
	Reverse	TTCAAGTGGGCCCCGGCCTT

Table 4. Oligonucleotide sequences for semi-quantitative RT-PCR

Transcript	Primer Sequences	
cTnT	Forward	CCAGCAGGCTCTTCATGC
	Reverse	TTCATTCAGGTGGTCGATGG
Nkx2-5	Forward	CAGCAACTTCGTCAACTTTGGC
	Reverse	AATCTGAGGGACAGGGCATAGTGG
Cdx1	Forward	ACAGAGCGGCAGGTAAAGATCTGG
	Reverse	GGAGACGGTGAAGCCTCAATCTTGT
Cdx2	Forward	AGCCAAGTGAAAACCAGGACAA
	Reverse	TGCAAGGAGGTCACAGGACT
Cdx4	Forward	GCATGGATGCGCAAAACTGT
	Reverse	CCAGAGTCACTTTGCACGGA
β-Actin	Forward	GCGGGAAATCGTGCGTGACATT
	Reverse	GATGGAGTTGAAGGTAGTTTCGTC

RNA-seq

Single cell RNA-seq was originally performed using E6.5-E7.75 whole embryos by Scialdone et al. (2016). Single cell read counts were downloaded from http://gastrulation.stemcells.cam.ac.uk and plotted against expression levels of Cdx family members.

FAIRE-PCR

Experiments were performed using E9.5 yolk sacs isolated from wild-type and DKO mutant embryos. Chromatin was sheared for seven 1-min intervals on ice using a Branson Sonifier 450 with a 30% duty cycle on power output 3, and DNA accessibility was assessed according to previously published protocols (Simon et al., 2012). Primers are listed in Table 5.

Table 5. Oligonucleotide sequences for FAIRE-PCR

Transcript	Primer Sequences	
Gata4 CDRE1	Forward	CACGTGCGCTCCAAAAGTC
	Reverse	GCCCCACGTCTTCTGAGATG
Gata4 CDRE2	Forward	GAAGTATCCCCGCAGCTGTT
	Reverse	GGGTCTGCCTCCCCAAGATC
Tbx5 CDREs1	Forward	ACCTCTCTGTTCCTATCCAGTC
	Reverse	GCCTGGACCGATCTCCAGCT
Tbx5 CDRE2	Forward	GCTCGCAGCTCTCACCAAAT
	Reverse	CCTGGGGTGTTGGTGAGG
Nkx2-5	Forward	CTTTCCTCTGTTCCCCTATTAGC
	Reverse	GGAAACTTGTTTTATGTGTG
β-Actin	Forward	CCCTAAGGCCAACCGTGAAA
	Reverse	GTCCTATGGGAGAACGGCAG

ACKNOWLEDGEMENTS

We thank Filippo Rijli for the *Actin::Cre-ER^T* mouse line, Benoit Bruneau for *Nkx2-5* and *Tbx5* in situ hybridization probes, Ilona Skerjanc for the *Mlc2v* in situ hybridization probe, David Cook for further analyses of the single cell RNAseq data, Sanzida Jahan for her expertise on FAIRE-PCR, and the University of Ottawa Animal Care and Veterinary Service for excellent mouse husbandry.

CHAPTER 3 - Cdx regulates gene expression through PRC2-mediated epigenetic mechanisms

Cdx regulates gene expression through PRC2-mediated epigenetic mechanisms

Tanya E. Foley, David Lohnes

Keywords: Cdx, transcription, yolk sac, epigenetics, PRC2

Article published December 30, 2021 in *Developmental Biology*, Volume 483, pp.22-33

AUTHOR CONTRIBUTIONS

Tanya Foley designed and conducted experiments, performed data analysis, and prepared the manuscript.

Travis Brooke-Bisschop provided images of whole mount yolk sacs.

David Lohnes designed experiments and helped to write the manuscript.

ABSTRACT

The extra-embryonic yolk sac contains adjacent layers of mesoderm and visceral endoderm. The mesodermal layer serves as the first site of embryonic hematopoiesis, while the visceral endoderm provides a means of exchanging nutrients and waste until the development of the chorioallantoic placenta. While defects in chorioallantoic fusion and yolk sac hematopoiesis have been described in Cdx mutant mouse models, little is known about the gene targets and molecular mechanisms through which Cdx members regulate these processes. To this end, we used RNA-seq to examine Cdx-dependent gene expression changes in the yolk sac. We find that loss of Cdx function impacts the expression of genes involved in yolk sac hematopoiesis, as previously described, as well as novel Cdx2 target genes. In addition, we observed Cdx-dependent changes in PRC2 subunit expression accompanied by altered H3K27me3 deposition at a subset of Cdx target genes as early as E7.5 in the embryo proper. This study identifies additional Cdx target genes and provides further evidence for Cdx-dependent epigenetic regulation of gene expression in the early embryo, and that this regulation is required to maintain gene expression programs in the extra-embryonic yolk sac at later developmental stages.

INTRODUCTION

During development, the post-implantation murine embryo is enveloped by the yolk sac, an extra embryonic structure that contains adjacent layers of mesoderm and visceral endoderm (Kaufman and Baard, 1999). The visceral endoderm derives from the primitive endoderm and consists of absorptive epithelial cells. As such, it serves as the primary site of nutrient, waste, and gas exchange between the embryo and the maternal circulation until chorioallantoic fusion occurs (E8.5-10.5), which then allows nutrients to be delivered via the chorioallantoic placenta (Gilman et al., 1948; Brent et al., 1990; Jollie et al., 1990; Lloyd, 1990; Lloyd, 1997; Farese et al., 1995; Cross et al., 1994; Zohn and Darkar, 2010). The transfer of nutrients by the visceral endoderm is facilitated by its close proximity to the underlying vasculature within the mesodermal layer, as well as by epithelial microvilli that aid in nutrient absorption (Bielinska et al., 1999). Parallels have been made between the yolk sac and the fetal liver based on the expression of liver-associated genes involved in nutrient transport and lipid, carbohydrate, and amino acid metabolism within the visceral endoderm, as well as its production of serum proteins and anti-coagulation factors (Farese et al., 1995; Duncan et al., 1994; Meehan et al., 1984; Kram and Klein, 1976; Young et al., 1980; Youn and Klein, 1983; Nakazawa et al., 2011).

In addition to nutrient and waste processing, the visceral endoderm produces a number of diffusible factors required for growth, patterning, and differentiation in the embryo, including Nodal, Lefty1, and retinoid-binding factors that mediate the transfer of retinol (Conlon et al., 1994; Varlet et al., 1997; Takaoka et al., 2011; Johansson et al., 1997). Additional signalling molecules originating in the visceral endoderm, including Indian hedgehog (Ihh) and Vegfa, are essential for vascularization within the underlying mesoderm (Becker et al., 1997; Farrington et al., 1997; Damert et al., 2002; Miura and Wilt, 1969; Beloussoff et al., 1998; Vokes and Krieg, 2002; Dyer et al., 2001). This is consistent with the finding that yolk sac vascularization is disrupted in embryos lacking visceral endoderm (Damert et al., 2002; Wilt, 1965; Bielinska et al., 1996), and that mesodermal explant

cultures form hematopoietic/vascular progenitors only when co-cultured with visceral endoderm or exogenous hedgehog proteins (Beloussoff et al., 1998; Dyer et al., 2001; Bielinska et al., 1996).

The yolk sac mesoderm is specified from progenitors that originate in the epiblast and egress through the posterior primitive streak before migrating extra-embryonically to populate the yolk sac (Huber et al., 2004; Medvinsky et al., 2011; Yamane, 2018). Within the yolk sac, these progenitors form blood islands, aggregates of hemangioblast cells that give rise to both primitive erythroid cells and vascular endothelium during the first wave of embryonic hematopoiesis, known as primitive hematopoiesis (Haar and Ackerman, 1971; Fehling et al., 2003; Jagannathan-Bogdan and Zon, 2013). During this process, blood islands merge to form the vascular plexus lined by hemogenic endothelium (Eilen et al., 2009; Lancrin et al., 2009). Primitive hematopoiesis sustains the embryo until definitive hematopoiesis is initiated in the embryo proper (Galloway and Zon, 2003).

Previous work by our group and others has shown that Cdx transcription factors are required for sustained differentiation of yolk sac hematopoietic progenitors (Brooke-Bisschop et al., 2017; Chawengsaksophak et al., 2004; Wang et al., 2008; McKinney-Freeman et al., 2008; Lengerke et al. 2008; Davidson and Zon, 2006; Davidson et al., 2003). The murine Cdx genes, *Cdx1*, *Cdx2*, and *Cdx4*, encode homeodomain transcription factors related to the gene *caudal* in *Drosophila*. In the embryo, each Cdx member is expressed in the posterior primitive streak and subsequently in all three germ layers of the developing tail bud, forming a nested pattern of expression from E6.5 through to E13.5 (Beck et al., 1995; Gamer and Wright, 1993; Meyer and Gruss, 1993; Strumpf et al., 2005; Foley et al., 2019; Silberg et al., 2000). In the extra-embryonic trophectoderm, *Cdx2* expression is initiated earlier, at E3.5, with *Cdx2* deletion resulting in early lethality due to its requirement in this lineage for implantation (Meyer and Gruss, 1993). At E13.5, Cdx expression is extinguished in all tissues with the exception of *Cdx1* and *Cdx2* in the hindgut endoderm where they persist in the intestinal epithelium throughout life (Silberg et al., 2000).

While *Cdx2*$^{-/-}$ mutants are peri-implantation lethal, *Cdx1*$^{-/-}$ and *Cdx4*$^{-/0}$ mice are viable. *Cdx1*$^{-/-}$ and *Cdx2*$^{+/-}$ mutants exhibit homeotic transformations of the cervical and thoracic vertebrae coupled with altered patterns of *Hox* gene expression (Subramanian et al., 1995; Chawengsaksophak et al., 1997). *Cdx4*$^{-/0}$ mice display no overt phenotype, however the loss of *Cdx4* exacerbates phenotypes associated with *Cdx1*$^{-/-}$ or *Cdx2*$^{+/-}$ mutants, suggestive of functional overlap among family members (Faas and Isaacs, 2009; Savory et al., 2011a; van den Akker et al., 2002; van Nes et al., 2006; Young et al., 2009). Consistent with this, Cdx can occupy, and regulate, a number of common target genes. Such genes include *Cyp26A1,* which encodes a cytochrome p450 required to maintain a retinoic acid depleted zone in the tail bud necessary for axial elongation (Young et al., 2009; Wingert et al., 2007; Savory et al., 2009a; Martin and Kimelman, 2010), a number of *Hox* genes essential for vertebral patterning and yolk sac hematopoiesis (Subramanian et al., 1995; van den Akker et al., 2002; Shashikant et al., 1995; Charite et al., 1998; Pownall et al., 1996; Isaacs et al., 1998; Gaunt et al., 2003; Gaunt et al., 2008; Davidson et al., 2003; Davidson and Zon, 2006; Lengerke et al., 2007), and other factors involved in yolk sac hematopoiesis, including *Scl/Tal-1* and *Runx1* (Brooke-Bisschop et al., 2017; Davidson et al., 2003; Lengerke et al., 2007).

To negate functional overlap between family members and early lethality inherent to loss of Cdx2 function, conditional *Cdx2* mutants were derived and crossed into a germ-line *Cdx1* null mutant background (Savory et al., 2011a; Stringer et al., 2012). Deletion of *Cdx2* at post-implantation stages with a global *CMV-Actin::Cre-ER*^{T} deletor yielded *Cdx1-Cdx2* compound mutants, termed DKO (double knockout) for simplicity, which lack expression of *Cdx4* and are thus functionally Cdx-null (Savory et al., 2011a).

While mechanisms underlying Cdx-dependent transcription are poorly understood, our group and others have shown that Cdx2 appears to regulate gene expression, in part, by impacting the chromatin landscape at its genomic targets. For instance, Cdx members interact directly with the Brg1

catalytic subunit of the SWI/SNF chromatin remodelling complex, and are necessary for recruitment of this complex to a number of Cdx targets, concomitant with altered chromatin accessibility at such loci (Foley et al., 2019; Yamamichi et al., 2009; Nguyen et al., 2017). In addition, Cdx2 inhibits the spread of repressive H3K27me3, which is deposited by Polycomb Repressive Complex 2 (PRC2), across target genes (Saxena et al., 2017; Mazzoni et al., 2013; Hojfeldt et al., 2018; Jung et al., 2010; Cao et al., 2002). Altered H3K27me3 density in Cdx mutants is associated with aberrant target gene expression and misspecification of cell fate (Saxena et al., 2017; Mazzoni et al., 2013).

We previously found that Cdx function is required for yolk sac hematopoiesis (Brooke-Bisschop et al., 2017), and that Cdx positively regulates the expression of pro-hematopoietic genes while repressing genes involved in cardiac differentiation from common progenitors (Foley et al., 2019). To better understand these relationships, we examined global patterns of gene expression in Cdx mutant yolk sacs using RNA-seq. We found that, in addition to maintaining hematopoietic gene expression programs, Cdx function is also required to maintain the expression of genes not previously reported to be Cdx-dependent. We show that certain of these are also occupied by Cdx2, and therefore represent novel direct Cdx targets. Further, we found that PRC2 subunits are misexpressed in Cdx mutants, coupled with altered H3K27me3 at Cdx target genes. These findings evoke novel roles for Cdx in regulating gene expression via PRC2-mediated H3K27me3 deposition at genomic targets, further demonstrating that Cdx members impact the expression of their targets by modulating the epigenetic landscape.

RESULTS

Differential gene expression in Cdx mutant yolk sacs

Cdx DKO mutants display a range of developmental defects, including caudal truncation at the level of the forelimb bud (e.g. Figure 47A), an open neural tube, aberrant cardiac morphogenesis, and defects in yolk sac hematopoiesis accompanied by a lack of yolk sac vascularization (Figure 47B) (Brooke-Bisschop et al., 2017; Chawengsaksophak et al., 2004; Lengerke et al., 2008; Davidson and Zon, 2006; Davidson et al., 2003; Want et al., 2008; Foley et al., 2019; Subramanian et al., 1995; Savory et al., 2011a; van den Akker et al., 2002; Young et al., 2009; Savory et al., 2009a; Epstein et al., 1997; van Rooijen et al., 2012). As regards the latter, previous work by our group and others revealed that Cdx function is required to maintain gene expression programs required for yolk sac hematopoiesis (Brooke-Bisschop et al., 2017; Chawengsaksophak et al., 2004; Wang et al., 2008; McKinney-Freeman et al., 2008; Davidson et al.,. 2003; Davidson and Zon, 2006). Visualization of E9.5 yolk sacs by H&E staining of transverse sections confirmed the lack of vasculature in mutants, as well as the absence of primitive erythrocytes typically observed within blood vessels (Figure 47C).

To better understand Cdx function in the yolk sac, we performed RNA-sequencing (RNA-seq), comparing DKO yolk sacs at E9.5 to untreated stage-matched CD1 controls (hereafter referred to as wild type (WT)). RNA was extracted from yolk sacs pooled from three litters of either genotype and processed for RNA-seq. Despite the fully penetrant yolk sac phenotype observed in mutants, complete loss of *Cdx2* Exon 2, as anticipated by the design of the conditional allele (Figure 47D), was not observed in any of the DKO samples (Figure 47E). This was likely due a tissue-specific inefficiency of the Cre recombinase in extra-embryonic lineages, as Cdx2 is consistently completely deleted in the embryo proper upon activation of the *CMV-Actin::CreER*^{T} used in this model, as well as with mesoderm-specific Cre drivers used in previous studies (Foley et al., 2019; Savory et al., 2009a). Cdx2

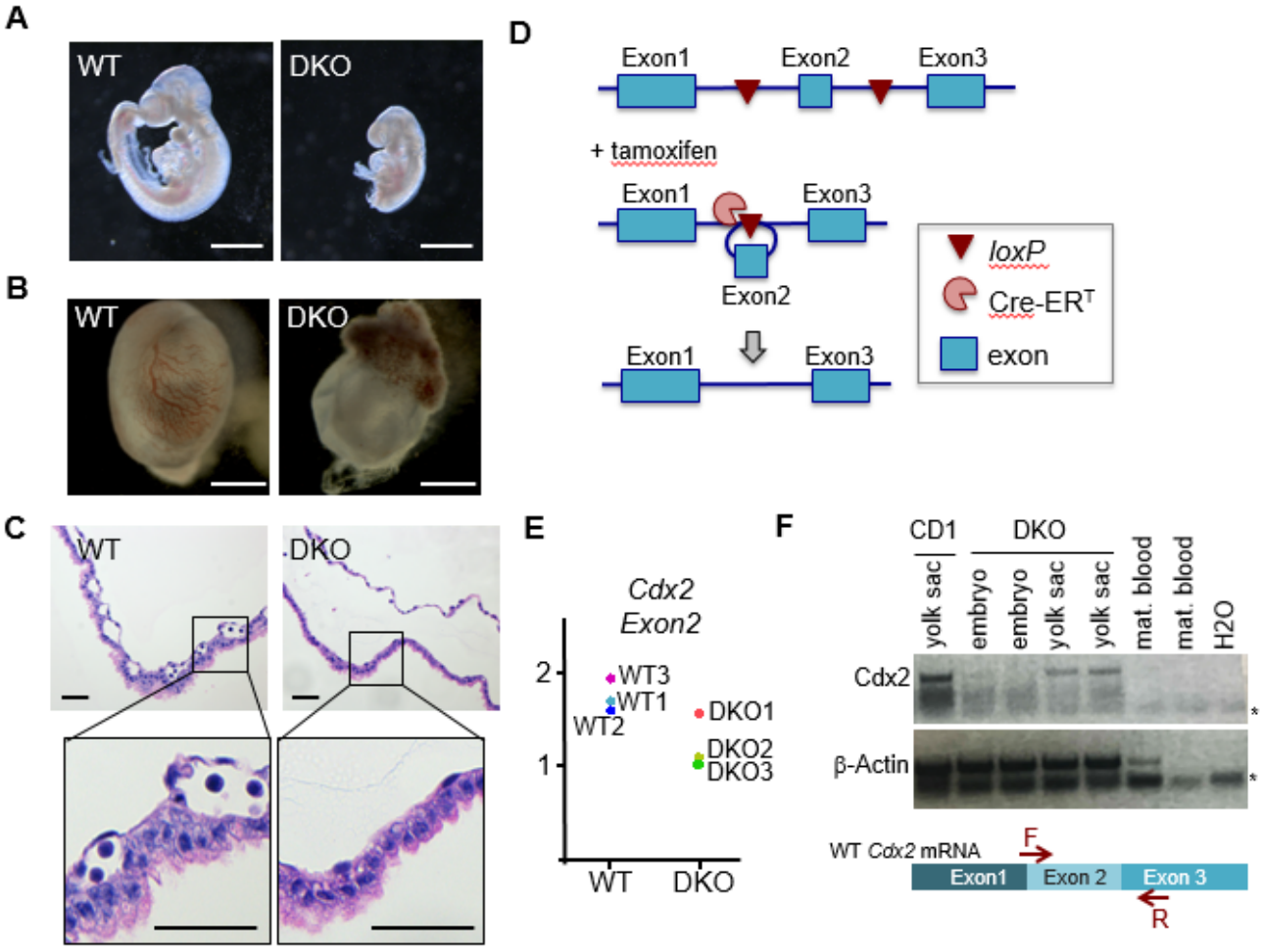


Figure 47. Cdx mutants display the expected phenotypes despite incomplete Cdx2 depletion. A. Whole mount WT and DKO embryos at E9.5. Scale bar represents 1 mm. **B.** Whole mount E9.5 WT and DKO yolk sacs at E9.5. Scale bar represents 2 mm. **C.** H&E staining of sectioned E9.5 WT and DKO yolk sacs. Scale bars represent 50 μm. **D.** Schematic representation of the Cdx2 locus showing the excision of exon 2 upon Cre recombination (Savory et al., 2011a). **E.** Relative levels of *Cdx2* exon 2in three WT and three DKO RNA-seq samples generated from E9.5 yolk sacs. **F.** Pregnant dams were crossed with *Cdx1*$^{-/-}$*Cdx2*$^{fl/fl}$ males carrying two *CMV-Actin::CreER*^{T} alleles. Females were treated with 4mg tamoxifen at E5.5. Embryos were harvested at E9.5, separated from yolk sacs, and material from each litter was pooled. Maternal blood was included as a control. *Cdx2* expression was assessed by RT-PCR in DKO mutants and WT controls, with *β-actin* used as a loading control. Asterisks (*) indicate primer dimers. A schematic representation of WT *Cdx2* mRNA is shown below with red arrows indicating regions complementary to forward (F) and reverse (R) primers.

transcripts were not detected in maternal blood (Figure 47F), excluding the possibility of contamination by this source during dissection. *Cdx2* ablation was particularly inefficient in sample DKO1 (Figure 47E, Figure 48), leading to its exclusion from subsequent analyses. *Cdx1* expression was not detected by RNA-seq in yolk sacs, irrespective of genotype, in agreement with previous work demonstrating that *Cdx1* is not required for primitive hematopoiesis (Wang et al., 2008). *Cdx4* transcripts were reduced in DKO yolk sacs relative to WT controls (Figure 49), consistent with *Cdx4* being a Cdx2 target gene (Savory et al., 2011b).

To compare gene expression between samples, $\log_2$ transformed gene counts were plotted, revealing that WT samples clustered together while DKO samples exhibited greater variability (Figure 50). Upon eliminating sample DKO1 from the analysis, PCA for the remaining datasets demonstrated that the DKO samples also clustered together (Figure 51A), as also observed with visualization of the Poisson distance between samples (Figure 51B). The greater variability among mutant samples relative to WT likely results from the incomplete loss of Cdx2 in the yolk sac.

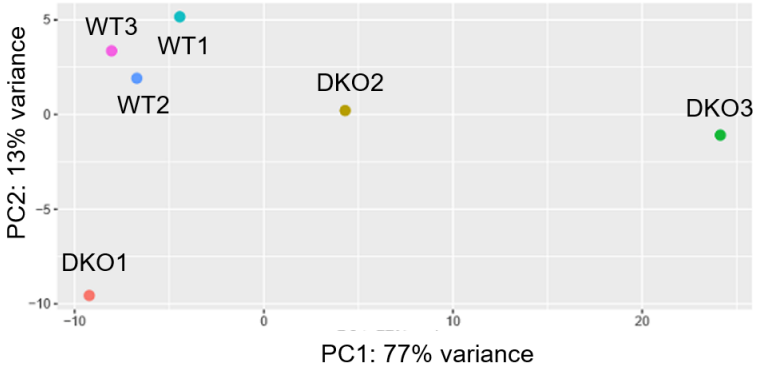


Figure 48. 2D PCA comparison of RNA-seq datasets. 2D principle component analysis (PCA) for RNA-seq datasets (WT1, WT2, WT3, DKO1, DKO2, DKO3) collected from pooled E9.5 WT and DKO yolk sacs. The percent total variance is indicated on the respective axes.

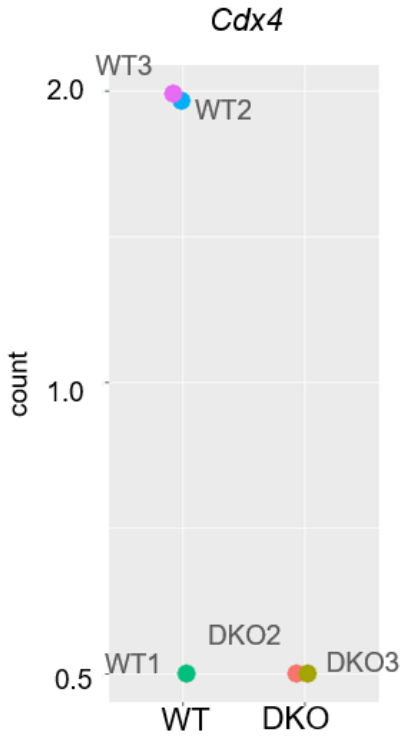


Figure 49. *Scl/Tal-1* expression in *Cdx1*$^{+}$ and *Cdx4*$^{+}$ cells. Normalized *Cdx4* transcript counts in WT and DKO E9.5 yolk sacs by RNA-seq.

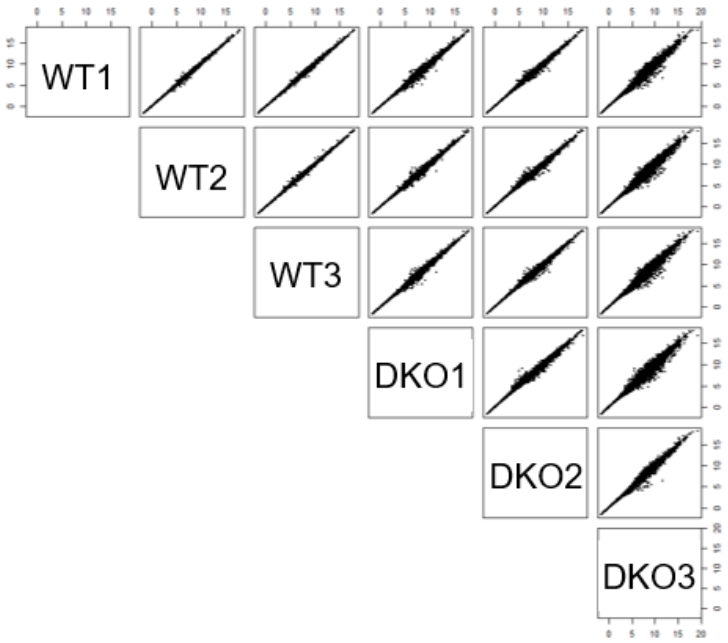


Figure 50. Log_2 transformed gene counts for six RNA-seq datasets. A comparison of log_2 transformed gene counts for WT1, WT2, WT3, DKO1, DKO2, and DKO3 RNA-seq samples.

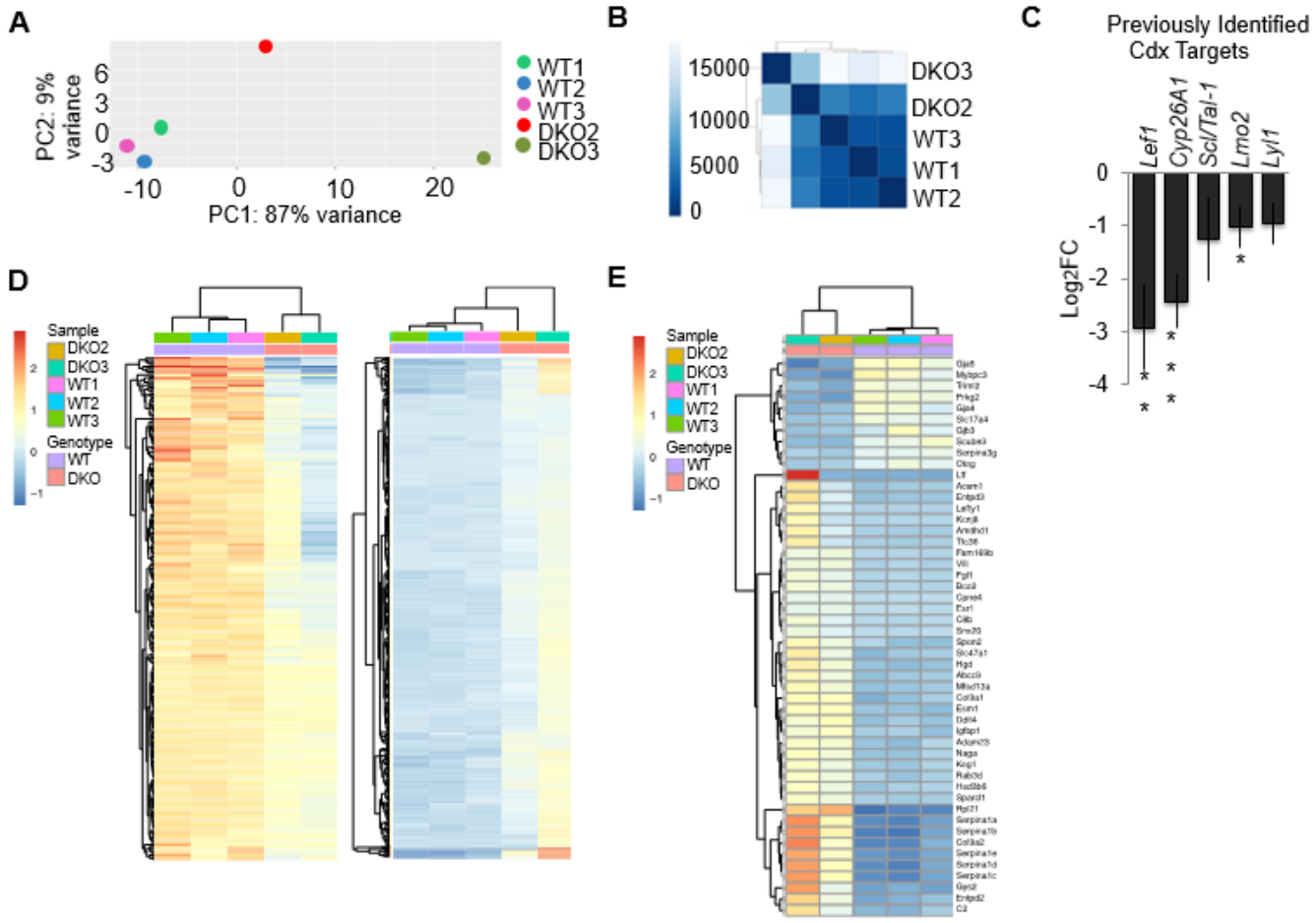


Figure 51. RNA-seq analysis of Cdx-dependent gene expression yolk sacs. A. 2D principle component analysis (PCA) for five RNA-seq datasets (WT1, WT2, WT3, DKO2, DKO3) collected from pooled litters E9.5 yolk sacs. The percent total variance is indicated on the respective axes. **B.** The Poisson distance between samples, represented by a heat-map, demonstrating sample-to-sample distances between datasets. **C.** Previously identified Cdx targets recovered in E9.5 DKO yolk sacs, represented as $\log_2$FC. **D.** Hierarchical clustering of 240 genes down-regulated in DKO yolk sacs ($\log_2$FC $\leq$ -1, left), and 673 genes up-regulated ($\log_2$FC $\geq$ 1, right), each with FDR $\leq$ 0.05. Samples are color-coded as described in the legend to the left of the panel. **E.** Hierarchical clustering of the top 50 most variable genes with 1 $\leq$ log2FC $\leq$ -1 and FDR $\leq$ 0.05, sorted by FDR.

Of the 18,890 genes mapped, 2921 genes were significantly affected (FDR ≤ 0.05). Among these genes, 913 experienced a 2-fold change in expression or greater (1 ≤ log2FC ≤ -1, FDR < 0.05), with 673 and 240 transcripts up- and down-regulated, respectively. Differentially expressed genes included the known Cdx target *Cyp26A1*, the Wnt effector *Lef1*, and *Scl/Tal-1, Lmo2,* and *Lyl1*, involved in Cdx-dependent yolk sac hematopoiesis (Figure 51C; Brooke-Bisschop et al., 2017; Savory et al., 2009a; Savory et al., 2011b; Shivdasani et al., 1995; Visvader et al., 1998; Warren et al., 1994; Souroullas et al., 2009). Heat-maps revealed that transcript levels were consistent across WT samples, but were variable among DKOs (Figure 51D). Hierarchical clustering of transcripts with the greatest variation between WT and DKO identified a number of additional differentially expressed genes (Figure 51E). These included *Wnt6,* associated with canonical Wnt signalling, *Triml2*, which is expressed in trophoblast-derived structures such as the yolk sac and placental tissues (Zhang et al., 2020), and the connexins *Gjα4* (*Cx37*), *Gjα5* (*Cx40*), and *Gjβ3* (*Cx31*), involved in the formation of gap junctions (Figure 51E). The latter observation is reminiscent of the aberrant tight junctions and the loss of cell polarity previously described in Cdx-deficient intestinal epithelium (Gao et al., 2010).

Cdx impacts expression of genes associated with nutrient and ion transport

Gene Ontology (GO) analysis revealed that the terms genes associated with GO terms *epithelium development*, *ion transport*, and *transmembrane transport* were overrepresented among the 240 genes significantly downregulated in DKO yolk sacs (Figure 52A). Differentially expressed genes associated with epithelial cell function, and also known to be involved in vessel formation, included the transcription factors *Dlx3*, *Tbx4*, *Lef1*, *Hey2*, and the signalling factors *Wnt7a* and *Efnb2* (Figure 52B), consistent with previously described roles for Cdx in yolk sac vascularization and hematopoiesis (Brooke-Bisschop et al., 2017; Chawengsaksophak et al., 2004; Davidson et al., 2003; Davidson and

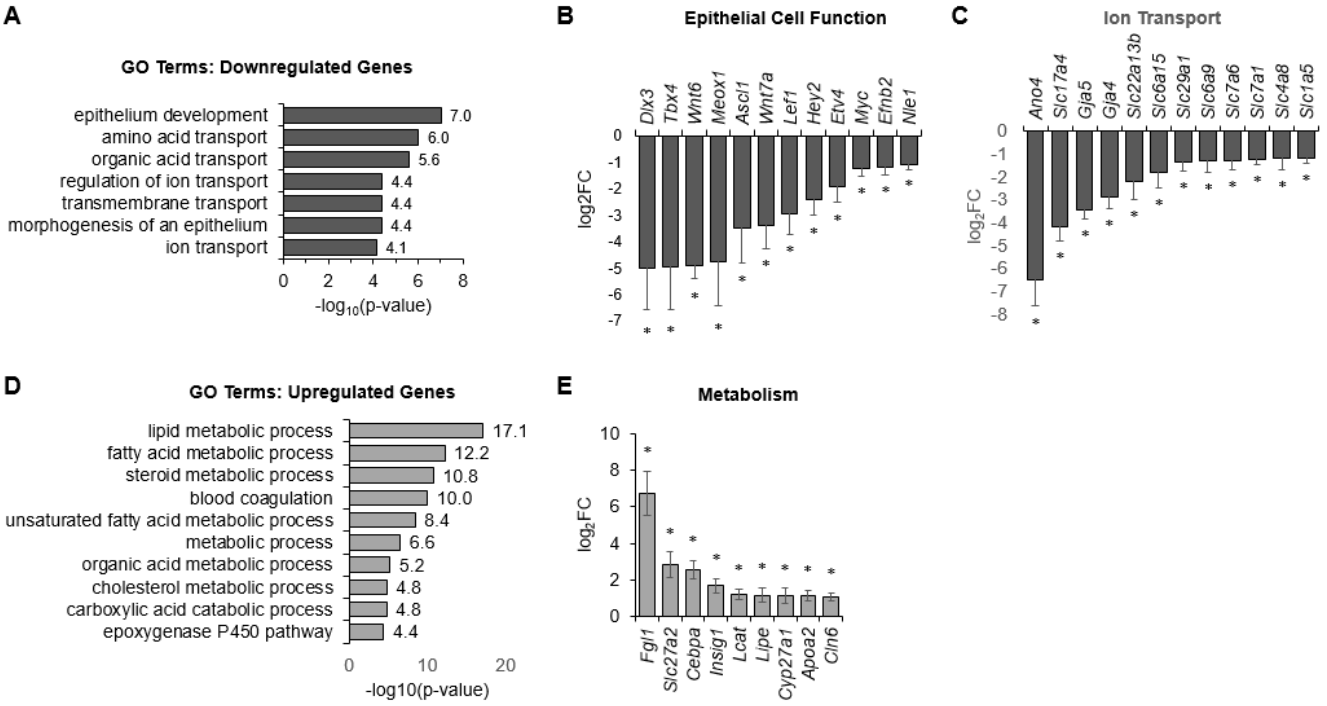


Figure 52. Genes involved in ion transport, blood vessel development, epithelial cell function, and metabolism are differentially expressed in DKO yolk sacs. A. GO analysis of genes downregulated in DKO yolk sacs relative to WT. Values represent $-\log_{10}$(p-value) for each term, with only significantly affected genes ($\log_2$FC $\geq$ 1, FDR $\leq$ 0.1) included in the analysis. **B.** Altered genes associated with epithelial cell function. Values represent $\log_2$FC $\pm$ s.e.m. Asterisks (*) indicate statistical significance (adjusted p-value (FDR) $\leq$ 0.05). C. Misregulated genes associated with ion and nutrient transport, as well as gap junctions. Values represent $\log_2$FC $\pm$ s.e.m. Asterisks (*) indicate statistical significance (adjusted p-value (FDR) $\leq$ 0.05). **D.** GO terms associated with increased gene expression in DKO mutant yolk sacs compared to WT. Values represent $-\log_{10}$(p-value) for each term, with only significantly affected genes ($\log_2$FC $\geq$ 1, FDR $\leq$ 0.05) included in the analysis. **E.** Select genes with increased transcript abundance in Cdx mutants associated with metabolic functions. Values represent $\log_2$FC $\pm$ s.e.m. Asterisks (*) indicate statistical significance (adjusted p-value (FDR) $\leq$ 0.05) as determined by paired Student's t-test.

Zon, 2006). Affected genes involved in ion and transmembrane transport included *Meox1*, *Ascl1, Etv4, Myc*, and *Nle1*, in addition to *Wnt6,* also involved in blood vessel formation (Figure 52B). Also among downregulated genes in this category were members of the *Slc* solute carrier family (*Slc17a4, Slc22a13b, Slc6a15, Slc29a1, Slc6a9, Slc7a6, Slc7a1, Slc4a8, Slc1a5*), the calcium-dependent non-selective anion channel *Ano4*, and genes encoding proteins associated with tight junctions (*Gjα4*, and *Gjα5*; Figure 52C). While misexpression of transport genes might suggest broad defects in visceral endoderm, the expression of canonical visceral endoderm markers like *Nodal*, *Gsc*, *Evx1*, and *Sox17* was unaffected in DKO mutants (Bielinska et al., 1996; Sherwood et al., 2007; Kanai-Azuma et al., 2002). Finally, GO terms associated with overexpressed transcripts included *metabolic processes* (*steroid*, *cholesterol*, *lipid*, and *fatty acid*; Figure 52D), comprised of genes like *Fgl1*, *Slc27a2*, *Cebpa, Lipe,* and *Apoa2,* among others (Figure 52E).

Identification of novel Cdx target genes in the yolk sac

To identify direct Cdx target genes in the yolk sac, we further examined *Tbx4*, *Sox9*, *Ascl1*, *Msx1*, *Ano4*, *Lef1*, and *Meox1,* as these transcripts were downregulated in DKO mutants by RNA-seq (Figure 53A). Reduced expression of all but *Meox1* was confirmed in E9.5 DKO yolk sacs by RT-qPCR (Figure 53B), with *Tbx4*, *Sox9*, *Ascl1*, and *Ano4* being significantly affected and *Tbx4* levels showing the strongest reduction.

Previous ChIP-seq analysis has demonstrated that Cdx2 occupies the above target loci in E8.5 embryos (Foley et al., 2019). To determine if this was also true for E9.5 yolk sacs, binding was interrogated by ChIP-PCR using primers designed to flank candidate Cdx response elements (CDRE) under previously identified ChIP-seq peaks (Foley et al., 2019). Despite Cdx2 occupancy at these loci in E8.5 embryos, no enrichment for binding was observed in yolk sac chromatin (data not shown). This

A

Gene Name	Log_2FC	P-value	FDR
Tbx4	-4.95	2.4×10^{-3}	1.8×10^{-2}
Sox9	-1.58	8.5×10^{-4}	8.0×10^{-3}
Ascl1	-3.49	8.1×10^{-3}	4.3×10^{-2}
Msx1	-1.03	1.2×10^{-2}	5.8×10^{-2}
Ano4	-6.5	6.19×10^{-9}	6.7×10^{-7}
Lef1	-2.94	2.9×10^{-4}	4.0×10^{-3}
Meox1	-4.74	4.9×10^{-3}	3.0×10^{-2}

B

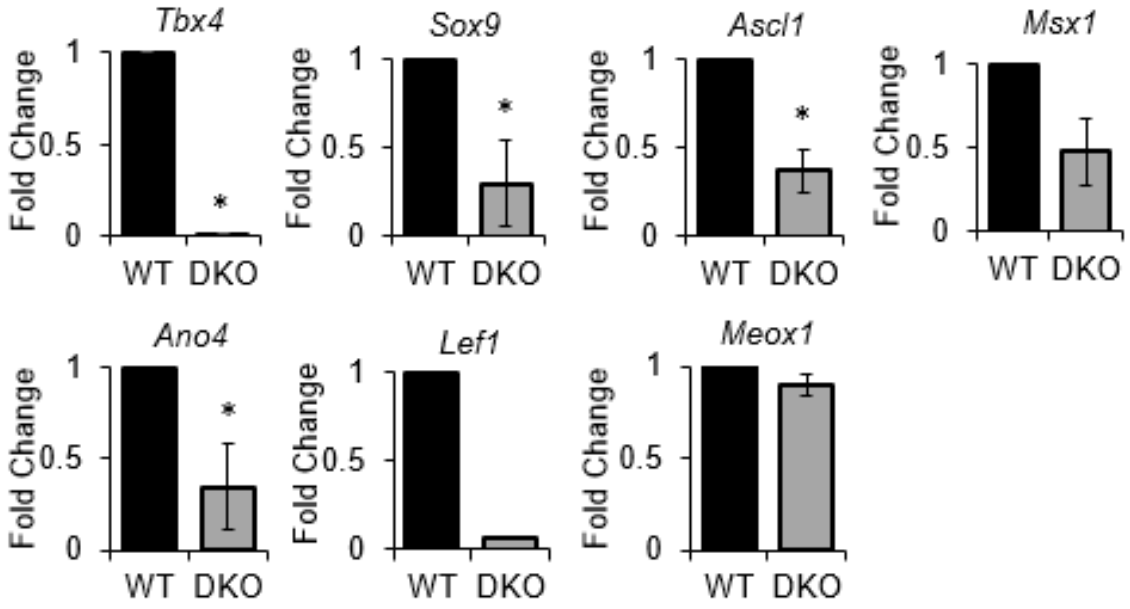


Figure 53. Differential gene expression in Cdx mutant yolk sacs. A. List of select Cdx-dependent genes in E9.5 yolk sacs as measured by RNA-seq with associated log_2FC values, p-values, and FDR. **B.** Transcript levels for *Tbx4*, *Sox9*, *Ascl1*, *Msx1*, *Ano4*, *Lef1*, and *Meox1* in E9.5 WT and DKO yolk sacs as assessed by RT-qPCR. Values represent the mean of three independent experiments $\pm$ s.e.m. for *Tbx4*, *Sox9*, *Ascl1*, *Msx1*, *Ano4*, and *Meox1*. Values for *Lef1* represent the mean of two independent experiments $\pm$ s.e.m. Asterisks indicate statistical significance ($p \leq 0.05$) as determined by paired Student's t-test.

suggests that the CDREs assayed may not be functional in the yolk sac at this stage, and that aberrant expression of these genes results from indirect mechanisms of regulation.

Previous work from our group suggested that Cdx members can act on targets in early mesodermal progenitor cells to establish chromatin architecture permissive to lineage-specific gene expression programs at later developmental stages, after Cdx expression is extinguished (Foley et al., 2019). To determine whether this might also be true for the candidate targets described here, Cdx2 occupancy at *Tbx4*, *Sox9*, *Ascl1*, and *Msx1* was assessed by ChIP-PCR in E7.5 embryos (Figure 54A), before mesodermal progenitors migrate to the yolk sac. In marked contrast to the yolk sac, Cdx2 binding was observed at each of these loci at E7.5, including at two CDREs proximal to both *Tbx4* and *Sox9*. Moreover, *Tbx4* and *Sox9* expression was significantly downregulated at this stage by RT-qPCR, while *Msx1* and *Ascl1* were not affected (Figure 54B). *Insm1*, which was upregulated in DKO yolk sacs by RNA-seq ($\log_2$FC = 3.3, p = 0.006, FDR = 0.04), was not occupied by Cdx2 at E7.5, serving as a negative control for Cdx2 binding. Taken together, these data suggest that Cdx2 regulates its target genes through locus-specific mechanisms, either impacting transcription at E7.5 directly, as occurs with *Tbx4* and *Sox9*, or through mechanisms that may prime targets for later expression in progeny, as with *Ascl1* and *Msx1,* and consistent with previous descriptions of Cdx-mediated gene regulation (Foley et al., 2019; Saxena et al., 2017; Mazzoni et al., 2013).

Cdx impacts PRC2-dependent gene regulation

Polycomb Repressive Complex 2 (PRC2) deposits H3K27me3, a repressive histone modification, onto genomic targets, and is composed of the core subunits Suz12, Eed, and one of two catalytic subunits, either Ezh1 or Ezh2 (Cao et al., 2002; Muller et al., 2002; Kuzmichey et al., 2002; Czermin et al., 2002; Margueron et al., 2008; Shen et al., 2008). Both RNA-seq and RT-qPCR analysis revealed that *Ezh1* transcripts were significantly increased in E9.5 DKO yolk sacs relative to WT

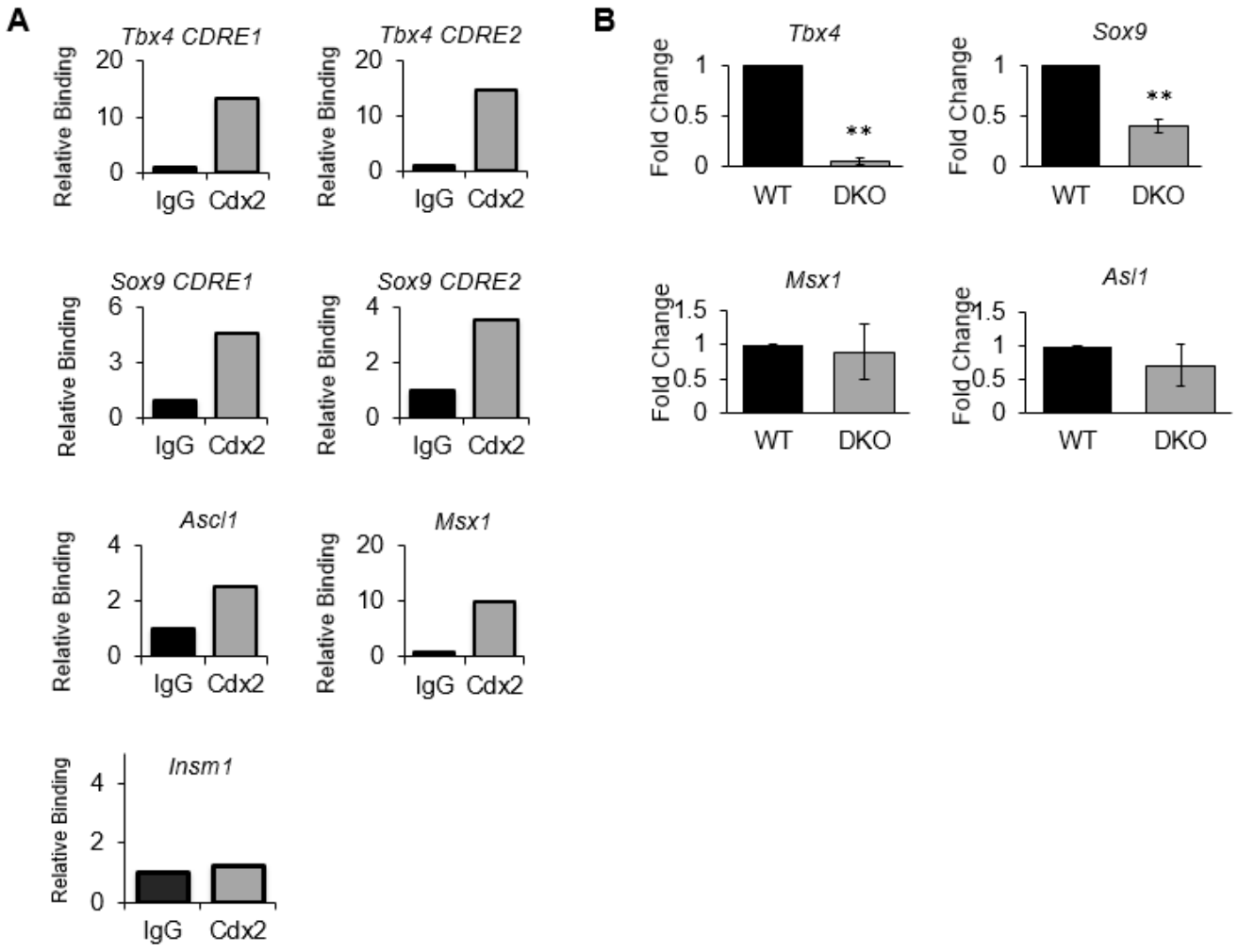


Figure 54. Cdx2 directly regulates *Tbx4* and *Sox9*. A. ChIP-PCR analysis of Cdx2 binding to *Tbx4*, *Sox9*, *Ascl1*, *Msx1,* and *Insm1* loci in E7.5 embryos. IgG was used as a negative control. Primers flanking putative CDREs identified from prior ChIP-seq analysis for Cdx2 occupancy were used for PCR (Foley et al., 2019). Values are representative of two independent experiments in which similar results were obtained. **B.** Expression of *Tbx4*, *Sox9*, *Msx1*, and *Ascl1* in E7.5 WT and DKO embryos as measured by RT-qPCR. Values represent fold change from the mean of at least three independent experiments ± s.e.m for *Tbx4*, *Sox9*, and *Msx1*. Values for *Ascl1* represent the mean of two independent experiments ± s.e.m. Asterisks (**) indicate statistical significance ($p \leq 0.001$) as determined by paired Student's t-test.

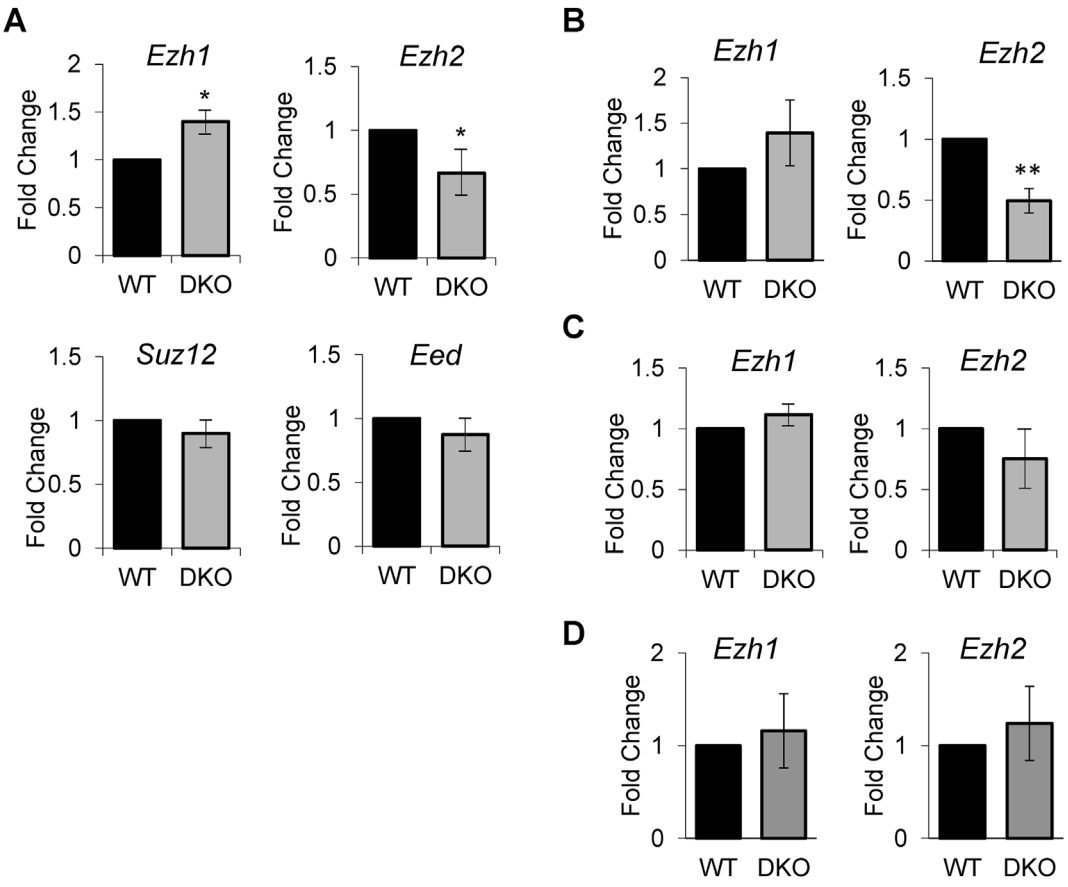


Figure 55. Cdx regulates *Ezh2* expression in the yolk sac. A. Normalized gene counts for *Ezh1*, *Ezh2*, *Suz12*, and *Eed* in E9.5 WT and DKO yolk sacs assessed by RNA-seq. Values represent fold change, with asterisks indicating statistical significance (FDR $\leq$ 0.1). **B.** *Ezh1* and *Ezh2* expression in E9.5 WT and DKO yolk sacs as measured by RT-qPCR. Values are expressed as fold change and represent the mean of 5 (*Ezh1*) and 6 (*Ezh2*) independent experiments $\pm$ s.e.m. Asterisks (**) indicate statistical significance ($p \leq 0.001$) as determined by paired Student's T-Test. No statistical significance is indicated by n.s. **C, D.** *Ezh1* and *Ezh2* expression in WT and DKO E8.5 tail buds (C) or E7.5 embryos (D) by RT-qPCR. Values represent the mean of two (C) or five (D) independent experiments $\pm$ s.e.m.

controls with a concomitant decrease in *Ezh2* levels, while *Eed* and *Suz12* were not affected (Figures 55A, B). *Ezh1* and *Ezh2* were modestly affected in E8.5 DKO tail buds (Figure 55C), while levels for both transcripts were unaffected at E7.5 (Figure 55D). These findings suggest that Cdx is required to maintain the expression of *Ezh1* and *Ezh2* in E8.5 embryo and the yolk sac, and that aberrant PRC2 subunit expression may contribute to misexpression of Cdx targets in the DKO yolk sacs.

Given prior work by our group showing that Cdx2 regulates gene expression by priming targets at early developmental stages (Foley et al., 2019), combined with work by others demonstrating that Cdx2 binding impacts H3K27me3 at target genes (Saxena et al., 2017; Mazzoni et al., 2013), we used ChIP-PCR to interrogate H3K27me3 density at the *Tbx4, Sox9, Ascl1,* and *Msx1* loci in E7.5 embryos (Figure 56A). H3K27me3 levels were markedly depleted in DKO embryos at each locus examined, despite normal *Ezh1* and *Ezh2* expression at this stage, suggesting that the deposition or retention of this repressive mark is Cdx-dependent.

To further investigate whether Cdx might impact H3K27me3 through locus-specific mechanisms, we intersected a previously published Cdx2 ChIP-seq dataset generated from E8.5 embryos (Foley et al., 2019) with a publicly available ChIP-seq dataset for Suz12 and H3K27me3 binding in embryonic stem cells collected at the mesoderm stage of differentiation to cardiomyocytes in culture (Figure 56B) (Alexander et al., 2015). Despite these datasets having been generated from different tissue types, this exercise identified regions of overlap between Cdx2 and Suz12/H3K27me3 at the *Tbx4, Sox9, Ascl1,* and *Msx1* loci flanked by regions void of binding. While these observations are speculative, they suggest that Cdx2 and PRC2 may co-regulate at least some common targets to maintain the fidelity of H3K27me3 marks, as suggested by prior work in the intestinal epithelium (Saxena et al., 2017).

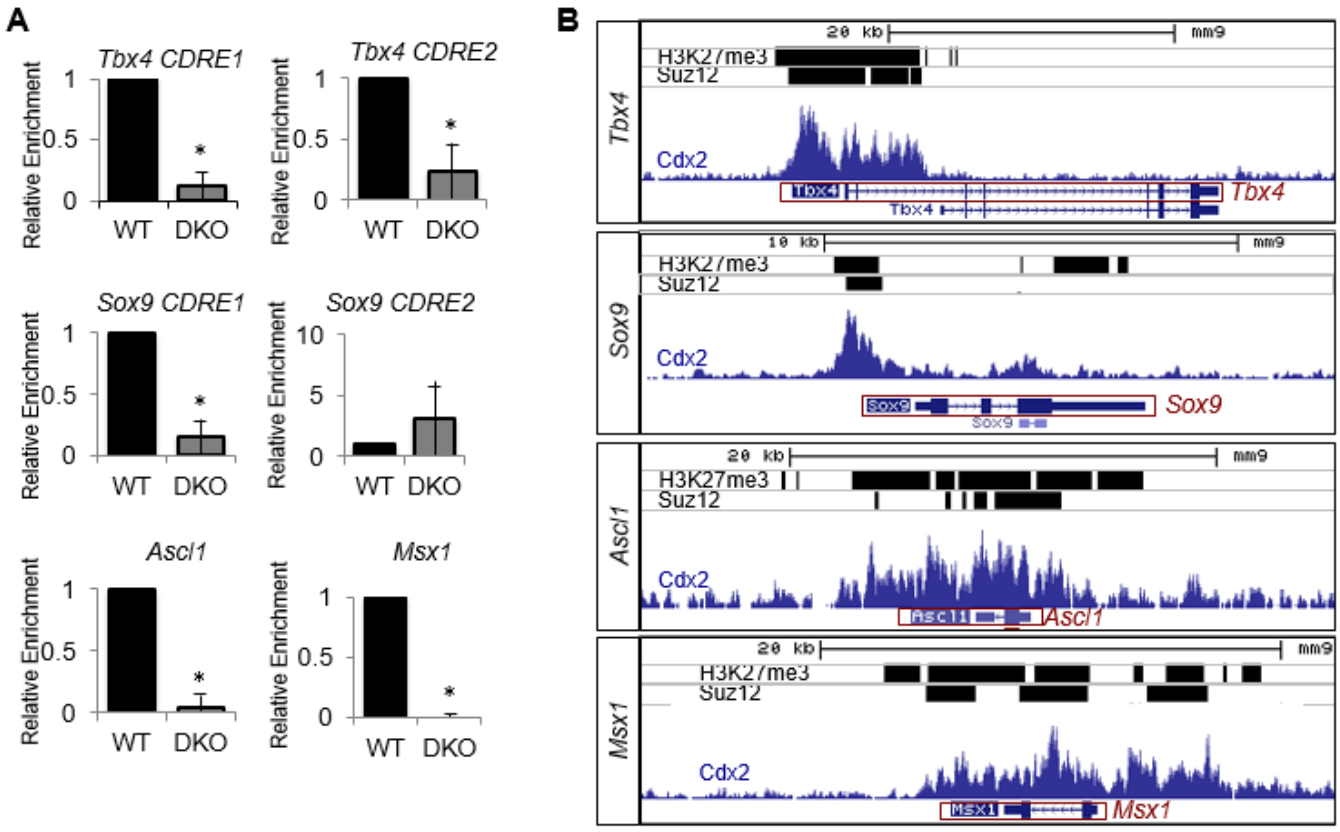


Figure 56. Cdx impacts H3K27me3 density at Cdx target genes. A. ChIP-PCR for H3K27me3 density at *Tbx4*, *Sox9*, *Ascl1*, and *Msx1* in E7.5 WT and DKO embryos. Values represent the mean of at least three independent experiments ± s.e.m. Asterisks (*) indicate statistical significance ($p \leq 0.05$) as determined by paired Student's t-test. **B.** ChIP-seq tracks for Cdx2 binding in E8.5 whole embryos (blue peaks) were visualized for *Tbx4*, *Sox9*, *Ascl1*, and *Msx1* and overlayed with previously published analyses (Alexander et al., 2015) for H3K27me3 and Suz12 (black bars, above) using the UCSC genome browser. Scale bars are shown above and exons are indicated by blue boxes below.

DISCUSSION

To better understand the role of Cdx in development of the yolk sac, we used a previously described conditional mutant to circumvent embryonic lethality associated with Cdx2 loss of function and negate functional overlap between family members (Savory et al., 2011a). Mutant yolk sacs exhibited altered expression of genes involved in hematopoiesis and vasculogenesis, consistent with previous observations (Brooke-Bisschop et al., 2017; Lengerke et al., 2008; Davidson and Zon, 2006; Davidson et al., 2003; Wang et al., 2008). Gene expression analyses combined with ChIP for Cdx2 occupancy identified a number of novel potential Cdx-dependent targets, including *Lef1*, *Ascl1*, *Ano4*, *Msx1*, *Sox9*, and *Tbx4*. In addition, we observed Cdx-dependent changes in expression of the catalytic PRC2 subunits *Ezh1* and *Ezh2*. Misexpression of *Tbx4*, *Sox9*, *Ascl1*, and *Msx1* in the yolk sac, coupled with selective Cdx2 occupancy and concomitant loss of H3K27me3 at these loci at E7.5, suggests that Cdx establishes gene expression programs in mesodermal progenitors through epigenetic mechanisms, and that these programs are deployed at later stages independent of Cdx occupancy (Figure 57).

Cdx and the yolk sac

Despite fully penetrant phenotypes in DKO embryos, including lack of blood and vascularization in mutant yolk sacs, wild-type *Cdx2* transcripts were unexpectedly detected in DKO yolk sacs. Yolk sac blood and vasculature are both derived from the hemangioblast, a mesodermal progenitor that is specified in the embryo proper during gastrulation that subsequently migrates to populate the yolk sac. As both yolk sac blood and vasculature were severely and consistently disrupted in DKO mutants, despite residual Cdx2 expression, it is likely that this phenotype reflects Cdx depletion from mesodermal lineages in the embryo proper, rather than cells of extra-embryonic origin in the yolk sac such as those within the visceral endoderm.

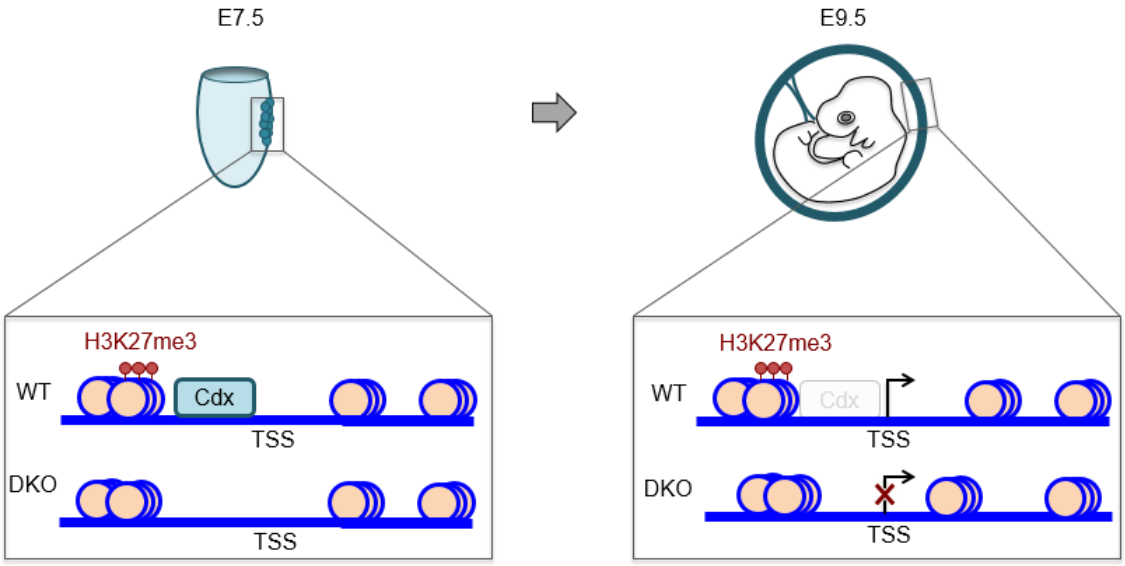


Figure 57. Model for Cdx function. Cdx2 binds to its targets at E7.5 when yolk sac progenitors are being specified from the primitive streak and impacts H3K27me3 density at certain of these sites which is required for gene expression in yolk sac progeny at E9.5. In DKO mutants, this epigenetic priming does not occur, resulting in altered H3K27me3 at Cdx target genes and aberrant gene expression in the yolk sac.

The visceral endoderm produces diffusible factors required for blood vessel formation within the underlying mesoderm, such as Ihh and Vegfa (Becker et al., 1997; Farrington et al., 1997; Damert et al., 2002; Miura and Wilt, 1969; Beloussoff et al., 1998; Vokes and Krieg, 2002; Dyer et al., 2001). While Cdx2 is expressed in the visceral endoderm (Scialdone et al., 2016; Pijuan-Sala et al., 2019), *Ihh* and *Vegfa* transcript levels were not impacted in DKO yolk sacs, making it unlikely that the vascular defects observed in DKO mutants result from aberrant signaling from the visceral endoderm. Indeed, an embryonic origin for Cdx-dependent yolk sac defects is further supported by previous studies in which *Cdx2* ablation in *Mesp1*$^{+}$ or *Tie2*$^{+}$ populations, specified in the primitive streak, phenocopied the DKO vascular lesions (Brooke-Bisschop et al., 2017; Foley et al., 2019). Together, these observations are consistent with a role for Cdx in regulating yolk sac hematopoiesis and vasculogenesis through the establishment of gene expression programs in the mesoderm, rather than in the visceral endoderm.

The visceral endoderm plays an important role in nutrient uptake and waste exchange until chorioallantoic fusion (Gillman et al., 1948; Brent et al., 1990; Jolie, 1990; Lloyd, 1990; Lloyd, 1997; Farese et al., 1995; Cross et al., 1994; Zohn and Sarkar, 2010). While critical functions for *Cdx2* in the trophectoderm and the allantois are known, roles for Cdx in the yolk sac visceral endoderm have not been described previously. The epithelium of the visceral endoderm is functionally and morphologically similar to that of the intestine (Bielinska et al., 1999), as both contain microvilli that facilitate nutrient absorption (Calarco et al., 1966). In the intestinal epithelium, Cdx directs the expression of genes involved in ion transport, including diverse members of the *Slc* solute carrier family (Verzi et al., 2011; Gao et al., 2009). While these specific transcripts were not aberrantly expressed in Cdx-deficient yolk sacs, misregulation of *Slc* family members with similar functions, including *Slc1a5, Slc4a8, Slc4a11, Slc6a9 Slc6a15*, *Slc7a1 Slc7a6, Slc22a13, Slc17a4*, and *Slc29a4* were observed, as was mis-expression of the calcium-dependent non-selective anion channel *Ano4* (Reichart et al., 2019), genes encoding tight junction proteins (*Gjα4*, *Gjα5*, and *Gjβ3*), and others involved in ion and nutrient transport. These observations suggest that Cdx factors may regulate analogous processes in the yolk sac and in the intestine. While Cdx2 is expressed in the visceral endoderm as early as E7.5 (Scialdone et al., 2016; Pijuan-Sala et al., 2019), derivation of an appropriate Cre driver will be necessary to better define the role of Cdx in this tissue.

Cdx primes gene expression programs

Prior work suggests that Cdx promotes mesoderm differentiation to hematopoietic lineages while concomitantly repressing cardiac fate from a common progenitor pool (Foley et al., 2019; Lengerke et al., 2011; Rao et al., 2016). Consistent with this, many genes affected in DKO yolk sacs in the present study are known regulators of hematopoiesis and vascularization. These included Cdx targets, *Scl/Tal-1*, *Lmo2*, and *Lyl1* (Brooke-Bisschop et al., 2017), as well as genes not previously

reported to be Cdx-dependent, such as *Msxl1*, *Hey1*, *Hey2,* and *Wt1* (Goupille et al., 2008; Fischer et al., 2004; Wagner et al., 2008). However, the ectopic expression of cardiogenic markers previously observed in Cdx mutant embryos (Foley et al., 2019) was not seen in yolk sacs, suggesting that such mis-specified progenitors are incapable of colonizing the yolk sac.

Cdx members influence gene expression, in part, via epigenetic mechanisms (Foley et al., 2019; Nguyen et al., 2017; Saxena et al., 2017; Mazzoni et al., 2013; Verzi et al., 2010). We previously proposed that Cdx establishes the chromatin landscape in E7.5 embryos necessary for the expression of lineage-specific gene expression programs in descendent lineages (Foley et al., 2019). Previous work also showed that yolk sac hematopoiesis is initiated in DKO mutants at E8.5, but is not maintained beyond this stage (Brooke-Bisschop et al., 2017). Consistent with these observations, Cdx target genes in the present study were bound by Cdx2 in E7.5 embryos, but not in yolk sac progeny at E9.5, further suggesting Cdx functions at these CDREs in early progenitors to prime targets for expression at later stages, when these elements are no longer functional. We cannot, however, exclude the possibility that Cdx binding to these targets at E7.5 regulates their expression in lineages that do not contribute to the yolk sac.

Among the novel Cdx target genes in this study, *Tbx4* was most dramatically downregulated in mutant yolk sacs, and was occupied by Cdx2 as early as E7.5, consistent with it being a direct target gene. *Tbx4* is well known for its role in hindlimb development (Chapman et al., 1996; Gibson-Brown et al., 1996), and is also highly expressed in the allantois where it is required for both allantoic growth and vasculogenesis during umbilical cord formation (Chapman et al., 1996; Naiche et al., 2011; Naiche et al., 2003). Like yolk sac mesoderm, the allantois is derived from $Flk1^{+}$ progenitors in the posterior primitive streak (Kattman et al., 2006). Both *Tbx4* and *Cdx2* are expressed in the allantois at E7.5, and mutants for either factor exhibit comparable defects in chorioallantoic fusion (Chawengsaksophak et al., 2004; Beck et al., 1995; Chapman et al., 1996; Naiche et al., 2003). The pronounced reduction in

Tbx4 transcripts in DKO mutants therefore suggests a mechanistic basis for defective chorioallantoic fusion in *Cdx* mutants (Chawengsaksophak et al., 2004).

Like *Tbx4, Sox9* was also occupied and regulated by Cdx2 at E7.5, and both *Tbx4* and *Sox9 loci* exhibited a marked reduction in H3K27me3 levels in DKO mutants at this stage. This reduced expression, coupled with lost Cdx2 occupancy and aberrant H3K27me3 deposition in mutants, suggests direct regulation of *Tbx4* and *Sox9* by Cdx2. In contrast, *Ascl1* and *Msx1* were not misregulated in E7.5 DKO mutants, despite decreased H3K27me3 and Cdx occupancy. This suggests that Cdx regulates its targets through multiple mechanisms, with early binding resulting in either direct regulation, as observed for *Tbx4* and *Sox9*, or epigenetic priming, as occurs for *Ascl1* and *Msx1,* which are only affected at later stages.

Cdx2 and PRC2

Cdx2 occupancy has been shown to oppose PRC2 function by preventing the spread of H3K27me3 across positively-regulated Cdx targets, thereby promoting a chromatin state permissive to transcription (Saxena et al., 2017; Mazzoni et al., 2013). In marked contrast, we found that H3K27me3 was abolished from positively-regulated Cdx targets in E7.5 mutant embryos. This suggests that H3K27me3, typically thought to mark gene repression, is not necessarily predictive of transcriptional activity, consistent with observations made by others (Miller et al., 2021). The absence of H3K27me3 from Cdx targets at E7.5 was not due to the altered expression of *Ezh1/Ezh2,* as both were unaffected at this stage. Rather, the absence of H3K27me3 correlates with loss of Cdx2 occupancy, consistent with previous work (Saxena et al., 2017).

Overlap was observed between genomic sites of Cdx2 occupancy in the embryo (Foley et al., 2019) and regions bound by Suz12/H3K27me3 in mesodermal progenitors differentiated from ESCs in culture (Alexander et al., 2015), despite these differences in tissue type. Given that both datasets

contain *Flk1*$^{+}$ mesoderm that contributes to both embryonic and extra-embryonic lineages, and that we suspect Cdx regulates yolk sac gene expression by priming mesodermal progenitors as they are specified from the streak, we feel that this comparison is relevant, despite being speculative. The overlap in Cdx2 and PRC2 occupancy, coupled with decreased H3K27me3 at Cdx targets in DKO mutants, suggests that Cdx2 and PRC2 may co-regulate shared targets, however whether this co-regulation occurs within the yolk sac, and in the same temporal window, remains unknown.

In contrast to earlier stages, *Ezh1* expression was significantly increased at E9.5. While Ezh1 and Ezh2 both have histone methyltransferase activity, they repress gene expression through different mechanisms. PRC2 complexes containing Ezh1 are less catalytically active than those containing Ezh2, yet are more efficient at compacting chromatin and through mechanisms independent of H3K27me3 (Margueron et al., 2008). Thus, in the absence of Cdx, alterations in the relative abundance of *Ezh1* and *Ezh2* may result in increased Ezh1-containing complexes, and therefore greater chromatin compaction and attenuation at target genes, impacting expression independent of H3K27me3 density and consistent with previously described Cdx-dependent changes in chromatin accessibility (Foley et al., 2019; Nguyen et al., 2017; Saxena et al., 2017; Mazzoni et al., 2013; Verzi et al., 2010).

Conclusions

Consistent with previous studies, we have shown that Cdx transcription factors are essential for the expression of genes involved in yolk sac hematopoiesis and vasculogenesis. Further, we identified novel direct Cdx targets, such as *Tbx4* and *Sox9,* and demonstrate that Cdx is required for ion and nutrient transport in the yolk sac, regulating processes that are analogous to Cdx-dependent functions in the intestine. The data presented here further suggest that Cdx is required to establish, or maintain, the epigenetic code at certain target gene loci, in part through PRC2 subunit expression and deposition of

H3K27me3 at Cdx targets (Figure 57). Through this, Cdx establishes an early chromatin architecture that ensures appropriate gene expression programs in descendant lineages.

MATERIALS AND METHODS

Mice

Cdx1$^{-/-}$*Cdx2*$^{fl/fl}$ and *CMV-Actin::CreER*^{T} lines have been previously described (Savory et al., 2009a; Santagati et al., 2005). For timed matings, *Cdx1*$^{-/-}$*Cdx2*$^{fl/fl}$ *CMV-Actin::CreER*^{T} males were crossed with *Cdx1*$^{-/-}$*Cdx2*$^{fl/fl}$ females and noon of the day of vaginal plug discovery was considered to be E0.5. *Cdx2* deletion was induced with 2 mg tamoxifen administered by oral gavage on E5.5. Wild-type (WT) controls were collected from timed matings between CD1 animals (Charles River), with pregnant dams left untreated. Animals were maintained according to guidelines established by the Canadian Council on Animal Care and the Animal Care and Veterinary Services at the University of Ottawa approved all experimental protocols.

Histology

Yolk sacs were dissected from WT or DKO embryos at E9.5, fixed in 4% paraformaldehyde at 4°C overnight, then transferred to 70% ethanol. Tissue was immobilized in agarose, embedded in paraffin, and 4 μm sections were prepared and mounted on slides. Hematoxylin and eosin (H&E) staining was performed by the Louise Pelletier Histology Core Facility at the University of Ottawa. Images were captured using a Zeiss AxioImager M2 with transmitted light and an AxioCam mRc colour camera.

Antibodies

Rabbit-anti-Cdx2 polyclonal antibodies were generated as previously described (Savory et al., 2009b). Polyclonal rabbit-anti-H3 and rabbit-anti-H3K27me3 were from Cell Signaling (9715S and 9733S, respectively). Control IgG antibodies were from Sigma (i8140).

Chromatin immunoprecipitation (ChIP)

Yolk sacs were cross-linked with 1% formaldehyde. ChIP was performed as previously described (Pilon et al., 2006) with the following modifications: chromatin was sonicated for six 1-minute intervals using a Branson Sonifier 450 at output 3, 30% duty cycle. 5 µg of either polyclonal rabbit-anti-H3K27me3 (Abcam) or rabbit-anti-IgG (Sigma) were coupled to 50 µl Protein A/G agarose beads (Santa Cruz) at 4°C overnight. Sample purification was performed with the QIAquick PCR Purification Kit (Qiagen) before PCR using primers as listed (Table 6). Statistical significance was determined by unpaired two-tailed Student's t-test ($p \leq 0.05$).

Table 6. List of ChIP-PCR primer sequences

Gene	Primer Sequence	
Tbx4 CDRE1	Forward	GGACGGCTTGAAAGTTTGCT
	Reverse	GCCATGGTTACCGCTCTTTTG
Tbx4 CDRE2	Forward	AGTGCTCCTTTTGGGATCGG
	Reverse	AAACTCGTCGCCCTGAGAAG
Sox9 CDRE1	Forward	GGCCCCTGGTCTCTTCAAATA
	Reverse	ATCTTAGTTGCCACCGGGC
Sox9 CDRE2	Forward	GCCTTTGTGCCAGAATACGTG
	Reverse	AAAGCGAATCGGCCTGTATC
Ascl1 (Mash1)	Forward	TAATGCTGACTGAATGCGGC
	Reverse	GTTCCCGTTCCTGTTCCGTT
Msx1	Forward	AAGATGCTCTGGTGAAGGC
	Reverse	TGGTCTTGTGCTTGCGTAG

ChIP-seq tracks for Suz12 and H3K27me3 were previously generated from embryonic stem cells collected at the mesodermal stage of *in vitro* differentiation to cardiac mesoderm in culture (Alexander et al., 2015). These publicly available tracks were intersected with tracks for Cdx2 binding in E8.5 embryos (Foley et al., 2019) using the UCSC genome browser (https://genome.ucsc.edu/).

Reverse-transcription quantitative PCR (RT-qPCR)

E8.5-9.5 embryos and yolk sacs were collected and RNA was extracted using Trizol (Gibco BRL) according to manufacturer's instructions. cDNA was prepared by conventional methods and amplified using a BioRad CFX96 Real-Time PCR System (C-1000 Touch Thermal Cycler) and GoTaq (Promega), with normalization to *Gapdh*. The ΔΔCt method was used to determine changes in gene expression, and statistical significance was determined using an unpaired two-tailed Student's t-test ($p \leq 0.05$). For semi-quantitative RT-PCR, cDNA was amplified a DNA Engine Tetrad 2 (Bio-Rad) using GoTaq (Promega), with *β-actin as* a loading control. Primers used were previously described (Foley et al., 2019) or as listed (Tables 7 and 8).

Table 7. List of qRT-PCR primer sequences

Gene	Primer Sequence	
Tbx4	Forward	TCCTTCATCTCTGTGACCTCC
	Reverse	ATACTCCTTTCTCTGCAACCG
Sox9	Forward	GAAGGCGAGTCGGAGCGGAG
	Reverse	GGAAGTCGGAGAGCCGAGAG
Msx1	Forward	AAGATGCTCTGGTGAAGGC
	Reverse	TGGTCTTGTGCTTGCGTAG
Ascl1 (Mash1)	Forward	CTCTCCTGGGAATGGACTTTG
	Reverse	GGCTGTCTGGTTTGTTTGTTT
Ano4	Forward	AAATCTATTACCTGCCCCGC
	Reverse	GTAGCAGTCATTCTCTTCCAGG
Meox1	Forward	AACCTGGACCTTTCTGAGC
	Reverse	TCTGAACTTGGAGAAGCTGC
Lef1	Forward	AGCCTGTTTATCCCATCACG
	Reverse	TGTTACAATAGCTGGATGAGGG
Ezh1	Forward	TCTTCCACGGCACCTATTTC
	Reverse	TTCTGTGCAGGGTTCATGAG
Ezh2	Forward	TCCCGTTAAAGACCCTGAATG
	Reverse	TGAAAGTGCCATCCTGATCC
Gapdh	Forward	GGCCGGTGCTGAGTATGTCG
	Reverse	TTCAAGTGGGCCCCGGCCTT

Table 8. List of RT-PCR primer sequences

Cdx2	Forward	AGCCAAGTGAAAACCAGGACAA
	Reverse	TGCAAGGAGGTCACAGGACT
β-Actin	Forward	GCGGGAAATCGTGCGTGACATT
	Reverse	GATGGAGTTGAAGGTAGTTTCGTG

Bulk RNA-sequencing

RNA was collected from E9.5 yolk sacs using the RNeasy Mini Kit (50) (Qiagen) according to the manufacturer's instructions, and library preparation and sequencing was conducted by the Genome Quebec Innovation Centre. Briefly, mRNA libraries were generated using NEB Next dual adapters. Quality control was performed using a bioanalyzer, and samples were multiplexed and sequenced to an average of 25M reads per library using the Illumina HiSeq 4000 SR50 platform. Reads were aligned to the *Mus musculus* mm10 reference genome and gene expression analysis performed in R using "RSamtools", "GenomicFeatures", "GenomicAlignments", and "DESeq2" packages, as described by Love and colleagues (Love et al., 2015). For statistical analyses, false discovery rates (FDR) were generated by the base R *p.adjust* function within the DESeq2 package, which adjusts for multiple testing using the Bejamini-Hochberg procedure. Significantly affected genes were considered to be those with a log2 fold change ($\log_2$FC) ≥ 1 and a FDR ≤ 0.1.

ACKNOWLEDGEMENTS

We thank Filipo Rijli for the *CMV-Actin::CreER^T* mouse line, the University of Ottawa Animal Care and Veterinary Service for excellent mouse husbandry, and the Louise Pelletier Histology Core Facility for the preparation of histological samples. We thank Travis Brooke-Bisschop for providing images of whole mount yolk sacs.

CHAPTER 4 – GENERAL DISCUSSION

Overview

This study sought to address unanswered questions relating to the role of Cdx function during mesoderm specification, and to identify the molecular mechanisms by which Cdx transcription factors regulate gene targets. To address these questions, we first explored the role of Cdx factors in derivatives of multipotential *Mesp1*$^{+}$ mesoderm. We identified a number of novel Cdx2 target genes involved in both cardiogenesis and yolk sac hematopoiesis, and provided evidence for direct regulation of these targets by Cdx2. Following this, we identified Brg1 and the SWI/SNF chromatin remodeling complex as a Cdx2 interacting partner at a number of these targets. We then showed that in the absence of Cdx2, Brg1 localization to cardiac targets is disrupted, resulting in aberrant chromatin organization at these loci (Foley et al., 2019). Thus, we propose that during gastrulation Cdx is required for the recruitment of Brg1 and the SWI/SNF complex to cardiac targets to establish a chromatin landscape that ensures the appropriate gene expression programs are induced at later developmental stages, thereby suggesting a model for the cardiac gene misexpression and aberrant heart morphogenesis seen in Cdx mutants (Foley et al., 2019).

Given that cardiac misspecification was observed in DKO mutants at the expense of the hematopoietic lineage, we next explored Cdx-dependent gene expression programs in the extra-embryonic yolk sac, the site of primitive hematopoiesis. We began by identifying affected gene targets and developmental processes in Cdx mutant yolk sacs (Foley et al., 2021), including the novel targets *Tbx4, Sox9*, *Msx1*, and *Ascl1*. Through subsequent experimentation, the yolk sac expression of these targets was shown to be maintained through Cdx-dependent epigenetic priming initiated earlier in development, at E7.5. We demonstrated that Cdx2 occupancy at these loci during gastrulation is associated with H3K27me3 maintenance, which is disrupted in DKO mutants and contributes to gene misregulation (Foley et al., 2021). The main conclusions from these studies are outlined in further detail below.

Cardiac defects in Cdx mutant embryos

Among the many developmental defects that result from Cdx depletion are defects in chorioallantoic fusion (Chawengsaksophak et al., 2004) and defects in yolk sac vascularization and primitive hematopoiesis (Brooke-Bisschop et al., 2017; Lengerke et al., 2007; Wang et al., 2008; Davidson and Zon, 2006; Davidson et al., 2003). Each of these contribute to poor oxygenation of developing tissues, including the heart, which begins to emerge at E8.5. This stage is concomitant with both hematopoietic development and formation of the chorioallantoic placenta. While it may be argued that cardiac defects in DKO mutant embryos are secondary to the absence of blood, Cdx2 occupancy at a number of cardiac loci suggests direct regulation of cardiac morphogenesis by Cdx factors. This is further supported by Cdx-dependent recruitment of the SWI/SNF complex to these sites, accompanied by changes in chromatin accessibility at loci aberrantly expressed in the cardiac crescent of DKO mutants.

Studies in zebrafish and mouse models have demonstrated a requirement for Cdx during embryonic hematopoiesis (Lengerke et al., 2007; Wang et al., 2008; Brooke-Bisschop et al., 2017; Davidson and Zon, 2006; Davidson et al., 2003). Prior to the studies presented here, however, little was known about the role of Cdx factors in cardiogenesis and much remains to be elucidated. In vitro studies have demonstrated an initial requirement for Wnt signaling during hESC induction to mesoderm, along with downstream Cdx function, followed by Wnt and Cdx inhibition for progression to cardiac lineages (Rao et al., 2016; Mendjan et al., 2014). Cdx factors and the Wnt pathway share a close relationship, with Cdx expression induced by Wnt signaling, coupled with Cdx-dependent expression of Wnt pathway elements, including *Wnt3a*, *Wnt5a*, and *Lef1* (Ikeya et al., 2001; Lickert et al., 2000; 2002; Prinos et al., 2001; Shimizu et al., 2005; Pilon et al., 2006; Rao et al., 2016; Mendjan et al., 2014; Nguyen et al., 2017; Savory et al., 2009a; Foley et al., 2019). The work presented here is consistent with these previous observations, suggesting that Cdx activity is incompatible with the

acquisition of a cardiac fate while being permissive to hematopoietic lineage specification (Mendjan et al., 2014; Rao et al., 2016; Lengerke et al., 2007; Lengerke et al., 2008; Wang et al., 2008; Brooke-Bisschop et al., 2017; Davidson and Zon, 2006; Davidson et al., 2003).

Ectopic cardiac gene expression in DKO mutants

In addition to cardiac defects, ectopic cardiogenesis is predicted to occur in mesodermal progenitors destined to populate the Cdx mutant yolk sac. Previous work by our group identified *Scl/Tal-1* as a Cdx target. *Scl/Tal-1* is required for yolk sac hematopoiesis, in part through the repression of cardiac transcription factors within mesodermal precursors (Shivdasani et al., 1995; Van Handel et al., 2012; Org et al., 2015). Yolk sac explant cultures generated from embryos deficient for *Scl/Tal-1* produce beating colonies and express cardiac markers like *cardiac troponin T* (*cTnT*; Van Handel et al., 2012), indicative of misspecification of hematopoietic progenitors to cardiac fates. We assessed the ability for Cdx-deficient yolk sac explant cultures and mouse embryoid bodies (EBs), differentiated from mESCs, to generate beating colonies. Explant cultures from DKO yolk sacs produced beating colonies (T.B.B and D.L., unpublished observations), however these observations were difficult to reproduce. EBs generated from both $Cdx1^{-/-}Cdx2^{fl/fl}$ $Actin::CreER^{T}$ mESCs differentiated with and without 4-OHT (control and DKO, respectively) produced spontaneously beating cells after 26 days of differentiation. We suspect the presence of beating cells in both mutant and control tissue was due to sub-optimal culture conditions. Despite this, the number of contracting colonies was greater in the DKO colonies than in controls (Appendix Figure 58), suggesting a greater potential for misspecification to cardiomyocytes in the absence of Cdx, which was further supported by increased *cTnT* expression in both DKO embryos and yolk sacs relative to controls at E8.5 (Appendix Figure 59). These observations are consistent with our model in which Cdx functions upstream of Scl to repress cardiogenesis within multipotential mesoderm.

While the appearance of spontaneously beating colonies and *cTnT* expression in DKO yolk sac and EB cultures points to ectopic cardiogenesis in Cdx mutants, GO terms associated with cardiogenesis were not overrepresented in E9.5 DKO yolk sacs as measured by RNA-seq. It may be that at E8.5, the stage at which *cTnT* levels were measured, cardiac gene expression is present in the yolk sac but is lost at E9.5 as cells become more dysfunctional. Alternatively, it may be that hematopoietic progenitors that are misspecified in the primitive streak are unable to colonize the yolk sac, as proposed in Chapter 3, or that ectopic *cTnT* in the yolk sac is produced by a different cell type that is also impacted by Cdx ablation. Further experimentation, such as *Cdx2*$^{+}$ lineage-tracing combined with cell-sorting at a range of developmental stages, may further elucidate the role of Cdx factors in mesoderm specification and address these outstanding questions.

Cdx2 occupancy across the genome

We used ChIP-seq to identify regions enriched for Cdx2 occupancy in E8.5 embryos. Transcription factor binding can occur near the promoter region of genomic targets, spanning distances between 1-5kb. ChIP-seq peaks generated by such transcription factor binding are generally discrete, and much narrower than those produced from histone modifications, which can cover hundreds of kilobases (Zhao et al., 2007; Hawkins et al., 2010). ChIP-seq studies of Cdx2 occupancy have been performed by a number of groups in various tissue types, including mouse epiblast stem cells and intestinal tissue from mice, humans, and differentiated from ESCs in culture (Kumar et al., 2019; Verzi et al., 2010; 2013; Saxena et al., 2016; Amin et al., 2016). While broad peaks have been observed at Cdx2-occupied sites in some of these studies (Kumar et al., 2019; Amin et al., 2016), peaks associated with Cdx2 are often narrow and consistent with what is expected from binding by a transcription factor (Verzi et al., 2010; 2013; Kumar et al., 2019; Amin et al., 2016). It is unlikely that the breadth of the Cdx2 binding peaks are associated with plasticity or developmental stage, as broad peaks were

observed in cells from adult intestine (Kumar et al., 2019), epiblast stem cells (Amin et al., 2016), and embryos as observed in our study (Foley et al., 2019). Instead, differences in the breadth of ChIP-seq peaks may result from differences in the anti-Cdx2 antibody employed in each study, or from the methods used to prepare chromatin prior to immunoprecipitation.

In our work, broad and narrow Cdx2 binding peaks were differentially localized across the genome, with narrow peaks at promoters and broad peaks localized to regions distal from the TSS of putative targets (Foley et al., 2019). The presence of broad Cdx2-binding peaks may suggest that CDREs are not essential for Cdx2 binding, however for both classes of Cdx2-peaks (broad and narrow), putative CDREs could be identified under Cdx2 peaks. Further, Cdx2-binding could be detected at these sites by ChIP-PCR using primers specifically designed to flank putative CDREs identified within broader Cdx2-occupied regions (Foley et al., 2019). It may be that the presence of this sequence is required for Cdx2 to be localized to its targets, but once it bound, Cdx2 may have some mobility across its target loci. This mobility may be conferred by its interaction with binding partners, such as the Brg1 subunit of the SWI/SNF complex, however at the present time this hypothesis is speculative.

In addition to both broad and narrow binding peaks, Cdx2 occupation occurred both distal from, and proximal to, the promoters of putative target genes (Foley et al., 2019). ChIP-seq in E8.5 embryos revealed Cdx-occupied regions were largely localized to the TSS of putative targets, with fewer binding sites within more distal regions (Foley et al., 2019). Despite this, a subset of Cdx2-bound regions were associated with intergenic regions. These particular peaks were broader than those expected from binding by a transcription factor, containing defined summits but spanning distances as large as 20 kb, as was observed at the genomic loci of mesodermal targets like *Tbx5* and *Nkx2-5*, among others (Foley et al., 2019). It is possible that Cdx2 regulates gene expression through context-specific mechanisms, with broad regions of Cdx2 occupation distal from gene bodies associated with

one mechanism of regulation, and narrow peaks at gene promoters indicative of a separate molecular mechanism.

To explore this further, sites occupied by Cdx2 in E8.5 embryos were compared to those bound by SWI/SNF and PRC2 in mesodermal progenitors differentiated from ESCs in vitro (Alexander et al., 2015). Sites of overlap between Cdx2-bound regions and regions occupied by Brg1, a catalytic subunit of the SWI/SNF complex, revealed 927 sites across the genome that were common to both factors (Appendix Figure 60), corresponding to 794 unique genes. Most of these shared sites were distal from associated target genes (50-500 kb from the TSS), and occurred at genes associated with biological processes such as *blood vessel morphogenesis*, *blood vessel development*, and *cardiac morphogenesis* (Appendix Figure 61).

Cdx2-bound regions in the embryo and those occupied by Suz12, a member of PRC2, identified 425 sites common to both factors (Appendix Figure 62) associated with 310 unique genes, with occupancy mostly within 5kb of transcription start sites (TSS). These genes were associated with biological processes such as *positive- and negative-regulation of transcription (*Appendix Figure 63). Finally, 1,159 binding sites associated with 768 unique genes contained overlapping binding regions for Cdx2 and H3K27me3, and were again largely located proximal to the TSS (Appendix Figure 64) and associated with genes involved in *retinoic acid signaling*, *cell fate commitment*, and *cardiac morphogenesis* (Appendix Figure 65). Together, these data suggest that Cdx2 shares binding sites with SWI/SNF distal from the TSS of common targets involved in blood vessel formation, possibly functioning at enhancers to positively regulate the expression of these targets. In contrast, Cdx2 occupancy overlaps with sites occupied by PRC2 and H3K27me3 at gene promoters involved in both transcriptional regulation and cardiac development. While these data are highly speculative due to the differences in tissue types from which ChIP-seq data for Cdx2 and potential interacting partners was generated, these observations further support Cdx-mediated gene regulation through at least two

distinct molecular mechanisms that are deployed during development in a context-dependent manner, associating with SWI/SNF at one subset of targets and PRC2 at another. Further, associations between Cdx2 and both SWI/SNF and PRC2 may provide an explanation for the broad Cdx2-binding peaks observed in E8.5 embryos by ChIP-seq, as noted above. Future work addressing these novel and complex relationships is sure to yield interesting results.

The model presented here suggests that Cdx interacts with the SWI/SNF complex at one set of genomic targets, and with the PRC2 complex and H3K27me3 at a unique set loci, allowing for differentiatial regulation of Cdx localization. For this to be the case, a mechanism must exist whereby Cdx2 preferentially interacts with one regulatory complex over the other. While little is known about the role of post-translational modifications in the regulation of Cdx function, such modifications may determine whether Cdx interacts with SWI/SNF or PRC2. Differential phosphorylation of Cdx2 on Serine-60 has previously been demonstrated along the crypt-villus axis of the small intestine, with higher levels of phospho-Cdx2 toward the base of the villi and within the crypts with both phosphorylated and unphosphorylated Cdx2 capable of translocating to the nucleus (Rings et al., 2001). Serine-60 resides within the N-terminal transactivation domain of Cdx2, and its phosphorylation affects transcriptional activation by Cdx (Rings et al., 2001). Apart from this, very little is known about the structure-function of Cdx proteins and the mechanisms by which they are regulated. This, it is possible that additional sites for post-translational modifications exist within Cdx proteins, and that such modifications may regulate interactions between Cdx factors and co-regulators, as has been previously proposed (Guo et al., 2010).

Cdx and the SWI/SNF complex

In addition to Brg1, other members of the SWI/SNF complex were identified as potential Cdx2-interacting proteins by stable isotope labeling of amino acids in culture followed by mass-spectrometry

(SILAC-MS) using human embryonic kidney (HEK293T) cells which express Cdx2 in abundance (Nguyen et al., 2017). Cdx2 was found to interact with Baf250, Baf57, and Baf155, each of which are ubiquitously expressed core members of the SWI/SNF complex (Ho and Crabtree, 2010; Nguyen et al., 2017). Thus, it is likely that interactions between Cdx2 and cell-type specific subunits may direct SWI/SNF activity to lineage specific gene targets.

Cell-type specific SWI/SNF subunits identified as Cdx interacting partners in this assay included Brahma/Brg1-associated factor (BAF) 250, BAF153, BAF57, BAF155, and BAF170 (Nguyen et al., 2017). While these interactions have yet to be studied in depth, it is possible that they represent lineage-specific binding partners, as the SWI/SNF complex includes different subunits in a lineage- and developmental-stage specific manner. It remains unknown whether Cdx2 interacts with SWI/SNF complex members other than Brg1 directly (Nguyen et al., 2017). Direct protein-protein interactions between Cdx2 and cell-type specific SWI/SNF complex members would provide a possible mechanism by which Cdx factors may be recruited to lineage-specific gene targets. For example, an interaction between Cdx2 and a Baf170-containing complex, whose inclusion is specific to neural progenitor and neuronal BAF complexes (Sokpor et al., 2017; Ho and Crabtree, 2010), may suggest a role for Cdx2 in neurogenesis. Further studies, such as in vitro pull-down assys in which the interaction between Cdx2 and SWI/SNF candidates is assessed in the absence of Brg1, will be required to determine whether the interactions identified by SILAC-MS are direct, and may provide evidence for a novel mechanism of Cdx2 recruitment to cell-type specific genomic targets.

Co-expression between Cdx and lineage-restricted SWI/SNF subunits was explored in the early embryo using a published single-cell RNA-seq dataset generated from E6.5-E7.75 embryos (Scialdone et al., 2016). A number of cells were positive for transcripts for both *Cdx2* and *Baf250a* (Appendix Figure 66). While it is considered part of the core SWI/SNF complex, murine *Baf250* is expressed at E6.5, the time of cardiac mesoderm specification, and its expression persists within the heart tube at

E9.5 (Singh et al., 2014). Further, depletion of this subunit results in defective cell commitment to mesodermal lineages and aberrant cardiac progenitor differentiation, suggesting a critical role in heart development (Alexander et al., 2015; Gao et al., 2008). Baf250 is thought to regulate cardiac differentiation through the recruitment of Brg1 to key cardiac loci during the early stages of heart development (Gao et al., 2008). While the interaction between Cdx2 and Brg1, the ATPase subunit of this complex, was investigated in this and other studies (Foley et al., 2019; Nguyen et al., 2017; Yamamichi et al., 2009), a specific association between Cdx2 and Baf250 remains unexplored.

The SWI/SNF subunit Baf60c is also specific to complexes involved in gene expression programs associated with differentiation to cardiac lineages (Sun et al., 2018). Baf60c was not identified as a Cdx2 interacting partner by SILAC-MS, perhaps due to the role of this subunit in promoting cardiac gene expression during differentiation (Sun et al., 2018), contrary to Cdx function. Indeed, as Cdx represses differentiation to cardiac fates in favour of hematopoietic lineages, it may be that Cdx does not interact with complexes containing Baf60c, and instead interacts with hematopoietic-specific SWI/SNF complexes that have yet to be identified. Alternatively, it may be that Cdx2 does interact with cardiac-specific SWI/SNF subunits, but that these subunits are not expressed in HEK239T cells. Further studies in relevant mesodermal cell types will be necessary to examine possible interactions between Cdx2 and cell-type specific SWI/SNF subunits, and whether these interactions direct chromatin remodeling activity to genes involved in differentiation to cardiac or other mesodermal lineages. Such work would contribute to our understanding of cell type-specific Cdx-dependent gene regulation, and further elucidate the mechanisms by which Cdx epigenetically regulates cell fate.

Temporal overlap between Cdx occupancy and regulatory partners at genomic targets

Brg1 localizes to cardiac targets occupied by Cdx2 in E9.5 embryos. It is unknown whether binding by Brg1 and the SWI/SNF complex is required first to render binding sites accessible for Cdx2, or whether initial Cdx2 binding is necessary to induce the recruitment of SWI/SNF, resulting in subsequent transcriptional regulation at the level of chromatin accessibility. Loss of Brg1 binding in Cdx mutants, coupled with changes in chromatin accessibility, suggest that Cdx2 binding is needed for SWI/SNF recruitment. This is consistent with work by others that has shown Cdx2 binding alone does not result in changes to chromatin architecture during intestinal development, and therefore is unlikely to act as a pioneer factor (Kumar et al., 2019). Instead, it is thought that Cdx2 binds to genomic targets as they become accessible, and that this binding maintains a chromatin configuration that is permissive to gene expression (Kumar et al., 2019). This is achieved, in part, through the exclusion of repressive H3K27me3 (Mazzoni et al., 2013; Saxena et al., 2016), as well as through the maintenance of active marks like H3K4me2, characteristic of active enhancers (Verzi et al., 2013; Heintzman et al., 2007; Verzi et al., 2010).

In addition to the interaction between Cdx2 and the SWI/SNF complex, the work presented here also identified a relationship between Cdx and PRC2. Preliminary co-immunoprecipitation experiments using an antibody against Cdx2 suggested a physical interaction between Cdx2 and Suz12, a core member of this complex (Appendix Figure 67). Whether this interaction is robust or direct remains unknown, yet is consistent with the observation that Cdx2 and Suz12/H3K27me3 share common targets within the genome, providing further evidence for PRC2-mediated regulation of Cdx targets. Further experimentation, including pull-down assays that examine direct interactions between Cdx2 and individual PRC2 subunits, combined with ChIP-seq and/or ChIP-reChIP experiments wherein simultaneous genomic occupancy by Cdx2 and Suz12 is assessed at the same loci across a series of developmental stages, will further elucidate PRC2-mediated mechanisms of regulation at Cdx targets.

While a protein-protein interaction between Cdx2 and Suz12 does support our working model in which Cdx2 and PRC2 share genomic targets within mesodermal progenitors, such an interaction is not necessarily required for co-regulation of common targets. Temporally distinct occupation of such targets would still allow for co-regulation. For instance, Cdx binding might result in the recruitment of SWI/SNF, or other transcription factors, that affect PRC2 recruitment and/or function at that locus. Apart from a single PRE identified at the *MafB/Kriesler* locus in mice (Sing et al., 2009), mammalian PREs and their role in PRC2 recruitment across the genome remain uncharacterized. Instead, PRC2 recruitment is thought to depend, in part, on the presence of chromatin-bound transcription factors (Woo et al., 2010; Yu et al., 2012; Pinello et al., 2014; Arnold et al., 2013). This hypothesis supports our model in which PRC2 localization is Cdx-dependent, and therefore impaired in Cdx-deficient tissues, contributing to decreased H3K27me3 at Cdx targets in Cdx-deficient tissues as was observed in DKO yolk sacs (Figure 56A).

H3K27me3 distribution across the Cdx targets *Tbx4*, *Sox9*, *Ascl1*, and *Msx1* was disrupted in Cdx-deficient yolk sacs at regions found to contain overlapping regions of occupation by Cdx and Suz12/H3K27me3 (Figure 56). In addition to these loci, a similar exercise was performed to identify regions of overlap between Cdx2 and Suz12/H3K27me3 at Cdx targets associated with hematopoietic and cardiac specification/differentiation (Appendix Figure 68). These included hematopoietic Cdx targets *Scl/Tal-1* and *Lyl1*, previously shown to be positive regulated by Cdx (Brook-Bisschop et al., 2017), as well as cardiac genes *Nkx2-5*, *Tbx5*, and *Gata4*, ectopically expressed in DKO mutants (Foley et al., 2019), and the bona fide Cdx target *Cyp26A1* (Savory et al., 2009a). As was observed for the loci that were previously examined, overlapping regions of occupancy by Cdx2 and Suz12/H3K23me3 were identified, suggesting a possibility for PRC2-mediated regulation of Cdx targets. Notably, Brg1 was absent from these loci (Alexander et al., 2015; Foley et al., 2019), further supporting our hypothesis that Cdx regulates genomic targets through multiple mechanisms.

While it appears that Cdx2 binding and PRC2/H3K27me3 occupancy overlap at Cdx targets in the yolk sac, it is possible that binding by these factors is temporally distinct. Transient Cdx binding early in development, and presumed SWI/SNF recruitment and chromatin rearrangement, may be required for the recruitment of unknown factors that utilize overlapping genomic regions to either facilitate the recruitment of PRC2, or maintain H3K27me3 levels, at these sites at later developmental stages. Thus, impaired SWI/SNF-mediated chromatin remodelling at Cdx target genes in Cdx mutants may interfere with binding by additional factors, resulting in aberrant PRC2 function and decreased H3K27me3 levels, contributing to altered patterns of gene expression. While we have no evidence to support the involvement of additional factors as of yet, SWI/SNF-dependement H3K27me3 has been observed by other groups during in vitro differentiation of ESCs to cardiac mesoderm (Alexander et al., 2016). This suggests there may be cooperativity between SWI/SNF and PRC2 at a unique subset of genomic loci, despite the generally antagonistic functions of these two complexes.

To determine whether there is a functional correlation to the overlap between Cdx and Suz12/H3K27me3 bound regions at cardiac and hematopoietic targets, H3K27me3 levels were assessed by ChIP-PCR in Cdx mutant embryos (Appendix Figure 69), as was previously done with *Tbx4*, *Sox9*, *Msx1*, and *Ascl1* (Figure 56). Among those genes examined were the hematopoietic loci *Scl/Tal-1*, *Lyl1*, and *Lmo2*, cardiogenic genes *Tbx5*, *Nkx2-5*, and *Gata4*, and the Cdx target *Cyp26A1* (Savory et al., 2009a). Based on our working model and previous reports (Mazzoni et al., 2013; Saxena et al., 2017), we predicted an increase in H3K27me3 at hematopoietic genes downregulated in Cdx-mutants, and a depletion of this mark at cardiogenic loci that are upregulated in the absence of Cdx. To our surprise, H3K27me3 levels were increased in mutant tissues relative to controls at each of the examined loci.

Changes in the relative expression of PRC2 subunits, as was observed in DKO yolk sacs (Figure 55), may impact PRC2 complex assembly and lead to its dysfunction. To determine whether

impaired H3K27me3 at Cdx targets in DKO yolk sacs was the result of PRC2 complex dysfunction, rather than due to specific misregulation at Cdx targets, we examined H3K27me3 protein levels relative to total histone H3 in wild type and DKO yolk sacs by western blot from nuclear extracts (Appendix Figure 70). While levels of histone H3 were largely unaffected in Cdx mutants, there was a great degree of variability in the amount of H3K27me3 protein detected among biological replicates, with some samples having almost no detectable H3K27me3 and others displaying a nearly 10-fold increase. Variability in H3K27me3 levels may result from incomplete Cdx deletion in the yolk sac, as we have shown (Figure 47). At E9.5, the stage at which this experiment was performed, the murine yolk sac is composed of primitive-streak derived mesoderm and trophectoderm-derived visceral endoderm (Kaufman and Baard, 1999). Based on these and other observations, we suspect that the visceral endoderm may be deficient in Cre expression, with the DKO yolk sac phenotype due to Cre-activation in the embryo proper where hematopoetic progenitors and yolk sac mesoderm are specified (Figure 47). Therefore, similar experiments in which cells are isolated at earlier stages of development, before cardiac and hematopoietic progenitors egress from the streak (E6.5-7.5), might be informative.

Alternatively, ChIP-re-ChIP could have been applied to determine whether Cdx2 and SWI/SNF, or Cdx2 and PRC2, co-occupy overlapping genomic regions within the same cell, or whether binding by Cdx2 and these proposed co-regulators to shared regulatory elements is mutually exclusive. Furthermore, isolating relevant cell populations using cell surface markers may also improve our experimental resolution, allowing for us to determine whether Cdx factors preferentially interact with Brg1 and the SWI/SNF complex, and/or PRC2 and H3K27me3, at certain Cdx targets in one cell lineage versus another. However, such an approach depends upon temporal overlap between Cdx2 occupancy and occupancy by SWI/SNF and/or PRC2, which, as explained above, may not be the mechanism by which co-regulation occurs. While we had considered taking this approach using the cell surface receptor *Flk1*, *Flk1*$^{+}$ cells are greatly reduced in DKO mutants relative to controls for unknown

reasons (D.L. and J.G.A.S., unpublished results). Thus, an alternative cell surface marker, or fluorescent reporter, present in both hematopoietic and cardiac progenitors will need to be identified for such an approach to be applied.

Functional significance of H3K27me3 at Cdx target genes

H3K27me3 is associated with gene repression, however H3K27me3 levels were decreased at Cdx2 targets that were downregulated in mutant yolk sacs (Foley et al., 2021). These observations were initially confounding, as the absence of a repressive mark is expected to result in gene expression. However, transcriptional activity at a given genomic locus is thought to result from input by a number of modifications to histone tails, known collectively as the 'histone code' (Strahl and Allis, 2000). This code is comprised of a host of post-translational modifications, including H3K4ac, H3K4me3, and H3K9ac, which mark active gene promoters, H3K27ac, associated with transcriptional activity at both promoters and enhancers, H3K79me2/3 and H3K36me3, associated with genes bodies undergoing active transcription, as well as repressive marks H3K4me1, H3K9me1, H3K20me3, and H2Aub (Gates et al., 2017). These marks are assumed to act in concert to induce or restrict gene expression alongside other mechanisms of regulation, like DNA methylation (Holliday and Pugh, 1975; Compere and Palmiter, 1981), lncRNA-mediated regulation of chromatin accessibility (Isoda et al., 2017; Mumbach et al., 2019), and other mechanisms not considered in this study. With these various aspects of transcriptional regulation taken together, it becomes clear that gene expression from a given locus may not be reliably predicted by examining the presence of a single histone modification. While decreased H3K27me3 levels, as observed in Cdx mutants, may contribute to the misexpression of Cdx-targets, aberrant gene expression as described in this study likely results from misregulation of multiple regulatory mechanisms. Future experiments in which additional histone modifications are examined,

along with assays to identify changes in chromatin accessibility, will provide further insight into the molecular mechanisms underlying Cdx-dependent gene expression.

H3K27me3 has been associated with functions in addition to transcriptional repression that are often overlooked. Work in ESCs and *Gata1*$^{+}$ megakaryocyte-erythroid (G1ME) cells has shown that H3K27me3 ChIP-seq peaks have three epigenetic profiles that uniquely affect gene expression (Young et al., 2011). The first marks bivalent promoters, and is characterized by sharp peaks of H3K27me3 located at transcriptional start sites, often accompanied by peaks of H3K27ac. The second is a broad H3K27me3 peak that spans gene bodies and is associated with gene repression. The final H3K27me3 profile is a sharp peak within a promoter and associated with gene expression. While the role of PRC2 in positive regulation of expression is seldom discussed, the absence of H3K27me3 from Cdx2 target genes in the yolk sac, as observed in our studies, correlated with reduced transcriptional activity from select targets in mutant yolk sacs. This is consistent with other instances in the literature where PRC2 activity positively affects transcription (Gao et al., 2014; Gentile et al., 2018; Zhao et al., 2017).

While specific histone modifications correlate with active or inhibited transcriptional states, there remains debate as to whether these marks are causal, or whether they might instead be the result of transcriptional regulation without being inherently functional (Gates et al., 2017; Henikoff and Shilatifard, 2011). Rather than serving as instructive cues for gene expression, these marks may instead be a record of transcriptional activity at a locus over time. If so, the absence of H3K27me3 at Cdx targets in Cdx-deficient yolk sacs can be reconciled with decreased expression from these targets, consistent with observations by others in which depletion of this "repressive" mark from certain loci occurs with decreased gene expression, and contrary to current dogma in which the absence of H3K27me3 should indicate relief of repression.

Conserved Cdx functions in the mouse extra-embryonic yolk sac and the adult intestine

At E9.5, the yolk sac contains mesodermal derivatives, in which hemangioblasts, progenitors for both primitive blood and yolk sac vasculature, are contained. Adjacent to this mesodermal layer is a layer of visceral endoderm, required for the transport of ions and nutrients and waste exchange by the embryo until chorioallantoic fusion (Gillman et al., 1948; Brent et al., 1990; Jollie, 1990; Lloyd, 1990, 1997; Farese et al., 1995; Cross et al., 1994; Zohn et al., 2010). While critical functions for *Cdx2* in the trophectoderm and the allantois are well documented, specific roles for Cdx in the yolk sac visceral endoderm have not been described.

Complete Cdx knockout was not achieved in the yolk sac (Foley et al., 2021). As a result, it remains unclear whether Cdx was abolished in some cell populations but not others, or whether it was incompletely depleted across all yolk sac cell types. Embryos from which yolk sacs were dissected displayed phenotypes associated with complete Cdx depletion, including caudal truncation rostral to the forelimb bud along with cardiac defects and an open neural tube. This suggests that Cdx was efficiently deleted within the embryo proper, extra-embryonic lineages like the visceral endoderm may not have been affected to the same extent for reasons that are not understood. Further studies using visceral-endoderm specific Cdx2 deletion will be required to elucidate Cdx function associated with this lineage, however at present no such Cre driver has been described.

Extracellular signals from the visceral endoderm, including Ihh and Vegfa, bind to cell surface receptors within underlying mesoderm, inducing the formation of blood vessels during primitive hematopoiesis (Becker et al., 1997; Farrington et al., 1997; Damert et al., 2002; Miura et al., 1969; Beloussof et al., 1998; Vokes and Krieg, 2002; Dyer et al., 2001). Cdx mutant yolk sacs lack vascularization, apparent by E9.5, however Ihh and Vegf expression in these mutants was not affected. Thus, yolk sac defects observed in Cdx mutants are independent of impaired signaling by the visceral

endoderm, as the expression of these factors was maintained in the absence of Cdx, despite the observed phenotype.

While these observations suggest that Cdx depletion was not achieved in the visceral endoderm, decreased expression of *Slc* family members, along with other ion transporters and and genes encoding gap junction proteins, indicates that some functions of the visceral endoderm may be impaired in Cdx mutants, despite incomplete Cdx2 deletion. The epithelium of the visceral endoderm is functionally and morphologically similar to that of the intestine (Bielinska et al., 1999), as both contain microvilli that facilitate nutrient absorption (Calarco et al., 1966). In the intestinal epithelium, Cdx regulates the expression of genes involved in ion transport, which include diverse members of the *Slc* solute carrier family (Verzi et al., 2011; Gao et al., 2009), as well as genes encoding tight junction proteins required for the maintenance of apicobasal polarity (Gao et al., 2010). While the specific transcripts misregulated in Cdx mutant intestine were not aberrantly expressed in Cdx-deficient yolk sacs, misregulation of *Slc* family members with similar functions, including *Slc1a5, Slc4a8, Slc4a11, Slc6a9 Slc6a15*, *Slc7a1 Slc7a6, Slc22a13, Slc17a4*, and *Slc29a4*, the calcium-dependent non-selective anion channel *Ano4* (Reichart et al., 2019), and genes encoding gap junction proteins *Gja4* and *Gja5*, was observed. This suggests that Cdx may regulate analogous processes in the yolk sac visceral endoderm and intestinal epithelium, perhaps via tissue-specific target genes with similar function. These observations are consistent with findings by Scialdone and colleagues who identified cells that co-expressed *Cdx2* and the visceral endoderm markers *Sox7* and *Lhx1* (Appendix Figure 71; Sherwood et al., 2007; Scialdone et al., 2016), indicating a possible role for Cdx in this tissue.

It may be that partial deletion in this lineage was achieved, or alternatively, that these changes in gene expression are secondary to the lack of blood. Impaired nutrient transport and cell-cell contact in DKO yolk sacs is consistent with previously described roles for Cdx in the intestinal epithelium, where Cdx factors similarly maintain both *Slc* gene expression and the expression of proteins required

for tight junctions, required for apicobasal polarity (Verzi et al., 2011; Gao et al., 2009). While affected gene targets are not entirely conserved between Cdx-mutant intestinal epithelium and yolk sac, affected genes appear to be involved in analogous processes, with ion and nutrient transport affected in both tissues lacking Cdx expression, pointing to a potentially conserved role for Cdx across different tissue types. Again, our understanding of roles for Cdx in these processes would benefit greatly from the identification of a visceral endoderm-specific Cre driver, allowing for targetted Cdx ablation within this lineage.

Conclusions

In summary, Cdx factors are required to maintain the balance between cardiac and hematopoietic lineage specification during gastrulation through regulation of genes involved in differentiation of multipotential mesoderm. In the absence of Cdx, cardiac gene expression is affected in the cardiac crescent at developmental stages where Cdx is no longer expressed. This may be due to aberrant chromatin organization at cardiac loci, as Cdx is required within progenitors to recruit the SWI/SNF complex to targets as cardiogenic cells are specified in the primitive streak. Impaired SWI/SNF recruitment to targets in the absence of Cdx results in disruption of the chromatin landscape, leading to miregulated and/or ectopic gene expression.

In the yolk sac, Cdx is required to maintain gene expression programs associated with both the mesoderm and visceral endoderm layers, including yolk sac hematopoiesis and ion and nutrient transport, among other processes. Ectopic cardiac gene expression is not observed in DKO mutant yolk sac, despite the role of Cdx in repressing cardiogenesis in favour of differentiation to hematopoietic lineages. This may be due to the impaired migration of misspecified mesodermal progenitors, which we expect to be incapable of colonizing the yolk sac. Nevertheless, a number of novel Cdx yolk sac targets were identified, with roles in ion and nutrient transport and chorioallantoic fusion. This work also

revealed Cdx-dependent processes within the yolk sac analogous to previously described roles for this factor in the intestinal epithelium, pointing to conserved Cdx functions across tissue types.

Within the yolk sac, Cdx maintains gene expression programs, in part, through the maintenance of H3K27me3 deposited at Cdx targets during gastrulation, before hematopoietic progenitors migrate from the streak. Cdx therefore primes genomic targets within hematopoietic mesoderm to establish appropriate gene expression patterns at later stages, when Cdx no longer occupies these genomic sites. Whether Cdx interacts with PRC2 directly to regulate this mark, or whether Cdx and PRC2 regulate overlapping regions of the genome but in a temporally distinct manner, remains unclear. However, the mechanism by which Cdx and PRC2 regulate shared targets appears to be separate from that involving the SWI/SNF complex, as genomic targets common to Cdx2 and PRC2 are unique from those common to Cdx2 and Brg1. This indicates that Cdx members interact with PRC2 and SWI/SNF through distinct epigenetic mechanisms that may be deployed in a cell-type specific manner to regulate cell fate.

REFERENCES

Abe, T., Kutsuna, N., Kiyonari, H., Furuta, Y., Fujimori, T. 2018. ROSA26 reporter mouse lines and image analyses reveal distinct region-specific cell behaviors in the visceral endoderm. Development 145, dev165852.

Afzelius, B. 1976. A human syndrome cause by immotile cylia. Science 193, 317-319.

Alexander, J., Rothenberg, M., Henry, G., Stainier, D. 1999. *casanova* plays an early and essential role in endoderm formation in zebrafish. Dev. Biol. 215, 343–357.

Alexander, J.M., Hota, S.K., He, D., Thomas, S., Ho, L., Pennacchio, L.A., Bruneau, B.G. 2015. Brg1 modulates enhancer activation in mesoderm lineage commitment. Development 142, 1418-1430.

Amin, A., Neijts, R., Simmini, S., van Rooijen, C., Tan, S.C., Kester, L., van Oudenaarden, A., Creyghton, M.P., Deschamps, J. 2016. Cell Reports 17, 3165-3177.

Antonica, F., Orietti, L.C., Mort, R.L., Zernicka-Goetz, M. 2019. Concerted cell divisions in embryonic visceral endoderm guide anterior visceral endoderm migration. Dev. Biol. 450, 132–140.

Andres-Delgado, L. and Mercader, N. 2016. Interplay between cardiac function and heart development. Biochim. Biophys. Acta Mol. Cell Res. 1863, 1707-1716.

Arnold, S.J. and Robertson, E.J. 2009. Making a commitment: Cell lineage allocation and axis patterning in the early mouse embryo. Nat. Rev. Mol. Cell Biol. 10, 91–103.

Atallah, J., Liu, N.H., Dennis, P., Hon, A., Larsen, E.W. 2009. Developmental constraints and convergent evolution in Drosophila sex comb formation. Evol. Dev. 11, 205–218

Aulehla, A. and Pourquié, O. 2010. Signaling gradients during paraxial mesoderm development. Cold Spring Harb. Perspect. Biol. 2, a000869.

Barbosa, A.C., Funato, N., Chapman, S., McKee, M.D., Richardson, J.A., Olson, E.N. Yanagisawa, H. 2007. Dev. Biol. 310, 154-168.

Barnes, R.M., Firulli, B.A., Conway, S.J., Vincentz, J.W., Firulli, A.B. 2010. Analysis of the Hand1 cell lineage reveals novel contributions to cardiovascular, neural crest, extra-embryonic, and lateral mesoderm derivatives. Dev. Dyn. 239, 3086-3097.

Barnes, R.M., Firulli, B.A., Van Dusen, N.J., Morikawa, Y., Conway, S.J., Cserjesi, P., Vincentz, J.W., Firulli, A.B. 2011. Hand1 loss-of-function in Hand1-expressing cells reveals distinct roles in epicardial and coronary vessel development. Circ. Res. 108, 940-949.

Bauer, M., Trupke, J., Ringrose, L. 2015. The quest for mammalian Polycomb response elements: are we there yet? Chromosoma. 125, 471-496..

Beccari, L., Moris, N., Girgin, M., Turner, D.A., Baillie-Johnson, P., Cossy, A.-C., Lutolf, M.P., Duboule, D., Arias, A.M. 2018. Multi-axial self-organization properties of mouse embryonic stem cells into gastruloids. Nature 562, 272-276.

Beck, F., Erler, T., Russell, A. James, R. 1995. Expression of Cdx2 in the mouse embryo and placenta: possible role in patterning of the extra-embryonic membranes. Dev. Dyn. 204, 219-227.

Beck, F., Chawengsaksophak, K., Luckett, J., Giblett, S., Tuci, J., Brown, J., Poulsom, R., Jeffery, R., Wright, N.A. 2003. A study of regional gut endoderm potency by analysis of Cdx null mutant chimaeric mice. Dev. Biol. 255, 399-406.

Beddington, R.S. 1994. Induction of a second neural axis by the mouse node. Development 120, 613-620.

Bellairs, R. 1986. The primitive streak. Anat. Embryol. 174, 1-14.

Belaoussoff, M., Farrington, S. M. and Baron, M. H. 1998. Hematopoietic induction and respecification of A-P identity by visceral endoderm signaling in the mouse embryo, Development 125, 5009-18.

Belo, J.A., Bouwmeester, T., Leyns, L., Kertesz, N., Gallo, M., Follettie, M., De Robertis, E.M. 1997. Cerberus-like is a secreted factor with neuralizing activity expressed in the anterior primitive endoderm of the mouse gastrula. Mech. Dev. 68, 45–57.

Ben-Haim, N., Lu, C., Guzman-Ayala, M., Pescatore, L., Mesnard, D., Bischofberger, M., Naef, F., Robertson, E.J., Constam, D.B. 2006. The Nodal precursor acting via Activin receptors induces mesoderm by maintaining a source of its convertases and BMP4. Dev. Cell. 11, 313–23.

Benson, D.W., Silberbach, G.M., Kavanaugh-McHugh, A., Cottrill, C., Zhang, Y., Riggs, S., Smalls, O., Johnson, M.C., Watson, M.S., Seidman, J.G., Seidman, C.E., Plowden, J., Kugler, J.D. 1999. Mutations in the cardiac transcription factor Nkx2- 5 affect diverse cardiac developmental pathways. J. Clin. Invest. 104, 1567-1573.

Bertrand, J.Y., Chi, N.C., Santoso, B., Teng, S., Stainier, D.Y., Traver, D. 2010. Heamatopoietic stem cells derive directly from aortic endothelium during development. Nature 464, 108-111.

Bielinska, M., Narita, N., Wilson, D.B. 1999. Distinct roles for visceral endoderm during embryonic mouse development. Int. J. Dev. Biol. 43: 183-205.

Blausen.com staff. 2014. Medical gallery of Blausen Medical 2014. WikiJournal of Medicine 1, 2.

Blumberg, B., Wright, C.V.E., De Robertis, E.M., Cho, K.W.Y., 1991. Organizer-specific homeobox

genes in Xenopus laevis embryos. Science 253, 194–196.

Boisset, J.C., van Cappellen, W., Andrieu-Soler, C., Galjart, N., Dzierzak, E., Robin, C. 2010. In vivo imaging of hematopoietic cells emerging from the mouse aortic endothelium. Nature 464, 116-120.

Bondue, A., Lapouge, G., Paulissen, C., Semeraro, C., Iacovino, M., Kyba, M., Blanpain, C. 2008. Mesp1 acts as a master regulator of multipotent cardiovascular progenitor specification. Cell Stem Cell 3, 69-84.

Bonhomme, C., Calon, A., Martin, E., Robine, S., Neuville, A., Kedinger, M., Domon-Dell, C., Duluc, I., Freund, J.-N. 2008. Cdx1, a dispensable homeobox gene for gut development with limited effect in intestinal cancer. Oncogene 27, 4497-4502.

Boucher, D.M., and Pedersen, R.A. 1996. Induction and differentiation of extra-embryonic mesoderm in the mouse. Reprod. Fertil. Dev. 8, 765-777.

Boyer, L.A., Plath, K., Zeitlinger, J., Brambrink, T., Medeiros, L.A., Lee, T.I., Levine, S.S., Wernig, M., Tajonar, A., Ray, M.K., Bell, G.W., Otte, A.P., Vidal, M., Gifford, D.K., Young, R.A., Jaenisch, R. 2006. Polycomb complexes repress developmental regulators in murine embryonic stem cell. Nature 441, 349-353.

Bracken, A.P., Dietrich, N., Pasini, D., Hansen, K.H., Helin, K. 2006. Genome-wide mapping of Polycomb target genes unravels their roles in cell fate transitions. Genes Dev. 20, 1123-1136.

Brand, M., Nakka, K., Zhu, J., Dilworth, F.J. 2019. Polycomb/Trithoriax antagonism: cellular memory in stem cell fate and function. Cell Stem Cell 24, 518-533.

Brennan, J., Norris, D.P., Robertson, E.J. 2002. Nodal activity in the node governs left-right asymmetry. Genes Dev. 16:2339-2344.

Brennan, J., Lu, C.C., Norris, D.P., Rodriguez, T.A., Beddington, R.S.P., Robertson, E.J. 2001. Nodal signalling in the epiblast patterns the early mouse embryo. Nature. 411, 965–969.

Brent, R.L., Jensen, B.M. and Koszalka, T.R. 1990. Experimental yolk sac dysfunction as a model for studying nutritional disturbances in the embryo during early organogenesis. Teratology 41, 405-413.

Bronner, M.E. 2012. Formation and migration of neural crest cells in the vertebrate embryo. Histochem. Cell Biol. 138, 179-186.

Brooke-Bisschop, T., Savory, J.G.A., Foley, T., Ringuette, R., Lohnes, D. 2017. Essential Roles for Cdx in Murine Primitive Hematopoiesis. Dev. Biol. 422, 115-124.

Bruneau, B.G. 2013. Signaling and transcriptional networks in heart development and regeneration.

Cold Spring Harb. Perspect. Biol. 5, a008292.

Bruneau, B.G., Logan, M., Davis, N., Levi, T., Tabin, C.J., Seidman, J.G., Seidman, C.E. 1999. Chamber-specific expression of Tbx5 and heart defects in Holt-Oram syndrome. Dev. Biol. 211, 100-108.

Bultman, S., Gebuhr, T., Yee, D., La Mantia, C., Nicholson, J., Gilliam, A., Randazzo, F., Metzger, D., Chambon, P., Crabtree, G., Megnuson, T. 2000. A Brg1 null mutation in the mouse reveal functional differences among mammalian SWI/SNF complexes. Mol. Cell. 6, 1287-1295.

Buckingham M, Meilhac S, Zaffran S. 2005. Building the mammalian heart from two sources of myocardial cells. Nat. Rev. Genet. 6, 826–35.

Bussmann, J., Bakkers, J., Schulte-Merker, S. 2007. Early endocardial morphogenesis requires Scl/Tal-1. Plos Genetics 3, e140.

Calcar, S., Qu, C., Ching, K.A., Wang, W., Weng, Z., Green, R.D., Crawford, G.E., Ren, B. 2007. Distinct and predictive chromatin signatures of transcriptional promoters and enhancers in the human genome. Nat. Genet. 39, 311–318.

Casanova, J.E., and Grabel, L.B. 1988. The role of cell interactions in the differentiation of teratocarcinoma derived from parietal and visceral endoderm. Dev. Biol. 129, 124-139.

Cai, C.L., Liang, X., Shi, Y., Chu, P.H., Pfaff, S.L., Chen, J., Evans, S. 2003. Isl1 identifies a cardiac progenitor population that proliferates prior to differentiation and contributes a majority of cells to the heart. Dev. Cell 5, 877–889.

Cairns BR, Kim YJ, Sayre MH, Laurent BC, Kornberg RD. 1994. A multisubunit complex containing the SWI1/ADR6, SWI2/SNF2, SWI3, SNF5, and SNF6 gene products isolated from yeast. Proc. Natl. Acad. Sci. U.S.A. 91, 1950–1954.

Celen, C., Chuang, J.-C., Luo, X., Nijem, N., alker, A.K., Chen, F., Zhang, S., Chung, A.S., Nguyen, L.H., Nassour, I., Budhipramono, A., Sun, X., Bok, L.A., McEntagart, M., Gevers, E.F., Birnbaum, S.G., Eisch, A.J., Powell, C.M., Ge, W.-P., Santen, G.W., Chahrour, M., Zhu, H. 2017. Arid1b haploinsufficient mice reveal neuropsychiatric phenotypes and reversible causes of growth impairment. Elife 6, e25730.

Chan, S.S.-K., Shi, X., Toyama, A., Arpke, R. W., Dandapat, A., Iacovino, M., Kang, J.-J., Le, G., Hagen, H. R., Garry, D. J., Kyba, M. 2013. Mesp1 patterns mesoderm into cardiac, hematopoietic, or skeletal myogenic progenitors in a context-dependent manner. Cell Stem Cell 12, 587-601.

Charron, F., Paradis, P., Bronchain, O., Nemer, G., Nemer, M. 1999. Cooperative interaction between

GATA-4 and GATA-6 regulates myocardial gene expression. Mol. Cell Biol. 19, 4355–4365.

Chen, M.J., Yokomizo, T., Zeigler, B.M., Dzierzak, E., Speck, N.A. 2009. Runx1 is required for the endothelial to haematopoietic cell transition but not thereafter. Nature 457, 887-891.

Chiba, H., Muramatsu, M., Nomoto, A., Kato, H. 1994. Two human homologues of Saccharomyces cerevisiae SWI2/SNF2 and Drosophila brahma are transcriptional coactivators cooperating with the estrogen receptor and the retinoic acid receptor. Nucleic Acids Res. 22, 1815–1820.

Christodoulou, N., Kyprianou, C., Weberling, A., Wang, R., Cui, G., Peng, G., Jing, N., Zernicka-Goetz. 2018. Sequential formation and resolution of multiple rosettes drive embryo remodelling after implantation. Nature Cell Biol. 20, 1278-1289.

Cindrova-Davies, T., Jauniaux, E., Elliot, M.G., Gong, S., Burton, G.J., Charnock-Jones, D.S. 2017. RNA-seq reveals conservation of function among the yolk sacs of human, mouse, and chicken. PNAS 114, E4753-E4761.

Chawengsaksophak, K., James, R., Hammond, V.E., Kontgen, F., Beck, F. 1997. Homeosis and intestinal tumors in Cdx2 mutant mice. Nature 386, 84-87.

Chawengsaksophak, K., de Graff, W., Rossant, J., Deschamps, J., Beck, F. 2004. Cdx is essential for axial elongation in mouse development. PNAS 101, 7641-7645.

Choi, K., Kennedy, M., Kazarov, A., Papadimitriou, J.C., Keller, G. 1998. A common precursor for hematopoietic and endothelial cells. Development 125, 725-732.

Ciruna, B., Rossant, J., 2001. FGF signaling regulates mesoderm cell fate specification and morphogenetic movement at the primitive streak. Dev. Cell 1, 37–49.

Ciruna, B., Schwartz, L., Harpal, K., Yamaguchi, T.P., Rossant, J. 1997. Chimeric analysis of fibroblast growth factor receptor-1 (Fgfr1) function: a role for FGFR1 in morphogenetic movement through the primitive streak. Development 124, 2829-2841.

Clapier, C.R., Iwasa, J., Cairns, B.R., Peterson, C.L. 2017. Mechanisms of action and regulation of ATP-dependent chromatin-remodelling complexes. Nat. Rev. Mol. Cell Biol. 18, 407–422.

Clevers, H. and Bevins, C.L. 2013. Paneth cells: maestros of the small intestinal crypts. Annu. Rev. Physiol. 75, 289-311.

Cohen, I., Zhao, D., Bar, C., Valdes, V.J., Dauber-Decker, K.L., Bguyen, M.B., Nakayama, M., Rendi, M., Bickmore, W.A., Koseki, H., Zheng, D., Ezhkova, E. 2018. PRC1 fine-tunes gene repression and activation to safeguard skin development and stem cell specification. Cell Stem Cell 22, 726-739.e7.

Compere, S.J., Palmiter, R.D. 1981. DNA methylation controls the inducibility of the mouse

metallothionein-I gene lymphoid cells. Cell 25, 233–240.

Conlon, F., Lyons, K., Takaesu, N., Barth, K., Hermann, B., Robertson, E. 1994. A primary requirement for nodal in the formation and maintenance of the primitive streak in the mouse. Development 129, 1919-1928.

Cooke, J., and Zeeman, E.C. 1976. A clock and wavefront model for control of the number of repeated structures during animal morphogenesis. J. Theor. Biol. 58, 455-476.

Copp, A.J. 1995. Death before birth: clues from gene knockouts and mutations. Trend. Genet. 11, 87-93.

Cosma, M.P., Tanaka, T., Nasmyth, K. 1999. Ordered recruitment of transcription and chromatin remodeling factors to cell cycle-and developmentally regulated promoter. Cell. 97, 299-311.

Cross, J.C., Werb, Z., Fisher, S.J. 1994. Implantation and the placenta: key pieces of the development puzzle. Science. 266, 1508-1518.

Cui, K., Zang, C., Roh, T.Y., Schones, D.E., Childs, R.W., Peng, W., Zhao, K. 2009. Chromatin signatures in multipotent human hematopoietic stem cells indicate that fate of bivalent genes during differentiation. Cell Stem Cell 4, 80-93.

Damert, A., Miquerol, L., Gertsenstein, M., Risau, W., Nagy, A. 2002. Insufficient VEGFA activity in yolk sac endoderm compromises haematopoietic and endothelial differentiation. Development 129, 1881-1892.

Davidson, A.J., Ernst, P., Wang, Y., Dekens, M.P.S., Kingsley, P.D., Palis, J., Korsmeyer, S.J., Daley, G.Q., Zon, L.I. 2003. cdx4 mutants fail to specify blood progenitors and can be rescued by multiple hox genes. Nature 425, 300-306.

Davidson, A.J. and Zon, L.I. 2004. The 'definitive' (and 'primitive') guide to zebrafish hematopoiesis. Oncogene. 23, 7233-7246.

Davidson, A.J. and Zon, L.I. 2006. The caudal-related homeobox genes cdx1a and cdx4 act redundantly to regulate hox gene expression and the formation of putative hematopoietic stem cells during zebrafish embryogenesis. Dev. Biol. 292, 506-518.

Dearolf, C.R., Topol, J., Parker, C.S. 1989. The caudal gene product is a direct activator of *fushi tarazu* transcription during Drosophila embryogenesis. Nature 341, 340-343.

Dersch, H. and Zile, M.H. 1993. Induction of normal cardiovascular development in the vitamin A-deprived quail embryo by natural retinoids. Dev. Biol. 160, 424-433.

Deschamps, J., van den Akker, E., Forlani, S., de Graaff, W., Oosterveen, T., Roelen, B., Roelfsema, J.

1999. Initiation, establishment and maintenance of Hox gene expression patterns in the mouse. Int. J. Dev. Biol. 43, 635-650.

Devine, W.P., Wythe, J.D., George, M., Koshiba-Takeuchi, K., Bruneau, B.G. 2014. Early patterning and specification of cardiac progenitors in gastrulating mesoderm. eLife 3, 1-23.

Dequéant, M.-L. and Pourquié, O. 2008. Segmental patterning of the vertebrate embryonic axis. Nat. Rev. Genet. 9, 370-382.

Dickman, E.D. and Smith, S.M. 1996. Selective regulation of cardiomyocyte gene expression and cardiac morphogenesis by retinoic acid. Dev. Dyn. 206, 39-48.

Di Croce, L., and Helin, K. 2013. Transcriptional regulation by Polycomb group proteins. Nat. Struct. Mol. Biol. 20, 1147-1155.

Dieterlen-Lievre, F. 1998. Hematopoiesis: progenitors and their genetic program. Curr. Biol. 8, R727-R730.

Dimova, D., Zeena, N., Furgeson, S., Eguchi, S., Osley, M.A. 1999. A role for transcriptional repressors in targeting the yeast Swi/Snf complex. Mol. Cell 4, 75-83.

Dingwall, A. K., Beek, S. J., McCallum, C. M., Tamkun, J. W., Kalpana, G. V., Goff, S. P. Scott, M. P. 1995. The Drosophila snr1 and brm proteins are related to yeast SWI/SNF proteins and are components of a large protein complex. Mol. Biol. Cell 6, 777-91.

Dodou, E., Verzi, M.P., Anderson, J.P., Xu, S.M., Black, B.L. 2004. Mef2c is a direct transcriptional target of ISL1 and GATA factors in the anterior heart field during mouse embryonic development. Development 131, 3931–3942.

Downs, K.M., and Bertler, C. 2000. Growth in the pre-fusion murine allantois. Anat. Embryol. 202, 323-331.

Downs, K.M., Gifford, S., Blahnik, M., Gardner, R.L. 1998. Vascularization in the murine allantois occurs by vasculogenesis without accompanying erythropoiesis. Development 125, 4507-4520.

Duprey, P., Chowdhury, K., Dressier, G., Balling, R., Simon, L. D., Guenet, J.-L., Gruss, P. 1988. A mouse gene homologous to the Drosophila gene caudal is expressed in epithelial cells from the embryonic intestine. Genes Dev. 2, 1647-1654.

Duval, M. 1891. The rodent placenta. Third part. The placenta of the mouse and of the rat. *J. Anat. Physiol. Normales et Pathol. de l'Homme et des Animaux* 27, 24-73; 344-395; 515-612

Dyer, L.A. and Kirby, M.L. 2009. Sonic hedgehog maintains proliferation in secondary heart field progenitors is required for normal arterial pole formation. Dev. Biol. 330, 305-317.

Eilken, H.M., Nishikawa, S., Schroeder, T. 2009. Continuous single-cell imaging of blood generating

from haemogenic endothelium. Nature 457, 896-900.

Elliot, D.A., Kirk, E., Yeoh, T., Chander, S., McKenzie, F., Taylor, P., Grossfeld, P., Fatkin, D., Jones, O., Hayes, P., Feneley, M., Harvey, R.P. 2003. NKX2-5 mutations and congenital heart disease: Associations with ASD and hyperplastic left heart syndrome. J. Am. Coll. Cardiol. 41, 2071-2076.

Endoh, M., Endo, T.A., Endoh, T., Isono, K., Sharif, J., Ohara, O., Toyoda, T., Ito, T., Eskeland, R., Bickmore, W.A., Vidal., M., Bernstein, B.E., Koseki, H. 2012. Histone H2A mono-ubiquitination is a crucial step to mediate PRC1-dependent repression of developmental genes to maintain ES cell identity. PLoS Genet. 8, e1002774.

Etchevers, H.C., Dupin, E., Le Douarin, N.M. 2019. The diverse neural crest: from embryology to human pathology. Development 146, dev169821.

Faas, L. and Isaacs, H.V. 2009. Overlapping functions of Cdx1, Cdx2, and Cdx4 in the development of the amphibian Xenopus tropicalis. Dev. Dyn. 238, 835-852.

Farese, R.V.Jr., Rulan, S.L., Flynn, L.M., Stokowski, R.P., Young, S.G. 1995. Knockout of the mouse apolipoprotein B gene results in embryonic lethality in homozygotes and protection against diet-induced hypocholesterolemia in heterozygotes. Proc. Natl. Acad. Sci. U.S.A. 92, 1774-1778.

Farrell, M., Waldo, K., Li, Y.-X., and Kirby, M.L. 1999. A novel role for cardiac neural crest in heart development. Trends Cardiovasc. Med. 9, 214-220.

Fehling, H.J., Lacaud, G., Kubo, A., Kennedy, M., Robertson, S., Keller, G., Kouskoff, V. 2003. Tracking mesoderm induction and its specification to the hemangioblasts during embryonic stem cell differentiation. Development 130, 4217-4227.

Feretti, E. and Hadjantonakis, A.-K. 2019. Mesoderm specification and diversification: from single cells to emergent tissues. Curr. Opin. Cell Biol. 61, 110-116.

Ferkowicz, M.J., Starr, M., Xie, X., Li, W., Johnson, S.A., Shelley, W.C., Morrison, P.R., Yoder, M.C. 2003. CD41 expression defined the onset of primitive and definitive hematopoiesis in the murine embryo. Development 130, 4393-4403.

Ferkowicz, M.J., Yoder, M.C. 2005. Blood island formation: longstanding observations and modern interpretations. Exp. Hematol. 33, 1041-1047.

Flores, M.V.C., Hall, C.J., Davidson, A.J., Singh, P.P., Mahagoankar, A.A., Zon, L.I., Crosier, K.E., Crosier, P.S. 2008. Intestinal differentiation in zebrafish requires Cdx1b, a functional equivalent of mammalian Cdx2. Gastroenterology 135, 1665-1675.

Flowers, S., Nagl, N.G., Beck, G.R., Moran, E. 2009. Antagonistic roles of BRM and BRG1 SWI/SNF complexes in differentiation. J. Biol. Chem. 284, 10067-10075.

Foley, T.E., Hess, B., Savory, J.G.A., Ringuette, R., Lohnes, D. 2019. Role of Cdx factors in early mesodermal fate decisions. Development 146, dev170498.

Francis, N.J., Kingstone, R.E., Woodcock, C.L. 2004. Chromatin compaction by a polycomb group protein complex. Science 306, 1574-1577.

Frankenberg, S., Gerbe, F., Bessonnard, S., Belville, C., Pouchin, P., Bardot, O., Chazaud, C. 2011. Primitive endoderm differentiates via a three-step mechanism involving Nanog and RK signaling. Dec. Cell 21, 1005-1013.

Frumkin, A., Rangini. Z., Ben-Yehuda, A., Gruenbaum, Y., Fainsod A. 1991. A chicken caudal homologue, Chox-cad, is expressed in the epiblast with posterior localization and in the early endodermal lineage. Development 112, 207–219.

Furuta, C., Ema, H., Takayanagi, S., Ogaeri, T., Okamura, D., Matsui, Y., Nakauchi, H. 2006. Discordant development waves of angioblasts and hemangioblasts in the early gastrulating mouse embryo. Development, 133, 2771-2779.

Furthauer, M., Van Celst, J., Thisse, C., Thisse, B. 2004. Fgf signaling controls the dorsoventral patterning of the zebrafish embryo. Development 131, 2853-2864.

Fyer, C.J., Archer, T.K. 1998. Chromatin remodelling by the glucocorticoid receptor requires the BRG1 complex. Nature 393, 88-91.

Gajewski, K., Fossett, N., Molkentin, J.D., Schulz, R.A. 1999. The zinc finger proteins Pannier and GATA4 function as cardiogenic factors in Drosophila. Development 126, 5679–5688.

Gamer, L.W. and Wright, C.V. 1993. Murine Cdx4 bears striking similarities to the Drosophila caudal gene in its homeodomain sequence and early expression pattern. Mech. Dev. 43, 71-81.

Gannon, M., and Bader, D. 1995. Initiation of cardiac differentiation occurs in the absence of anterior endoderm. Development 121, 2439-2450.

Gao, N., White, P., Kaestner, K.H. 2009. Establishment of intestinal identity and epithelial-mesenchymal signaling by Cdx2. Dev. Cell 16, 588-599.

Gao, N and Kaestner, K.H. 2010. Cdx2 regulates endo-lysosomal function and epithelial cell polarity. Genes Dev. 24, 1295-1305.

Gao, Z., Lee, P., Stafford, J.M., von Schimmelmann, M., Schaefer, A., and Reinberg, D. 2014. An AUTS2-Polycomb complex activates gene expression in the CNS. Nature 516, 349-354.

Gardner, R.L. 1982. Investigation of cell lineage and differentiation in the extraembryonic endoderm of the mouse embryo. J. Embryol. Exp. Morphol. 68, 175-198.

Gardner, R.L. 1983. Origin and differentiation of extraembryonic tissues in the mouse. Int. Rev. Exp. Pathol. 24, 63-133.

Gardner, R.L. 1989. Cell allocation and lineage in the early mouse embryo. Ciba Found. Symp. 144, 172-181.

Gardner, R.L. and Beddington, R.S. 1988. Multi-lineage "stem" cells in the mammalian embryo. J. Cell. Sci. Suppl. 10, 11-27.

Gates, L., Foulds, C.E., O'Malley, B.W. 2017. Histone marks in the 'driver's seat: functional roles in steering the transcription cycle. Trends Biochem. Sci. 42, 977-989.

Gentile, C., Paquette, D., Mayran, A., Guerard-Millet, F., Berlivet, S., Dostie, J., Kmita, M. 2018. PRC2-dependent tissue-specific 3D architecture in the developing limb reveals a possible mechanism for the atypical role of PRC2 in gene activation. Dev. Cell 50, 184-196.e4.

George, R.M., and Firulli, A.B. 2019. Hand factors in cardiac development. Anat. Rec. (Hoboken) 302, 101-107.

Goldmuntz, E. 2001. The epidemiology and genetics of congenital heart disease. Clin. Perinatol. 28, 1-10.

Gorman, C. and Bullock, C. 2000. Site-specific gene targeting for gene expression in eukaryotes. Curr. Opin. Biotechnol. 11, 455–460.

Gove, C., Walmsley, M., Nijjar, S., Bertwistle, D., Guille, M., Partington, G., Bomford, A., Patient, R. 1997. Over-expression of GATA-6 in Xenopus embryos blocks differentiation of heart precursors. EMBO J. 16, 355–368.

Grainger, S., Hryniuk, A., Lohnes, D. 2012. Cdx1 and Cdx2 exhibit transcriptional specificity in the intestine. Plos One 8, e54757.

Grepin, C., Robitaille, L., Antakly, T., Nemer, M. 1995. Inhibition of transcription factor GATA-4 expression blocks in vitro cardiac muscle differentiation. Mol. Cell Biol. 15, 4095–4102.

Grepin, C., Nemer, G., Nemer, M. 1997. Enhanced cardiogenesis in embryonic stem cells overexpressing the GATA- 4 transcription factor. Development 124, 2387–2395.

Guo, R.J., Suh, E.R., Lynch, J.P. 2004. The role of Cdx proteins in intestinal development and cancer. Cancer Biol. Ther. 3, 593-601.

Gutierrez-Roelens I, Sluysmans T, Gewillig M, Devriendt K, Vikkula M. 2002. Progressive AV-block

and anomalous venous return among cardiac anomalies associated with two novel missense mutations in the CSX/NKX2-5 gene. Hum Mutat. 20, 75–76.

Haack, T. and Abdelilah-Seyfried, S. 2016. The force within: endocardial development, mechanotransduction and signalling during cardiac morphogenesis. Development. 143, 373–386.

Haar, J.L. and Ackerman, G.A. 1971. A phase and electron microscopic study of vasculogenesis and erythropoiesis in the yolk sac of the mouse. Anat. Rec. 170, 199-223.

Hadidy, N.E. and Uversky, V.N. 2019. Intrinsic disorder of the BAF complex: roles in chromatin remodeling and disease development. 20, 5260.

Hahn, C. and Schwartz, M.A. 2009. Mechanotransduction in vascular physiology and atherogenesis. Nature Rev. Mol. Cell Biol. 10, 53–62.

Hamburger, V. 1988. The Heritage of Experimental Embryology: Hans Spemann and the Organizer. Oxford University Press 12.

Hansen, K.H., Bracken, A.P., Pasini, D., Dietrich, N., Gehani, S.S., Monrad, A., Rappsilber, J., Lerdrup, M., Helin, K. 2008. A model for transmission of the H3K27me3 epigenetic mark. Nat. Cell Biol. 10, 1291–1300.

Harvey R.P. 1996. NK-2 homeobox genes and heart development. Dev. Biol. 178: 203.

Hashimoto, K. and Nakatsuji, N. 1989. Formation of the primitive streak and mesoderm cells in mouse-embryos-detailed scanning electron microsco-pical study. Dev. Growth Diff. 31, 209–218.

Hawkins, R.D., Hon, G.C., Lee, L.K., Ngo, Q., Lister, R., Pelizzola, M., Edsall, L.E., Kuan, S., Luu, Y., Klugman, S., Antosiewicz-Bourget, J., Ye, Zhen, Espinoza, C., Agarwahl, S., Shen, L., Ruotti, V., Wang, W., Stewart, R., Thomson, J.A., Ecker, J.R., Ren, B. 2010. Cell Stem Cell 6, 479-491.

Hayashi, S. and McMahon, A. P. 2002. Efficient recombination in diverse tissues by a tamoxifen-inducible form of Cre: A tool for temporally regulated gene activation/inactivation in the mouse. Dev. Biol. 244, 305–318.

Heckel, E., Boselli, F., Roth, S., Krudewig, A., Belting, H.-G., Charvin, G., Vermot, J. 2015. Oscillatory flow modulates mechanosensitive *klf2a* expression through *trpv4* and *trpp2* during heart valve development. Curr. Biol. 25, 1354–1361.

Heine, U.I., Roberts, A.B., Munoz, E.F., Roche, N.S., Sporn, M.B. 1985. Effects of retinoid deficiency on the development of the heart and vascular system on the quail embryo. Virchows Arch. B. Cell Pathol. Incl. Mol. Pathol. 50, 135-152.

Heintzman, N.D., Stuart, R.K., Hon, G., Fu, Y., Ching, C.W., Hawkins, R.D., Barrera, L.O., Van

Ho, L. and Crabtree, G.R. 2010. Chromatin remodelling during development. Nature 463, 474-484.

Ho, L., Ronan, J.L., Wu, J., Staahl, B.T., Chen, L., Kuo, A., Lessard, J., Nesvizhskii, A.I., Ranish, J., Crabtree, G.R. 2009. An embryonic stem cell chromatin remodelling complex, esBAF, is essential for embryonic stem cell self-renewal and pluripotency. PNAS 106, 5181-5186.

Hojfeldt, J.W., Laugesen, A., WIllumsen, B.M., Damhofer, H., Hedehus, L., Tvardovskiy, A., Mohammad, F., Jensen, O.N., Helin, K. 2018. Accurate H3K27me3 methylation can be established de novo by SUZ12-directed PRC2. Nat. Struct. Mol. Biol. 25, 225-232.

Hogan, B.L.M., and Tilly, R. 1981. Cell interactions and endoderm differentiation in cultured mouse embryos. J. Embryol. Exp. Morphol. 62, 379-394.

Hogan, B., Beddington, R., Constantini, F., Lacy, E. 1994. Manipulating the mouse embryo: a laboratory manual. Cold Spring Harbor, N.Y. Cold Spring Harbor Press.

Hogers, B., DeRuiter, M.C., Gittenberger-de Groot, A.C., Poelmann, R.E. 1997. Unilateral vitelline vein ligation alters intracardiac blood flow patterns and morphogenesis in the chick embryo. Circ. Res. 80, 473–481.

Holliday, R. and Pugh, J.E. 1975. DNA modification mechanisms and gene activity during development. Science 187, 226–232.

Hove, J.R., Koster, R.W., Forouhar, A.S., Acevedo-Bolton, G., Fraser, S.E., Gharib, M. 2003. Intracardiac fluid forces are an essential epigenetic factor for embryonic cardiogenesis. Nature 421, 172–177.

Hryniuk, A., Grainger, S., Savory, J.G.A., Lohnes, D. 2012. Cdx function is required for maintenance of intestinal identity in the adult. Dev. Biol. 363, 426-437.

Huber, T.L., Kouskoff, V., Fehling, H.J., Palis, J., keller, G. 2004. Haemangioblast commitment is initiated in the primitive streak of the mouse embryo. Nature 432, 625-630.

Huelsken, J., Vogel, R., Brinkmann, V., Erdmann, B., Birchmeier, C., Birchmeier, W. 2000. Requirement for β-catenin in anterior-posterior axis formation in mice. J. Cell Biol. 148, 567–578.

Iida, M., Heike, T., Yoshimoto, M., Baba, S., Doi, H., Nakahata, T. 2005. Indentification of cardiac stem cells with FLK1, CD31, and VE-cadherin expression during embryonic stem cell differentiation. FASEB J. 19, 371-378.

Ikeya M, Takada S. Wnt-3a is required for somite specification along the anteroposterior axis of the mouse embryo and for regulation of cdx-1 expression. Mech. Dev. 2001. 103, 27–33

Ikeya, M. and Takada, S. 2001. Wnt-3a is required for somite specification along the anteroposterior axis of the mouse embryo and for regulation of cdx-1 expression. Mech. Dev. 103, 27-33.

Inman, K.E. and Downs, K.M. 2006. Brachyury is required for elongation and vasculogenesis in the murine allantois. Development 133, 2947-2959.

Inman, K.E. and Downs, K.M. 2007. The murine allantois: emerging paradigms in development of the mammalian umbilical cord and its relation to the fetus. Genesis 45, 237-258.

Isaacs, H.V., Pownall, M.E., Slack, J.M. 1998. Regulation of Hox gene expression and posterior development by the Xenopus caudal homologue Xcad3. EMBO J. 17, 3413–3427.

Ishitobi, H., Wakamatsu, A., Lui, F., Azami, T., Hamada, M., Matsumoto, K., Kataoka, H., Kobayashi, M., Choi, K., Nishikawa, S.-I., Takahashi, S., Ema, M. 2011. Molecular basis for Flk1 expression in hemato-cardiovascular progenitors in the mouse. Development 138, 5357-5368.

Isoda, T., Moore, A.J., He, Z., Chandra, V., Aida, M., Denholtz, M., van Hamburg, J.P., Fisch, K.M., Change, A.N., Fahl, S.P., Wiest, D.L., Murre, C. 2017. Non-coding transcription instructs chromatin folding and compartmentalization to dictate enhancer–promoter communication and T cell fate. Cell 171, 103–119.e18.

Iovino, N., Ciabrelli, F., Cavalli, G. 2013. PRC2 controls Drosophila oocyte cell fate by repressing cell cycle genes. Dev. Cell 26, 431-439.

James, R., and Kazenwadel, J. 1991. Homeobox gene expression in the intestinal epithelium of adult mice. J. Biol. Chem. 266, 3246-3251.

Johnson, G.R., Moore, M.A.S. 1975. Role of stem cell migration in initiation of mouse foetal liver haematopoiesis. Nature 258, 726-728.

Johnson, M.H. and Ziomek, C.A. 1981. The foundation of two distinct cell lineages within the mouse morula. Cell 24, 71-81.

Jollie, W.P. 1990. Development, morphology, and function of the yolk-sac placenta of laboratory rodents. Teratology 41, 361–381.

Jones, E.A., le Noble, F., Eichmann, A. 2006. What determines blood vessel structure? Genetic prespecification vs. hemodynamics. Physiology 21, 388-395.

Kadam, S., and Emerson, B.M. 2003. Transcriptional specificity of human SWI/SNF BRG1 and BRM chromatin remodelling complexes. Mol. Cell. 11, 377-389.

Kalb, R., Latwiel, S., Baymaz, H.I., Jansen, P.W.T.C., Muller, C.W., Vermeulen, M., Muller, J. 2014. Histone H2A monoubiquitination promotes histone H2 methylation in Polycomb repression. Nat. Struct. Mol. Biol. 21, 569-571.

Kattman, S.J., Huber, T.L., Keller, G.M. 2006. Multipotent flk-1+ cardiovascular progenitor cells give rise to the cardiomyocytes, endothelial, and vascular smooth muscle lineages. Developmental Cell 11, 723-732.

Kattman, S.J., Witty, A.D., Gagliardi. M., Duboid, N.C., Niapour, M., Hotta, A., Eliis, J., Keller, G. 2011. Stage-specific optimization of activin/nodal and BMP signaling promotes cardiac differentiation of mouse and human pluripotent stem cell lines. Cell Stem Cell 8, 228-240.

Keegan, B.R., Feldman, J.L., Begemann, G., Ingham, P.W., Yelon, D. 2005. Retinoic acid signaling restricts the cardiac progenitor pool. Science 307, 247-249.

Keller, G. 1995. In vitro differentiation of embryonic stem cells. Curr. Opin. Cell Biol. 7, 862–869.

Keller, G. 2005. Embryonic stem cell differentiation: emergence of a new era in biology and medicine. Genes Dev. 19, 1129-1155.

Kemp, C., Willems, E., Abdo, S., Lambiv, L., Leyns, L. 2005. Expression of all Wnt genes and their secreted antagonists during mouse blastocyst and postimplantation development. Dev. Dyn 233, 1064–1075.

Kennedy, M., D'Souza, S., Lynch-Kattman, M., Schwantz, S., Keller, G. 2007. Development of the hemangioblasts defines the onset of hematopoiesis in human ES cell differentiation cultures. Blood 10, :2679-2687.

Khavari, P.A., Peterson, C.L., Tamkun, J.W., Mendel, D.B., Crabtree, G.R. 1993. BRG1 contains a conserved domain of the SWI2 / SNF2 family necessary for normal mitotic growth and transcription. Nature 366, 170–174.

Kia, S.K., Gorski, M.M., Giannakopoulos, S., Verrijzer, C.P. 2008. SWI/SNF mediates Polycomb eviction and epigenetic reprogramming of the INK4b-ARF-INK4a locus. Mol. Cell. Biol 28, 3457-3464.

Kinder, S.J., Tsang, T.E., Quinlan, G.A., Hadjantonakis, A.K., Nagy, A., Tam, P.P. 1999. The orderly allocation of mesodermal cells to the extraembyonic structures and the anteroposterior axis during gastrulation of the mouse embryo. Development 126, 4691-4701.

Kirby, M.L., and Waldo, K.L. 1990. Role of neural crest in congenital heart disease. Circulation 82, 332-340.

Kirby, M.L., and Waldo, K.L. 1995. Neural crest and cardiovascular patterning. Circ. Res. 77, 211-215.

Kissa, K. and Herbomel, P. 2010. Blood stem cells emerge from aortic endothelium by a novel type of cell transition. Nature 464, 112-115.

Koefoed, K., Veland, I.R., Pedersen, L.B., Larsen, L.A., Christensen, S.T. 2014. Cilia and coordination of signaling networks during heart development. Organogenesis 10, 108–125

Kopp, A. 2011. Drosophila sex combs as a model of evolutionary innovations. Evol. Dev. 13, 504–522.

Kowalski, W.J., Pekkan, K., Tinney, J.P., Keller, B.B. 2014. Investigating developmental cardiovascular biomechanics and the origins of congenital heart defects. Front. Physiol. 5, 408.

Kowenz-Leutz, E., Leutz, A. 1999. A C/EBP isoform recruits the SWI/SNF complex to activate myeloid genes. Mol. Cell. 4, 735-743.

Krebs, J.E., Kuo, M.H., Allis, C.D., Peterson, C.L. 1999. Cell cycle-regulated histone acetylation required for expression of the yeast HO gene. Genes Dev. 13, 1412-1421.

Ku, M., Koche, R.P., Rheinbay, E., Mendenhall, E.M., Endoh, M., Mikkelsen, T.S., Presser, A., Nusbaum, C., Xie, X., Chi, A.S., Adli, M., Kasif, S., Ptaszek, L.M., Cowan, C.A., Lander, E.S., Koseki, H., Bernstein, B.E. 2008. Genomewide analysis of PRC1 and PRC2 occupancy identified two classes of bivalent domains. PLoS Genet. 4, e1000242.

Kumar, N., Tsai, Y.-H., Chen, L., Zhou, A., Banerjee, K.K., Saxena, M., Huang, S., Toke, N.H., Xing, J., Shivdasani, R.A., Spence, J.R., Verzi, M.P. 2019. The lineage-specific transcription factor CDX2 navigates dynamic chromatin to control distinct stages of intestine development. Development 146, dev172189.

Kuo, C.T., Morrissey, E.E., Anandappa, R., Sigrist, K., Lu, M.M., Parmacek, M.S., Soudais, C., Leiden, J.M. 1997. GATA4 transcription factor is required for ventral morphogenesis and heart tube formation. Genes Dev. 11, 1048-1060.

Kwon, G.S., Viotti, M., Hadjantonakis, A.-K. 2008. The endoderm of the mouse embryo arises by dynamic widespread interacalation of embryonic and extraembryonic lineages. Dev. Cell 15, 509-520.

Kwon, H., Imbalzano, A.N., Khavari, P.A., Kingston, R.E., Green, M.R. 1994. Nucleosome disruption and enhancement of activator binding by a human SW1/SNF complex. Nature 370, 477–481.

Lancrin, C., Sroczynska, P., Stephenson, C., Allen, T., Kouskoff, V., Lacaud, G. 2009. The hemangioblast generates hematopoietic cells through a haemogenic endothelium stage. Nature 457, 892-895.

Lane, M.C. and Smith, W.C. 1999. The origins of primitive blood in Xenopus: implications for axial patterning. Development 126, 423-434.

Laurent, B. C., Treich, I. and Carlson, M. 1993. The yeast SNF2/SWI2 protein has DNA-stimulated ATPase activity required for transcriptional activation. Genes Dev. 7, 583-91.

Lawson, K.A., Dunn, N.R., Roelen, B.A., Zeinstra, L.M., Davis, A.M., Wright, C.V., Korving, J.P., Hogan, B.L. 1999. Bmp4 is required for the generation of primordial germ cells in the mouse embryo. Genes Dev. 13, 424-436.

Lawson, K.A. and Hage, W.J. 1994. Clonal analysis of the origin of primordial germ cells in the mouse. In: Germline Development, Ciba. Found. Symp. Vol. 182, Wiley, Chichester, pp. 68-91.

Lawson, LA, Meneses, JJ, Pedersen, RA. 1991. Clonal analysis of epiblast fate during germ layer formation in the mouse embryo. Development 113, 891-911.

Lee, T.I., Jenner, R.G., Boyer, L.A., Guenther, M.G., Levine, S.S., Kumar, R.M., Chevalier, B., Johnstone, S.E., Cole, M.F., Isono, K., Koseki, H., Fuchikami, T., Abe, K., Murray, H.L., Zucker, J.P., Yuan, B., Bell, G.W., Herbolsheimer, E., Hannett, N.M., Sun, K., Odom, D.T., Otte, A.P., Volkert, T.L., Bartel, D.P., Melton, D.A., Gifford, D.K., Jaenisch, R., Young, R.A. 2006. Control of developmental regulators by Polycomb in human embryonic stem cells. Cell 125, 301-313.

Leeb, M., Pasini, D., Novatchkova, M., Jaritz, M., Helin, K., Wutz, A. 2010. Polycomb complexes act redundantly to repress genomic repeats and genes. Genes Dev. 24, 265-276.

Lengerke, C., McKinney-Freeman, S., Naveiras, O., Yates, F., Wang, Y., Bansal, D., Daley, G.Q. 2007. The cdx-hox pathway in hematopoietic stem cell formation from embryonic stem cells. Ann. N. Y. Acad. Sci. 1106, 197-208.

Lewis, P.H. 1949. PC: Polycomb. Drosophila Information Service 21, 69.

Lewis, E.B. 1978. A gene complex controlling segmentation in Drosophila. Nature 276, 565-570.

Li, W., Ferkowicz, M.J., Johnson, S.A., Shelly, W.C., Yoder, M.C. 2005. Endothelial cells in the early murine yolk sac give rise to CD41-expression hematopoietic cells. Stem Cells Dev. 14, 44-54.

Lickert, H., Domon, C., Huls, G., Wehrle, C., Duluc, I., Clevers, H., Meyer, B.I., Freund, J.N., Kemler, R. 2000. Wnt/(beta)-catenin signaling regulation the expression of the homeobox gene Cdx1 in embryonic intestine development. 127, 3805-3813.

Lickert, H. and Kemler, R. 2002. Functional analysis of cis-regulatory elements controlling initiation and maintenance of early Cdx1 gene expression in the mouse. Dev. Dyn. 225, 216-220.

Lickert, H., Takeuchi, J.K., von Both, I., Walls, J.R., McAuliffe, F., Adamson, S.L., Henkelman, R.M., Wrana, J.L., Rossant, J., Bruneau, B.G. 2004. Baf60c is essential for function of BAF chromatin remodelling complexes in heart development. Nature 432, 107-112.

Lin, Q., Schwarz, J., Bucana, C., Olson, E.N. 1997. Control of mouse cardiac morphogenesis and

myogenesis by transcription factor MEF2C. Science 276, 1404–1407.

Lints, T.J., Parsons, L.M., Hartley, L., Lyons, I., Harvey, R.P. 1993. Nkx-2.5: A novel murine homeobox gene expressed in early heart progenitor cells and their myogenic descendants. Development 119, 969.

Lipkin, M. 1985. Growth and development of gastrointestinal cells. Annu. Rev. Physiol. 47, 175-197.

Lloyd, J.B. 1990. Cell physiology of the rat visceral yolk sac: a study of pinocytosisand lysosome function. Teratology 41: 383-393.

Lohnes, D.L. 2003. The Cdx1 homeodomain protein: an integratory of posterior signaling in the mouse. BioEssays 25, 971-980.

Lu, S.-J., Feng, Q., Caballero, S., Chen, Y., Moore, M.A.S., Grant, M.B., Lanza, R. 2006. Generation of functional hemangioblasts from human embryonic stem cells. Nat. Mathods 6, 501-509.

Lu, C.X., Gong, H.R., Liu, X.Y., Wang, J., Zhao, C.M., Huang, R.T., Xue, S., Yang, Y.Q. 2016. A novel HAND2 loss-of-function mutation responsible for tetralogy of Fallot. Int. J. Mol. Med. 27, 445-451.

Lu, C.C. and Robertson, E.J. 2004. Multiple roles for Nodal in the epiblast of the mouse embryo in the establishment of anterior-posterior patterning. Dev. Biol 273, 149–159.

Lynch, J., Keller, M., Guo, R.-J., Yang, D., Traber, P. 2003. Cdx1 inhibits the proliferation of human colon cancer cells by reducing cyclin D1 gene expression. Oncogene 22, 6395-6407.

Lyons, I., Parsons, L.M., Hartley, L., Li, R., Andrews, J.E., Robb, L., Harvey, R.P. 1995. Myogenic and morphogenetic defects in the heart tubes of murine embryos lacking the homeobox gene Nkx2-5. Genes Dev. 9. 1654.

Mae, S.-I., Shono, A., Shiota, F., Yasuno, T., Kajiwara, M., Gotoda-Nishimura, N., Arai, S., Sato-Otubo, A., Toyoda, T., Takahashi, K., Nakayama, N., Cowan, C.A., Aoi, T., Ogawa, S., McMahon, A.P., Yamanaka, S., Osafune, K. 2013. Monitoring and robust induction of nephrogenic intermediate mesoderm from human pluripotent stem cells. Nat. Comm. 4, 1367.

Macdonald, P.M. and Struhl, G. 1986. A molecular gradient in early Drosophila embryos and its role in specifying the body pattern. Nature 324, 537–545.

Maître, J.-L. 2017. Mechanics of blastocyst morphogenesis: Mechanics of blastocyst morphogenesis. Biol. Cell 109, 323-338.

Margueron, R., Li, G., Sarma, K., Blais, A., Zavadil, J., Woodcock, C.L., Dynlacht, B.D., Reinberg, D. 2008. Ezh1 and Ezh2 maintain repressive chromatin through different mechanisms. Mol. Cell. 32, 503-518.

Margueron, R., Justine, N., Ohno, K., Sharpe, M.L., Son, J., Drury 3rd, W.J., Voigt, P., Martin, S.R., Taylor, W.R., De Marco, V., Pirrotta, V., Reinberg, D., Gamblin, S.J. 2009. Role of the polycomb protein EED in the propagation of repressive histone marks. Nature. 461, 762-767.

Margueron, R. and Reinberg, D. 2011. The polycomb complex PRC2 and is mark on life. Nature 469, 343-349.

Mazzoni, E.O., Mahony, S., Peljto, M., Patel, T., Thornton, S.R., McCuine, S., Reeder, C., Boyer, L.A., Young, R.A., Gifford, D.K., Wichterle, H. 2013. Saltatory remodeling of Hox chromatin in response to rostro-caudal patterning signals. Nat. Neurosci. 16, 1191-1198.

Medvinsky, A. and Dzierzak, E. 1996. Definitive hematopoiesis is autonomously initiated by the AGM region. Cell 86, 897-906.

Mendenhall, E.M., Koche, R.P., Truong, T., Zhou, V.W., Issac, B., Chi, A.S., Ku, M., Bernstein, B.E. 2010. GC-rich sequence elements recruit PRC2 in mammalian ES cells. PLoS Genet. 6, e1001244.

Mendjan, S., Ortmann, D., Ortiz, M., Karjosukarso, D.Q., Ng, Y., Moreau, T., Pedersen, R.A. 2014. NANOG and CDX2 pattern distinct subtypes of human mesoderm during exit from pluripotency. Cell Stem Cell 15, 310-325.

Meslamani, J., Smith, S.G., Sanchez, R., Zhou, M.-M. 2016. Structural features and inhibitors of bromodomains. Drug Discov. Today Technol. 19, 3–15.

Meyer, B.I. and Gruss, P. 1993. Mouse Cdx2 expression during gastrulation. Development 117, 191-203.

Midgett, M. and Rugonyi, S. 2014. Congenital heart malformations induced by hemodynamic altering surgical interventions. Front. Physiol. 5, 287.

Midgett, M., Thornburg, K.L., Rugonyi, S. 2017b. Blood flow patterns underlie developmental heart defects. Am. J. Physiol. Heart Circ. Physiol. 312, H632–H642.

Migeotte, I., Omelchenko, T., Hall, A., Anderson, K.V. 2010. Rac1-dependent collective cell migration is required for specification of the anterior–posterior body axis of the mouse. PLoS Biol. 8, e1000442.

Mlodzik, M., Fjose, A., Gehring, W.J. 1985. Isolation of caudal, a Drosophila homeo box-containing gene with maternal expression, whose transcripts form a concentration gradient at the pre-blastoderm stage. EMBO J. 4, 2961-2969.

Mlodzik, M., Gehring, W.J. 1987. Expression of the caudal gene in the germ line of Drosophila: formation of an RNA and protein gradient during early embryogenesis. Cell 48, 465–478.

Mlodzik, M., Gibson, G., Gehring, W.J. 1990. Effects of ectopic expression of caudal during Drosophila development. Development 109, 271–277.

Mohamed, O.A., Clarke, H.J., Dufort, D. 2004. β-Catenin signaling marks the prospective site of primitive streak formation in the mouse embryo. Dev. Dyn. 231, 416–424.

Molkentin, J.D., Lin, Q., Duncan, S.A., Olson, E.N. 1997. Requirement of the transcription factor GATA4 for heart tube formation and ventral morphogenesis. Genes Dev. 11, 1061-1072.

Moore, M.A.S. and Metcalf, D. 1970. Ontogeny of the haematopoietic system yolk sac origin of in vivo and in vitro colony forming cells in the developing mouse embryo. Br. J. Haematol. 18, 279-296.

Moretti, A., Caron, L., Nakano, S., Lam, J.T., Bernhausen, A., Chen, Y., Qyang, Y., Bu, L., Sasaki, M., Martin-Puig, S., Sun, Y., Evans, S.M., Laugwitz, K.-L., Chien, K.R. 2006. Multipotent embryonic isl1+ progenitor cells lead to cardiac, smooth muscle, and endothelial cell diversification. Cell 127, 1151-1165.

Morris, S.A., Teo, R.T., Li, H., Robson, P., Glover, D.M., Zernicka-Goetz, M. 2010. Origin and formation of the first two distinct cell types of the inner cell mass in the mouse embryo. Proc. Natl. Acad. Sci. U.S.A. 107, 6364-6369.

Moustakim, M., Clark, P.G.K., Hay, D.A., Dixon, D.J., Brennan, P.E. 2016. Chemical probes and 652 inhibitors of bromodomains outside the BET family. Medchemcomm. 7, 2246–2264.

Muchardt, C. and Yaniv, M. 1993. A human homologue of Saccharomyces cerevisiae SNF2/SWI2 and Drosophila brm genes potentiates transcriptional activation by the glucocorticoid receptor. EMBO J. 12, 4279-90.

Mulley, J.F., Chiu, C.-H., Holland, P.W.H. 2006. Breakup of a homeobox cluster after genome duplication in teleosts. Proceedings of the National Academy of Sciences. 103, 10369-10372.

Mumbach, M.R., Granja, J.M., Flynn, R.A., Raoke, C.M., Satpathy, A.T., Rubin, A.J., Qi, Y., Jiang, Z., Shams, S., Louie, B.H., Gui, J.K., Gennert, D.G., Corces, M.R., Khavari, P.A., Atianand, M.K., Artandi, S.E., Fitzgerald, K.A., Greenleaf, W.J., Chang, H.Y. 2019. HiChIRP reveals RNA-associated chromosome conformation. Nat. Methods 16, 489–492.

Murray, P.D.F. 1932. The development in vitro of the blood of the early chick embryo. Proc. R. Soc. Lond. B. 111, 497-520.

Nagy, A. 2000. Cre recombinase: The universal reagent for genome tailoring. Genesis 26, 99–109.

Narita, N., Bielinska, M., Wilson, D.B. 1997. Cardiomyocyte differentiation by GATA-4-deficient embryonic stem cells. Development 124, 3755–3764.

Nascone, N. and Mercola, M. 1995. An inductive role for the endoderm in Xenopus cardiogenesis. Development 121, 515-523.

Neely, K.E., Hassan, A.H., Wallberg, A.E., Steger, D.J., Cairns, B.R., Wright, A.P.H., Workman, J.L. 1999. Activation domain-mediated targeting of the SWI/SNF complex to promoters stimulates transcription from nucleosome arrays. Mol. Cell. 4, 649-655.

Nguyen, T.T., Savory, J.G.A., Brooke-Bisschop, T., Ringuette, R., Foley, T., Hess, B.L., Mulatz, K.J., Trinkle-Mulcahy, L., Lohnes, D. 2017. Cdx2 regulates gene expression through recruitment of Brg1-associated Switch-Sucrose Non-fermentable (SWI-SNF) chromatin remodeling activity. J. Biol. Chem. 292, 3389-3399.

Nishamatsu, S. and Thomsen, G.H. 1998. Ventral mesoderm induction and patterning by bone morphogenetic protein heterodimers in Xenopus embryos. Mech. Dev. 74, 75-88.

Nishikawa, S.-I. Nishikawa, S., Hirashima, M., Matsuyoshi, N., Kodama, H. 1998. Progressive lineage analysis by cell sorting and culture identifies FLK1+VE-cadherin+ cells at a diverging point of endothelial and hematopoietic lineages. Development 125, 1747-1757.

Niwa, H., Toyooka, Y., Shimosato, D., Strumpf, D., Takahashi, K., Yagi, R., Rossant, J. 2005. Interaction between Oct3/4 and Cdx2 determines trophectoderm differentiation. Cell 123, 917-29.

Nonaka, S., Shiratori, H., Saijoh, Y., Hamada, H. 2002. Determination of left–right patterning of the mouse embryo by artificial nodal flow. Nature 418, 96–99.

Nonaka, S., Tanaka, Y., Okada, Y., Takeda, A., Harada, A., Kanai, Y., Kido, M., Hirokawa, N. 1998. Randomization of left-right asymmetry due to loss of nodal cilia generating leftward flow of extraembryonic fluid in mice lacking KIF3B motor protein. Cell 95, 829-837.

Norris, D.P. and Robertson, E.J. 1999. Asymmetric and node-specific nodal expression patterns are controlled by two distinct cis-acting regulatory elements. Genes Dev. 13, 1575-1588.

Northrop, J.L. and Kimelman, D. 1994. Dorsal-ventral differences in Xcad-3 expression in response to FGF-mediated induction in Xenopus. Dev. Biol. 161, 490-503.

Okada, Y., Nonaka, S., Tanaka, Y., Saijoh, Y., Hamada, H., Hirokawa, N. 1999. Abnormal nodal flow precedes situs inversus in iv and inv mice. Mol. Cell 4, 459– 468.

Omelchenko, T., Rabadan, M.A., Hernáandez-Martínez, R., Grego-Bessa, J., Anderson, K.V., Hall, A. 2014. BPix directs collective migration of anterior visceral endoderm cells in the early mouse embryo. Genes Dev. 28, 2764–2777.

Org, T., Duan, D., Ferrari, R., Montel-Hagen, A., Van Handel, B., Kerenyi, M.A., Sasidharan, R.,

Rubbi, L., Fujiwara, Y., Pellegrini, M., Orkin, S.H., Kurdistani, S.K., Mikkola, H.K.A. 2015. Scl binds to primed enhancers in the mesoderm to regulate hematopoietic and cardiac fate divergence. EMBO J. 34, 759-777.

Ostlund Farrants, A.K., Blomquist, P., Kwon, H., Wrange, O. 1997. Glucocorticoid receptor-glucocorticoid response element binding stimulates nucleosome disruption by the SWI/SNF complex. Mol. Cell Biol. 17, 895-905.

Oudenaarden, A., Clevers, H., Deschamps, J. 2014. Transformation of intestinal stem cells into gastric stem cells on loss of transcription factor Cdx2. Nature Comm. 5, 5728.

Padron-Barthe, L., Temino, S., Villa Del Campo, C., Carramolino, L., Isern, J., Torres, M. 2014. Clonal analysis identifies hemogenic endothelium as the source of the blood-endothelial common lineage in the mouse embryo. Blood 124, 2523-2532.

Palis, J., McGrath, K.E., Kingsley, P.D. 1995. Initiation of hematopoiesis and vasculogenesis in murine yolk sac explants. Blood 86, 156-163.

Pan, G., Tian, S., Nie, J., Yang, C., Ruotti, V., Wei, H., Jonsdottir, G.A., Stewart, R., Thomson, J.A. 2007. Whole-genome analysis of histone H3 lysine 4 and lysine 27 methylations in human embryonic stem cells. Cell Stem Cell 1, 299-312.

Papaioannou, V.E. 1982. Lineage analysis of inner cell mass and trophectoderm using microsurgically reconstituted blastocysts. J. Embryol. Exp. Morphol. 68, 199-209.

Parameswaran, M. and Tam, P.P.L. 1995. Regionalisation of cell fate and morphogenetic movement of the mesoderm during mouse gastrulation. Dev. Genet. 17, 16-28.

Pedersen, H. and Mygind, N. 1976. Absence of axonemal arms in nasal mucosa cilia in Kartagener's syndrome. Nature 262, 494-495.

Perea-Gomez, A., Vella, F.D.J., Shawlot, W., Oulad-Abdelghani, M., Chazaud, C., Meno, C., Pfister, V., Chen, L., Robertson, E., Hamada, H., Behringer, R.R., Ang, S.L. 2002. Nodal antaginists in the anterior visceral endoderm prevent the formation of multiple primitive streaks. Dev. Cell 3, 745–756.

Peterson, C. L., Dingwall, A., Scott, M. P. 1994. Five SWI/SNF gene products are components of a large multisubunit complex required for transcriptional enhancement Proc. Natl. Acad. Sci. U.S.A. 91, 2905-2908.

Pilon, N., Oh, K., Sulvestre, J.-R., Bouchard, N., Savory, J., Lohnes, D. 2006. Cdx4 is a direct target of the canonical Wnt pathway. Dev. Biol. 289, 55-63.

Pinello, L., Xu, J., Orkin, S.H., Yuan, G.-C. 2014. Analysis of chromatin-state plasticity identifies cell-

type-specific regulators of H3K27me3 patterns. PNAS 111, E344-353.

Plusa, B., Piliszek, A., Frankenburg, S., Artus, J., Hadjantonakis, A.K. 2008. Distinct sequential cell behaviours direct primitive endoderm formation in the mouse blastocyst. Development 35, 3081-3091.

Prinos, P., Joseph, S., Oh, K., Meyer, B.I., Gruss, P., Lohnes, D. 2001. Multiple pathways governing Cdx1 expression during murine development. Dev. Biol. 239, 257-269.

Puri, P.L. and Mercola, M. 2012. BAF60 A, B, and Cs of muscle determination and renewal. Genes Dev. 26, 2673–2683.

Ralston, A. and Rossant, J. 2008. Cdx2 acts downstream of cell polarization to cell-autonomously promote trophectoderm fate in the early mouse embryo. Dev. Biol. 313, 614-629.

Ramakrishnan, A.B., Chen, L., Burby, P.E., Cadigan, K.M. 2021. Wnt target enhancer regulation by a CDX/TCF transcription factor collective and a novel DNA motif. Nucleic Acids Res. 49, 8625-864.

Randazzo, F. M., Khavari, P., Crabtree, G., Tamkun, J. and Rossant, J. 1994. Brg1: a putative murine homologue of the Drosophila brahma gene, a homeotic gene regulator Dev. Biol. 161, 229-42.

Rayon, T., Menchero, S., Rollan, I., Ors, I., Helness, A., Crespo, M., Nieto, A., Azuara, V., Rossant, J., Manzanares, M. 2016. Distinct mechanisms regulate Cdx2 expression in the blastocyst and in trophoblast stem cells. Scientific Reports 6, 27139.

Redkar, A., Mongomery, M., Litvin, J. 2001. Fate map of early avian cardiac progenitor cells. Development 128, 2269.

Reiter, J.F., Alexander, J., Rodaway, A., Yelon, D., Patient, R., Holder, N., Stainier, D.Y. 1999. Gata5 is required for the development of the heart and endoderm in zebrafish. Genes Dev. 13, 2983–2995.

Reyes, J.C., Barra, J., Muchardt, C., Camus, A., Babinet, C., Yaniv, M. 1998. Altered control of cellular proliferaction in the absence of mammalian brahman (SNF2alpha). EMBO J. 17, 6979-6991.

Ringrose, L. and Paro, R. 2007. Polycomb/Trithorax response elements and epigenetic memory of cell identity. Development 134, 223–232.

Rings, E.H.H., Boudreau, F., Taylor, J.K., Moffett, J., Suh, E.R., Traber, P.G. 2001. Phosphorylation of the serine 60 residue within the Cdx2 activation domain mediates its transactivtion capacity. Gastroenterology 121, 1437-1450.

Robb, L., Lyons, I., Li, R., Hartley, L., Kontgen, F., Harvey, R.P., Metcalf, D., Begley, C.G. 1995.

Absence of yolk sac hematopoiesis form mice with a targeted disruption of the scl gene. Proc. Natl. Acad. Sci. USA. 92, 7075-7079.

Rossant, J., Chazaud, C., Yamanaka, Y. 2003. Lineage allocation and asymmetries in the early mouse embryo. Philos. Trans. R. Soc. Lond. B. Biol. Sci. 358, 1341-1348.

Rossant, J. and McMahon, A. 1999. "Cre"-ating mouse mutants—A meeting review on conditional mouse genetics. Gene Dev. 13, 142–145.

Rossant, J. and Tam P.P.L. 2009. Blastocyst lineage formation, early embryonic assymmetries and axis patterning in the mouse. Development 136, 701-713.

Rosenquiest, G.C. 1970. Location and movements of cardiogenic cells in the chick embryo: the heart-forming portion of the primitive streak. Dev. Biol. 22, 461-475.

Sabin, F.R. 1920. Studies on the origin of blood vessels and of rest corpuscles as seen in the living blastoderm of chicks during the second day of incubation. Contrib. Embryol. 9, 213-262.

Saga, Y., Hata, N., Kobayashi, S., Magnuson, T., Seldin, M.F., Taketo, M.M. 1996. MesP1: a novel basic helix-loop-helix protein expressed in the nascent mesodermal cells during mouse gastrulation. Development 122, 2769-2778.

Saga, Y., Miyagawa-Tomita, S., Takagi, A., Kitajima, S., Miyazaki, J., Inoue, T. 1999. Mesp1 is expressed in the heart precursor cells and required for the formation of a single heart tube. Development 126, 3437-3447.

Saijoh, Y., Adachi, H., Sakuma, R., Yeo, C.Y., Yashiro, K., Watanabe, M., Hashiguchi, H., Mochida, K., Ohishi, S., Kawabata, M., Miyazono, K., Whitman, M., Hamada, H. 2000. Left-right assymetric expression of lefty2 and nodal is induced by a signaling pathway that includes the transcription factor FAST2. Mol. Cell 5, 35-47.

Savory, J.G.A., Bouchard, N., Pierre, V., Pijili, F.M., De Repentigny, Y., Kothary, R., Lohnes D. 2009a. Cdx2 regulation of posterior development through non-Hox targets. Development 136, 4099-4110.

Savory, J.G.A., Pilon, N., Grainger, S., Sylvestre, J.-R., Beland, M., Houle, M., Oh, K., Lohnes D. 2009b. Cdx1 and Cdx2 are functionally equivalent in vertebral patterning. Dev. Biol. 330, 114-122.

Savory, J.G.A., Bouchard, N., Pierre, V., Rijili, F.M., De Repentigny, Y., Kothary, R., Lohnes, D. 2011a. Cdx2 regulation of posterior developing through non-Hox targets. Development 136, 4099-4110.

Savory, J.G.A., Mansfield, M., St. Louis, C., Lohnes, D. 2011b. Cdx4 is a Cdx2 target gene. Mech.

Dev. 128, 41-48.

Saxena, M., San Roman, A., O'Neill, N.K., Sulahian, R., Jadhav, U., Shivdasani, R.A. 2017. Transcription factor-dependent 'anti-repressive' mammalian enhancers exclude H3K27me3 from extended genomic domains. Genes Dev. 31, 2391-2404.

Schier, A.F. 2003. Nodal signaling in vertebrate development. Annu. Rev. Cell Dev. Biol. 19, 589–621.

Schier, A.F. and Talbot, W.S. 2005. Molecular genetics of axis formation in zebrafish. Annu. Rev. Genet. 39, 561-613.

Schott, J.J., Benson, D.W., Basson, C.T., Silberbach, G.M., Moak, J.P., Maron, B.J., Seidman, C.E., Seidman, J.G. 1998. Congenital heart disease caused by mutations in the transcription factor Nkx2-5. Science 281, 108-111.

Schuettengruber, B., Chourrout, D., Vervoort, M., Leblanc, B., Cavalli, G. 2007. Genome regulation by polycomb and trithorax proteins. Cell 128, 735–745.

Schultheiss, T.M., Xydas, S., Lassar, A.B. 1995. Induction of avian cardiac myogenesis by anterior endoderm. Development 121, 4203-4214.

Schumacher, J.A., Bloomekatz, J., Garavito-Aguilar, Z.V., Yelon, D. 2013. tal1 regulates the formation of intercellular junctions and the maintenance of identity in the endocardium. Dev. Biol. 383, 214-226.

Schwartz, Y.B., Kahn, T.G., Nix, D.A., Li, X.Y., Bourgon, R., Biggin, M., Pirotta, V. 2006. Genome-wide analysis of Polycomb targets in Drosophila melanogaster. Nature Gen. 38, 700-705.

Schwartz, Y.B., and Pirotta, V. 2014. Ruled by ubiquitylation: a new order for Polycomb recruitment. Cell Rep. 8, 321-325.

Scialdone, A., Tanaka, Y., Jawaid, W., Moignard, V., Wilson, N.K., Macaulay, I.C., Marioni, J.C., Gottgens, B. 2016. Resolving early mesoderm diversification through single-cell expression profiling. Nature 535, 289-293.

Selleck, M. A. and Stern, C. D. 1991. Fate mapping and cell lineage analysis of Hensen's node in the chick embryo. Development 112, 615-626.

Shen, M.M. 2007. Nodal signaling: Developmental roles and regulation. Development 134, 1023–1034.

Shioi, G., Hoshino, H., Abe, T., Kiyonari, H., Nakao, K., Meng, W., Furuta, Y., Fujimori, T., Aizawa, S. 2017. Apical constriction in distal visceral endoderm cells initiates global, collective cell rearrangement in embryonic visceral endoderm to form anterior visceral endoderm. Dev. Biol. 429, 20–30.

Shimizu, T., Bae, Y.-K., Muraoka, O., Hibi, M. 2005. Interaction of Wnt and caudal-related genes in zebrafish posterior body formation. Dev. Biol. 279, 125-141.

Shiratori, H., Sakuma, R., Watanabe, M., Hshiguchi, H., Mochida, K., Sakai, Y., Nishino, J., Saijoh, Y., Whitman, M., Hamada, H. 2001. Two-step regulation of left-right assymetric expression of Pitx2: initiation by nodal signaling and maintenance of Nkx2. Mol. Cell 7, 137-149.

Shivdasani, R.A., Mayer, E.L., Orkin, S.H. 1995. Absence of blood formation in mice lacking the T-cell leukaemia oncoprotein tal-1/SCL. Nature 373, 432-434.

Silver, L. and Palis, J. 1997. Initiation of murine embryonic erythropoiesis: a spatial analysis. Blood 89, 1154-1164.

Simmini, A., Bialecka, M., Huch, M., Kester, L., van de Wetering, M., Sato, T., Beck, F., van Oudenaarden, A., Clevers, H., Deschamps, J. 2014. Transformtion of intestinal stem cells into gastric stem cells on loss of transcription factor Cdx2. Nar. Commun. 5, 5728.

Sing, A., Pannell, D., Karaiskakis, A., Sturgeon, K., Djabali, M., Ellis, J., Lipshitz, H.D., Cordes, S.P. 2009. A vertebrate Polycomb response element governs segmentation of the posterior hindbrain. Cell 138, 885-897.

Singh, A.P., Archer, T.K. 2014. Analysis of the SWI/SNF chromatin-remodeling complex during early heart development and BAF250a repression cardiac gene transcription during P19 cell differentiation. Nucleic Acids Res. 42, 2958-2975.

Simon, J. A. and Kingston, R. E. 2009. Mechanisms of polycomb gene silencing: knowns and unknowns. Nature Rev. Mol. Cell Biol. 10, 697–708.

Sokpor, G., Xie, Y., Rosenbusch, J., Tuoc, T. 2017. Chromatin remodeling BAF (SWI/SNF) complexes in neural development and disorders. Front. Mol. Neurosci. 10, 243.

Spemann, H. Embryonic Development and Induction. Yale University Press; New Haven, Conn: 1938. reprinted by Hafner publishing company, 1962.

Srinivas, S., Rodriguez, T., Clements, M., Smith, J.C., Beddington, R.S.P. 2004. Active cell migration drives the unilateral movements of the anterior visceral endoderm. Development 131, 1157–1164.

Stanton, B.Z., Hodges, C., Calarco, J.P., Braun, S.M., Ku, W.L., Kadoch, C., Zhao, K., Crabree, G.R. 2017. Smarca4 ATPase mutations disrupt direct eviction of PRC1 from chromatin. Nat. Genet. 49, 282-288.

Strahl, B.D., Aliss, C.D. 2000. The language of covalent histone modifications. Nature 403, 41-45.

Stern, C.D. and Downs, K.M. 2012. The hypoblast (visceral endoderm): an evo-devo perspective.

Development 139, 1059-1069.

Smith, A.G. 2001. Embryo-derived stem cells: Of mice and men. Annu. Rev. Cell Dev. Biol. 17, 435–462.

Squazzo, S.L., O'Green, H., Komashko, V.M., Krig, S.R., Jin, V.X., Jang, S.-w., Margueron, R., Reinberg, D., Green, R., Farnham, P.J. 2006. Suz12 binds to silenced regions of the genome in a cell-type-specific manner. Genome Res. 16, 890-900.

Srivastava, D. 2006. Making or breaking the heart: from lineage determination to morphogenesis. Cell 126, 1037-1048.

Strumpf, D., Mao, C-A., Yamanaka, Y., Ralston, A., Chawengsaksophak, K., Beck, F., Rossant, J. 2005. Cdx2 is required for correct cell fate specification and differentiation of trophectoderm in the mouse blastocyst. Development 132, 2093-2102.

Subramanian, V., Meyer, B.I., Gruss, P. 1995. Disruption of the murine homeobox gene Cdx1 affects axial skeletal identities by altering the mesodermal expression domains of Hox genes. Cell 83, 641-653.

Sulik, K., Dehart, D.B., Iangaki, T., Carson, J.L., Vrablic, T., Gesteland, K., Shoenwolf, G.C. 1994. Morphogenesis of the murine node and notochordal plate. Dev. Dyn. 201, 260-278.

Sun, X., Meyers, E.N., Lewandoski, M., Martin, G.R. 1999. Targeted disruption of Fgf8 causes failure of cell migration in the gastrulating mouse embryo. Genes Dev. 13, 1834–1846.

Sun, X., Hota, S.K., Zhou, T.-Q., Novak, S., Miguel-Perez, D., Chistodoulou, D., Siedman, C.E., Seidman, J.G., Gregorio, C.C., Henkelman, R.M., Rossant, J., Bruneau, B.G. 2018. Cardiac-enriched BAF chromatin-remodeling complex subunit Baf60c regulates gene expression programs essential for heart development and function. Development 7, bio029512.

Supp, D.M., Brueckner, M., Kuehn, M.R., Witte, D.P., Lowe, L.A., McGrath, J., Corrales, J., Potter, S.S. 1999. Targeted deletion of the ATP binding domain of left–right dynein confirms its role in specifying development of left–right asymmetries. Development 126, 5495 – 5504.

Takaoka, K., Nishimura, H., Hamada, H. 2017. Both Nodal signalling and stochasticity select for prospective distal visceral endoderm in mouse embryos. Nat. Commun. 8, 1–3.

Takaoka, K., Yamamoto, M., Hamada, H. 2011. Origin and role of distal visceral endoderm, a group of cells that determines anterior-posterior polarity of the mouse embryo. Nat. Cell Biol. 13, 743-752.

Takeda, S., Yonekawa, Y., Tanaka, Y., Okada, Y., Nonaka, S., Hirokawa, N. 1999 Left –right

asymmetry and kinesin superfamily protein KIF3A: new insights in determination of laterality and mesoderm induction by kif3A2/2 mice analysis. J. Cell Biol. 145, 825– 836.

Tam, P. and Beddington, R.S. 1987. The formation of mesodermal tissues in the mouse embryo during gastrulation and early organogenesis. Development 99, 109-126.

Tam, P.P.L. and Behringer, R.R. 1997. Mouse gastrulation: the formation of a mammalian body plan. Mech. Dev. 68, 3-25.

Tam, P.P. and Gad, J.M. 2004. Gastrulation of the mouse embryo. In *Gastrulation* (ed. Stern C. D.), pp. 223–262. Cold Spring Harbor, NY: Cold Spring Harbour Laboratory Press.

Tam, P.P.L., Parameswaran, M., Kinder, S.J., Weinberger, R.P. 1997. The allocation of epiblast cells to the embryonic heart and other mesodermal lineages: the role of ingression and tissue movement during gastrulation. Development 124, 1631-1642.

Tam, P.L. and Schoenwolf, G.C. 1999. Cardiac fate maps: Lineage allocation, morphogenetic movement, and cell commitment. In Heart development (ed. R.P. Harvey and N. Rosenthal), p. 3. Academic Press, San Diego, California.

Tam, P.P.L., Williams, E.A., Chan, W.Y. 1993. Gastrulation in the mouseembryo: ultrastructural and molecular aspects of germ layermorphogenesis. Microsci. Res. Tech. 26, 301–328.

Tam, P.P.L. and Zhou, S.X. 1996. The allocation of epiblast cells to ectodermal and germ-line lineages is influenced by the position of cells in the gastrulating mouse embryo. Dev. Biol. 178, 124-132.

Tavares, L., Dimitrova, E., Oxley, D., Webster, J., Poot, R., Demmers, J., Bezstarosti, K., Taylor, S., Ura, H., Koide, H., Wutz, A., Vidal, M., Elderkin, S., Brockdorff, N. 2012. RYBP-PRC1 complexes mediate H2A ubiquitulation at polycomb target sites independently of PRC2 and H3K27me3.

Taylor, J.K., Boll, W., Levy, T., Suh, E., Siang, S., Mantei, N., Traber, P.G. 1997a. Comparison of intestinal phospholipase A/lysophospholipase and sucrase-isomaltase genes suggest a common structure for enterocyte-specific promoters. DNA Cell Biol. 16, 1419-1428.

Taylor, J.K., Levy, T., Suh, E.R., Traber, P.G. 1997b. Activation of enhancer elements by the homeobox gene Cdx2 is cell line specific. Nucleic Acids Res. 25, 2293-300.

Tamkun, J.W., Deuring, R., Scott, M.P., Kissinger, M., Pattatucci, A.M., Kaufman, T.C., Kennison, J.A. 1992. Brahma: a regulator of Drosophila homeotic genes structurally related to the yeast transcriptional activator SNF2/SWI2. Cell 68, 561-72.

Thomas, P. and Beddington, R. 1996. Anterior primitive endoderm may be responsible for patterning

the anterior neural plate in the mouse embryo. Curr. Biol. 6, 1487-1496.

Thomas, P.Q., Brown, A., Beddington, R.S. 1998. Hex: a homeobox gene revealing peri-implantation asymmetry in the mouse embryo and an early transient marker of endothelial cell precursors. Development 125, 85-94.

Thompson, K.W., Marquez, S.B., Lu, L., Reisman, D. 2015. Induction of functional Brm protein from Brm knockout mice. Oncoscience 2, 349-361.

Trinh, K.Y., Jin, T., Drucker, D.J. 1999. Identification of domains mediating transcriptional activa- tion and cytoplasmic export in the caudal homeobox protein Cdx-3. J. Biol. Chem.274, 6011-6019.

Tolkunova, E., Cavaleri, F., Eckardt, S., Reinbold, R., Christenson, L.K., Scholer, H.R., Tomilin, A. 2006. The caudal-related protein cdx2 promotes trophoblast differentiation of mouse embryonic stem cells. Stem Cells 24: 139-144.

Turner, D.A., Girgin, M., Alonso-Cristomo, L., Trivedi, V., Baillie-Johnson, P., Glodowski, C.R., Hayward, P.C., Collignon, J., Gustavsen, C., Serup, P., Steventon, B., Lutolf, M.P., Arias, A.M. 2017. Anteroposterior polarity and elongation in the absence of extraembryonic tissues and of spatially localised signaling in gastruloids: mammalian embryonic organoids. Development 144, 3894-3906.

van den Akker, E., Forlani, S., Chawengsaksophak, K., de Graaff, W., Beck, F., Meyer, B.I., Deschamps, J. 2002. Cdx1 and Cdx2 have overlapping functions in anteroposterior patterning and posterior axis elongation. Development 129, 2181–2193.

van den Brink, S.C., Baillie-Johnson, P., Balayo, T., Hadjantonakis, A.-K., Nowotschin, S., Turner, D.A., Martinez Arias, A. 2014. Symmetry breaking, germ layer specification and axial organisation in aggregates of mouse embryonic stem cells. Development 141, 4231–4242.

van de Ven, C., Bialecka, M., Neilts, R., Young, T., Rowland, J.E., Stringer, E.J., Van Rooijen, C., Meijlink, F., Novoa, A., Freund, J.-N., Mallo, M., Beck, F., Deschamps, J. 2011. Concerted involvement of Cdx/Hox genes and Wnt signaling in morphogenesis of the caudal neural tube and cloacal derivatives from the posterior growth zone. Development 138, 3451-3462.

Van Handel, B., Mongel-Hagen, A., Sasidharan, R., Nakano, H., Ferrari, R., Boogerd, C.J., Schredelseker, J., Wang, Y., Hunter, S., Org, T., Zhou, J., Li, X., Pellegrini, M., Chen, J.N., Orkin, S.H., Kurdistani, S.K., Evans, S.M., Nakano, A., Mikkola, H.K. 2012. Scl represses cardiomyogenesis in prospective hemogenic endothelium and endocardium. Cell 150, 590-605.

van Nes, J., de Graaf, W., Lebrin, F., Gerhard, M., Beck, F., Deschamps, J. 2006. The Cdx4 mutation

affects axial development and reveals an essential role for Cdx genes in the ontogenesis of the placental labyrinth in mice. Development 133, 419-428.

Varner, V.D. and Taber, L.A. 2012. Not just inductive: a crucial mechanical role for the endoderm during heart tube assembly. Development 139, 1680-1690.

Verzi, M.P., McCulley, D.J., De Val, S., Dodou, E., Black, B.L. 2005. The right ventricle, outflow tract, and ventricular septum comprise a restricted expressiondomain within the secondary/anterior heart field. Dev Biol. 287, 134-145.

Verzi, M.P., Shin, H., He, H.H., Sulahian, R., Meyer, C.A., Montgomery, R.K., Fleet, J.C., Brown, M., Liu, X.S., Shivdasani, R.A. 2010. Differentiation-specific histone modifications reveal dynamic chromatin interactions and partners for the intestinal transcription factor CDX2. Dev. Cell 19, 713–726.

Verzi, M.P., Shin, H., Roman, A.K.S., Liu, X.S., Shivdasani, R.A. 2013. Intestinal master transcription factor CDX2 controls chromatin access for partner transcription factor binding. Mol. Cell Biol. 33, 281-292.

Vincentz, J.W., Barnes, R.M., Rodgers, R., Firulli, B.A., Conway, S.J., Firulli, A.B. 2008. An absence of Twist1 results in aberrant cardiac neural crest morphogenesis. Dev Biol. 320, 131–139.

Visvader, J.E., Fujiwara, Y., Orkin, S.H. 1998. Unsuspected role for the T-cell leukemia protein SCL/tal-1 in vascular development. Genes Dev. 12, 473-479.

Vogeli, K.M., Jin, S.-W., Martin, G.R., Stainier, D.Y.R. 2006. A common progenitor for haematopoietic and endothelial lineages in the zebrafish gastrula. Nature 443, 337-339.

Wang, Y., Yabuuchi, A., McKinney-Freeman, S., Ducharme, D.M., Ray, M.K., Chawengsaksophak, \ K., Archer, T.K., Daley, G.Q. 2008. Cdx gene deficiency compromises embryonic hematopoiesis in the mouse. PNAS 105, 7756-7761.

Wang, W., Cote, J., Xue, Y., Zhou, S., Khavari, P.A., Biggar, S.R., Muchardt, C., Kalpana, G.V., Goff, S.P., Yaniv, M., Workman, J.L., Crabtree, G.R. 1996. Purification and biochemical heterogeneity of the mammalian SWI-SNF complex. EMBO J. 15, 5370–5382.

Warga, R. M. and Nüsslein-Volhard, C. 1999. Origin and development of the zebrafish endoderm. Development 126, 827-838.

Wasiak, S. and Lohnes, D. 1999. Retinoic acid affects left-right patterning. Dev. Biol. 215, 332-342.

Watson, E.D., Cross, J.C. 2005. Development of structures and transport functions in the mouse placenta. Physiology 20, 180–193.

Waxman, J.S., Keegan, B.R., Roberts, R.W., Poss, K.D., Yelon, D. 2008. Hoxb5b acts downstream of

retinoic acid signaling in the forelimb field to restrict heart field potential in zebrafish. Dev. Cell 15, 923–34.

Wells, J.M. and Melton, D.A. 1999. Vertebrate endoderm development. Annu. Rev. Cell Dev. Biol. 15, 393-410.

Wilson, V. and Beddington, R.S. 1996. Cell fate and morphogenetic movement in the late mouse primitive streak. Mech. Dev. 55, 79-89.

Winnier, G., Blessing, M., Labosky, P.A., Hogan, B.L. 1995. Bone morphogenetic protein-4 is required for mesoderm formation and patterning in the mouse. Genes Dev. 9, 2105–2116.

Wolpert, L. 1996. One hundred year of positional information. Trends Genet. 12, 359-364.

Woo, C.J., Kharchenko, P.V., Daheron, L., Park, P.J., Kingston, R.E. 2010. A region of the human HOXD cluster that confer Polycomb-group responsiveness. Cell 140, 99-110.

Wright, C.V. 2001. Mechanisms of left-right asymmetry: what's right and what's left? Dev. Cell 1, 179-186.

Wu, L.H., and Lengyel, J.A. 1998. Role of caudal in hindgut specification and gastrulation suggests homology between Drosophila amnioproctodeal invaginations and vertebrate blastopore. Development 125, 2433-2442.

Xin, M., Olson, E.N., Bassel-Duby, R. 2013. Mending broken hearts: cardiac development as a basis for adult heart regeneration and repair. Nat. Rev. Mol. Cell Biol. 14, 529-541.

Xu, Z., Meng, X., Cai, Y., Koury, M.J., Brandt, S.J. 2006. Recruitment of the SWI/SNF protein Brg1 by a multiprotein complex effects transcriptional repression in murine erythroid progenitors. Biochem. J. 399, 297-304.

Yan, Z., Wang, Z., Sharova, L., Sharov, A.A., Ling, C., Piao, Y., Aiba, K., Matoba, R., Wang, W., Ko, M.S. 2008. BAF250B-associated SWI/SNF chromatin-remodeling complex is required to maintain undifferentiated mouse embryonic stem cells. Stem Cells 26, 1155-1165.

Yamagishi, H. 2021. Cardiac neural crest. Cold Spring Harb. Perspect. Biol. 13, a036715.

Yamaguchi, T.P., Dumont, D.J., Conlon, R.A., Breitman, M.L., Rossant, J. 1993. flk-1, an flt-related receptor tyrosine kinase is an early marker for endothelial cell precursors. Development 118, 489-498.

Yamamichi, N., Inada, K.-I., Furukawa, C., Sakurai, K., Tando, T., Ishizaka, A., Haraguchi, T., Mizutani, T., Fujishiro, M., Shimomura, R., Oka, M., Ichinose, M., Tsutsumi, Y., Omata, M., Iba, H. 2009. Cdx and the Brm-type SWI/SNF complex cooperatively regulate villin expression in gastrointestinal cells. Expt. Cell Res. 315, 1779-1789.

Yamamoto, M., Beppu, H., Takaoka, K., Meno, C., Li, E., Miyazono, K., Hamada, H. 2009. Antagonism between Smadl and Smad2 signaling determines the site of distal visceral endoderm formation in the mouse embryo. J. Cell Biol. 184, 323–334.

Yamanaka, Y., Ralston, A., Stephenson, R.O., Rossant, J. 2006. Cell and molecular regulation of the mouse blastocyst. Dev. Dyn. 235, 2301-14.

Yatskievych, T., Ladd, A., Antin, P. 1997. Induction of cardiac myogenesis in avian pregastrula epiblast: the role of the hypoblast and activin. Development 124, 2561–2570.

Yoshinaga, S.K., Peterson, C.L., Herskowitz, I., Yamamoto, K. 1992. Roles of SWI1, SWI2, and SWI3 proteins for transcriptional enhancement by steroid receptors. Science 258, 1598-1604.

Young, T., Rowland, J.E., van de Ven, C., Bialecka, M., Novoa, A., Carapuco, M., van Nes, J., de Graaf, W., Duluc, I., Fruend, J.-N., Beck, F., Mallo, M., Dechamps, J. 2009. Cdx and Hox genes differentially regulate posterior axial growth in mammalian embryos. Dev. Cell 17, 516-526.

Young, M.D., Wilson, T.A., Wakefield, M.J., Trounson, E., Hilton, D.J., Blewitt, M.E., Oshlack, A., Majewski, I.J. 2011. ChIP-seq analysis reveals distinct H3K27me3 profiles that correlate with transcriptional activity. Nucleic Acids Res. 39, 7415-7427.

Yu, M., Mazor, T., Huang, H., Huang, H.T., Kathrein, K.L., Woo, A.J., Chouinard, C.R., Labadorf, A., Akie, T.E., Moran, T.B., Xie, H., Zacharek, S., Taniuchi, I., Roeder, R.G., Kim, C.F., Zon, L.I., Fraenkel, E., Cantor, A.B. 2012. Direct recruitment of Polycomb repressive complex 1 to chromatin by core binding transcription factors. Mol. Cell 45, 330-343.

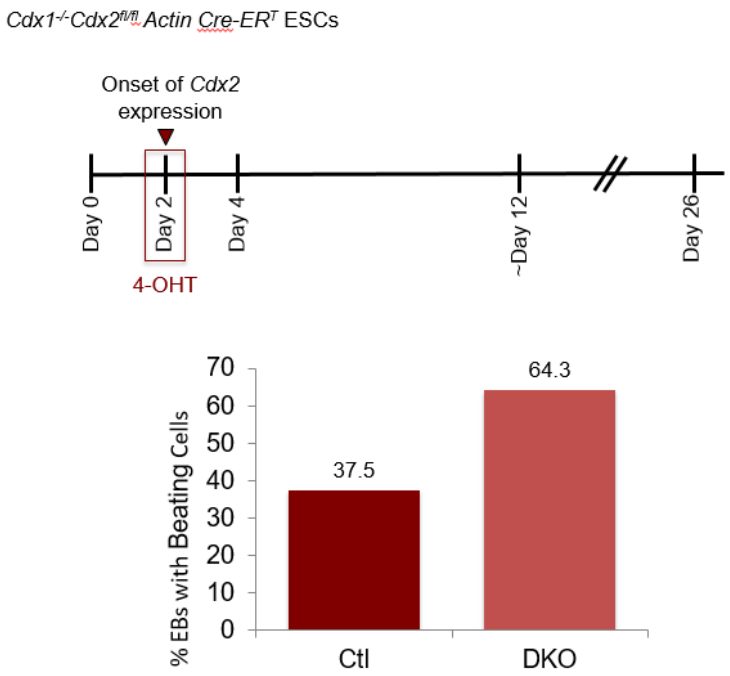
Yutzey, K.E. and Kirby, M.L. 2002 Wherefore heart thou? Embryonic origins of cardiogenic mesoderm. Dev. Dyn. 223, 307–320.

Zhao, X.D., Han, X., Chew, J.L., Liu, J., Chiu, K.P., Choo, A., Orlov, Y.L., Sung, W-K., Shahab, A., Kuznetsov, V.A., Bourque, G., Oh, S., Ruan, Y., Ng, H-H., Wei, C-L. 2007. Whole-genome mapping of histone H3 Lys4 and 27 trimethylations reveals distinct genomic compartments in human embryonic stem cells. Cell Stem Cell 1, 286-298.

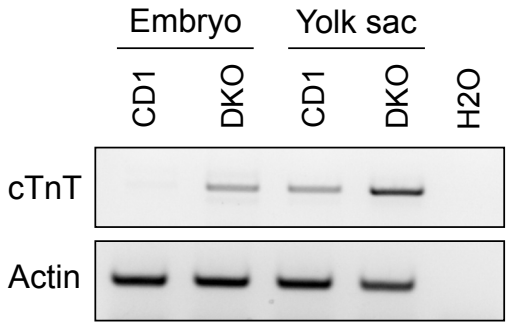
Zhao, W., Huang, Y., Zhang, J., Liu, M., Ji, H., Wang, C., Cao, N., Li, C., Xia, Y., Jiang, Q., Qin, J. 2017. Polycomb group RING finger proteins 3/5 activate transcription via interaction with the pluripotency factor Tex10 in embryonic stem cells. J. Biol. Chem. 292, 21527-21537.

Zovein, A.C., Hofmann, J.J., Lynch, M., French, W.J., Turlo, W.J., Yang, Y., Becker, M.S., Zanetta, L., Dejana, E., Gasson, J.C., Tallquist, M.D., Iruela-Arispe, M.L. 2008. Fate tracing reveals the endothelial origin of hematopoietic stem cells. Cell Stem Cell 3, 625-636.

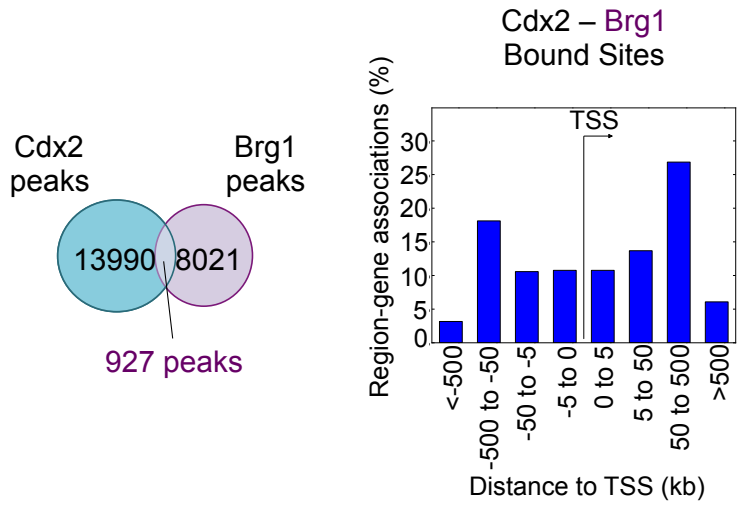
APPENDIX



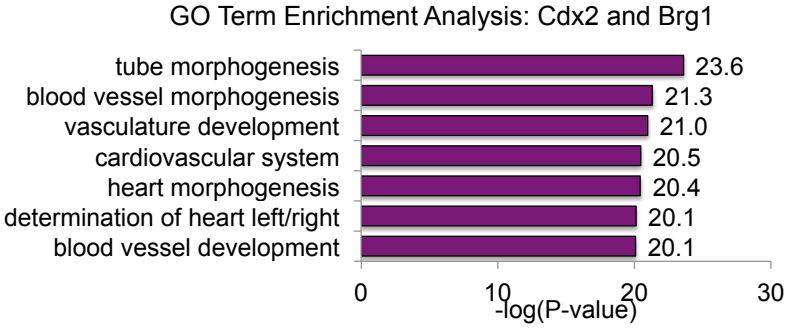
Appendix Figure 58. DKO embryoid bodies produce spontaneously beating colonies. *Cdx1*$^{-/-}$ *Cdx2*$^{fl/fl}$ *Actin::CreER*^{T} mESCs were maintained in hanging droplets for 2 days to induce differentiation through the formation of embryoid bodies (EBs). On day 2, when Cdx2 expression is normally induced, EBs were transferred to suspension cultures in the absence or presence of 4-OHT (control (Ctl) and DKO, respectively). On day 4, single EBs were transferred from suspension to 24-well culture dishes to which the cells could adhere, with each EB in a single well. The resulting colonies were monitored for spontaneous beating. The number of beating colonies Ctl and DKO EBs was quantified on day 26 and expressed as a percentage of the total (n=1).



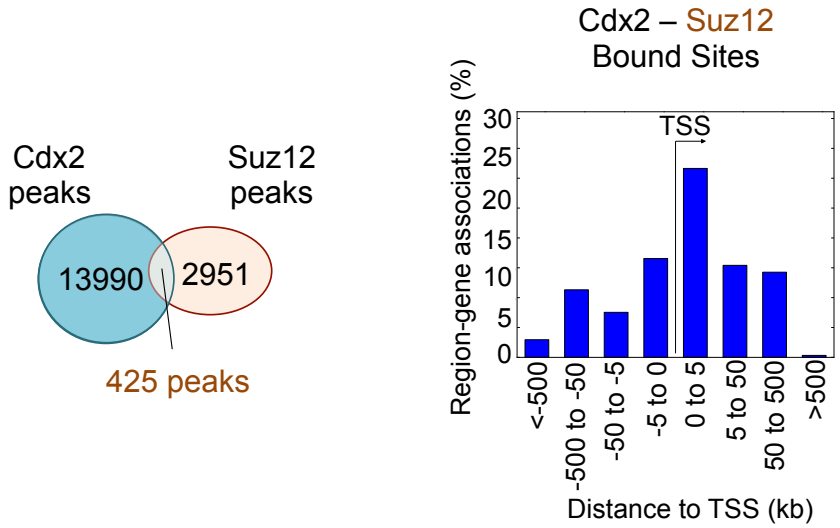
Appendix Figure 59. cTnT is ectopically expressed in E8.5 DKO embryos and yolk sacs. cTnT transcript levels were measured in wild type (CD1) and DKO embryos and yolk sacs at E8.5 by RT-PCR (n=1). β-Actin was included as a loading control.



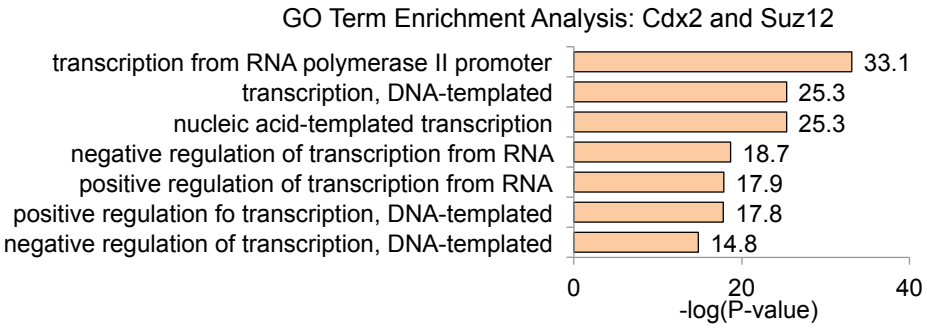
Appendix Figure 60. Cdx2 and Brg1 share genomic binding sites. Cdx2 binding sites identified in E8.5 embryos overlap with regions occupied by Brg1 in mouse embryonic stem cells differentiated to mesodermal progenitors in culture. Overlap occurs at 927 sites, largely within regions distal from the TSS of shared targets.



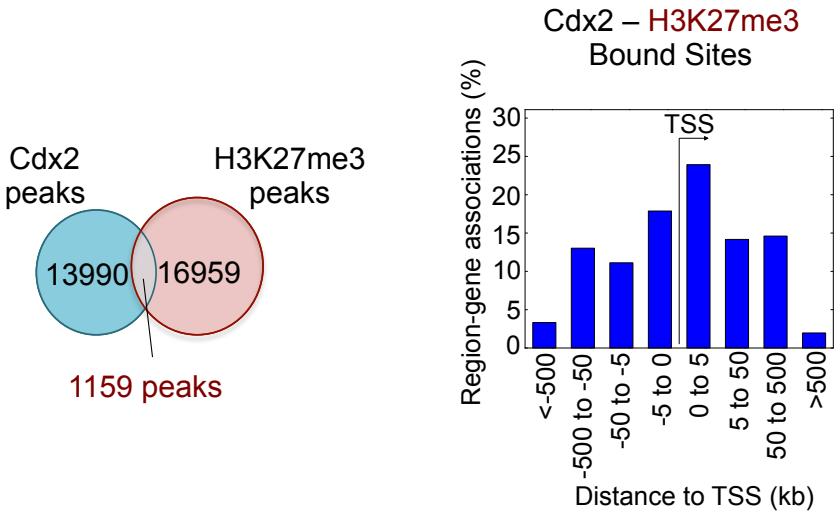
Appendix Figure 61. Cdx2 and Brg1 overlap at targets associated with vascular morphogenesis. Gene ontology (GO) terms associated with genes occupied by Cdx2 in E8.5 embryos and by Brg1 in mesodermal progenitors.



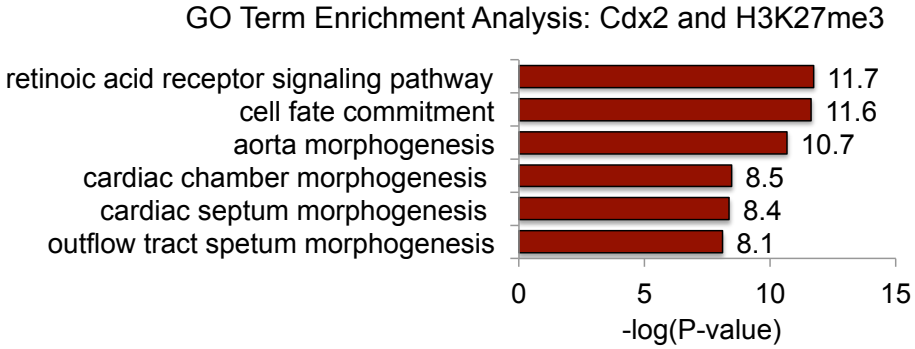
Appendix Figure 62. Cdx2 and Suz12 share genomic binding sites. Cdx2 binding sites identified in E8.5 embryos overlap with regions occupied by Suz12 in mouse embryonic stem cells differentiated to cardiac mesoderm in culture. Overlap between Cdx2 and H3k27me3 was observed at 425 sites, largely near the TSS of shared targets.



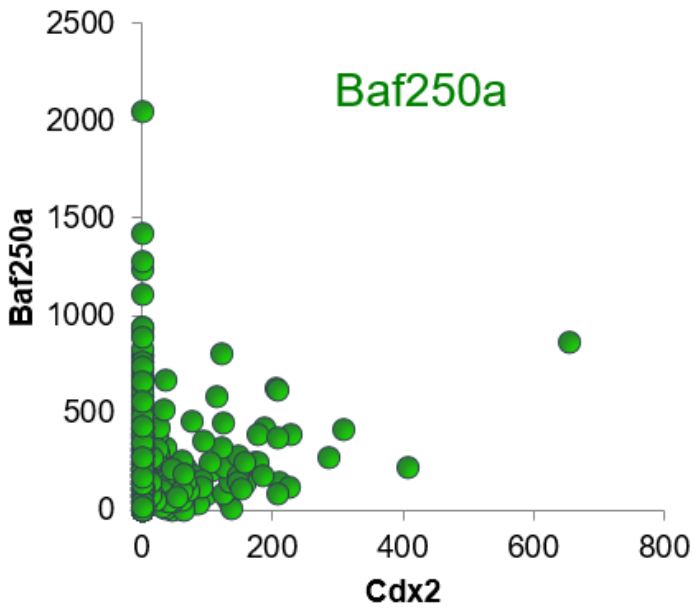
Appendix Figure 63. Cdx2 and Suz12 overlap at targets associated with transcriptional regulation. Gene ontology (GO) terms associated with genes occupied by Cdx2 in E8.5 embryos and by Suz12 in mesodermal progenitors.



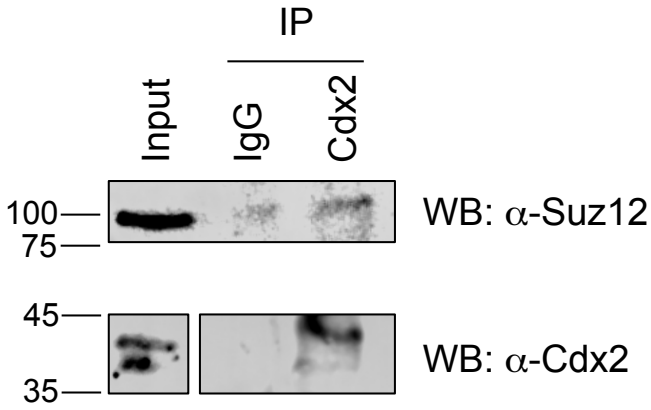
Appendix Figure 64. Cdx2 and H3K27me3 share genomic binding sites. Cdx2 binding sites identified in E8.5 embryos overlap with regions occupied by H3K27me3 in mouse embryonic stem cells differentiated to cardiac mesoderm in culture. Overlap between Cdx2 and H3k27me3 was observed at 1159 sites, largely near the TSS of shared targets.



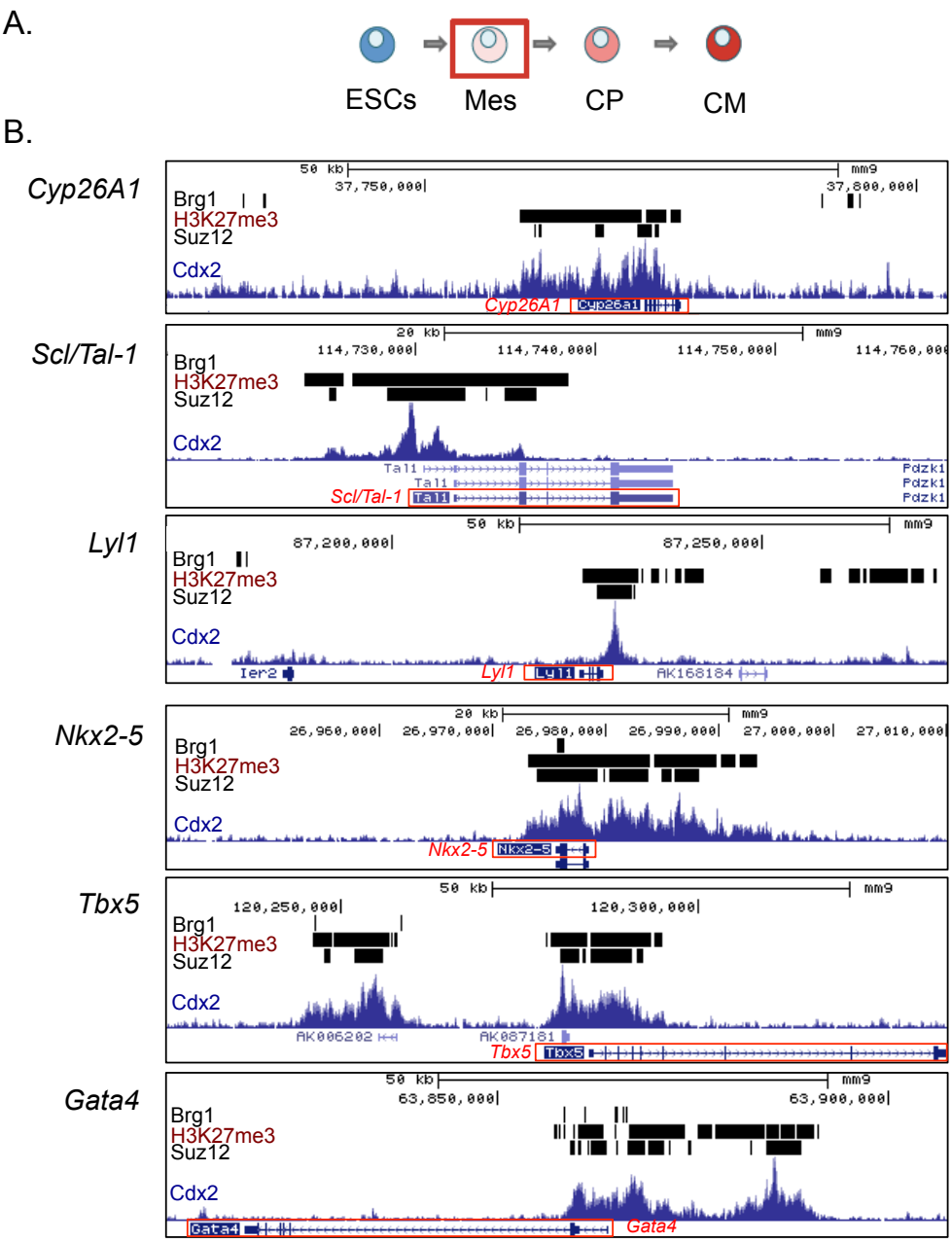
Appendix Figure 65. Cdx2 and H3K27me3 overlap at targets associated with cardiac development. Gene ontology (GO) terms associated with genes occupied by Cdx2 in E8.5 embryos and by H3K27me3 in mesodermal progenitors.



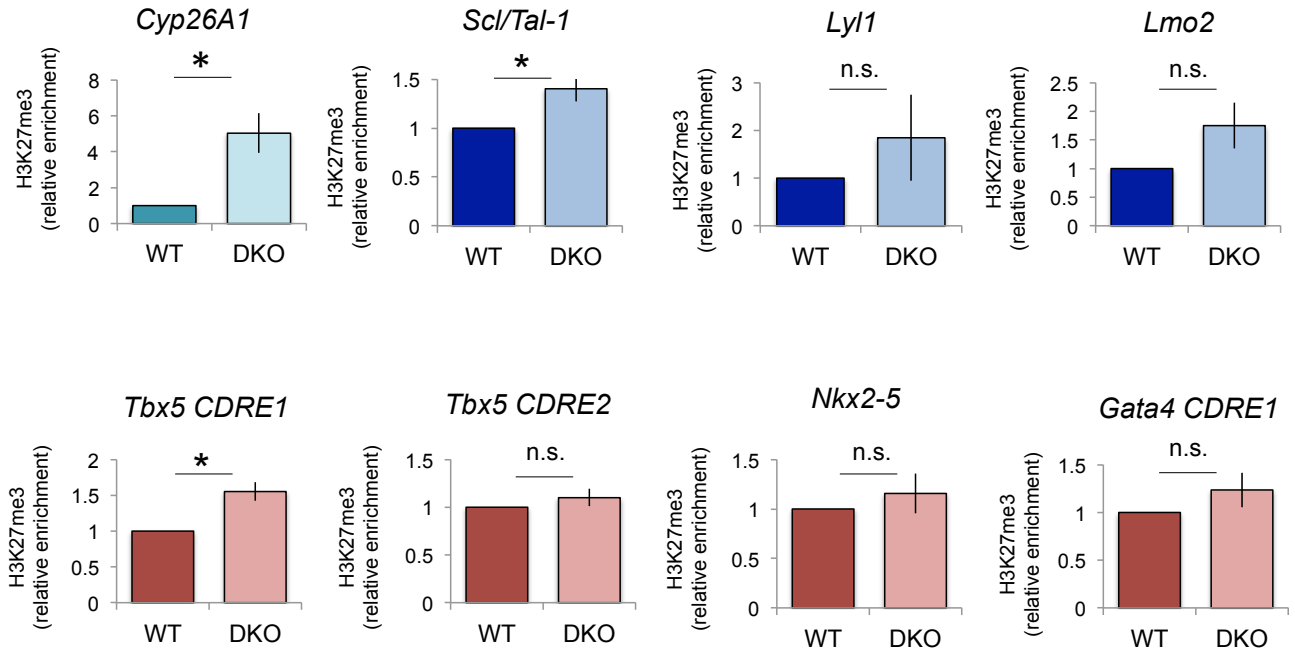
Appendix Figure 66. Cdx2 and Baf250a are co-expressed in single cells at E6.5-E7.75. Correlation plots using a single-cell RNA-seq dataset in E6.25-7.5 whole embryos generated by Scialdone and colleagues (Scialdone et al., 2016) demonstrate co-expression of *Cdx2* and *Baf250a.*



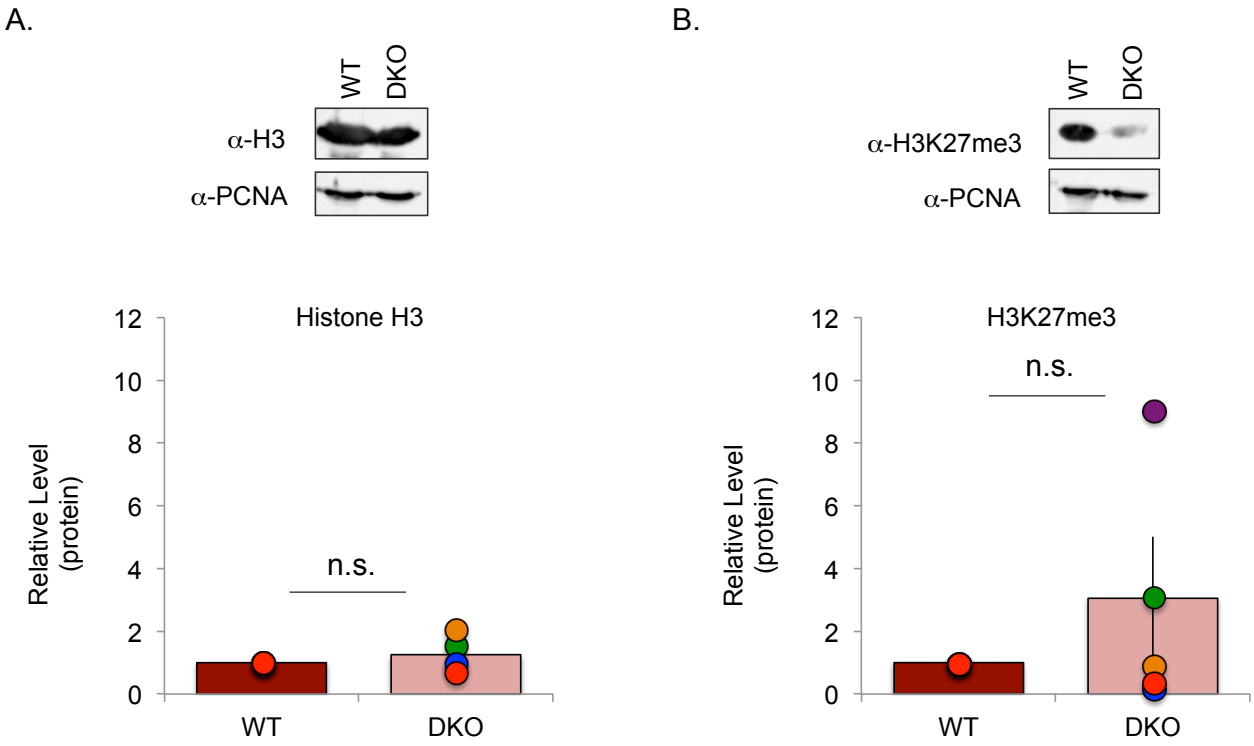
Appendix Figure 67. Cdx2 interacts with Suz12. Cdx2 was immunoprecipitated from whole cell lysates collected from E9.5-E10.5 wild type tail buds, and Suz12 binding was detected by western blot. The Cdx2 input lane is shown separately from the IP lanes, despite being from the same blot, due to differences in exposure time required for band visualization. Western blots are representative of four independent experiments. Molecular weights are indicated in kDa to the left.



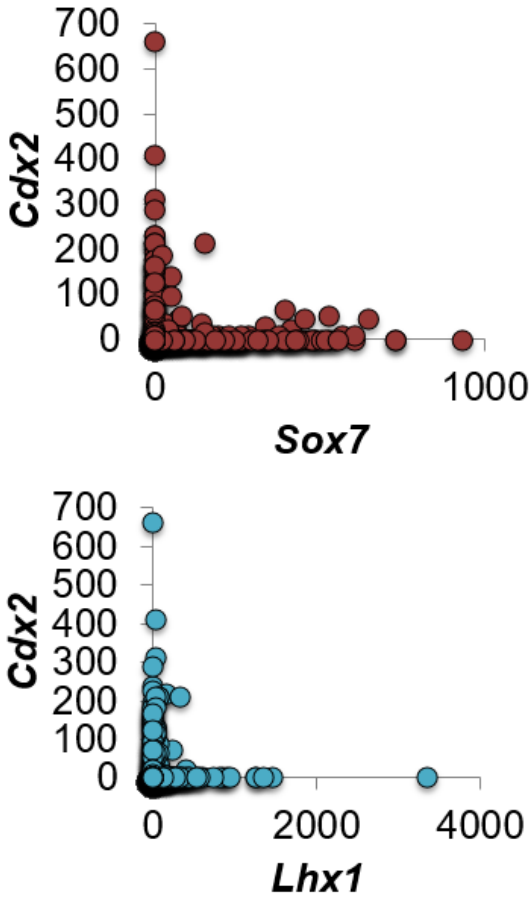
Appendix Figure 68. Cdx2 occupied sits overlap with binding by Suz12 and H3K27me3 in mesodermal precursors. A. Embryonic stem cells were differentiated to cardiomyocytes in vitro and collected at the mesoderm stage of differentiation for ChIP-seq by Alexander *et al.* (2015). ESCs, embryonic stem cells; Mes, mesoderm; CP, cardiac progenitors; CM, cardiomyocytes. **B.** ChIP-seq was performed in mesodermal cells (described in A.) using antibodies against Suz12, H3K27me3, and Brg1 (black bars, top; Alexander et al., 2015). These data were intersected with ChIP-seq data for Cdx2 binding in E8.5 whole embryos (blue peaks, below; Foley et al, 2019). Gene loci (*Cyp26A1*, *Scl/Tal-1*, *Tbx5*, *Nkx2-5,* and *Gata4*) are indicated beneath the peaks with exons represented by blue boxes.



Appendix Figure 69. H3K27me3 levels are increased at a subset of cardiogenic and hematopoietic Cdx-targets in Cdx-mutant yolk sacs. ChIP-PCR was performed in E9.5-10.5 yolk sacs to assess levels of H3K27me3 at known Cdx2 target genes. Primers flanked previously identified Cdx2-occupied regions of *Cyp26A1*, previously described as a Cdx2-target gene (Savory et al., 2009), the hematopoietic genes *Scl/Tal-1*, *Lyl1*, *Lmo2*, *Meis1*, (Brooke-Bisschop et al., 2017), and cardiogenic genes *Nkx2-5, Tbx5,* and *Gata4* (Foley et al., 2019). CDRE1 and CDRE2 denote separate putative Cdx-response elements at the *Tbx5* and *Gata4* loci. Background (IgG) was subtracted before normalization to inputs. Values represent the mean of at least three independent experiments $\pm$ standard error of the mean (s.e.m). Asterisks indicate statistical significance as determined by Student's t-test, $p \leq 0.05$, with n.s. indicative of no statistical significance.



Appendix Figure 70. Cdx-mutant embryos have highly variable levels of total H3K27me3. Nuclear extracts were collected from E9.5 wild type and DKO embryos (Schechter et al., 2007), and global levels of histone H3 (**A**) and H3K27me3 (**B**) were assessed by western blot. Bands were quantified by densitometry and normalized to a nuclear loading control, proliferating cell nuclear antigen (PCNA). Representative images of the western blots are shown above, with variability in H3 and H3K27me3 represented by the dot plots below. Bar graphs represent the mean of five independent experiments ± s.e.m, with no statistical significance (n.s.).



Appendix Figure 71. Cdx2 and markers of visceral endoderm are co-expressed in single cells at E6.5-E7.75. Correlation plots using a single-cell RNA-seq dataset in E6.25-7.5 whole embryos generated by Scialdone and colleagues (Scialdone et al., 2016) demonstrate co-expression of *Cdx2* and visceral endoderm markers *Sox7* and *Lhx1*.